

7000 ·

This is to certify that the dissertation entitled

MICROBIAL SYNTHESES OF CHEMICALS FROM RENEWABLE FEEDSTOCKS

presented by

Wei Niu

has been accepted towards fulfillment of the requirements for the

Ph.D. degree in Chemistry

Major Professor's Signature

Date

MSU is an Affirmative Action/Equal Opportunity Institution

LIBRARY fichigan State University **PLACE IN RETURN BOX** to remove this checkout from your record. **TO AVOID FINES** return on or before date due. **MAY BE RECALLED** with earlier due date if requested.

DATE DUE	DATE DUE	DATE DUE

6/07 p:/CIRC/DateDue.indd-p.1

MICROBIAL SYNTHESES OF CHEMICALS FROM RENEWABLE FEEDSTOCKS

Ву

Wei Niu

A DISSERTATION

Submitted to
Michigan State University
in partial fulfillment of the requirements
for the degree of

DOCTOR OF PHILOSOPHY

Department of Chemistry

2004

ABSTRACT

MICROBIAL SYNTHESES OF CHEMICALS FROM RENEWABLE FEEDSTOCKS

By

Wei Niu

Microbial syntheses of chemicals from renewable feedstocks are emerging as indispensable alternatives to current petroleum-based syntheses of industrial chemicals. In addition to key advantages of microbial syntheses over chemical syntheses such as chemical selectivity, molecular diversity, and environmental friendliness, a long-term application of microbial syntheses entails replacement of hydrocarbons with renewable resources and therefore addresses the issue of sustainability in chemical manufacture. Owing to recent technological advances in metabolic engineering, fermentation process, microbial genomics, and protein engineering, industrial application of microbial syntheses is on the verge of significant growth. In this thesis, microbial syntheses of 3-dehydroshikimate from glycerol, adipate from D-glucose, 1,2,4-butanetriol from D-xylose and L-arabinose are presented to illustrate challenging aspects in design, development, and utilization of microbial biocatalysts.

Choice of starting material is a critical issue in microbial syntheses of commercial chemicals. The phosphoenolpyruvate:carbohydrate phosphotransferase system (PTS) imposes a severe limitation on the yield of shikimate pathway metabolites synthesized by wild-type *E. coli* strains using glucose as the sole carbon source. The concentrations and the yields of 3-dehydroshikimate synthesized by a series of recombinant *E. coli* strains from glycerol, a PTS-independent carbon source, have been examined under fed-batch

fermentor conditions. One construct detailed in this dissertation research, *E. coli* KL3.21/pWN3.062A, synthesized 65 g/L of 3-dehydroshikimate from glycerol in 20% yield.

Adipic acid is one of the two precursors in the synthesis of nylon 6,6. Synthesis of adipate from glucose was achieved using a microbe-catalyzed conversion of glucose into *cis*,*cis*-muconate followed by chemical hydrogenation of the *cis*,*cis*-muconate into adipate. The design, construction, and evaluation of *E. coli* WN1/pWN2.248 is detailed, which synthesized 36.8 g/L of *cis*,*cis*-muconate in 22% yield from glucose under fedbatch fermentor conditions. Partially purified *cis*,*cis*-muconate in cell-free, protein-free culture medium was hydrogenated (500 psi H₂) over 10% Pt on C (5 mol%) for 2.5 h at ambient temperature to afford a 97% conversion of *cis*, *cis*-muconate into adipate.

The lack of a practical synthesis of 1,2,4-butanetriol has hindered widespread utilization of 1,2,4-butanetriol trinitrate, which is less shock sensitive, more thermally stable, less volatile, and has a lower freezing point relative to nitroglycerin. To explore alternatives to the current commercial synthesis of racemic D,L-1,2,4-butanetriol, a biosynthetic pathway, which does not occur in nature, was created to synthesize D- or L-1,2,4-butanetriol, respectively, from D-xylose or L-arabinose. Oxidation of D-xylose by *Pseudomonas fragi* provides D-xylonate in 70% yield. *E. coli* DH5α/pWN6.186A then catalyzes the conversion of D-xylonate into D-1,2,4-butanetriol in 25% yield. *P. fragi* also oxidizes L-arabinose to a mixture of L-*arabino*-1,4-lactone and L-arabinonate in 54% overall yield. Following hydrolysis of the lactone, L-arabinonate is converted into L-1,2,4-butanetriol in 35% yield using *E. coli* BL21(DE3)/pWN6.222A. In order to improve the overall yield of 1,2,4-butanetriol synthesized from pentose starting materials, directed evolution of a key enzyme in the created biosynthetic pathway is examined.

Copyright by Wei Niu 2004 To my parents, my brother, and my friends

For their love and encouragement

ACKNOWLEDGMENTS

I would first like to express my great gratitude to Prof. John W. Frost for his patience, encouragement and guidance throughout the course of my Ph.D. studies. His overly enthusiasm and integral view on science, and his mission for providing high-quality work has made a huge influence on me. I would like to thank the members of my graduate committee, Prof. Babak Borhan, Prof. Milton Smith III, and Prof. David P. Weliky for their intellectual input during the preparation of this thesis.

I am deeply indebted to Dr. Karen Draths for her patient instructions on experimental skills and invaluable inputs to my research. As a mentor of mine, her insights in science and wisdoms about life helped me make it through the toughest times in my graduate studies. Her word "Life is all about balance" will always be remembered.

I would especially like to thank Dr. Kai Li, Dr. Spiros Kambourakis, and Dr. Chad A. Hansen for their helps during the early stages in my graduate studies. Thanks are also due to other current and former group members: Dr. Sunil Chandran, Dr. Jessica Barker, Dr. Dave Knop, Dr. Padmesh Venkitasubramanian, Dr. Jiantao Guo, Dr. Jian Yi, Dr. Dongming Xie, Dr. Jihane Achkar, Ningqing Ran, Mapitso Molefe, Heather Stueben, Wensheng Li, Xiaofei Jia, Justas Jancauskas, Man-Kit Lau, Jinsong Yang, and Kin Sing Stephen Lee for their assistance and pleasant companion.

Finally and heartfully, I would like to thank my parents and my brother for their unconditional love and support. They are the source of inspiration to my journey of life. This thesis is dedicated to them.

TABLE OF CONTENTS

LIST OF FIGURES	XI
LIST OF TABLES	XV
LIST OF ABBREVIATIONS	XVII
CHAPTER ONE	1
INTRODUCTION	1
Metabolic Engineering of The Shikimate Pathway	3
The Shikimate Pathway	
Chemicals Derived from The Shikimate Pathway	6
Aromatic Amino Acids	
Shikimic Acid and Quinic Acid	8
Compounds Accessed via the Intermediacy of 3-Dehydroshikimate	
Titer and Yield Optimization of Escherichia coli Biocatalysts	
Microbial Syntheses of Non-Native Metabolites	
CHAPTER TWO	23
BIOSYNTHESIS OF 3-DEHYDROSHIKIMATE BY RECOMBINANT ESCHE	
COLI USING GLYCEROL AS CARBON SOURCE	
Background	
Theoretical Maximum Yield Analysis for Biosynthesis of 3-Dehydroshikima	
Biocatalysts and Fed-Batch Fermentor Conditions for	
3-Dehydroshikimate Synthesis	29
Common Genetic and Recombinant Elements	
Fed-Batch Fermentor Conditions	
Fed-Batch Fermentor Synthesis of 3-Dehydroshikimate from Glycerol	
Fermentations Employing E. coli KL3 as Host Strain	
E. coli KL3/pKD11.291A	32
E. coli KL3/pKL5.17A	
Fermentations Employing E. coli KL3.21 as the Host Strain	
Isolation of E. coli KL3.21	
E. coli KL3.21/pKD11.291A and E. coli KL3.21/pKL5.17A	
Impact of Glycerol Kinase Overexpression on	11
3-Dehydroshikimate Biosynthesis	44
Discussion and Future Work	
CHAPTER THREE	61
SYNTHESIS OF ADIPIC ACID FROM D-GLUCOSE	
Background	
Microbial Synthesis of cis, cis-Muconic Acid from D-Glucose	
Host Strain Construction	
Overview	
- · · · · · · · · · · · · · · · ·	

Synthesis of the <i>tktAaroZ</i> Cassette	66
Genomic Insertion of the tktAaroZ Cassette into the lacZ Locus of E. of	coli
KL7 to Generate E. coli WN1	68
Plasmid Construction	72
Overview	
Construction of pWN1.162A and pWN1.184A	73
Construction of pWN2.100B	81
Construction of pWN2.248	
Fed-Batch Fermentor Synthesis of cis, cis-Muconic Acid	87
Fed-Batch Fermentor Conditions	
Synthesis of cis, cis-Muconic Acid Using E. coli KL7/pWN1.162A	88
3-Dehydroshikimate Dehydratase Activity	
The Impact of Increased Oxygen Availability on Synthesis of cis, cis-	
Muconic Acid Using E. coli WN1/pWN1.162A	
Catechol 1,2-Dioxygenase Activity	95
Hydrogenation of cis, cis-Muconic Acid to Adipic Acid	99
Discussion and Future Work	99
CHAPTER FOUR	
MICROBIAL SYNTHESIS OF 1,2,4-BUTANETRIOL FROM D-XYLOSE AND I	
ARABINOSE	
Background	
Microbial Synthesis of D- and L-1,2,4-Butanetriol	
Biosynthesis of D-Xylonic Acid and L-Arabinonic Acid	
Overview	
Microbial Synthesis of D-Xylonic Acid	
Microbial Synthesis of L-Arabinonic Acid	
D-Xylonate Dehydratase and L-Arabinonate Dehydratase	
Overview	
Purification of D-Xylonate Dehydratase from P. fragi	
D-Xylonate Dehydratase Activity in E. coli	116
Isolation of Gene Encoding P. fragi (ATCC 4973)	100
L-Arabinonate Dehydratase	120
2-Keto Acid Decarboxylase and Alcohol Dehydrogenase	
Overview	
Screening for Alcohol Dehydrogenase Activity	
Screening for 2-Keto Acid Decarboxylase Activity	
Microbial Synthesis of D- and L-1,2,4-Butanetriol	
Construction of a D-1,2,4-Butanetriol-Synthesizing Microbe	
Construction of an L-1,2,4-Butanetriol-Synthesizing Microbe	
Biosynthesis of D- and L-1,2,4-Butanetriol	148
Directed Evolution of Benzoylformate Decarboxylase to Improve Microbial	1.50
Synthesis of 1,2,4-Butanetriol	
Background	
Directed Evolution of Benzoylformate Decarboxylase Construction of Benzovlformate Decarboxylase Mutant Libraries	
Construction of Denzovitormate Decardoxylase ivitiant Libraries	132

Development of a Screening Method	153
Isolation of Benzoylformate Decarboxylase Mutants	156
Characterization of Selected Mutants	
Discussion and Future Work	162
CHAPTER FIVE	166
EXPERIMENTAL	
General Methods	
Chromatography	
Spectroscopic Measurements	
Bacterial Strains and Plasmids	
Storage of Bacterial Strains and Plasmids	
Culture Medium	
General Fed-Batch Fermentor Conditions	
Analysis of Fermentation Broth	
Genetic Manipulations	
General	
PCR (Polymerase Chain Reaction)	
Determination of DNA Concentration	
Large Scale Purification of Plasmid DNA	
Small Scale Purification of Plasmid DNA	
Purification of Genomic DNA	
Restriction Enzyme Digestion of DNA	
Agarose Gel Electrophoresis	
Isolation of DNA from Agarose	
Treatment of Vector DNA with Calf Intestinal Alkaline Phosphatase.	
Treatment of DNA with Klenow Fragment	
Ligation of DNA	
Preparation and Transformation of Competent Cells	
Enzyme Assays	
General	186
DAHP Synthase	186
Glycerol Kinase	187
Catechol 1,2-Dioxygenase	188
3-Dehydroshikimate Dehydratase	188
Transketolase	
D-Xylonate Dehydratase and L-Arabinonate Dehydratase	189
2-Keto Acid Decarboxylase	190
Alcohol Dehydrogenase	
Protein SDS-PAGE Analysis	
CHAPTER TWO	
Strain Constructions	
E. coli KL3.21	
Plasmid pWN3.062A	
Plasmid pWN3.120A	196
Microbial Synthesis of 3-Dehydroshikimate	196

CHAPTER THREE	196
Strain Constructions	196
E. coli WN1	196
Plasmid pWN1.162A	198
Plasmid pWN1.184A	199
Plasmid pWN2.100B	199
Plasmid pWN2.248	200
Microbial Synthesis of cis, cis-Muconic Acid	
Hydrogenation of cis, cis-Muconic Acid to Adipic Acid	201
CHAPTER FOUR	
Purification of D-Xylonate Dehydratase from	
Pseudomonas fragi (ATCC 4973)	202
Buffers	202
Purification of D-Xylonate Dehydratase	202
Pseudomonas fragi Genomic DNA Library Construction	204
Plasmids	205
Plasmid pWN5.150A	205
Plasmid pWN5.022A	
Plasmid pWN5.284A	206
Plasmid pWN5.238A	206
Plasmid pWN6.186A	
Plasmid pWN6.120A	
Plasmid pWN6.222A	207
Microbial Oxidation of Pentoses	208
Fermentor-Controlled Cultivation Conditions	208
Purification of Fermentation Products	209
Microbial Synthesis of 1,2,4-Butanetriol	210
Fermentor-Controlled Cultivation Conditions	
Analysis of 1,2,4-Butanetriol for Enantiometric Purity	211
Directed Evolution of Benzoylformate Decarboxylase	212
Construction of Benzoylformate Decarboxylase Mutant Libraries	
Error-Prone PCR	213
DNA Shuffling	213
Screening of Benzoylformate Decarboxylase Mutant Libraries	
Biosynthesis of 1,2,4-Butanetriol by E. coli W3110 Expressing W	ild-Type
and Mutant Benzoylformate Decarboxylase	
Purification of Recombinant 6-His Tagged	
Benzoylformate Decarboxylase	216
Analysis of Decarboxylation Product of 3-Deoxy-D,L-glycero-per	
Acid for Enantiomeric Purity	
EFERENCES	220

LIST OF FIGURES

Figure 1. The shikimate pathway in Escherichia coli	.4
Figure 2. Biocatalytic synthesis of aspartame and indigo	.8
Figure 3. Chemical and biocatalytic synthesis of hydroquinone	.9
Figure 4. Chemicals biosynthesized from D-glucose via the intermediacy of 3-dehydroshikimate	10
Figure 5. Chemical and biocatalytic synthesis of vanillin	l 1
Figure 6. In vivo synthesis of E4P in E. coli	14
Figure 7. Metabolic pathways and reactions related to generation and consumption of phosphoenolpyruvate	15
Figure 8. Theoretical flux analysis of carbon flow into the shikimate pathway when glucose is transported using PTS	16
Figure 9. Biosynthesis of poly(3-hydroxybutyrate) (PHB) from glucose by **Ralstonia eutropha** 1	19
Figure 10. Biosynthesis of novel carotenoids 3,4,3',4'-tetradehydrolycopene and torulene in recombinant <i>E. coli</i>	
Figure 11. Metabolism of glycerol by E. coli	24
Figure 12. Biosynthesis of 3-dehydroshikimate by recombinant <i>E. coli</i> using glycerol as the sole carbon source	
Figure 13. Preparation of plasmid pKD11.291A3	34
Figure 14. Biosynthesis of 3-dehydroshikimate under fed-batch fermentor conditions3	17
Figure 15. Preparation of plasmid pKL5.17A3	19
Figure 16. Biosynthesis of 3-dehydroshikimate under fed-batch fermentor conditions4	12
Figure 17. Preparation of plasmid pSK1.171A4	6
Figure 18. Preparation of plamid pWN3.042A4	7
Figure 19. Preparation of plamid pWN3.052A4	8

Figure 20. Preparation of plamid pWN3.062A	49
Figure 21. Biosynthesis of 3-dehydroshikimate under fed-batch fermentor conditions	52
Figure 22. The structures of adipic acid and nylon 6,6	61
Figure 23. Industrial production of adipic acid via cyclohexane as intermediate	62
Figure 24. Solutia benzene-phenol process for adipic acid production	62
Figure 25. Alternatives to synthesize adipic acid from hydrocarbons	63
Figure 26. Synthesis of adipic acid from D-glucose	6 4
Figure 27. Preparation of plasmid pWN1.200A	67
Figure 28. Preparation of plasmid pWN2.038A	70
Figure 29. Preparation of plasmid pWN2.050B	71
Figure 30. Preparation of plasmid pWN1.028A	75
Figure 31. Preparation of plasmid pWN1.079A	76
Figure 32. Preparation of plasmid pWN1.094A	77
Figure 33. Preparation of plasmid pWN1.106A	78
Figure 34. Preparation of plasmid pWN1.162A	79
Figure 35. Preparation of plasmid pWN1.184A	80
Figure 36. Preparation of plasmid pWN2.064A	82
Figure 37. Preparation of plasmid pWN2.084A	83
Figure 38. Preparation of plasmid pWN2.100B	84
Figure 39. Preparation of plasmid pWN2.242A	85
Figure 40. Preparation of plasmid pWN2.248	86
Figure 41. Biosynthesis of <i>cis,cis</i> -muconic acid by <i>E. coli</i> KL7/pWN1.162A under	90

Figure 42.	. Biosynthesis of cis, cis-muconic acid under fed-batch fermentor conditions	92
Figure 43.	Biosynthesis of cis,cis-muconic acid by E. coli WN1/pWN1.162A when oxygen availability was increased	95
Figure 44.	Biosynthesis of cis,cis-muconic acid by E. coli WN1/pWN2.248	97
Figure 45.	Structures of 1,2,4-butanetriol and 1,2,4-butanetriol trinitrate	104
Figure 46.	Current commercial synthesis of 1,2,4-butanetriol	105
Figure 47.	Catalytic hydrogenation of malic acid towards 1,2,4-butanetriol	106
Figure 48.	Chemoenzymatic synthesis of 1,2,4-butanetriol from L-ascorbic acid	107
Figure 49.	Biosynthetic pathway of D- and L-1,2,4-butanetriol	108
Figure 50.	Microbial oxidation of D-xylose and L-arabinose	110
Figure 51.	Synthesis of D-xylonic acid by <i>P. fragi</i> (ATCC 4973)	112
Figure 52.	Synthesis of L-arabino-1,4-lactone and L-arabinonic acid by P. fragi	113
Figure 53.	Catabolism of D-xylonic acid and L-arabinonic acid in <i>P. fragi</i> (ATCC 4973)	115
Figure 54.	NH ₂ -terminal sequences of D-xylonate dehydratase from <i>P. fragi</i> (ATCC 4973)	116
Figure 55.	Catabolism of D-xylose and L-arabinose in E. coli	117
Figure 56.	E. coli catabolism of D-gluconate and D-galactonate	118
Figure 57.	Proposed pathway for E. coli catabolism of D-xylonic acid	119
Figure 58.	Restriction map of the 5.0 kb <i>P. fragi</i> (ATCC 4973) genomic DNA fragmer encoding the L-arabinonate catabolic gene cluster	
Figure 59.	Preparation of plasmid pWN5.150A	126
Figure 60.	The DNA sequence of <i>P. fragi</i> (ATCC 4973) L-arabinonate dehydratase	127
Figure 61.	Chemical synthesis of 3-deoxy-D,L-glycero-pentulosonic acid and D,L-3,4-dihydroxybutanal	129
Figure 62	In vitro reaction of alcohol dehydrogenase	131

Figure 63.	Preparation of plasmid pWN5.238A	136
Figure 64.	Preparation of plasmid pWN6.186A	140
Figure 65.	Preparation of plasmid pWN6.086A	142
Figure 66.	Preparation of plasmid pWN6.120A	144
Figure 67.	Preparation of plasmid pWN6.126A	145
Figure 68.	Preparation of plasmid pWN6.222A	146
Figure 69.	The DNA sequence of an L-arabinonic acid transport protein from <i>P. fragi</i> (ATCC 4973)	147
Figure 70.	Biosynthesis of D-1,2,4-butanetriol by E. coli DH5α/pWN6.186A	148
Figure 71.	Biosynthesis of L-1,2,4-butanetriol by E. coli BL21(DE3)/pWN6.222A	149
Figure 72.	Reaction of Purpald with D,L-3,4-dihydroxybutanal and 3-deoxy-D,L-glycero-pentulosonic aicd	154
Figure 73.	Reaction of Schiff's reagent with D,L-3,4-dihydroxybutanal	155
Figure 74.	1,2,4-Butanetriol production by <i>E. coli</i> W3110 expressing wild-type and mutant benzoylformate decarboxylases	157

LIST OF TABLES

Table 1.	Yields and concentrations of 3-dehydroshikimate and shikimate pathway byproducts synthesized by <i>E. coli</i> KL3/pKD11.291A and <i>E. coli</i> KL3/pKL5.17A cultured on glycerol as the sole source of carbon for 48 h under fermentor-controlled conditions
Table 2.	Yields and concentrations of 3-dehydroshikimate and shikimate pathway byproducts synthesized by <i>E. coli</i> KL3.21/pKD11.291A and <i>E. coli</i> KL3.21/pKL5.17A cultured on glycerol as the sole source of carbon for 48 h under fermentor-controlled conditions
Table 3.	Impact of varying IPTG concentration on glycerol kinase specific activities and cell growth characteristics for <i>E. coli</i> KL3.21/pWN3.062A51
Table 4.	Yields and concentrations of 3-dehydroshikimate and shikimate pathway byproducts synthesized by <i>E. coli</i> KL3.21/pWN3.120A and <i>E. coli</i> KL3.21/pWN3.062A cultured on glycerol as the sole source of carbon for 48 h under fermentor-controlled conditions
Table 5.	Glycerol kinase specific activities of <i>E. coli</i> KL3.21/pWN3.120A and KL3.21/pWN3.062A during cultivation under fermentor-controlled conditions
Table 6.	Comparison of yields and concentrations of biosynthesized 3-dehydroshikimate as a function of strategy employed to increase phosphoenolpyruvate availability
Table 7.	Product and byproducts synthesized by <i>E. coli</i> KL7/pWN1.162A after 48 h of cultivation under fermentor-controlled conditions
Table 8.	Product and byproducts synthesized by E. coli KL7/pWN1.184A and E. coli WN1/pWN1.162A after 48 h of cultivation under fermentor-controlled conditions
Table 9.	DAHP synthase and 3-dehydroshikimate dehydratase specific activities93
Table 10	Product and byproducts synthesized by E. coli WN1/pWN1.162A under modified fed-batch fermentor conditions after 48 h of cultivation
Table 11	. Catechol 1,2-dioxygenase specific activities96
Table 12	2. Product and byproducts synthesized by E. coli WN1/pWN2.248 after 48 h of cultivation under fermentor-controlled conditions98

Table 13	. Purification of P. fragi D-xylonate dehydratase	116
Table 14	. Sub-cloning of 5.0 kb P. fragi (ATCC 4973) genomic DNA fragments	123
Table 15	. L-Arabinonate dehydratase specific activity	125
Table 16	. Annotation of loci in the L-arabinonate catabolic gene cluster	128
Table 17	. Alcohol dehydrogenase activities	131
Table 18	. 2-Keto acid decarboxylase activities	133
Table 19	. E. coli growth characteristic in D-xylonic acid and synthesis of 1,2,4-butanetriol	138
Table 20	. Cultivation of E. coli in medium containing L-arabinonate	143
Table 21	Enantiomeric purity analysis of 1,2,4-butanetriol synthesized in the in vitro enzymatic reactions	
Table 22.	. Characterization of benzoylformate decarboxylase mutants	160
Table 23.	. Kinetic data of wild-type and mutant benzoylformate decarboxylases	161

LIST OF ABBREVIATIONS

ADH alcohol dehydrogenase

Ap ampicillin

ATP adenosine triphosphate

bp base pair

BT 1,2,4-butanetriol

BTX benzene, toluene, xylene

ccMA cis,cis-muconic acid

CIAP calf intestinal alkaline phosphatase

Cm chloramphenicol

DAH 3-deoxy-D-arabino-heptulosonic acid

DAHP 3-deoxy-D-*arabino*-heptulosonic acid 7-phosphate

DEAE diethylaminoethyl

DHAP dihydroxyacetone phosphate

DHQ 3-dehydroquinate

DHS 3-dehydroshikimate

DNA 3-deoxyribonucleic acid

D.O. dissolved oxygen

DTT dithiothreitol

E4P D-erythrose 4-phosphate

1,6-FDP 1,6-fructose diphosphate

F6P D-fructose 6-phosphate

FBR feed back resistant

G3P sn-glycerol 3-phosphate

G6P D-glucose 6-phosphate

GAP D-glyceraldehyde 3-phosphate

GA gallic acid

GRAS generally regard as safe

h hour

His L-histidine

HPLC high pressure liquid chromatography

IPTG isopropyl β-D-thiogalactopyranoside

Kan kanamycin

kg kilogram

LB luria broth

M molar

mg milligram

mL milliliter

μL microliter

mM millimolar

min minute

NAD nicotinamide adenine dinucleotide, oxidized form

NADH nicotinamide adenine dinucleotide, reduced form

NADP nicotinamide adenine dinucleotide phosphate, oxidized form

NADPH nicotinamide adenine dinucleotide phosphate, reduced form

NMR nuclear magnetic resonance

OD optical density

orf open reading frame

PCA protocatechuic acid

PEG polyethylene glycol

PEP phosphoenolpyruvate

PCR polymerase chain reaction

PMSF phenylmethylsulfonyl floride

ppm parts per million

psi pounds per square inch

PTS phosphoenolpyruvate:carbohydrate phosphotransferase systems

R5P D-ribose 5-phosphate

rpm revolutions per minute

rt room temperature

Ru5P D-ribulose 5-phosphate

S7P D-sedoheptulose 7-phosphate

SA shikimate

SDS sodium dodecyl sulfate

SDS-PAGE SDS polyacrylamide gel electrophoresis

TCA cycle tricarboxylic acid cycle

TSP sodium 3-(trimethylsilyl)propionic-2,2,3,3-d₄

UV ultraviolet

X5P D-xylulose 5-phosphate

CHAPTER ONE

INTRODUCTION

Biocatalytic syntheses provide the material basis for the very existence of all living creatures. For thousands of years, humans also have been trying to harness these processes as tools to generate chemicals for our survival, comfort and luxury. In ancient times, biocatalysis was mainly practiced for the production of foods and beverages by employing microorganisms.¹ Some well-known examples include the fermentative conversion of sugars to alcohol and the oxidation of ethanol to vinegar. One interesting case is the production of cheese by enzymatic breakdown of milk proteins, an invention by ancient Greeks dating back to 800 B.C. However, it was not until the late 1800's that enzymes were recognized as the catalytic components in biosynthetic reactions, which was due to the pioneering studies on yeast fermentation conducted by Pasteur, Liebig, and Fischer.² Small-scale productions of amylase and trypsin initiated by the textile and detergent industries in the early 1900's represent the first application of enzyme biotechnology.³ Nevertheless, it was the discovery of microbe-synthesized penicillin by Sir Alexander Fleming in 1928 and its later application as an antibiotic that revolutionized people's view about the value of microbial biosynthetic products.⁴

Biocatalytic conversions attract synthetic chemists for their substrate specificity, high enantio- and regioselectivity, mild reaction conditions, employment of ambient temperatures and pressures, and avoidance of starting materials or intermediates that are toxic or flammable. Microbial cells and enzymes are therefore increasingly being exploited for the production of important chemicals. By the end of the 20th century,

biocatalysis emerged as an important tool in industrial chemical synthesis. Examples include the use of nitrile hydratase in the enzymatic production of acrylamide from acrylonitrile;⁵ microbial synthesis of pharmaceutical intermediates such as the shikimic acid used as the starting material for the manufacture of the antiinfluenza drug Tamiflu;⁶ microbial synthesis of amino acids such as L-lysine; and the use of thermolysin in the manufacture of the low-calorie sweetener aspartame.⁷

An emerging long-term application of biocatalysis entails replacement of hydrocarbons with renewable feedstocks in route to establishing a sustainable chemical industry. Currently, the 1.5 trillion dollar chemical industry is mainly built upon fossil fuels including petroleum, coal and natural gas. Because their formation from biomass takes millions of years, fossil fuels are not renewable in the time frame during which they are currently consumed. On the other hand, terrestrial and marine plants annually fix billions of tons of carbon as biomass, which consists of approximately 25% lignin and 75% carbohydrate polymers (cellulose and hemicellulose). Renewable feedstocks derived from biomass include corn stover and corn fiber, wheat straw, wood residues and sugar cane bagasse.9

This dissertation presents research results for the synthesis of chemicals from several renewable feedstocks through microbe-catalyzed routes. In Chapter 2 of this thesis, shikimate pathway metabolites were synthesized by recombinant *E. coli* strains under fed-batch fermentor conditions. This study explored the possibility of circumventing the in vivo limitation of phosphoenolpyruvate availability by exploiting glycerol as a sole carbon source for microbial growth and metabolism. In Chapter 3 of this thesis, adipic acid was synthesized via the intermediacy of *cis,cis*-muconic acid,

which was microbially synthesized from D-glucose employing recombinant *Escherichia* coli under fed-batch fermentor conditions. Chapter 4 of this thesis examined the synthesis of 1,2,4-butanetriol via the creation of a biosynthetic pathway that is not found in nature. Oxidation of D-xylose or L-arabinose by *Pseudomonas fragi* strain afforded the corresponding sugar carboxylates, which were converted into optically pure D- or L-1,2,4-butanetriol by *Escherichia coli* biocatalysts. Directed evolution was used to improve the catalytic activity of a key enzyme in the created biosynthetic pathway.

Metabolic Engineering of The Shikimate Pathway

A. The Shikimate Pathway

The shikimate pathway is responsible for the biosynthesis of aromatic amino acids and aromatic vitamins in plants and microorganisms, including both bacteria and fungi (Figure 1).¹² The shikimate pathway consists of seven biosynthetic reactions that catalyze the overall conversion of phosphoenolpyruvic acid (PEP) and D-erythrose 4-phosphate (E4P) into chorismic acid. The three aromatic amino acids, L-tryptophan, L-tyrosine, and L-phenylalanine, are synthesized from chorismic acid via three terminal pathways.¹² Chorismic acid is also converted into *p*-hydroxybenzoic acid, *p*-aminobenzoic acid, and 2,3-dihydroxybenzoic acid, which are the precursors for the biosynthesis of, respectively, ubiquinone, folic acid, and enterobactin. Ubiquinone (coenzyme Q) functions in the respiratory chain as an electron transporter, folic acid is a carrier of one-carbon units in biosynthetic reactions, and enterobactin is a chelating agent in bacterial iron uptake.¹³

Figure 1. The shikimate pathway in Escherichia coli. Enzymes (encoding genes) (a) DAHP synthase (aroF, aroG, aroH); (b) DHQ synthase (aroB); (c) DHQ dehydratase (aroD); (d) shikimate dehydrogenase (aroE); (e) shikimate kinase (aroL, aroK); (f) EPSP synthase (aroA); (g) chorismate synthase (aroC). Abbreviations: phosphoenolpyruvate (PEP), D-erythrose 4-phosphate (E4P), 3-deoxy-D-arabino-heptulosonic acid 7-phosphate (DAHP), 3-dehydroquinate (DHQ), 3-dehydroshikimate (DHS), shikimate 3-phosphate (S3P), 5-enolpyruvylshikimate 3-phosphate (EPSP), p-hydroxybenzoic acid (PHB), p-aminobenzoic acid (PABA).

The important biological functions of metabolites derived from the shikimate pathway led to considerable research efforts directed toward pathway elucidation, delineating in vivo pathway regulation, biosynthetic gene identification, and enzymological evaluation of individual biosynthetic enzymes.^{12b,14} The first step of the shikimate pathway (Figure 1), condensation of phosphoenolpyruvate and E4P to yield 3deoxy-D-arabino-heptulosonic acid 7-phosphate (DAHP), is catalyzed by DAHP synthase. 15 Wild-type E. coli produces three feedback inhibition sensitive isozymes, whose in vivo activities are inhibited by tyrosine, phenylalanine, and tryptophan. The corresponding structural genes, aroF, aroG, and aroH, are scattered over the E. coli chromosome. 16 Transcription of the aroF and aroG genes is also regulated by a global regulatory protein, TyrR. In vitro analysis of pure DAHP synthase indicates they are metallo proteins, while the metal requirement can be satisfied by several divalent cations, including Fe²⁺ and Zn²⁺. The second step of the shikimate pathway (Figure 1) is the cyclization of DAHP to generate 3-dehydroquinate, which is catalyzed by aroB-encoded 3-dehydroquinate synthase in E. coli. This conversion proceeds through a sequence of reactions, including oxidation, elimination, reduction, ring opening, and intramolecular aldol condensation. This reaction requires catalytic NAD, which is tightly bound in the active site of 3-dehydroquinate synthase. 18 The third step in the shikimate pathway (Figure 1) involves the dehydration of 3-dehydroquinate to form 3-dehydroshikimate. The aroD-encoded E. coli 3-dehydroquinate dehydratase catalyzes the syn elimination of water from 3-dehydroquinate.¹⁹ The fourth step in the shikimate pathway (Figure 1) is the reduction of 3-dehydroshikimate to shikimate. In E. coli, this reaction is catalyzed by an NADP-dependent shikimate dehydrogenase, encoded by the aroE gene. 20 Shikimate

kinase catalyzes the fifth reaction of the shikimate pathway (Figure 1), which is the transfer of a phosphoryl group from ATP to shikimate to yield shikimate 3-phosphate (S3P). *E. coli* genes *aroK* and *aroL* encode two corresponding shikimate kinase isozymes, while the transcription of *aroL* is controlled by both TyrR and TrpR repressor proteins. In the sixth step of the shikimate pathway (Figure 1), shikimate 3-phosphate further condenses with phosphoenolpyruvate to yield 5-enolpyruvylshikimate 3-phosphate (EPSP) and inorganic phosphate. *E. coli* EPSP synthase encoded by *aroA* locus catalyzes this reversible reaction. The final step in the shikimate pathway (Figure 1) involves the *trans* 1,4-elimination of phosphate from EPSP to yield chorismate. Chorismate synthase encoded by the *aroC* gene catalyzes this reaction in *E. coli*. The first two crystal structures of chorismate synthase (from *Streptococcus pneumoniae* and *Saccharomyces cerevisiae*) were solved recently. These data should provide valuable information to help resolve questions related to the catalytic mechanism of this enzyme.

The absence of the shikimate pathway in animals has led to the targeting of enzymes in this pathway for inhibition in route to the development of new nontoxic herbicides and antibiotics.²⁶ One example is the successful marketed broad-spectrum herbicide, glyphosate (N-phosphonomethylglycine), which inhibits EPSP synthase as a competitive inhibitor with respect to binding of phosphoenolpyruvate at this enzyme's active site.²⁷

B. Chemicals Derived from the Shikimate Pathway

Presently, the benzene, toluene, xylene (BTX) fraction of petroleum refining is the major source of aromatic building blocks required for the synthesis of both aromatic and non-aromatic industrial chemicals.²⁸ As a consequence, the prices of these compounds reflect global petroleum pricing and availability. As nature's predominant route for the biosynthesis of primary aromatic metabolites, the shikimate pathway might likewise serve as a route for the biocatalytic manufacture of industrial aromatic chemicals. Biocatalytic syntheses of aromatic and nonaromatic compounds via the shikimate pathway might thus provide alternatives to existing industrial manufacturing processes. Furthermore, the multiple stereocenters in the intermediates of the shikimate pathway can be exploited as valuable chiral synthons. In this section, examples are presented of industrial and academic exploitation of the shikimate pathway for the synthesis of value-added chemicals.

Aromatic Amino Acids

Currently, the aromatic amino acids L-phenylalanine and L-tryptophan are mainly manufactured through microbial fermentations.²⁹ Bacteria including *Corynebacterium*, *Brevibacterium* and *Escherichia* species are among the reported host strains.³⁰ The U.S. market for L-phenylalanine is estimated to be 3.2 × 10⁶ kg for 2004.³⁰ L-Phenylalanine is used in the manufacture of the low-calorie sweetener aspartame, which is also referred to by the trade names of NutraSweet and EQUAL. Industrial synthesis of aspartame relies upon the thermolysin-catalyzed dipeptide formation between protected aspartate and phenylalanine (Figure 2).³¹ L-Tryptophan is mainly used as a livestock feed additive. Expression of tryptophanase and naphthalene dioxygenase in a tryptophan-synthesizing *E. coli* strain resulted in a biocatalyst capable of converting D-glucose into indigo dye (Figure 2).³²

Figure 2. Biocatalytic synthesis of aspartame and indigo. (a) thermolysin; (b) hydrogenation; (c) tryptophanase; (d) naphthalene dioxygenase; (e) spontaneous dehydration and oxidation.

Shikimic Acid and Quinic Acid

Shikimic acid is the starting material for the synthesis of the neuraminidase inhibitor Tamiflu, which is an antiinfluenza drug currently marketed by Roche. The traditional source of shikimic acid is the fruit of *Illicium* plants, which is commonly known as the anise tree. Currently, shikimic acid is produced from D-glucose under fermentation conditions employing a genetically engineered *E. coli* biocatalyst that lacks shikimate kinase activity. The first reported shikimate-producing *E. coli* biocatalyst synthesized a maximum of 27 g/L shikimic acid in a 1 L cell culture. After genetic and fermentation process modifications, *E. coli* strains and culture conditions are now available that can lead to biosynthesis of 71-84 g/L concentrations of shikimic acid. Shikimic acid thus provides an example of how microbial synthesis can be used to increase the availability of a relatively scarce or difficult-to-isolate natural product derived from plants.

Figure 3. Chemical and biocatalytic synthesis of hydroquinone. (a) shikimate dehydrogenase; (b) $Ag_3PO_4/K_2S_2O_8$; (c) HOCl; (d) heat.

Quinic acid, which is currently isolated from *Cinchona* bark, is a widely used chiral starting material in organic synthesis. This hydroaromatic has also been identified as a byproduct synthesized by shikimate-producing biocatalysts. Its formation has been attributed to the catalytic promiscuity of shikimate dehydrogenase, which in addition to catalyzing the reduction of 3-dehydroshikimate, can also catalyze the reduction of 3-dehydroquinate to quinic acid. High-titer, high-yielding microbial syntheses of quinic acid have subsequently been established based on overexpression of shikimate dehydrogenase in 3-dehydroquinate-synthesizing *E. coli* strains. Although quinic acid is not currently involved in any industrial process, research in the Frost group has demonstrated its potential application in hydroquinone production. As a pseudocommodity chemical mainly used for photographic developing, the approximate 4.5×10^7 kg/yr production of hydroquinone is derived from aniline, phenol, and *p*-diisopropylbenzene, which are all manufactured from benzene. Quinic acid in partially

purified fermentation broth was readily converted into hydroquinone employing HOCl or Ag₃PO₄/K₂S₂O₈ (Figure 3).

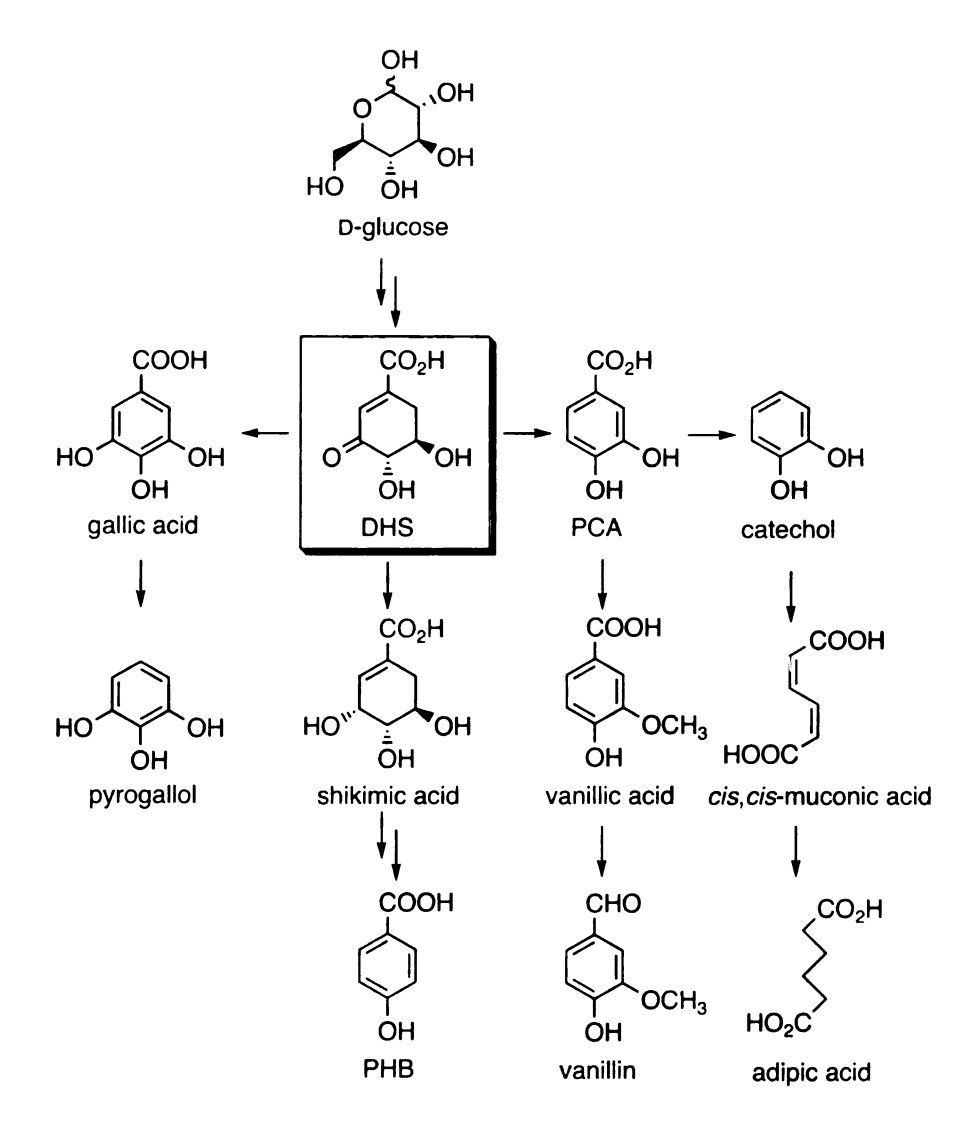


Figure 4. Chemicals biosynthesized from D-glucose via the intermediacy of 3-dehydroshikimate. Abbreviations: 3-dehydroshikimate (DHS), protocatechuic acid (PCA), p-hydroxybenzoic acid (PHB).

Compounds Accessed via the Intermediacy of 3-Dehydroshikimate

3-Dehydroshikimate is a hydroaromatic molecule with potent antioxidant activity.³⁶ It also serves as an intermediate in the microbial biosynthesis of shikimic acid,⁶ gallic acid,³⁷ pyrogallol,^{37a} p-hydroxybenzoic acid,³⁸ protocatechuic acid, catechol,³⁹

cis,cis-muconic acid,^{10,106} and vanillic acid⁴⁰ (Figure 4). Some of these compounds, such as p-hydroxybenzoic acid and catechol, are essential building blocks of the chemical industry. Some of these compounds could be converted into more valuable molecules through chemical or enzymatic reactions. The enzymatic conversion of vanillic acid to vanillin is an intriguing example.

Figure 5. Chemical and biocatalytic synthesis of vanillin. Abbreviations: 3-dehydroshikimate (DHS), protocatechuic acid (PCA).

Vanillin is one of the most important aromatic flavor compounds used in foods, beverages, perfumes, and pharmaceuticals. Due to the limited availability of its natural source, which is the beans of the orchid *Vanilla planifolia*, the annual production of more than 1.0×10^7 kg of vanillin is mainly through chemical synthesis. Currently, the dominant industrial process (Figure 5) employs catechol as starting material, which is manufactured from phenol. The increasing worldwide demand for natural vanillin flavor promotes research into biocatalytic transformation of renewable feedstocks into vanillin. Microbial synthesis of vanillin has been achieved by manipulation of the

shikimate pathway (Figure 5).⁴⁰ Heterologous expression of the *Klebsiella pneumoniae* 3-dehydroshikimate dehydratase (AroZ) and rat-liver catechol-*O*-methyltransferase (COMT) in an *E. coli* biocatalyst lacking shikimate dehydrogenase activity resulted in the conversion of 3-dehydroshikimate into vanillic acid via the intermediacy of protocatechuic acid. Under fed-batch fermentor conditions, *E. coli* KL7/pKL5.96A synthesized 5.0 g/L of vanillic acid from D-glucose when the culture was supplemented with L-methionine. Vanillic acid was subsequently reduced to vanillin in 91% yield using aryl aldehyde dehydrogenase that was partially purified from *Neurospora crassa*. The biosynthetic route developed for converting glucose into vanillin (Figure 5) differs from all the other biosynthetic routes previously developed for the synthesis of vanillin. It is also the only known method to produce vanillin from abundant and inexpensive D-glucose.

C. Titer and Yield Optimization of Escherichia coli Biocatalysts

Although biosynthetic processes that rely on renewable feedstocks have the advantage of sustainability, their industrial applications require cost competitiveness relative to current chemical processes. Therefore, biocatalytic conversions that lead to high concentrations and high yields of products are desirable. Microbes are frequently capable of altering gene expression and enzyme activity to ensure their survival under a variety of environmental conditions. However, these metabolic configurations are not necessarily optimal for synthesis of chemicals. Modification of cell metabolism is usually required to redirect metabolic activity for overproducing desired chemicals. Metabolic engineering of the shikimate pathway in *E. coli* has focused on elimination of

•

•

enzymes and pathways consuming the final product, increasing the catalytic activity of rate-limiting enzymes, and improving the in vivo availability of substrates for key biosynthetic reactions.

Early attempts to increase productivity of aromatic amino acid-synthesizing E. coli biocatalysts were limited to overexpression of enzymes in terminal biosynthetic pathway and elimaination of product-degrading pathways.⁴² However, minor successes resulting from these strategies indicated the need for manipulation of central E. coli metabolism to increase carbon flow directed into the shikimate pathway. The initial factor limiting the flow of carbon directed into aromatic amino acid biosynthesis has been shown to be the in vivo catalytic activity of DAHP synthase, the first enzyme in the common pathway. To eliminate the inhibition of the three DAHP synthase isozymes (AroF, AroG, and AroH) by aromatic amino acids, feedback insensitive (FBR) mutants were generated.⁴³ Overexpression of an AroF^{FBR} enzyme together with several other biosynthetic proteins led to an E. coli biocatalyst that produced 52 g/L L-phenylalanine when cultured under fermentor-controlled conditions.⁴⁴ Further increases in aroF^{FBR} encoded DAHP synthase activity have been achieved by relieving its transcriptional repression imposed by the promoter-binding repressor protein, TyrR. Strategies designed for this purpose include the use of a host strain that does not express TyrR repressor, 12b plasmid-localization of two aroFFBR genes, inclusion of extra TyrR-binding regions on the plasmid, and switching the transcriptional control of the aroF gene to a promoter not regulated by TyrR.⁴⁵ Successful application of the last three strategies resulted in three E. coli strains that synthesized twofold higher concentrations of 3-dehydroshikimate relative to a strain with a single plasmid-localized aro F^{FBR} gene.⁴⁵

However, DAHP synthase activity can eventually reach a level where additional increases in activity do not translate into improved synthesis of aromatic amino acids or their biosynthetic precursors. In 1990, Frost and coworkers published the first work indicating that in vivo E4P availability could limit increased carbon flow directed into the shikimate pathway even with amplified expression levels of DAHP synthase. E4P is a four-carbon aldose phosphate serving as a precursor in both the shikimate pathway and the biosynthesis of pyridoxal 5-phosphate. In wild-type *E. coli*, E4P is synthesized through three enzymatic reactions, which are catalyzed by transketolase (encoded by *tktA* or *tktB*) and transaldolase (encoded by *talA* or *talB*) (Figure 6). Overexpression of either transketolase or transaldolase was proven to be an effective method for increasing both the concentration and yield of biosynthesized shikimate pathway metabolites. For example, amplified expression of *tktA*-encoded transketolase in *E. coli* strain containing

Figure 6. In vivo synthesis of E4P in E. coli. Enzymes (encoding genes) (a) transketolase (tktA, or tktB); (b) transaldolase (talA, or talB).

the $aroG^{FBR}$ gene led to a twofold increase in the carbon flow directed into the shikimate pathway.^{43b}

As another precursor of the shikimate pathway, the intracellular availability of phosphoenolpyruvate has been a subject of intense research interests. Phosphoenolpyruvate is a direct product of glycolysis and serves multiple biological functions in *E. coli* (Figure 7). Conversion of phosphoenolpyruvate to oxaloacetate catalyzed by phosphoenolpyruvate carboxylase is an anaplerotic reaction responsible for replenishment of the C₄-dicarboxylic acid pool. Phosphoenolpyruvate could also be converted to pyruvate through a pyruvate kinase-catalyzed reaction. Most importantly, phosphoenolpyruvate is the cosubstrate in the phosphoenolpyruvate:carbohydrate phosphotransferase system (PTS), which brings carbohydrate molecules, such as glucose and fructose, into *E. coli* cells through a group translocation mechanism. For every

Figure 7. Metabolic pathways and reactions related to generation and consumption of phosphoenolpyruvate. (a) phosphoenolpyruvate:carbohydrate phosphotransferase system; (b) pyruvate kinase; (c) phosphoenolpyruvate synthase; (d) phosphoenolpyruvate carboxylase; (e) DAHP synthase; (f) pyruvate dehydrogenase; (g) citrate synthase.

1. 47.

N

35

.

λ.

ĵ.;

.

1911年11日 11日 11日

molecule of sugar transported and phosphorylated, one phosphoenolpyruvate molecule is converted to pyruvate.

Strategies for improving phosphoenolpyruvate availability by blocking phosphoenolpyruvate consumption using *E. coli* mutants without phosphoenolpyruvate carboxylase or pyruvate kinase activity led to a modest increase in aromatic amino acid biosynthesis. It was later recognized that PTS-mediated glucose transport is the major consumer of phosphoenolpyruvate. Based on a stoichiometric analysis, the theoretical yield of shikimate pathway products synthesized by *E. coli* biocatalyst is 43% (mol/mol) when glucose is provided as the sole carbon source (Figure 8). However, if phosphoenolpyruvate consumption in the carbohydrate transport process could be recovered or circumvented, the theoretical yield becomes 86% (mol/mol). 45, 49a

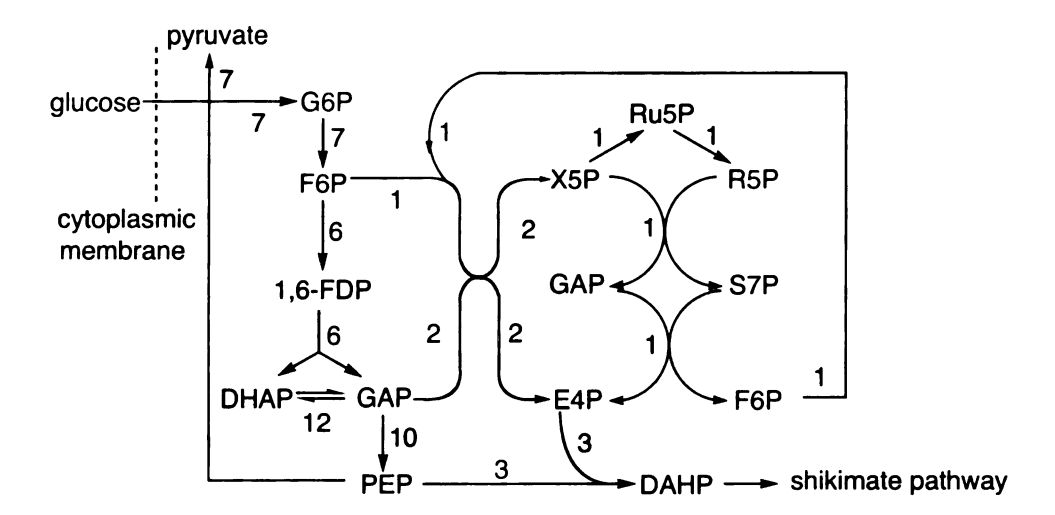


Figure 8. Theoretical flux analysis of carbon flow into the shikimate pathway when glucose is transported using PTS. The numbers represent the fluxes required to convert 7 mol of glucose into DAHP. Abbreviations: glucose 6-phosphate (G6P), fructose 6-phosphate (F6P), 1,6-fructose diphosphate (1,6-FDP), dihydroxyacetone phosphate (DHAP), glyceraldehyde 3-phosphate (GAP), ribulose 5-phosphate (Ru5P), xylulose 5-phosphate (X5P), ribose 5-phosphate (R5P), sedoheptulose 7-phosphate (S7P), phosphoenolpyruvate (PEP), D-erythrose 4-phosphate (E4P), 3-deoxy-D-arabino-heptulosonic acid 7-phosphate (DAHP).

One solution to relieve the phosphoenolpyruvate limitation is to express ppsencoded phosphoenolpyruvate synthase, which catalyzes the reaction of ATP with pyruvate to form phosphoenolpyruvate, AMP, and inorganic phosphate.⁴⁹ Work combining this phosphoenolpyruvate recycling strategy with amplified expression of $aroF^{FBR}$ and tktA resulted in an E. coli strain that synthesized shikimate pathway metabolites in a yield of 51% (mol/mol) utilizing glucose as the sole carbon source.⁵⁰ The phosphoenolpyruvate consumption by the PTS system could also be avoided by replacing the PTS system with phosphoenolpyruvate-independent glucose transport systems. In 1994, Ingram and coworkers successfully expressed the Zymomonas mobilis glucose facilitator (encoded by glf) and glucose kinase (encoded by glk) in an E. coli pts mutant.⁵¹ Following Glf-mediated facilitated diffusion of glucose, subsequent phosphorylation of glucose in the cytoplasm was catalyzed by Glk. This resulted in the expenditure of one ATP per transported glucose molecule, while phosphoenolpyruvate was not expended. Alternatively, the combined activities of E. coli galP-encoded galactose permease and Zymomonas mobilis glk-endoded glucose kinase were also recruited to replace PTS-mediated glucose transport.⁵² Independent implementation of these two glucose transport systems in E. coli attendant with amplified expression of feedback-insensitive DAHP synthase and transketolase resulted in total yields of 3dehydroshikimate and shikimate pathway byproducts synthesized from glucose of 41-43% (mol/mol).⁵³ The third strategy for avoiding the competition between the starting material transport system and the shikimate pathway for intracellular phosphoenolpyruvate is to use starting materials that do not rely on a PTS system for transport. For example, D-xylose and L-arabinose are transported into the E. coli

cytoplasm by high-affinity permeases. Therefore, for every molecule of D-xylose or L-arabinose transported, one mole of ATP is consumed. Use of D-xylose or L-arabinose as the starting materials in *E. coli* biosynthesis of 3-dehydroshikimate led to a total yield of 3-dehydroshikimate and shikimate pathway byprodcuts ranging from 45-47% (mol/mol).⁵⁴

Microbial Syntheses of Non-Native Metabolites

Traditionally, microbial syntheses are established and improved using extensive screening for microorganisms that synthesize the desired compounds in high concentration and/or yield. Whereas this approach has been reasonably successful, the type of compound synthesized has been typically restricted to molecules that are part of a given microbe's natural metabolism. Owing to the developments in areas such as molecular biology, genomics, metabolic engineering and protein engineering, microbes can now be manipulated to synthesize non-native metabolites. Biosynthetic pathways designed for this purpose can be divided into two categories based on the origins of enzymatic reactions involved: naturally existing biosynthetic pathways and artificially assembled biosynthetic pathways.

Expression of a naturally existing biosynthetic pathway in a heterologous host strain may be preferred for variety of reasons such as growth properties and the availability of genetic engineering procedures for the host strain. An intriguing example is from the current efforts directed toward the large-scale production of polyhydroxyalkanoates. Polyhydroxyalkanoates are biodegradable polymers that have similar material properties as conventional petrochemical-derived polymers.⁵⁵ Although

polyhydroxyalkanoates could be biosynthesized from renewable resources by a variety of bacteria (Figure 9), their current production employs the recombinant non-natural producer, *Escherichia coli*. As compared to natural polyhydroxyalkanoates producers, such as *Ralstonia eutropha* and *Alcaligenes latus*, *E. coli* grows faster and reaches a higher cell density when cultured in a fermentor. Readily available information concerning metabolism and genetic regulation along with the availability of genetic engineering techniques for *E. coli* cells allows for genetic manipulation in route to achieving improved performance of this microbe. One *E. coli* polyhydroxyalkanoates-producing construct is able to synthesize 157 g/L of polyhydroxyalkanoate representing 77% of the cell dry weight in 49 h. 55b Furthermore, because *E. coli* cells are more fragile than microbes that naturally produce polyhydroxyalkanoates, product purification avoids complicated extraction steps.

Figure 9. Biosynthesis of poly(3-hydroxybutyrate) (PHB) from glucose by *Ralstonia eutropha*. Enzymes (encoding genes) (a) β -ketothiolase (phbA); (b) acetoacetyl CoA reductase (phbB); (c) poly(3-hydroxybutyrate) polymerase (phbC).

The rationale for creating biosynthetic pathways is to expand the repertoire of microbially synthesized molecules by recruiting enzymatic reactions that do not naturally

coexist in any single microbe. Microorganisms, plants and animals are capable of synthesizing immense variety of metabolites from carbon sources such as CO₂ and D-glucose. Certain microorganisms are also capable of degrading various synthetic chemicals to generate catabolic intermediates with unique structures. If each metabolite were considered as a point, and enzymes that catalyze the bioconversions between these metabolites were considered as the lines connecting them, we could envision a network that represents the sum total of anabolic and catabolic pathways found in nature. Within this network, biosynthetic pathways can be rewired, and microbial biocatalysts can be developed to synthesize metabolites that are not native to a given microbe. Additionally, many enzymes accept nonnative substrates, ⁵⁶ and protein engineering techniques such as directed evolution and rational design can further broaden the substrate specificity of enzymes as well as increase the catalytic activity of enzymes towards nonnative substrates. Novel biosynthetic routes can therefore be created for microbial synthesis of molecules that are not found in nature.

Carotenoids are natural pigments synthesized by plants and microorganisms. They make up a diverse group of polyene molecules that are of interest as pharmaceuticals and food additives. The sale of carotenoids as food and feed supplements is estimated to be approximately 5×10^8 /yr. Discoveries that carotenoids have antioxidant activity and tumor repression activity has further boosted their pharmaceutical potential. Functional carotenoid pathways have been established in non-carotenogenic *E. coli* by utilizing the biosynthetic precursor generated from the *E. coli* isoprenoid biosynthesis pathway in combination with the expression of carotenoid biosynthetic genes from several natural carotenoid producers. To expand the structural

Figure 10. Biosynthesis of novel carotenoids 3,4,3',4'-tertradehydrolycopene and torulene in recombinant E. coli. (a) E. coli nonmevolonate pathway; (b) E. coli isoprenoid biosynthesis pathway; (c) geranyl geranylpyrophosphate synthase; (d) phytoene synthase; (e) phytoene desaturase; (f) evolved phytoene desaturase I14; (g) evolved lycopene cyclase, Y2. Abbreviations: glyceraldehyde 3-phosphate (G3P); isopentenyl diphosphate (IPP); dimethylallyl diphosphate (DMPP). Nonnatural carotenoids molecule are marked with •.

diversity of carotenoids biosynthesized by *E. coli*, both combinatorial biosynthesis and molecular evolution strategies have been applied. Albrecht and coworkers demonstrated the biosynthesis of novel hydroxycarotenoids through a combinatorial approach.^{61b} By

4. ¥... 3.3 3. ٠٠٠٠ د روه coexpressing three different carotenoid desaturases together with a carotenoid hydratase, a cyclase, and a hydroxylase in *E. coli*, they synthesized four novel acyclic carotenoids with improved antioxidative properties. In a separate study, Schmidt-Dannert and coworkers evolved mutant phytoene desaturases and lycopene cyclases using DNA family shuffling.⁶² When these mutant enzymes were expressed in carotenoid-synthesizing *E. coli*, novel structures including fully conjugated carotenoid 3,4,3',4'-tetradehydrolycopene and cyclic carotenoid torulene were synthesized (Figure 10).

CHAPTER TWO

BIOSYNTHESIS OF 3-DEHYDROSHIKIMATE BY RECOMBINANT ESCHERICHIA COLI USING GLYCEROL AS CARBON SOURCE

Background

Choice of starting material is a critical issue in microbial syntheses of commercial chemicals. Cost, availability, and the efficiency with which a carbon source can be converted to product are major factors that determine the commercial viability of a microbial synthesis. Due to the abundance of the feedstock from which it is derived and the well-developed processing techniques for its isolation and purification, ⁶³ D-glucose derived from corn starch is the dominant carbon source used for current microbecatalyzed chemical syntheses. However, a yield limitation exists when glucose is used as the starting material for syntheses catalyzed by E. coli. Wild-type E. coli cells utilize the phosphoenolpyruvate:carbohydrate phosphotransferase system (PTS) to transport glucose into their cytoplasm from the culture medium.⁶⁵ Transport and phosphorylation of each molecule of glucose catalyzed by the PTS system consumes one phosphoenolpyruvate molecule, which is converted into pyruvate and further oxidized through the TCA cycle into CO₂. Based on stoichiometric analysis, the maximum theoretical yield for the conversion of glucose into the shikimate pathway metabolite 3dehydroshikimate is 43% (mol/mol).⁶⁴ As discussed in Chapter 1, one solution to avoid generating pyruvate is to use a carbon source whose transport into the cytoplasm is not mediated by the PTS system. Pentose carbon sources such as D-xylose and L-arabinose are transported into the cytoplasm of E. coli by ATP-driven high-affinity permease systems. 66 As a consequence, the maximum theoretical yield for the biosynthesis of the

shikimate pathway metabolite 3-dehydroshikimate from pentoses is 71% (mol/mol).^{64b} D-Xylose and L-arabinose are derived from hemicellulose, which typically constitutes 10-35% of plant biomass.⁶⁷ The Frost group has demonstrated the biosynthesis of 3-dehydroshikimate by *E. coli* using xylose or arabinose individually and as a 3/3/2 molar mixture of glucose, xylose, and arabinose.⁶⁸ The carbohydrate mixture is used to approximate the composition of corn fiber, an inexpensive byproduct of wet milling.⁶⁹ Yields for the microbial synthesis of 3-dehydroshikimate and shikimate pathway byproducts ranged from 44-47% when pentoses were used as starting materials.⁶⁸

Figure 11. Metabolism of glycerol by $E.\ coli.$ Enzymes (encoding genes) (a) glycerol facilitator (glpF); (b) glycerol kinase (glpK); (c) G3P dehydrogenase (glpD); (d) triose phosphate isomerase (tpiA); (e) fructose 1,6-diphosphate aldolase (fsaA, or fbaA); (f) fructose 1,6-diphosphatase (fbp, or glpX). Abbreviations: glycerol 3-phosphate (G3P), dihydroxyacetone phosphate (DHAP), glyceraldehyde 3-phosphate (GAP), 1,6-fructose diphosphate (1,6-FDP), fructose 6-phosphate (F6P).

In contrast to glucose and pentoses, glycerol enters the *E. coli* cytoplasm by facilitated diffusion across the cytoplasmic membrane (Figure 11).⁶⁶ The *glpF*-encoded facilitator protein provides a channel for energy-independent diffusion of glycerol

molecules into the *E. coli* cytoplasm. Glycerol is phosphorylated in the cytoplasm by the *glpK*-encoded glycerol kinase with the expenditure of ATP to form *sn*-glycerol 3-phosphate. Under aerobic conditions, the *glpD*-encoded glycerol 3-phosphate dehydrogenase oxidizes *sn*-glycerol 3-phosphate into dihydroxyacetone phosphate, which is catabolized via glycolysis. Therefore, glycerol theoretically should not suffer the yield limitation associated with PTS-driven glucose utilization. In this chapter, the use of glycerol as the starting material for microbial synthesis of 3-dehydroshikimate is examined utilizing *Escherichia coli* biocatalysts cultured under fed-batch fermentor conditions.

Figure 12. Biosynthesis of 3-dehydroshikimate by recombinant E. coli using glycerol as the sole carbon source. Enzymes (encoding genes) (a) DAHP synthase $(aroF^{EBR})$; (b) 3-dehydroquinate synthase (aroB); (c) 3-dehydroquinate dehydratase (aroD); (d) shikimate dehydrogenase (aroE). Abbreviations: phosphoenolpyruvate (PEP), Derythrose 4-phosphate (E4P), 3-deoxy-D-arabino-heptulosonic acid 7-phosphate (DAHP), 3-dehydroquinate (DHQ), 3-dehydroshikimate (DHS).

į
;
i
5
B
;
;
4
ς.

The Frost group has been using the biosynthesis of 3-dehydroshikimate as a model system to study the impact of different substrate transport mechanisms on microbial synthesis of shikimate pathway metabolites.^{68,72} 3-Dehydroshikimate is the most advanced precursor common to the synthesis of industrially synthesized bioproducts (L-phenylalanine, ^{73a} L-tryptophan, ^{73b} and shikimic acid⁶) as well as the reported synthesis of commodity chemicals (adipic acid, ^{10,106} phenol ^{73c}), pseudocommodity chemicals (catechol, ³⁹ *p*-hydroxybenzoic acid ³⁸), fine chemicals (vanillin, ⁴⁰ indigo ³²) and ultrafine chemicals (gallic acid, ³⁷ pyrogallol ^{37a}). Strategies developed to improve the concentration and yield of 3-dehydroshikimate synthesized from glycerol could be applied to syntheses of the various molecules derived from 3-dehydroshikimate.

Glycerol metabolism in $E.\ coli$ is regulated at both the transcriptional level and the protein level. Genes that comprise the glp regulon encode enzymes involved in the utilization of glycerol in $E.\ coli$. A constitutively expressed protein encoded by glpR represses the transcription of other genes of the glp regulon in the absence of the inducer molecule, sn-glycerol 3-phosphate. As with other inducible catabolic pathways, the induction of the glp system in $E.\ coli$ mutants with an impaired PTS system is severely impeded because of cAMP deficiency and the inability to accumulate sn-glycerol 3-phosphate. Glycerol kinase activity controls the overall rate of glycerol utilization by $E.\ coli$ cells. This enzyme is subjected to noncompetitive allosteric inhibition by fructose 1,6-biphosphate and the nonphosphorylated form of enzyme III^{Glc} in the PTS system.

Glycerol is currently produced as a byproduct by the oleochemical industry and the rapidly growing biodiesel industry.⁷⁷ It is becoming increasingly attractive as an alternative starting material derived from renewable feedstock. Microbial syntheses of

<u>:</u>}: دد. دده . . ŀ. 3. $i\lambda$...

in:

ا الما

Ŭ.

.

30.

chemicals including 1,3-propanediol⁷⁸ and succinic acid⁷⁹ from glycerol have been demonstrated. Although the current cost and availability of glycerol may be prohibitive for the syntheses of commodity and psuedocommodity chemicals, it could be attractive for certain small volume, high value chemicals such as shikimic acid. More importantly, understanding the impact of varying transport mechanisms attendant with varying feedstocks and starting materials may lead to strategies that are more broadly applicable to the syntheses of the variety of chemicals derived from 3-dehydroshikimate.

Theoretical Maximum Yield Analysis for Biosynthesis of 3-Dehydroshikimate

The different transport mechanisms utilized by $E.\ coli$ cells for D-glucose, D-xylose, L-arabinose, and glycerol are reflected in the different theoretical maximum yields of 3-dehydroshikimate synthesized from these individual starting materials. A stoichiometric analysis method was used to determine the theoretical maximum yield for the synthesis of 3-dehydroshikimate from glucose and pentoses using $E.\ coli$ as the biocatalyst.⁶⁴ This calculation is built upon the assumption that the branching pathways are blocked and the carbon flow is directed by the most efficient pathways with minimum loss to CO_2 and other metabolites.

PEP + E4P 2 H ₃ PO ₄ + H ₂ O + DHS	Eq. 1
x glucose ——► PEP + E4P + x pyruvic acid	Eq. 2a
x 6 (C)	Eq. 2b
x pentose ——► PEP + E4P	Eq. 3a
x 5 (C) → 3 (C) + 4 (C)	Eq. 3b
x glycerol ——► PEP + E4P	Eq. 4a
x 3 (C)	Eq. 4b

Taking the theoretical yield determination for use of glucose as the starting material as an example, the calculation begins with balancing the phosphoenolpyruvate and E4P inputs with the 3-dehydroshikimate and other byproducts outputs (Eq. 1). The phosphoenolpyruvate and E4P are then equated to the amount of D-glucose required for the formation of these substrates (Eq. 2a). A pyruvate acid term is included in Eq. 2a to reflect the generation of pyruvate as a byproduct during the transport of glucose by PTS system. To balance the number of carbon atoms in glucose with the total number of carbon atoms in phosphoenolpyruvate, E4P, and pyruvate, a coefficient is determined (Eq. 2b), which leads to a maximum theoretical yield of 43% (mol of 3dehydroshikimate/mol of glucose) for microbial synthesis of 3-dehydroshikimate from glucose. Similar calculations (Eq. 3b and Eq. 4b) result in a maximum theoretical yield of 71% (mol of 3-dehydroshikimate/mol of pentoses) for microbial synthesis of 3dehydroshikimate from pentoses and 43% (mol of 3-dehydroshikimate/mol of glycerol) for microbial synthesis of 3-dehydroshikimate from glycerol. Because the results in the above calculations are expressed as the formation of 3-dehydroshikimate from each mol of starting material, the differences in the number of carbon atoms in a starting material molecule are not taken into consideration. As a consequence, direct comparison of the calculated theoretical maximum yields for different starting materials do not reflect the efficiency of carbon utilization. To solve this problem, the results from the previous calculations are normalized by representing the theoretical maximum yield using the formation of 3-dehydroshikimate per mol of C in glucose, xylose, arabinose, or glycerol (Eq. 5). Following Eq. 5, the theoretical maximum yield is 7.2% for glucose, 14.3% for xylose, 14.3% for arabinose, and 14.3% for glycerol. In the case of glucose, PTS-

generated pyruvate is considered to be the carbon source required for the generation of E. coli cellular biomass. However, when pentoses or glycerol was used as the sole carbon source, some of the carbon sources must be diverted to biomass production. As a result, the calculated yield must be considered to be the upper limit for the theoretical maximum yield for pentoses and glycerol.

Biocatalysts and Fed-Batch Fermentor Conditions for 3-Dehydroshikimate Synthesis

A. Common Genetic and Recombinant Elements

 $E.\ coli$ biocatalysts employed in 3-dehydroshikimate synthesis shared several genetic and recombinant traits including a mutationally inactivated genomic aroE locus, a second copy of the aroB gene inserted into the genomic serA locus, and plasmid-localized serA, $aroF^{FBR}$ and P_{aroF} . The KL3 host strain was derived from $E.\ coli$ AB2834, a strain that lacks the ability to express catalytically active shikimate dehydrogenase due to a mutated genomic aroE locus. As a result, 3-dehydroshikimate, the substrate of shikimate dehydrogenase, is exported into the culture supernatant. Aromatic amino acids (L-phenylalanine, L-tyrosine, and L-tryptophan) and aromatic vitamins (p-aminobenzoic acid, p-hydroxybenzoic acid, and 2,3-dihydroxybenzoic acid) are added to the minimal salts culture medium in order for cell growth to occur.

When increased carbon flow is directed into the shikimate pathway due to increased in vivo activity of DAHP synthase, the 3-dehydroquinate synthase activity of E. coli AB2834 is inadequate to convert substrate DAHP into product 3-dehydroquinate at a

rate that is rapid enough to avoid substrate accumulation. As a consequence, DAHP undergoes dephosphorylation to 3-deoxy-D-arabino-heptulosonic acid (DAH), which is exported into the culture supernatant causing a reduction in the yield and concentration of biosynthesized 3-dehydroshikimate. To remove this impediment to carbon flow, *E. coli* KL3 carried a second genomic copy of the *aroB* gene, which resulted in an approximately twofold increase in 3-dehydroquinate synthase specific activity relative to wild-type strains. This strategy has been previously employed to reduce the accumulation of DAH when carbon flow into the common pathway is increased. Insertion of the *aroB* gene into the 3-phosphoglycerate dehydrogenase-encoding *serA* locus also abolished the ability of *E. coli* KL3 to synthesize L-serine. Therefore, survival of *E. coli* KL3 in minimal medium without L-serine supplementation required the existence of a plasmid-localized *serA* gene. This strategy of enforcing plasmid maintenance by nutritional pressure has been successfully employed under fed-batch fermentor conditions. The construction of *E. coli* KL3 was described previously.

In addition to the serA gene, all plasmids used in this study carried a feedback-insensitive allele of DAHP synthase, encoded by $aroF^{FBR}$, 83 and an additional copy of the promoter region of the aroF gene, designated P_{aroF} . Feedback inhibition constitutes the most important factor in E. coli controlling the flow of carbon into the common pathway of aromatic amino acid biosynthesis. 17a Therefore, a feedback-insensitive mutant of aroF, which was generated by photochemical mutagenesis, 84 was utilized by 3-dehydroshikimate-synthesizing biocatalysts. The P_{aroF} sequence contains three binding sequences for the TyrR repressor protein. 85 Inclusion of P_{aroF} resulted in less of this

repressor binding to the promoter region of $aroF^{FBR}$ gene. As a consequence, transcription of feedback-insensitive DAHP synthase increased. 64c

B. Fed-Batch Fermentor Conditions

Fed-batch fermentations were performed in a 2.0 L working capacity Biostat MD B-Braun fermentor equipped with a DCU-3 system and a Dell Optiplex Gs⁺ 5166M personal computer utilizing B-Braun MFCS/win software (v1.1) for data acquisition and automatic process monitoring. Temperature, pH, and glycerol feeding were controlled by PID control loops. Temperature was maintained at 36 °C by water flow through a water jacket surrounding the fermentor vessel. The pH was maintained at 7.0 by the addition of concentrated ammonium hydroxide or 2 N H₂SO₄. Dissolved oxygen (D.O.) was measured using a Mettler-Toledo 12 mm sterilizable O₂ sensor fitted with an Ingold A-type O₂ permeable membrane. D.O. level was maintained at 20% of air saturation. Antifoam (Sigma 204) was added manually as needed. Fed-batch fermentations were run in duplicate, and reported results represent an average of the two runs.

Inoculants were started by introduction of a single colony picked from an M9 agar plate containing glycerol into 5 mL of M9 glycerol medium. Cultures were grown at 37 °C with agitation at 250 rpm until they were turbid and subsequently transferred to 100 mL of fresh M9 glycerol medium. After culturing at 37 °C and 250 rpm for an additional 10 h, the inoculant ($OD_{600} = 1.0$ -3.0) was transferred into the fermentation vessel and the batch fermentation was initiated (t = 0 h). The initial glycerol concentration in the fermentation medium ranged from 17 to 22 g/L according to the growth requirement of different constructs.

	:
	;
	:

Cultivation under fermentor-controlled conditions was divided into three stages with each stage corresponding to a different method for controlling D.O. In the first stage, the airflow was kept constant at 0.06 L/L/min and the impeller speed was increased from 50 rpm to 1100 rpm to maintain the D.O. at 20%. Once the impeller speed reached its preset maximum of 1100 rpm, the mass flow controller started to maintain the D.O. by increasing the airflow from 0.06 L/L/min to 1.0 L/L/min. Depending on the construct under examination, the two stages took a total of 12 to 14 h for completion. At constant impeller speed and constant airflow rate, the D.O. level was maintained at 20% for the remainder of the fermentation by use of an O₂ sensor to control glycerol feeding. At the beginning of the third stage, the D.O. concentration fell below 20% due to the residual glycerol initially added to the medium. This lasted from approximately 10 min to 30 min before glycerol feeding (600 g/L) started. Fermentation cultures typically entered the stationary phase between 24 and 30 h after inoculation of the fermentor's culture medium. Cell density reached a maximum of 20-25 g/L of dry cell weight. Due to the formation of gallate, the culture medium gradually turned into a dark brown color over the course of the runs. The maximum productivity for synthesis of 3-dehydroshikimate generally started at 12 h and continued until 42 h. Fermentations were run for 48 h.

Fed-Batch Fermentor Synthesis of 3-Dehydroshikimate from Glycerol

A. Fermentations Employing E. coli KL3 as the Host Strain

E. coli KL3/pKD11.291A

Biosynthesis of 3-dehydroshikimate by *E. coli* strains is first dictated by the in vivo activity of DAHP synthase. Therefore, the first 3-dehydroshikimate-synthesizing

biocatalyst was constructed by transforming $E.\ coli$ KL3 with plasmid pKD11.291A, which encodes $aroF^{FBR}$, serA genes and a P_{aroF} fragment. Plasmid pKD11.291A was directly constructed from plasmid pKL4.33B, a pSU18⁸⁶ derivative (Figure 13). Insertion of a 0.15 kb DNA fragment encoding the promoter region of aroF into the XbaI site on pKL4.33B afforded this 5.6 kb plasmid. Transcription from P_{aroF} was in the same direction as the transcription of the serA gene.

Previous reports indicated that the growth rate of E. coli on glycerol could vary over a considerable range, depending upon the particular strain and the composition of the minimal salts medium.⁸⁷ Although E. coli KL3 has long been cultured in laboratories, its ability to metabolize glycerol was unknown. E. coli KL3 competent cells were transformed with plasmid pKD11.291A and spread onto agar plates containing glycerol as the sole carbon source. After approximately 90 h of incubation at 37 °C, the transformants were able to form colonies with a diameter of 1 mm. However, when the same transformants were incubated on agar plates containing glucose as the sole carbon source, it took approximately 24 h to form colonies of the same size. A slow growth rate was also observed after single colonies of E. coli KL3/pKD11.291A grown on M9 glycerol plates were inoculated into 5 mL of M9 minimal salts containing glycerol as the sole carbon source and cultured at 37 °C with agitation. However, when the 5 mL inoculant was transferred into 100 mL of M9 minimal salts containing glycerol as the sole carbon source, the cells growth rate was almost the same as when glucose was provided as the sole carbon source. To clarify if the initial slow growth rate of E. coli KL3/pKD11.291A on glycerol was a constitutive phenotype of the host strain, E. coli KL3 competent cells were subjected to the conditions employed for transformation, yet

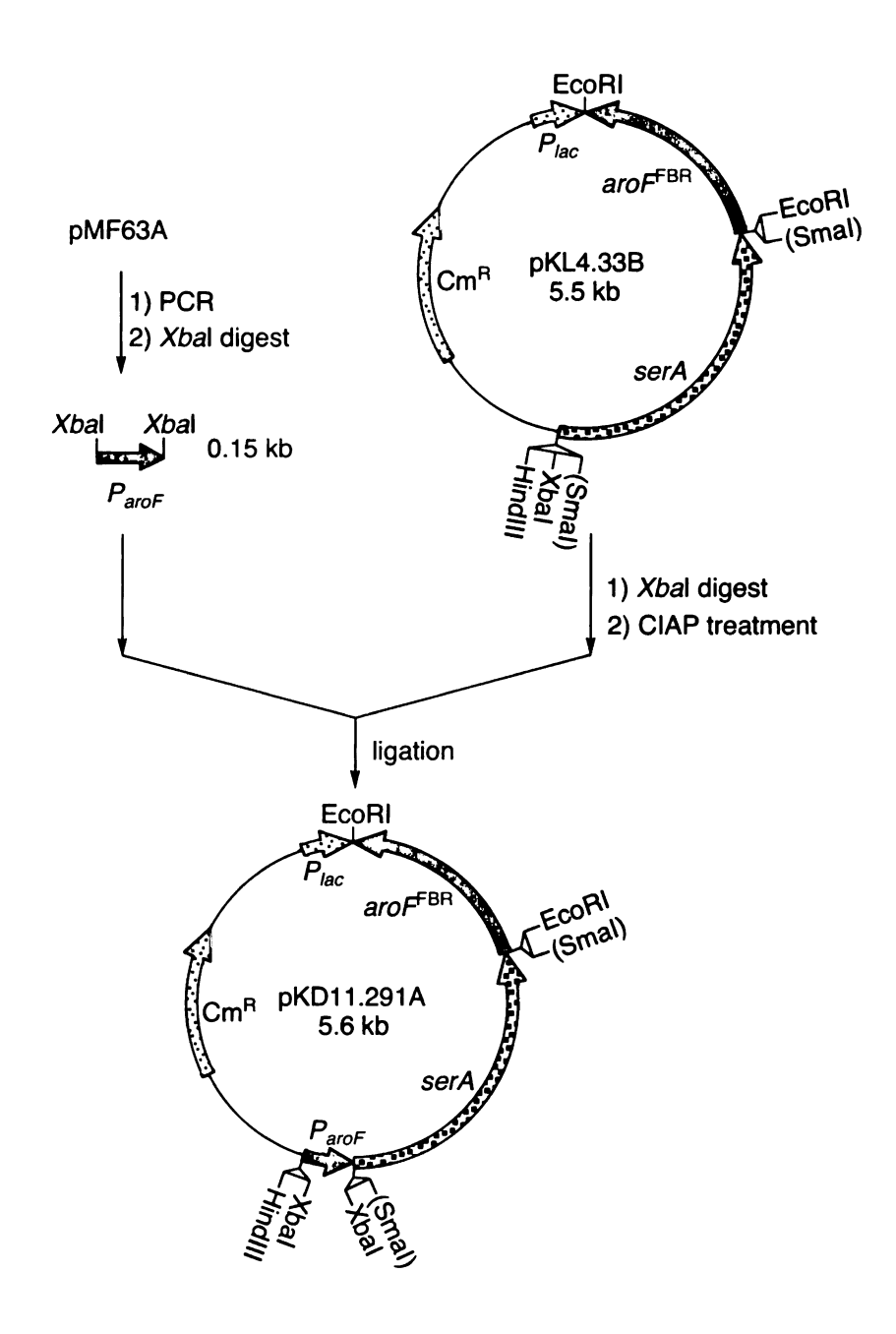


Figure 13. Preparation of plasmid pKD11.291A.

no plasmid DNA was included. Cells were then respectively spread on agar plates containing glycerol or glucose as the sole carbon source. In contrast to the significantly slower growth rate for *E. coli* KL3/pKD11.291A transformants on glycerol relative to on glucose, the growth rate of *E. coli* KL3 that had been subjected to transformation conditions in the absence of plasmid DNA on glycerol and on glucose was indistinguishable. *E. coli* KL3/pKD11.291A contained plasmid-localized copies of genes encoding feedback-insensitive DAHP synthase and 3-phosphoglycerate dehydrogenase. Resulting overexpression of these enzymes is likely a burden on cellular metabolism. Additionally, cellular carbon and energy were divided between the requirements for cell growth and biosynthesis of 3-dehydroshikimate in *E. coli* KL3/pKD11.291A. Theses factors may have collectively been responsible for the slower growth rate of *E. coli* KL3/pKD11.291A on glycerol.

Construct KL3/pKD11.291A was further examined under fed-batch fermentor conditions. Cell growth reached stationary phase around 24 h after the fermentor's culture medium had been inoculated. 3-Dehydroshikimate was mainly synthesized from 12 h to 42 h. The rate of synthesis of 3-dehydroshikimate significantly slowed down beyond 42 h (Figure 14A). When the fermentation was terminated at 48 h, 32 g/L of 3-dehydroshikimate had been synthesized of 10% yield (mol/mol) based on the total amount of glycerol consumed by the cells (Table 1). Other metabolites in the culture supernatant included 3-dehydroquinate (3.8 g/L) and gallic acid (4.8 g/L). 3-Dehydroquinate is the direct metabolic precursor to 3-dehydroshikimate, and gallic acid is derived from 3-dehydroshikimate via a route that remains to be elaborated. Both 3-dehydroquinate and gallic acid represent carbon flow directed into the shikimate

pathway. DAH, which is the dephosphorylation product of DAHP was not observed in the culture medium. This observation indicated that the expression levels of 3-dehydroquinate dehydratase were adequate throughout the runs. The total yield of 3-dehydroshikimate and shikimate pathway byproducts 3-dehydroquinate and gallate synthesized by *E. coli* KL3/pKD11.291A was 13% (mol/mol). DAHP synthase activity, which was measured in cell-free lysate at three time points during the fermentation runs, reached 0.39 U/mg at 24 h and dropped to 0.12 U/mg by 48 h (Table 1).

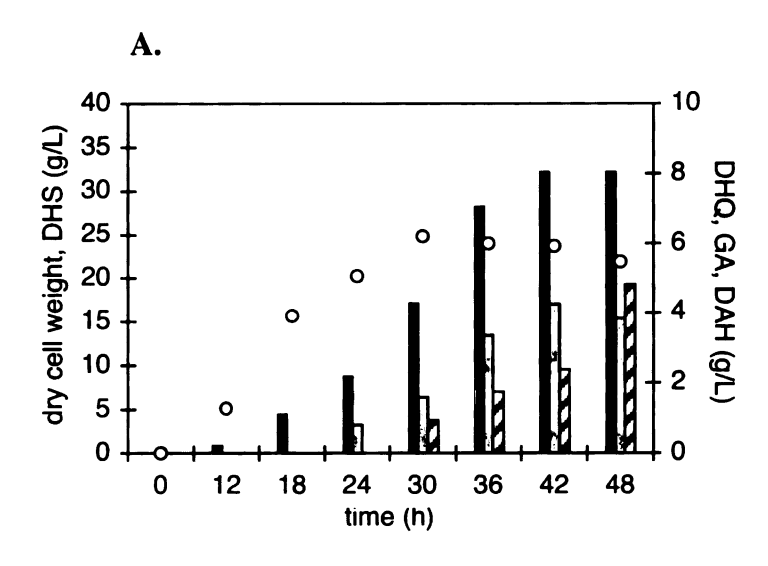
Table 1. Yields and Concentrations of 3-Dehydroshikimate and Shikimate Pathway Byproducts Synthesized by *E. coli* KL3/pKD11.291A and *E. coli* KL3/pKL5.17A Cultured on Glycerol as the Sole Source of Carbon for 48 h Under Fermentor-Controlled Conditions.

Construct	[DHS]"	DHS yield	[DAH]	[DHQ]	[GA]	Total yield (%) ^c	DAHP synthase activity (U/mg) 24 h 36 h 48 h			
	(B/L)	$(\%)^{b}$	(8/12)	(6/12)	(8/12)		24 h	36 h	48 h	
KL3/pKD11.291A			0.0	3.8	4.8		0.39			
KL3/pKL5.17A	25	8.7	0.0	2.5	3.3	12	0.37	0.10	0.10	

^a Abbreviations: 3-dehydroshikimate (DHS), 3-deoxy-D-arabino-heptulosonic acid (DAH), 3-dehydroquinate (DHQ), gallic acid (GA); ^b Given as (mol of DHS)/(mol of glycerol); ^c Given as (mol of DHS + mol of DAH + mol of DHQ + mol of gallic acid)/(mol of glycerol).

E. coli KL3/pKL5.17A

To further improve 3-dehydroshikimate biosynthesis from glycerol, the impact of increased transketolase activity was examined. *E. coli* KL3/pKL5.17A contained a plasmid-localized *tktA* gene, which encodes *E. coli* transketolase. Transketolase functions in the nonoxidative branch of the pentose phosphate pathway and catalyzes the synthesis of D-erythrose 4-phosphate (E4P), one of the two substrates of DAHP synthase (Figure 1). Previous research had demonstrated that the in vivo availability of



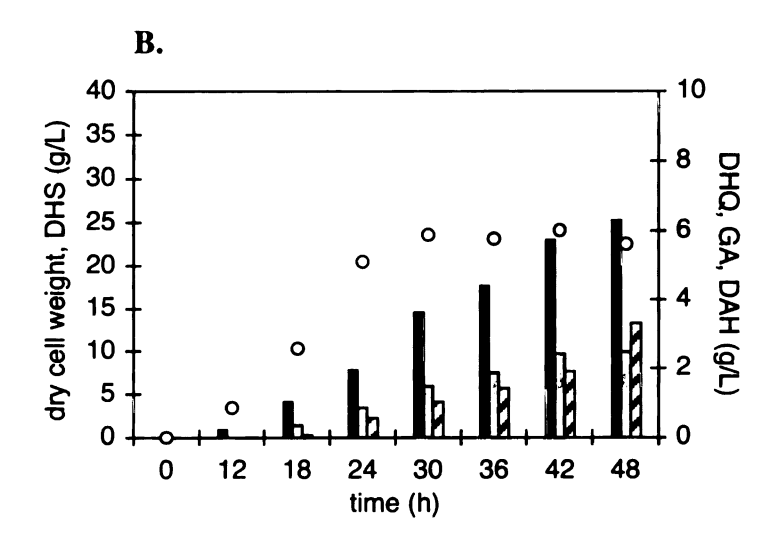


Figure 14. Biosynthesis of 3-dehydroshikimate under fed-batch fermentor conditions. (A) E. coli KL3/pKD11.291A, (B) E. coli KL3/pKL5.17A: • dry cell weight; — 3-dehydroshikimate (DHS); — 3-dehydroquinate (DHQ); — gallic acid (GA).

E4P is also an important limiting factor in the biosynthesis of shikimate pathway metabolites. Overexpression of transketolase in *E. coli* biocatalysts with increased DAHP synthase activity increased the concentration and the yield of 3-dehydroshikimate synthesized when glucose was employed as the carbon source. The 7.8 kb plasmid pKL5.17A was created by replacing the 1.0 kb *NcoI/SphI* fragment of pKD11.291A with a 3.2 kb *NcoI/SphI* fragment from pKL4.130B that contained the *tktA* gene (Figure 15). Digestion of pKD11.291A with *NcoI* and *SphI* afforded a 4.6 kb DNA fragment while similar digestion of pKL4.130B yielded a 3.2 kb DNA fragment. Ligation of these two purified fragments resulted in pKL5.17A.

Construct *E. coli* KL3/pKL5.17A showed similar growth characteristics on glycerol as *E. coli* KL3/pKD11.291A throughout the process of preparing inoculants for fed-batch fermentations and during fermentor runs (Figure 14B). After 48 h of cultivation, 25 g/L of 3-dehydroshikimate was synthesized in a yield of 8.7% (mol/mol) from glycerol (Table 2). Both 3-dehydroquinate (2.5 g/L) and gallic acid (3.3 g/L) were also synthesized. The total yield of 3-dehydroshikimate and shikimate pathway byproducts 3-dehydroquinate and gallate was 12% (mol/mol). During the fermentation, comparable DAHP synthase specific activities were observed for *E. coli* KL3/pKD11.291A and *E. coli* KL3/pKL5.17A (Table 1). The fact that overexpression of transketolase in *E. coli* KL3 didn't improve 3-dehydroshikimate biosynthesis when glycerol was the carbon source stands in contrast to previous results when glucose was employed as the sole source of carbon.^{64c.68} This observation indicated that E4P availability was not a factor limiting the in vivo catalytic activity of DAHP synthesis in *E. coli* cultured on glycerol as a sole source of carbon.

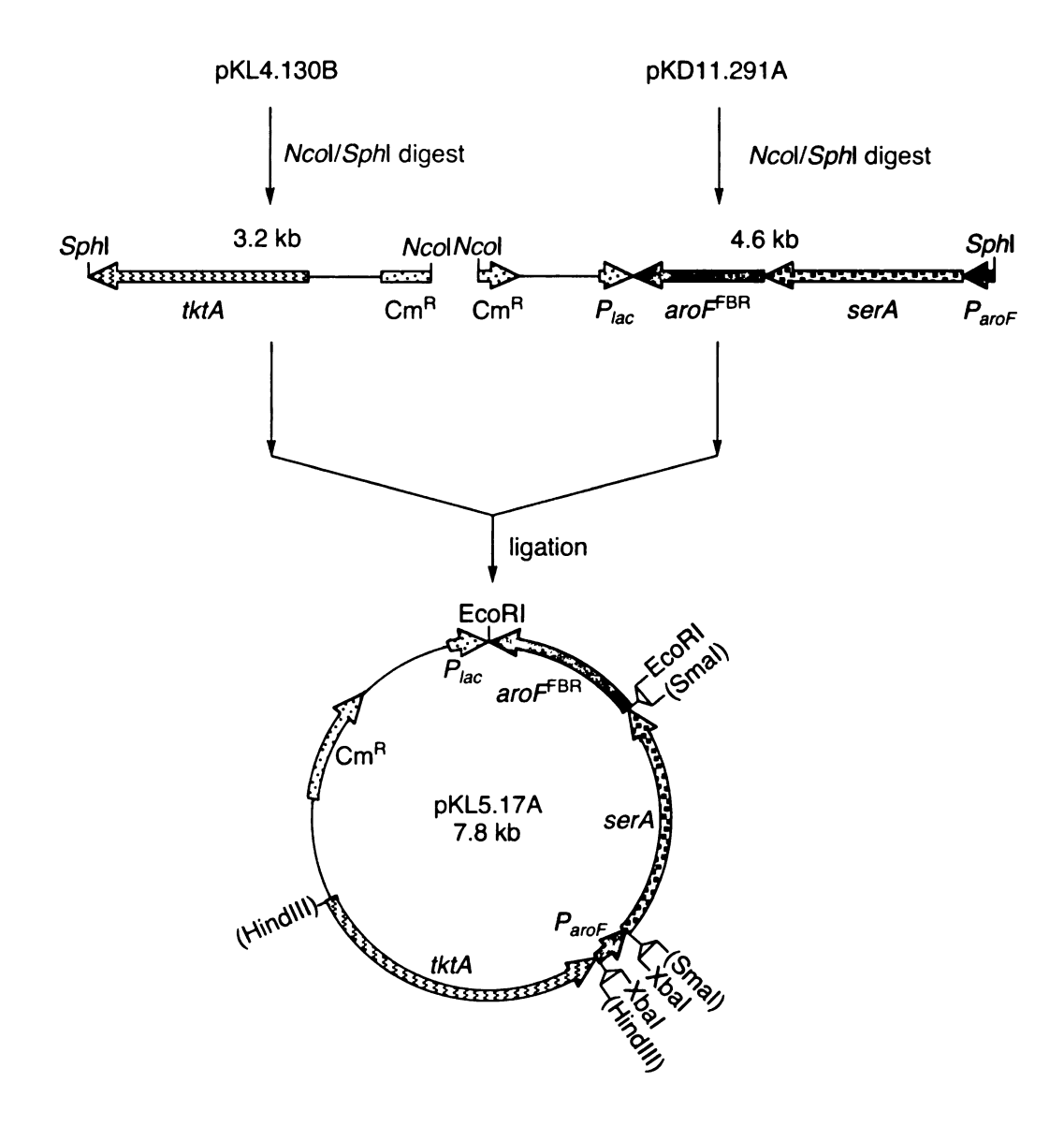


Figure 15. Preparation of plasmid pKL5.17A.

B. Fermentations Employing E. coli KL3.21 as the Host Strain

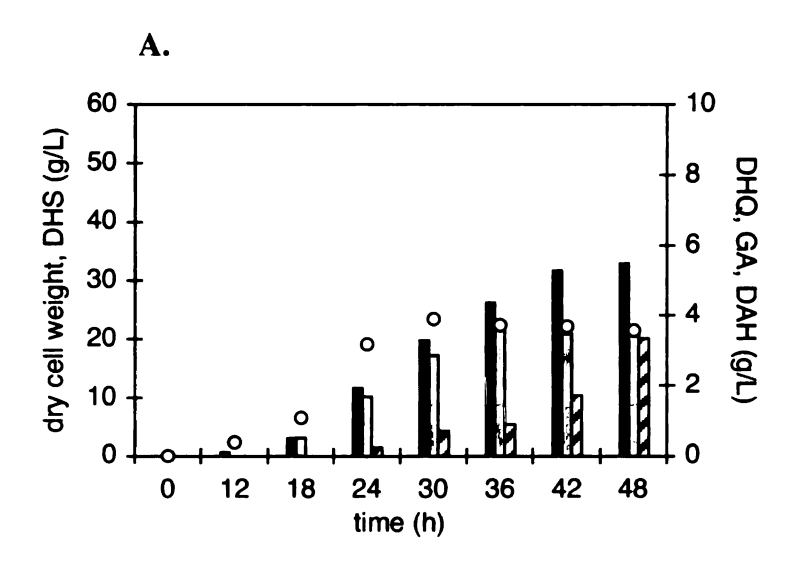
Isolation of E. coli KL3.21

E. coli KL3.21 is a spontaneous mutant of E. coli KL3 which was isolated after repeated selection for enhanced growth rate of E. coli KL3 on minimal salts medium containing glycerol as the sole carbon source. Single colonies of E. coli KL3/pKL5.17A were streaked out onto M9 glycerol plates and incubated at 37 °C. Colonies with an enhanced growth rate were streaked onto fresh M9 glycerol plates to identify cells with even faster growth rates. After three rounds of selection for faster growth on agar plates, a single colony was cultured under fed-batch fermentor conditions using glycerol as the sole carbon source. An aliquot of cells was withdrawn from the fermentor after 24 h of culturing. After serial dilution with M9 salts, cells were plated onto an M9 glycerol plate. Following 48 h of incubation at 37 °C, two types of colonies were observed on the plate: colonies of large size and colonies of small size, which indicated the existence of cells with different growth rates on glycerol. To isolate a possible plasmid-free E. coli KL3 mutant strain with an elevated growth rate on glycerol, a single colony of large size was inoculated into 5 mL of LB medium to provide culturing conditions lacking nutritional or antibiotic pressure. Following cultivation at 37 °C for 12 h, the culture was then diluted in LB (1:20,000), and three more cycles of growth at 37 °C for 12 h each were carried out to enrich cultures for cells that had lost the plasmid. Serial dilutions of culture were then spread onto LB plates and incubated at 37 °C overnight. The resulting colonies were first screened for the retention of the phenotype of E. coli KL3: growth on M9 glycerol containing L-serine, aromatic amino acids, and aromatic vitamins; no growth on M9 glycerol; no growth on M9 glycerol containing L-serine and shikimic acid. E. coli mutant KL3.21 was characterized for the loss of plasmid pKL5.17A: growth on LB; no growth on LB containing Cm.

E. coli KL3.21/pKD11.291A and E. coli KL3.21/pKL5.17A

E. coli KL3.21 was transformed with pKD11.291A and pKL5.17A to generate E. coli KL3.21/pKD11.291A and E. coli KL3.21/pKL5.17A. After 36 h of incubation at 37 °C, cells formed colonies with a diameter of 1 mm. This corresponds to less than one-half the amount of the time that E. coli KL3 transformants took to reach a similar size, but was approximately 12 h slower relative to the same transformants cultured on glucose. However, when single colonies of each construct were cultured in 5 mL of M9 glycerol medium, the growth rate was similar to cells supplemented with glucose as the sole carbon source. To evaluate the impact of accelerated growth rate on 3-dehydroshikimate biosynthesis, E. coli KL3.21/pKD11.291A and E. coli KL3.21/pKL5.17A were examined under fed-batch fermentor conditions.

E. coli KL3.21/pKD11.291A showed similar growth character during cultivation under fermentor-controlled condition as E. coli KL3/pKD11.291A. Cell growth reached stationary phase around 24 h after the inoculation of the fermentor's culture medium and achieved a maximum dry cell weight of 23 g/L (Figure 16A). Upon cessation of the fermentation at 48 h, 3-dehydroshikimate had accumulated at 33 g/L in a yield of 11% (mol/mol) based on the glycerol consumed (Table 2). 3-Dehydroquinate (3.5 g/L) and gallic acid (3.4 g/L) were also detected in the culture medium. The total yield of synthesized 3-dehydroshikimate and shikimate pathway byproducts 3-dehydroquinate and gallate for E. coli KL3.21/pKD11.291A was 14% (mol/mol). The nearly identical



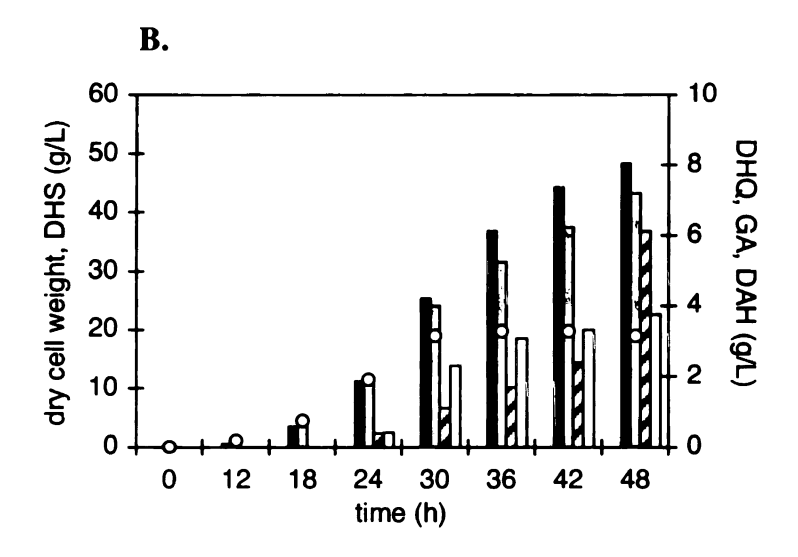


Figure 16. Biosynthesis of 3-dehydroshikimate under fed-batch fermentor conditions. (A) E. coli KL3.21/pKD11.291A, (B) E. coli KL3.21/pKL5.17A: o dry cell weight; 3-dehydroshikimate (DHS); 3-dehydroquinate (DHQ); gallic acid (GA); 3-deoxy-D-arabino-heptulosonic acid (DAH).

Table 2. Yields and Concentrations of 3-Dehydroshikimate and Shikimate Pathway Byproducts Synthesized by *E. coli* KL3.21/pKD11.291A and *E. coli* KL3.21/pKL5.17A Cultured on Glycerol as the Sole Source of Carbon for 48 h Under Fermentor-Controlled Conditions.

Construct	[DHS] ^a	DHS yield	[DAH] (g/L)	[DHQ]	[GA]	Total yield (%)	DAHP synthase activity (U/mg)		
(,	(g/L)	$(\%)^{b}$	(5/12)	(g/L)	(g/L)		24 h	36 h	48 h
KL3.21/ pKD11.291A	33	11	0.0	3.5	3.4	14	0.27	0.19	0.11
KL3.21/ pKL5.17A	48	17	3.8	7.2	6.1	22	0.35	0.21	0.18

^a Abbreviations: 3-dehydroshikimic acid (DHS), 3-deoxy-D-arabino-heptulosonic acid (DAH), 3-dehydroquinic acid (DHQ), gallic acid (GA); ^b Given as (mol of DHS)/(mol of glycerol); ^c Given as (mol of DHS + mol of DAH + mol of DHQ + mol of gallic acid)/(mol of glycerol).

metabolite accumulation profiles and yields obtained during cultivation of *E. coli* KL3.21/pKD11.291A (Table 2) and *E. coli* KL3/pKD11.291A (Table 1) under fermentor-controlled conditions indicated that an elevated growth rate for a host strain on glycerol had no impact on 3-dehydroshikimate biosynthesis when plasmid pKD11.291A was employed.

However, *E. coli* KL3.21/pKL5.17A performed much differently relative to *E. coli* KL3/pKL5.17A under fed-batch fermentor conditions. Cell growth was slower during the fermentation, with cells entering stationary phase about 30 h after the fermentation was initiated, which was nearly 6 h later than *E. coli* KL3/pKL5.17A (Figure 16B). The highest dry cell weight was 19 g/L, which was approximately 4 g/L lower than that achieved by *E. coli* KL3/pKL5.17A. Nevertheless, the reduction in biomass synthesis was accompanied by an increase in metabolite accumulation. After 48 h of cultivation, *E. coli* KL3.21/pKL5.17A synthesized 48 g/L of 3-dehydroshikimate in a

yield of 17% (mol/mol) based on the glycerol consumed (Table 2). Increased 3-dehydroquinate (7.2 g/L) and gallic acid (6.1 g/L) synthesis were also observed. Another significant change in this run was the accumulation of DAH (3.8 g/L) in the cultivation medium. This indication of insufficient 3-dehydroquinate synthase activity suggested that increased carbon flow was being directed into the shikimate pathway of *E. coli* KL3.21/pKL5.17A. The total yield of 3-dehydroshikimate and shikimate pathway byproducts 3-dehydroquinate, gallate, and DAH was 22% (mol/mol) (Table 2), which was almost double the total yield achieved with *E. coli* KL3/pKL5.17A (Table 1). *E. coli* KL3.21/pKL5.17A (Table 2) showed a similar overexpression level of DAHP synthase as *E. coli* KL3/pKL5.17A (Table 1) during its cultivation under fermentor-controlled conditions.

Comparison of *E. coli* KL3.21/pKL5.17A with *E. coli* KL3.21/pKD11.291A indicated that overexpression of transketolase resulted in an increase in both the concentration and the yield of 3-dehydroshikimate synthesized from glycerol, and also in the total yield of 3-dehydroshikimate and shikimate pathway byproducts synthesized from glycerol (Table 2). The impact of transketolase overexpression in *E. coli* KL3.21 cultured on glycerol under fermentor-controlled conditions upon 3-dehydroshikimate synthesis was comparable to the impact of transketolase overexpression in *E. coli* constructs cultured on glucose under fermentor-controlled conditions.

C. Impact of Glycerol Kinase Overexpression on 3-Dehydroshikimate Biosynthesis

Glycerol kinase is the pacemaker for the catabolism of glycerol in E. coli. The in vivo glycerol kinase activity is regulated by fructose 1,6-diphosphate through feedback

inhibition. When $E.\ coli$ is cultured on glycerol, the intracellular concentration of fructose 1,6-diphosphate has been estimated to be 1.7 mM, which is sufficient to cause significant inhibition of wild-type glycerol kinase given fructose 1,6-diphosphate's K_i value of 0.5-1.0 mM. Previous research has indicated an enhanced growth rate for $E.\ coli$ mutant strains expressing a feedback-insensitive glycerol kinase relative to wild-type strains when grown on medium containing glycerol as the sole carbon source. To explore the impact of accelerated metabolism of glycerol rate on microbial synthesis of 3-dehydroshikimate by an $E.\ coli\ KL3.21$ strain, feedback-insensitive and wild-type glycerol kinase were expressed in two 3-dehydroshikimate-synthesizing biocatalysts $E.\ coli\ KL3.21$ /pWN3.062A and $E.\ coli\ KL3.21$ /pWN3.120A.

The 12.3 kb plasmid pWN3.062A is a pJF118EH-based plasmid that encodes $aroF^{FBR}$, P_{aroF} , $glpK^{FBR}$, serA, tktA, and $lact^Q$. Ligation of a 1.25 kb $aroF^{FBR}$ DNA fragment into pJF118EH afforded plasmid pJY1.131. Insertion of a 0.15 kb DNA fragment encoding P_{aroF} into the BamHI site of plasmid pJY1.131 resulted in plasmid pSK1.171A (Figure 17). The 1.5 kb feedback-insensitive $glpK^{FBR}$ gene was amplified from genomic DNA of E. coli Lin43,75 a spontaneous E. coli mutant showing an increased growth rate on glycerol. Sequencing of the $glpK^{FBR}$ gene reveals a Gly-305 to Ser-305 point mutation that renders the $glpK^{FBR}$ -encoded glycerol kinase insensitive to the feedback inhibition of fructose 1,6-diphosphate. Localization of the PCR product into the EcoRI site of pSK1.171A resulted in plasmid pWN3.042A (Figure 18). The transcription of $glpK^{FBR}$ in pWN3.042A was initiated by the plasmid-localized tac promoter. A 1.9 kb DNA fragment containing the serA gene was ligated into the smal site of pWN3.042A, which yielded plasmid pWN3.052A (Figure 19). Final localization

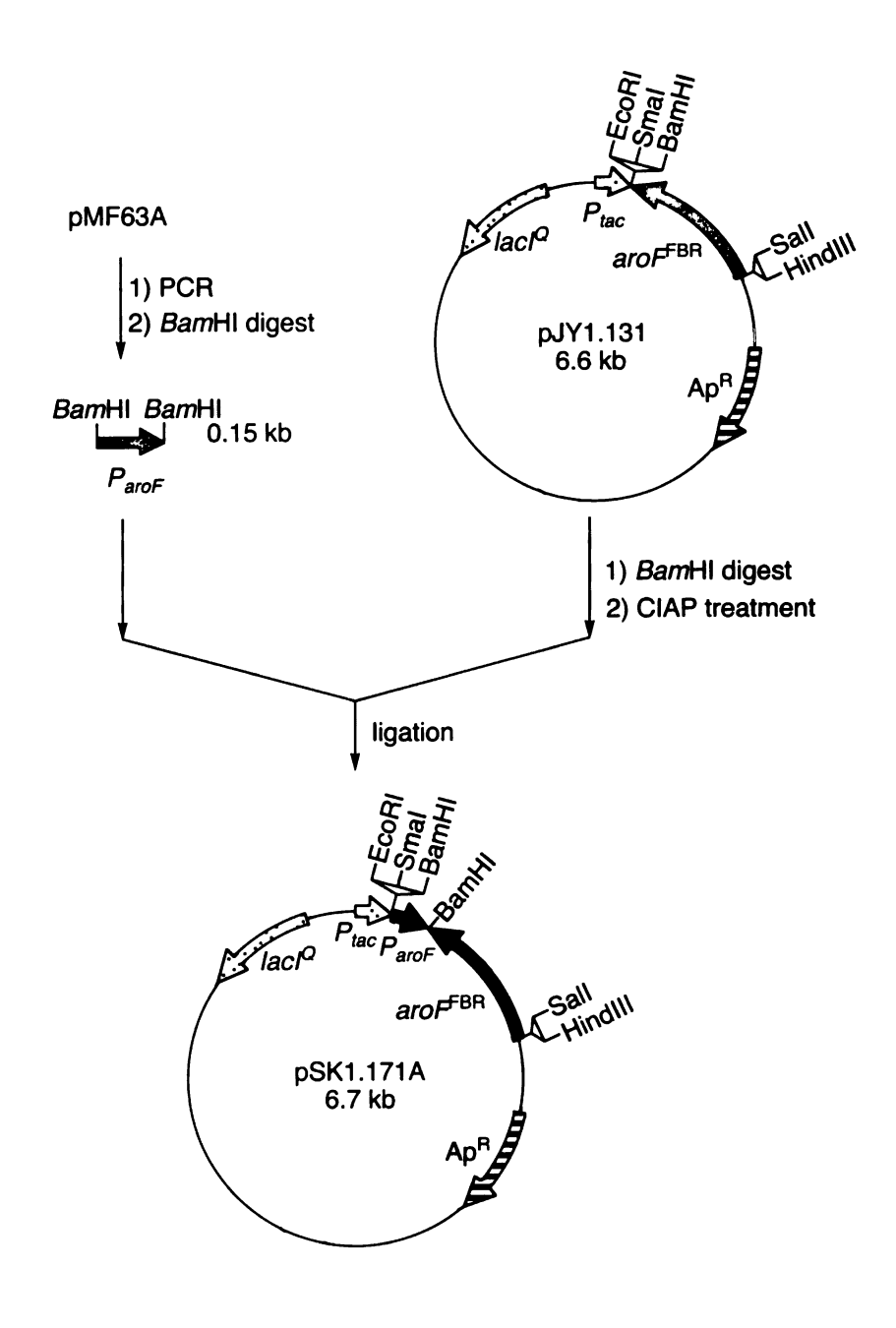


Figure 17. Preparation of plasmid pSK1.171A.

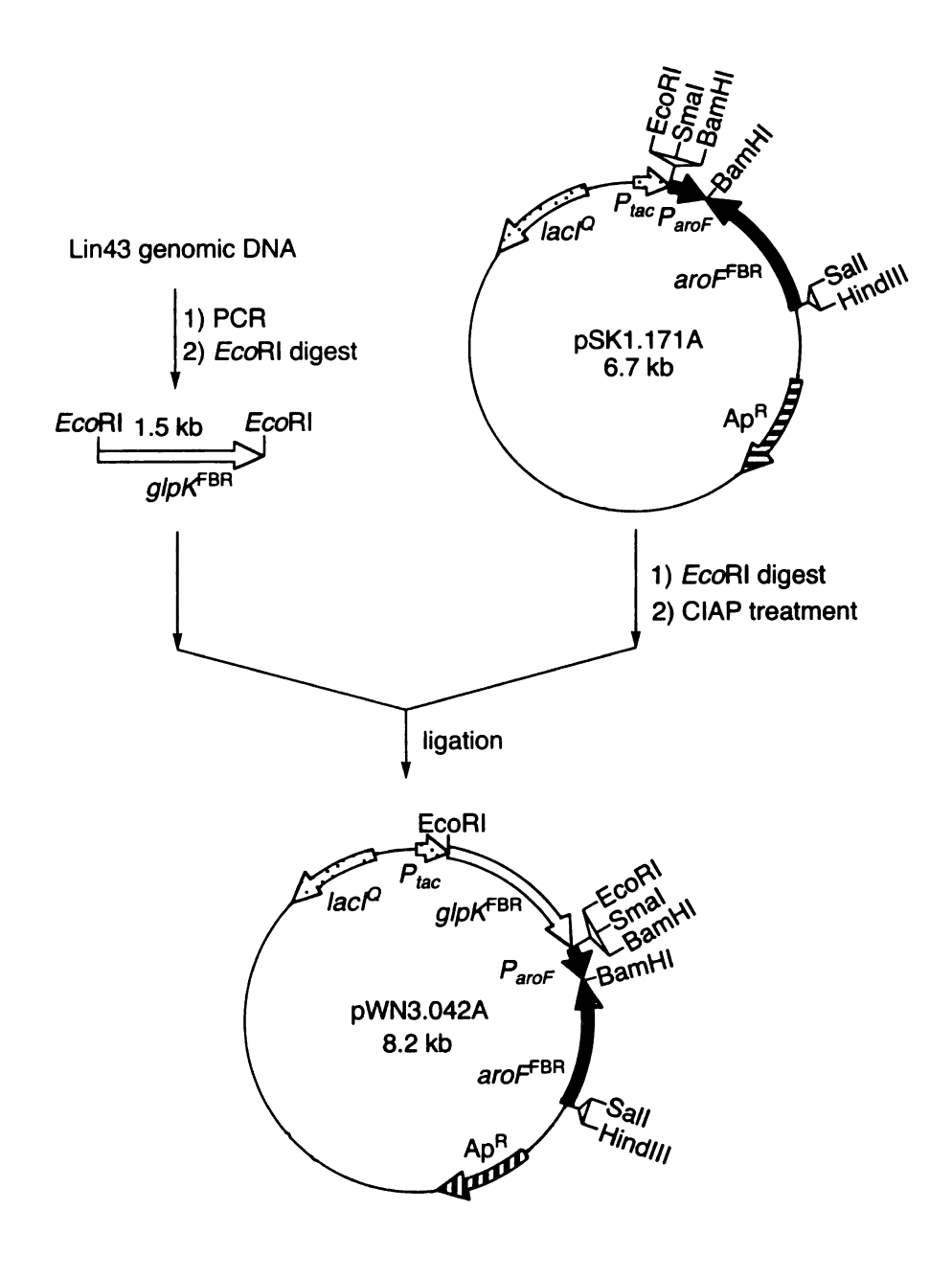


Figure 18. Preparation of plasmid pWN3.042A.

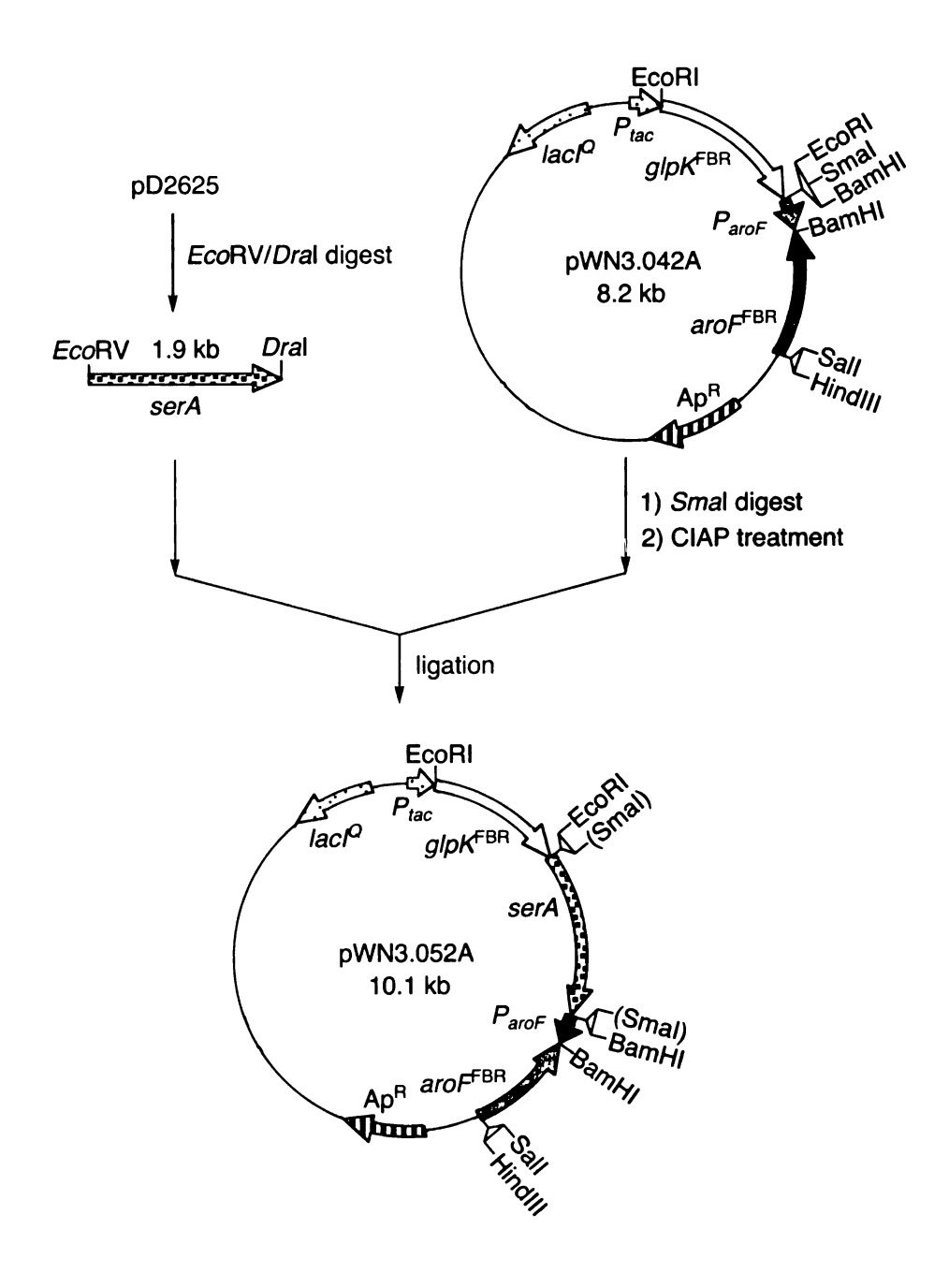


Figure 19. Preparation of plasmid pWN3.052A.

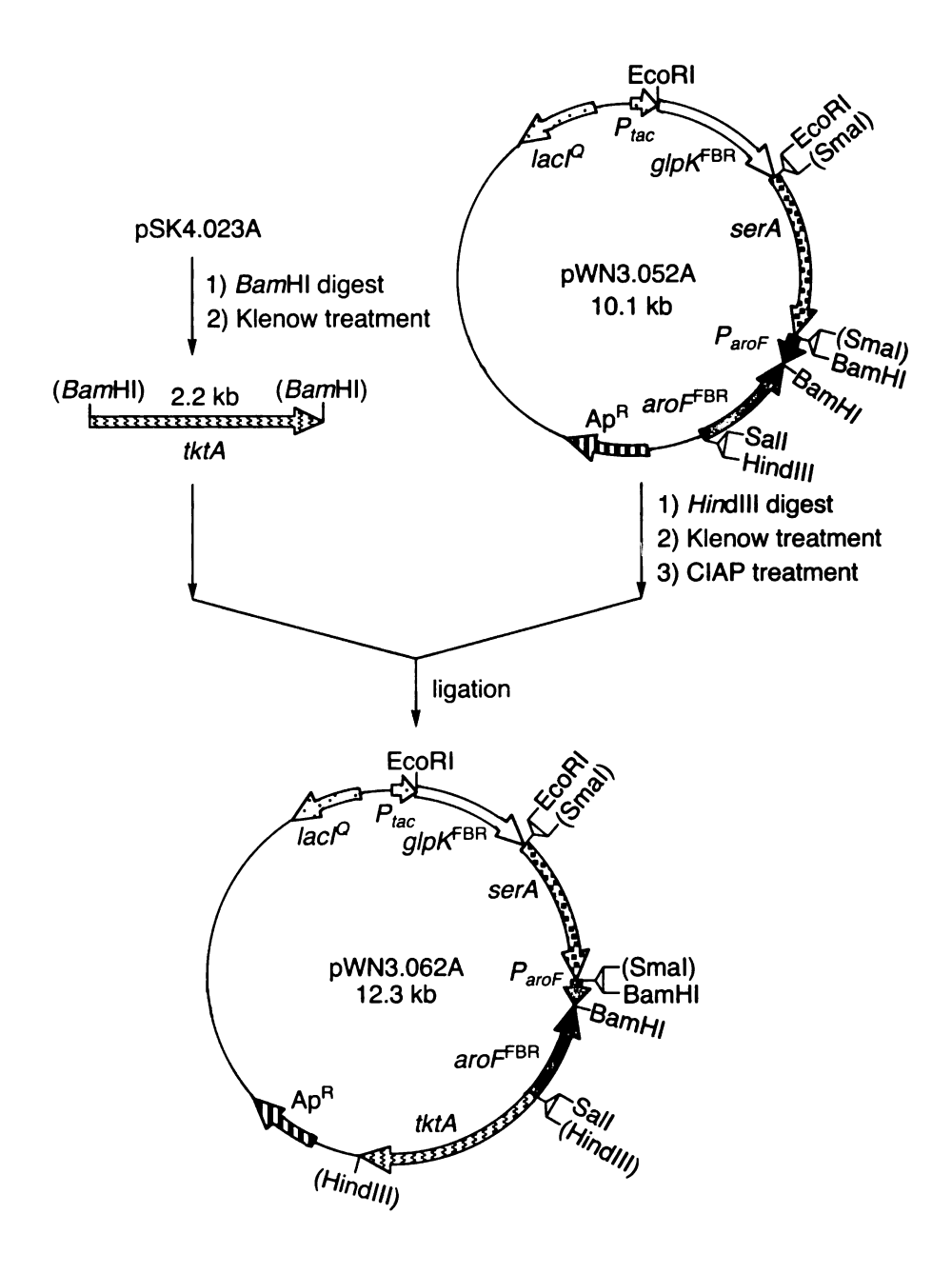


Figure 20. Preparation of plasmid pWN3.062A.

of the Klenow fragment-treated 2.2 kb DNA fragment encoding tktA gene into the Klenow fragment-treated HindIII site on pWN3.052A afforded plasmid pWN3.062A (Figure 20). The 12.3 kb plasmid pWN3.120A is a pJF118EH-based plasmid that encodes $aroF^{FBR}$, P_{aroF} , glpK, serA, and tktA. The construction of plasmid pWN3.120A followed the same strategy as pWN3.062A but via different intermediate plasmids. The glpK-encoded wild-type glycerol kinase was amplified from the genomic DNA of E. coli RB791.

Due to the formation of bactericidal methylglyoxal from dihydroxyacetone phosphate during unregulated glycerol metabolism, high expression levels of feedback-insensitive glycerol kinase are detrimental to $E.\ coli$ cells grown on medium containing glycerol as the sole carbon source. The control of the $lact^Q$ gene on plasmid pWN3.062A was designed to control the expression level of feedback-insensitive glycerol kinase. The Lac repressor protein encoded by the $lact^Q$ gene represses gene transcriptions initiated by the plasmid-localized tac promoter by binding to the operator sequence. However, binding of lactose and other molecules such as isopropyl β -D-thiogalactopyranoside (IPTG) to the Lac repressor causes a conformational change of the repressor so that the repressor no longer binds to the operator. Transcription of the gene under the control of the tac promoter is thus depressed. In plasmid pWN3.062A, the open reading frame of $glpK^{FBR}$ was localized directly behind the tac promoter. Therefore, the transcriptional level of the $glpK^{FBR}$ gene could be modulated by the concentration of IPTG added to the culture medium.

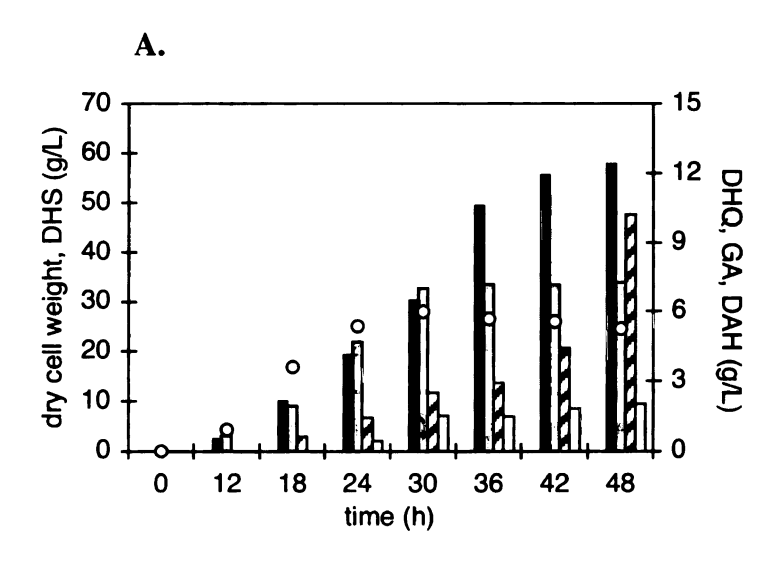
To determine the appropriate IPTG concentration in culture medium, *E. coli* KL3.21/pWN3.062A cultures were assayed for glycerol kinase activities. Varied

Table 3. Impact of Varying IPTG Concentration on Glycerol Kinase Specific Activities and Cell Growth Characteristics for *E. coli* KL3.21/pWN3.062A.

entry	1	2	3	4	5
IPTG (mM)	0	0.02	0.05	0.1	0.5
cell growth after induction	+	+	+		_
glycerol kinase specific activity (U/mg)	0.20	0.60	0.36	0.20	0.21

amounts of IPTG were added to cell cultures, and glycerol kinase was assayed in the cell crude lysate (Table 3). Without IPTG addition, the basal activity of glycerol kinase was 0.20 U/mg. After adding 0.02 mM of IPTG to relieve the binding of repressor protein to the *tac* promoter, the specific activity of glycerol kinase increased to 0.60 U/mg. However, further increase of the IPTG concentration caused a decline in specific activity and slower cell growth. When the IPTG concentration in the culture medium reached 0.1 mM, cells stopped growing.

E. coli KL3.21/pWN3.120A and E. coli KL3.21/pWN3.062A were respectively examined under fermentor-controlled culture conditions. After the inoculation of the fermentor's culture medium for 14 h, IPTG was added in the fermentation medium to a concentration of 0.02 mM to initiate the transcription of glycerol kinase. The two constructs displayed similar cell growth profiles. They both reached stationary phase about 24 h after inoculation of culture medium (Figure 21). The total amount of glycerol consumed by both biocatalysts was about 50 g higher than the amount consumed by constructs without glycerol kinase overexpression. After 48 h of cultivation, E. coli KL3.21/pWN3.120A produced 58 g/L of 3-dehydroshikimate, which is 10 g/L higher than E. coli KL3.21/pKL5.17A (Table 4). However, both the yield of 3-dehydroshikimate (17%, mol/mol) and the total yield of 3-dehydroshikimate and



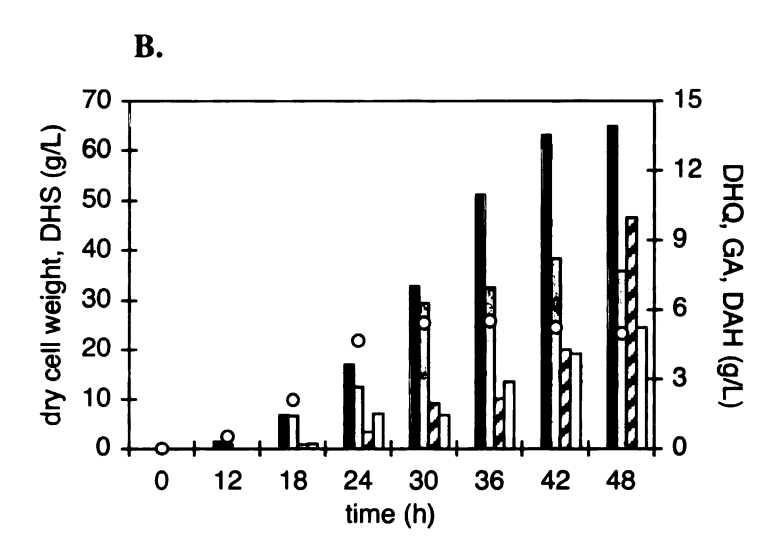


Figure 21. Biosynthesis of 3-dehydroshikimate under fed-batch fermentor conditions. (A) E. coli KL3.21/pWN3.120A, (B) E. coli KL3.21/pWN3.062A: • dry cell weight; — 3-dehydroshikimate (DHS); — 3-dehydroquinate (DHQ); — gallic acid (GA); — 3-deoxy-D-arabino-heptulosonic acid (DAH).

K U -

1. T

- 10

Tal col Cor

in in

Table 4. Yields and Concentrations of 3-Dehydroshikimate and Shikimate Pathway Byproducts Synthesized by *E. coli* KL3.21/pWN3.120A and *E. coli* KL3.21/pWN3.062A Cultured on Glycerol as the Sole Source of Carbon for 48 h Under Fermentor-Controlled Conditions.

Construct	[DHS] ^a (g/L)	DHS yield (%) ^b	[DAH] (g/L)	[DHQ] (g/L)	[GA] (g/L)	Total yield (%) ^c	DAHP synthase activity (U/mg)		
							24 h	36 h	48 h
KL3.21/ pWN3.120A	58	17	2.0	7.3	10	23	0.25	0.21	0.12
KL3.21/ pWN3.062A	65	20	5.2	7.7	10	26	0.36	0.27	0.22

^a Abbreviations: 3-dehydroshikimic acid (DHS), 3-deoxy-D-*arabino*-heptulosonic acid (DAH), 3-dehydroquinic acid (DHQ), gallic acid (GA); ^b Given as (mol of DHS)/(mol of glycerol); ^c Given as (mol of DHS + mol of DAH + mol of DHQ + mol of gallic acid)/(mol of glycerol).

shikimate pathway byproducts 3-dehydroquinate, gallate, and DAH (23%, mol/mol) achieved by *E. coli* KL3.21/pWN3.120A were close to *E. coli* KL3.21/pKL5.17A. *E. coli* KL3.21/pWN3.062A synthesized 65 g/L of 3-dehydroshikimate, which is a 7 g/L increase relative to *E. coli* KL3.21/pWN3.120A (Table 4). An improved yield of 3-dehydroshikimate (20%, mol/mol) and total yield of 3-dehydroshikimate and shikimate pathway byproducts 3-dehydroquinate, gallate, and DAH (26%, mol/mol) were also observed. Enzyme assays performed on lysates obtained from cells harvested during fermentor-controlled cultivation showed similar in vitro glycerol kinase specific activities

Table 5. Glycerol Kinase Specific Activities of *E. coli* KL3.21/pWN3.120A and *E. coli* KL3.21/pWN3.062A During Cultivation Under Fermentor-Controlled Conditions.

Construct	Glycerol kinase activity (U/mg)					
	12 h	24 h	36 h	48 h		
KL3.21/pWN3.120A	0.15	0.31	0.30	0.20		
KL3.21/pWN3.062A	0.15	0.32	0.29	0.20		

for *E. coli* KL3.21/pWN3.120A and *E. coli* KL3.21/pWN3.062A (Table 5). Therefore, the increased concentration and yield of 3-dehydroshikimate and shikimate pathway byproducts synthesized by *E. coli* KL3.21/pWN3.062A could be attributed to the expression of feedback-insensitive glycerol kinase.

Discussion and Future Work

Glycerol is one of the traditional carbon sources used for culturing microorganisms. The metabolism of glycerol in *Escherichia coli* was extensively studied during the 1970's and 1980's.⁶⁶ Genes that encode enzymes involved in glycerol metabolism have also been identified.⁶⁶ However, the possibility of using glycerol as a starting material in microbe-catalyzed synthesis of commercial chemicals has not been actively explored. A large amount of glycerol may become available as a byproduct of biodiesel production.⁷⁷ Since the current supply of glycerol generated by the oleochemical industry satisfies the market demands, the supply of glycerol attendant with the emergence of a biodiesel industry will likely exceed demand.⁹⁴ Therefore, studies of employing glycerol as an alternate renewable feedstock-derived starting material for the microbial synthesis of value-added chemicals are important. The development of the biodiesel industry is part of a broader effort to reduce dependence on imported petroleum. Utilization of a byproduct of biodiesel production as the starting material for microbial synthesis of value-added chemicals is a strategically reasonable consideration.

Research has shown that mechanisms employed by microbes to transport carbohydrate starting materials from the culture medium into the cytoplasm have a significant impact on the yields of biosynthesized products.^{68,72,95} The biosynthesis of

shikimate pathway products from glucose by wild-type E. coli biocatalysts represents a typical case. Phosphoenolpyruvate is one of the precursors in the biosynthesis of shikimate pathway products. However, phosphoenolpyruvate is also consumed during PTS-mediated transport of glucose to form pyruvate. As a consequence, the theoretical maximum yield for biosynthesis of 3-dehydroshikimate and shikimate pathway byproducts is 43% (mol of 3-dehydroshikimate/mol of glucose) or 7.2% (mol of 3dehydroshikimate/mol of carbon) from glucose based on a stoichiometric analysis.⁶⁴ This yield reflects the fundamental limitation imposed on microbial synthesis by the mechanism employed for glucose transport. In contrast to glucose, glycerol is transported into the cytoplasm of E. coli by a facilitated diffusion mechanism, which does not consume phosphoenolpyruvate. Stoichiometric analysis shows that the maximum theoretical yield for biosynthesis of 3-dehydroshikimate and shikimate pathway byproducts is 43% (mol of 3-dehydroshikimate/mol of glycerol) or 14.3% (mol of 3dehydroshikimate/mol of carbon) from glycerol without considering carbons needed for biomass formation. Employing glycerol as the carbon source in microbial synthesis of shikimate pathway products could therefore increase product yield by twofold.

The Frost group has been evaluating different strategies to increase the in vivo availability of phosphoenolpyruvate during $E.\ coli$ biosynthesis of shikimate pathway products through a series of experiments using $E.\ coli$ biosynthesis of 3-dehydroshikimate under fed-batch fermentor conditions as a model system. To effectively compare the product yields obtained when glycerol was the sole source of carbon with product yields realized using other carbon sources, the 3-dehydroshikimate-synthesizing model system was also used in this study. Host strain $E.\ coli$ KL3 and its

mutant *E. coli* KL3.21 were derived from the same parent strain as host strains used in previous studies of the impact of carbon source transport on product yields. Under the same temperature, pH, and dissolved O₂ control settings, the fermentor-controlled cultivation conditions provided consistent culture environments from study to study. At the end of microbe-catalyzed synthesis of 3-dehydroshikimate using different carbon sources, 3-dehydroshikimate was typically not the only metabolite biosynthesized. Byproducts include DAH, 3-dehydroquinate and gallic acid. 3-Dehydroquinate, DAH, and gallic acid represent carbon flow directed into the shikimate pathway that did not result in the formation of 3-dehydroshikimate. Therefore, the evaluation of the impact of carbon source on product yield requires comparison of the yield of DAH, 3-dehydroquinate, 3-dehydroshikimate, and gallic acid (Table 6).

Using glycerol as the sole carbon source (entry 6, Table 6) led to significant improvements in the yield of 3-dehydroshikimate and the total yield of shikimate pathway byproducts relative to the 5.5% combined yield of *E. coli* KL3/pKL5.17A (entry 1, Table 6), a strain that relies on PTS-mediated glucose transport. The 8.7% total yield achieved using *E. coli* KL3.21/pWN3.062A (entry 6, Table 6) is similar to the total product yield observed for *E. coli* KL3/pJY1.216A (entry 2, Table 6), which utilized amplified expression of phosphoenolpyruvate synthase to recycle PTS-generated pyruvate back to phosphoenolpyruvate. In comparison to strains utilizing altered glucose transport mechanisms, including *E. coli* JY1/pJY2.183A, in which PTS-mediated glucose transport was replaced by glucose facilitator-mediated transport and glucose kinase-catalyzed phosphorylation (entry 3, Table 6), and *E. coli* JY1.3/pKL5.17A, which uses the galactose permease for glucose transport and glucose kinase for phosphorylation of

Table 6. Comparison of Yields and Concentrations of Biosynthesized 3-Dehydroshikimate as a Function of Strategy Employed to Increase Phosphoenolpyruvate Availability.

entry	strain	carbon source	transport mechanism	DHS (g/L) yield ^{d,e,g}	total yield ^e	theoretical yield ^{e,f}
1	KL3/pKL5.17A ^{72b}	glucose	PTS	(49) 4.3%	5.5%	7.2%
2	KL3/pJY1.216A ^{72a}	glucose	PTS^a	(69) 5.8%	8.5%	14.3%
3	JY1/pJY2.183A ^{72b}	glucose	Glf^{\flat}	(60) 5.7%	6.8%	14.3%
4	JY1.3/pKL5.17A ^{72b}	glucose	GalP	(60) 6.0%	7.2%	14.3%
5	KL3/pKL4.124A ⁶⁸	xylose	permease	(43) 6.6%	9.4%	14.3%
6	KL3.21/ pWN3.062A	glycerol	facilitated diffusion	(65) 6.7%	8.7%	14.3%

^a Recycling of PTS-generated pyruvate to phosphoenolpyruvate with amplified phosphoenolpyruvate synthase expression; ^b Glucose transported by facilitated diffusion; ^c With galactose permease transport system; ^d Given as (mol of DHS)/(mol of carbon); ^e Numbers were recalculated using Equation 5 from original references; ^f Given as (mol of DHS + mol of DAH + mol of DHQ + mol of gallic acid)/(mol of carbon); ^g Abbreviations: 3-dehydroshikimic acid (DHS), 3-deoxy-D-arabino-heptulosonic acid (DAH), 3-dehydroquinic acid (DHQ).

transported glucose (entry 4, Table 6), *E. coli* KL3.21/pWN3.062A synthesized 3-dehydroshikimate and shikimate pathway byproducts in a higher total yield using glycerol as the sole carbon source. This yield was slightly lower relative to that realized when KL3/pKL4.124A was cultured on D-xylose (entry 5, Table 6). Collectively, these data indicated that phosphoenolpyruvate availability increases when glycerol was used as the sole carbon source for *E. coli* biosynthesis of shikimate pathway products. This conclusion is derived from comparisons with biosynthetic systems that employed increased E4P availability and overexpression of feedback-insensitive DAHP synthase. Therefore, replacement of glucose with glycerol is competitive in terms of biosynthesized product yields with all other strategies employed to date to circumvent PTS-mediated transport of the carbon source.

Central to the successful biosynthesis of 3-dehydroshikimate from glycerol is the identification of a spontaneous *E. coli* mutant strain KL3.21, which showed a significantly improved growth rate on glycerol, and elevated concentration and yield for 3-dehydroshikimate biosynthesis when transformed with plasmid pKL5.17A. Establishing the genetic basis for this phenotype change will be important in the future for identification of the limiting factor(s) in the biosynthesis of shikimate pathway products from glycerol. This information will be critical to the formulation of strategies for achieving further improvements in product concentrations and yields.

A previous report attributed the fast growth phenotype of *E. coli* mutant strains on glycerol to the existence of a fructose 1,6-diphosphate feedback-insensitive glycerol kinase. When the gene encoding this mutated enzyme was overexpressed in *E. coli* KL3.21/pWN3.062A, the biocatalyst synthesized both 3-dehydroshikimate and shikimate pathway byproducts in higher yields relative to *E. coli* KL3.21/pWN3.120A which overexpressed a wild-type glycerol kinase. Therefore, a possible mutation of *E. coli* KL3.21 is the acquisition of a feedback-insensitive glycerol kinase. However, the amount of glycerol consumed by *E. coli* KL3 and *E. coli* KL3.21 harboring the same plasmid (pKD11.291A or pKL5.17A) during fermentor-controlled cultivation was very close, indicating the faster growth rate of *E. coli* KL3.21 on glycerol was not accompanied by a faster glycerol metabolism rate. This observation is inconsistent with the existence of a feedback-insensitive glycerol kinase, which could elevate the rate of glycerol metabolism in *E. coli*.⁷⁵

The metabolism of *E. coli* KL3/pKL5.17A may be burdened by the amplified expression of plasmid-localized genes and biosynthesis of elevated concentrations and

yields of 3-dehydroshikimate and shikimate pathway byproducts. The improved growth rate of E. coli KL3.21/pKL5.17A thus could result from mutation(s) that relieve these metabolic burdens. Growth rate differences of E. coli KL3/pKL5.17A on glycerol and glucose indicates that the extra metabolic burdens might be caused by the different metabolic flux distribution during cultivation of E. coli on these two different carbon sources. One significant change in the carbon flux distribution observed in a flux analysis of an E. coli wild-type strain grown on glycerol and glucose is the carbon flow directed through D-fructose 6-phosphate, which is 5% for glycerol and 82% for glucose.% D-Fructose 6-phosphate is one of the intermediates of the nonoxidative pentose phosphate pathway, which is responsible for the biosynthesis of D-erythrose 4-phosphate (one of the biosynthetic precursors of shikimate pathway, Figure 6) and C₅ small molecule building blocks of nucleosides biosynthesis.⁸⁸ A low carbon flux through D-fructose 6-phosphate when glycerol is used as the carbon source could result in a limited availability of metabolic intermediates and biosynthetic products derived from the nonoxidative pentose pathway. For example, the observed slow growth rate of E. coli KL3/pKL5.17A cultured on glycerol could reflect a limitation in the availability of nucleosides attendant with reduced availability of pentose phosphate products. A further indication of the limited carbon flow directed through D-fructose 6-phosphate when E. coli KL3 was cultured on glycerol is the observation that transketolase overexpression didn't result in improvements in concentrations and yields of 3-dehydroshikimate and shikimate pathway byproducts biosynthesized from glycerol by E. coli KL3/pKL5.17A. Transketolase catalyzes the biosynthesis of D-erythrose 4-phosphate from D-fructose 6-phosphate in the nonoxidative pentose phosphate pathway (Figure 6). Overexpression of transketolase

byproducts synthesized by *E. coli* KL3/pKL5.17A when glucose was the sole carbon source. However, if carbon flow directed through D-fructose 6-phosphate was limited, overexpression of *tktA* gene would not result in increased E4P availability. Collectively, phenotype changes in *E. coli* KL3.21 could originate from mutation(s) that increase the carbon flow directed through D-fructose 6-phosphate when cultured on glycerol. Further experiments are required to evaluate this hypothesis.

CHAPTER THREE

SYNTHESIS OF ADIPIC ACID FROM D-GLUCOSE

Background

Adipic acid is the common name for 1,6-hexanedioic acid (Figure 22). It is one of the top 50 synthetic chemicals in United States produced annually in terms of volume. Global production of adipic acid in 1999 reached 2.1 × 109 kg, and it is estimated to increase to 2.4 × 109 kg by 2004. The majority of this chemical is used in the production of nylon 6,6 polyamide via its reaction with 1,6-hexanediamine (Figure 22). Nylon 6,6, invented by W. H. Carother's research team at the DuPont company in the early 1930s, is a polymer widely used in carpet fibers, upholstery, tire reinforcements, auto parts, apparel, and other products. The steady growth in demand for nylon 6,6 has resulted in the large-scale production of high purity adipic acid. This availability, in turn, has led to the use of adipic acid in other applications. Due to its GRAS (Generally Regard As Safe) status, adipic acid monomer is also used as a food acidulant in jam, jellies, and gelatins.

$$HO_2C$$
 adipic acid HO_3C HO_2C HO_2C

Figure 22. The structures of adipic acid and nylon 6,6.

Since the commercial introduction of nylon 6,6 in 1939, industrial manufacture of adipic acid has been constantly improved. However, all the current large-scale

productions employ two major steps. The first step involves the production of intermediates cyclohexanol and cyclohexanone from benzene via the intermediacy of cyclohexane (Figure 23), phenol (Figure 24), or cyclohexene. The second step carries oxidation of the mixture of cyclohexanol and cyclohexanone using nitric acid.

benzene cyclohexanol cyclohexanone
$$CO_2H$$

$$+ C CO_2H$$

$$+ N_2C$$

$$+ N_2C$$
adipic acid

Figure 23. Industrial production of adipic acid via cyclohexane as intermediate. (a) Ni-Al₂O₃, H₂, 2550-5500 kPa, 150-250 °C; (b) Co, O₂, 830-970 kPa, 150-160 °C; (c) Cu, NH₄VO₃, 60% HNO₃, 60-80 °C.

As a gaseous phase byproduct of the second step, 0.15-0.3 ton of nitrous oxide (N₂O) is generated for every ton of adipic acid that is produced.⁹⁷ As the major source of stratospheric nitric oxide (NO), N₂O has a global warming potential many times higher than that of carbon dioxide. N₂O also contributes to other environmental problems such as ozone depletion, acid rain, and smog.⁹⁸ In 1991, approximately 10% of the annual increase in atmospheric N₂O was attributed to the adipic acid manufacturing industry.⁹⁹ To reduce the N₂O emission, various N₂O abatement processes have been employed since

Figure 24. Solutia benzene-phenol process for adipic acid production. (a) Fe-ZSM-5, N₂O, 310 kPa, 300-500 °C; (b) Pd/Al₂O₃, H₂, 110 kPa, 130-160 °C; (c) Cu, NH₄VO₃, 60% HNO₃, 60-80 °C.

the middle 1990s. One unique example is the N_2O recycling process developed by Solutia (Figure 24). This innovation benefits from the use of the recycled byproduct N_2O to oxidize benzene to phenol. Cyclohexanol and cyclohexanone are then produced from phenol.

In order to eliminate N₂O emission, routes to adipic acid have been developed utilizing either H₂O₂ or air as the oxidant to convert cyclohexene and *n*-hexane into adipic acid (Figure 25).¹⁰¹ A gene cluster encoding enzymes for converting cyclohexanol to adipic acid also has been identified from *Acinetobacter* sp. strain SE19 (Figure 25).¹⁰² Nevertheless, benzene remains the starting material employed in these processes. Currently, benzene is solely obtained from the BTX fraction of petroleum,¹⁰³ a nonrenewable fossil fuel whose price and availability is increasingly subject to cartel politics. As a result, prices of standard resin-grade adipic acid for 1960-1989 have paralleled raw material and energy costs (petroleum and natural gas) and are growing at a rate of 1.7%/year.⁹⁷ In the early 1990s, the price for resin-grade adipic acid leveled off

A
$$CO_2H$$
 $+ 4 H_2O_2$ \xrightarrow{a} $+ 4 H_2O$ CO_2H $+ 4 H_2O$ CO_2H CO_2H

Figure 25. Alternatives to synthesize adipic acid from hydrocarbons. (A)^{101a} (a) Na₂WO₄, [CH₃(n-C₈H₁₇)₃N]HSO₄, 75-90°C. (B)¹⁰² Enzymes (encoding genes) (a) alcohol dehydrogenase (chnA); (b) cyclohexanone monooxygenase (chnB); (c) hydrolase (chnC); (d) alcohol dehydrogenase (chnD); (e) aldehyde dehydrogenase (chnE).

around \$1.37/kg.⁹⁷ By the late 1990s, it jumped to \$1.53/kg.⁹⁷ Additionally, benzene is also a carcinogen 104 linked to acute myeloid leukemia and non-Hodgkin's lymphoma. 105

ÓН

catechol

cis, cis-muconic acid

adipic acid

Figure 26. Synthesis of adipic acid from D-glucose. Enzymes (encoding genes) (a) DAHP synthase $(aroF^{FBR})$; (b) DHO synthase (aroB); (c) DHO dehydratase (aroD); (d) DHS dehydratase (aroZ); (e) PCA decarboxylase (aroY); (f) catechol 1,2-diooxygenase (catA); (g) 10% Pt/C, H₂, 500 psi, 25 °C. Abbreviations: phosphoenolpyruvate (PEP), Derythrose 4-phosphate (E4P), 3-deoxy-D-arabino-heptulosonic acid 7-phosphate (DAHP), 3-dehydroquinate (DHQ), 3-dehydroshikimate (DHS), protocatechuic acid (PCA).

ÓН

PCA

DHS

In 1994, the Frost group reported the synthesis of adipic acid from D-glucose. 106 In this chapter, improvements in this synthesis will be discussed (Figure 26). Glucose is first converted into cis, cis-muconic acid utilizing a recombinant Escherichia coli biocatalyst under fed-batch fermentor conditions. Subsequent hydrogenation converted cis, cis-muconic acid to adipic acid. This synthesis substituted nontoxic, renewable glucose as a starting material for currently employed carcinogenic, nonrenewable benzene. At the same time, the synthesis of adipic acid from glucose avoids generation of N₂O as a byproduct.

Microbial Synthesis of cis, cis-Muconic Acid from D-Glucose

A. Host Strain Construction

Overview

Two Escherichia coli host strains, KL7107 and WN1, were employed in the microbial conversion of D-glucose into cis, cis-muconic acid. E. coli WN1 is a derivative of E. coli KL7, which was derived from AB2834, an E. coli aroE strain. Other genomic elements shared by the two host strains include site-specific insertion of an aroZaroB cassette into the serA locus of E. coli AB2834. The lack of aroE-encoded shikimate dehydrogenase activity in E. coli KL7 and E. coli WN1 results in the synthesis of 3-dehydroshikimate when carbon flow is directed into the shikimate pathway. Direction of biosynthesized 3-dehydroshikimate into cis, cis-muconic acid biosynthesis requires 3-dehydroshikimate dehydratase activity, which is not native to E. coli strains. Genomic insertion of the Klebsiella pneumoniae 3-dehydroshikimate dehydrataseencoding gene, aroZ, 109 catalyzes the conversion of 3-dehydroshikimate to protocatechuic acid. Previous research in this group revealed that aroB-encoded 3-dehydroguinate synthase is a rate-limiting enzyme when elevated carbon flow is directed into the common pathway.¹¹⁰ A separate study indicated that insertion of one additional copy of aroB into the E. coli genome could remove the rate limitation. The insertion of the aroZaroB cassette into the serA locus also results in strains that lack D-3phosphoglycerate dehydrogenase activity, which is an enzyme necessary for L-serine biosynthesis. Microbial growth in minimal medium without L-serine supplementation is only possible when the plasmid-localized serA gene is maintained by the serA strain. This strategy of employing nutritional pressure for plasmid maintenance is more

in the state of th

00; Dig

, ed

WQ

il.

(4F)

economical relative to using antibiotics and plasmid-localized genes encoding antibiotic resistance for plasmid maintenance during large-scale microbial cultivation. E. coli WN1 contains a second chromosomal insertion consisting of a tktAaroZ cassette inserted into the lacZ locus of the E. coli KL7 genome. E. coli transketolase encoded by tktA has been identified as one of the enzymes whose amplified expression results in increased availability of E4P, 112 one of the two substrates of DAHP synthase. Elevated transketolase activities increase the carbon flow into the shikimate pathway when DAHP synthase expression is amplified. Inclusion of a second copy of the aroZ gene enables more 3-dehydroshikimate be converted into protocatechuic acid by increasing the in vivo expression level of 3-dehydroshikimate dehydratase. The construction of E. coli KL7 has been described previously. Therefore, only the construction of E. coli WN1 is described in detail in this chapter.

Synthesis of the tktAaroZ Cassette

The 4.5 kb plasmid pSK4.99A was derived from the cloning vector pSU18.86 It contained a 2.2 kb DNA sequence encoding the *aroZ* gene and its native promoter. Digestion of pSK4.99A with restriction enzyme *SmaI* resulted in a linearized plasmid with an intact *aroZ* gene and two blunt-ended termini. The 2.2 kb *tktA* gene with its native promoter was obtained by digestion of plasmid pSK4.203A with *BamHI*. Further treatment of the DNA fragment with DNA polymerase I Klenow fragment converted the two termini into blunt-ends. Ligation of the *tktA* fragment with the modified pSK4.99A afforded plasmid pWN1.200A (Figure 27), in which both genes are transcribed in the same direction relative to the *lac* promoter of pSU18. Restriction enzyme digestion and

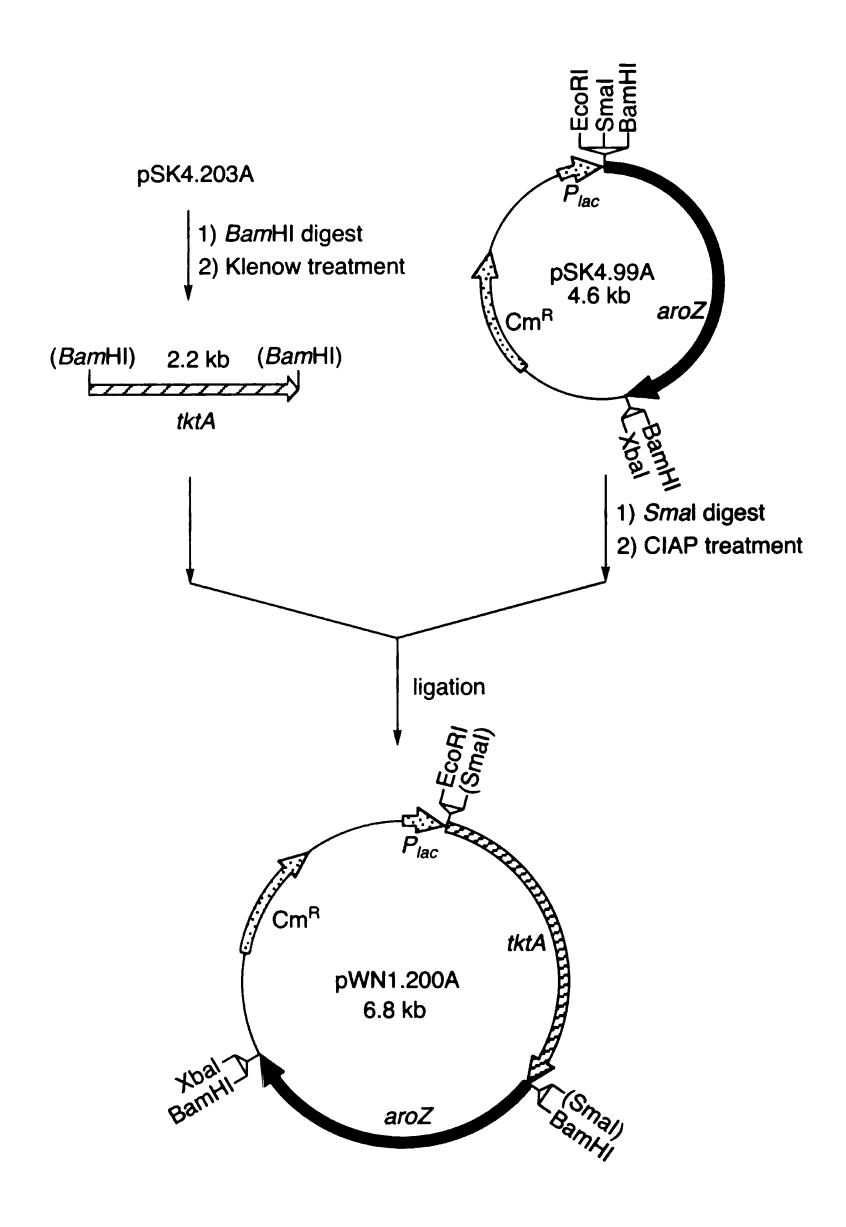


Figure 27. Preparation of plasmid pWN1.200A.

enzyme assay experiments verified that both *tktA* and *aroZ* genes carried by pWN1.200A encoded functional enzymes. The 2.5 kb *tktAaroZ* cassette was liberated from plasmid pWN1.200A by complete digestion with *XbaI* followed by partial digestion with *EcoRI*.

Genomic Insertion of the tktAaroZ Cassette into the lacZ Locus of E. coli KL7 to Generate E. coli WN1

Homologous recombination, a spontaneous event occurring in living organisms, is the process of exchanging sequence information between two homologous DNAs. It plays a major role in maintaining genome integrity and generating genetic diversity. Exploitation of this phenomenon led to the development of in vivo site-specific chromosomal modification methods applicable to microbe and plant systems.¹¹⁴ Genetic events including deletion, insertion, and single nucleotide mutation are achievable using homologous recombination methods.

In the process of constructing *E. coli* WN1, genomic insertion into the *lacZ* gene was guided by flanking the plasmid-localized *tktAaroZ* cassette with *lacZ* sequence. Successful genomic modification relies on two homologous recombination events consisting of integration of the whole plasmid containing *tktAaroZ* cassette into the genome, following by extrusion of a plasmid containing the entire *lacZ* gene out of the genome. As a consequence, the *tktAaroZ* cassette was inserted into the genomic *lacZ* locus. The homologous recombination experiment was carried out using plasmid pMAK705, which has a temperature-sensitive pSC101 replicon and a chloramphenicol resistance marker. Since derivatives of pMAK705 replicate at 30 °C but are unstable at 44 °C, isolation of all pMAK705 derivatives required culturing cells at 30 °C in the presence of Cm. However, identification of cells that harbor the plasmid inserted into the

genome must be carried out at 44 °C in the presence of Cm. After the second homologous recombination event, the *lacZ* locus is disrupted. The *lacZ* gene encodes β-galactosidase, which is essential for the metabolism of lactose in *E. coli*. Therefore, cells without functional β-galactosidase can be detected by observation of their growth characteristics on MacConkey agar containing lactose. MacConkey agar contains a pH indicator molecule, neutral red, which turns red under acidic pH. Since acidic molecules are produced when *E. coli* cells metabolize lactose, colonies of white color grown on MacConkey agar containing lactose should have a disrupted *lacZ* gene. For the purpose of maintaining strain stability, cells were cultured in medium without antibiotics to promote plasmid loss.

Construction of plasmids employed in the homologous recombination experiment was initiated by amplification of the *lacZ* gene from *E. coli* RB791 genome. Following digestion of the 3.1 kb PCR product with *Bam*HI, the DNA fragment was ligated with pMAK705 linearized with *Bam*HI. The resulting plasmid, pWN2.038A (Figure 28), contained the intact *lacZ* gene with its transcription under the control of *lac* promoter on pMAK705. Approximately 1.1 kb away from the start codon on the *lacZ* gene of pWN2.038A, there existed a unique *Eco*RV restriction enzyme recognition site, which facilitated the insertion of the synthetic cassette. After treatment of the 4.5 kb *tktAaroZ* cassette with DNA polymerase I Klenow fragment, it was subsequently inserted into the *Eco*RV site of pWN2.038A to yield plasmid pWN2.050B (Figure 29). Both *tktA* and *aroZ* genes are transcribed in the opposite direction relative to the *lac* promoter of pWN2.050B.

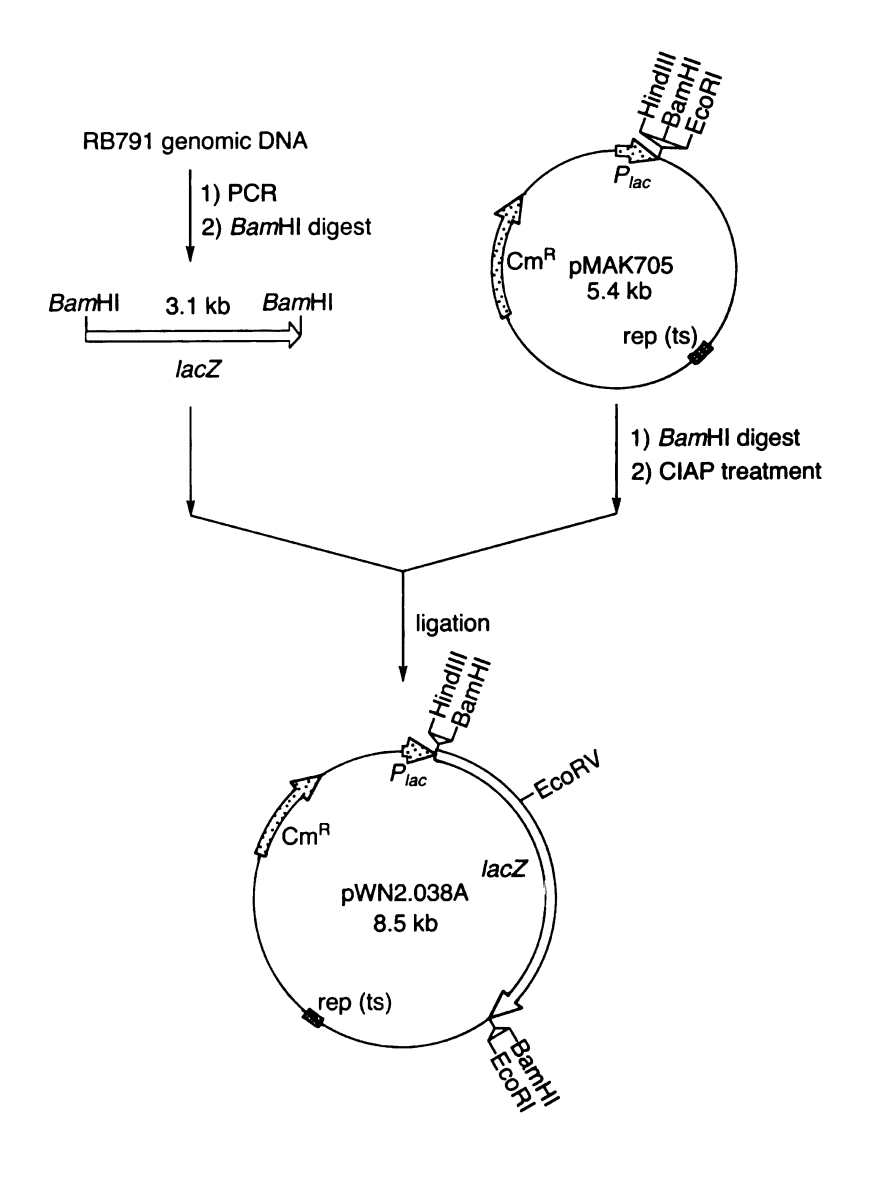


Figure 28. Preparation of plasmid pWN2.038A.

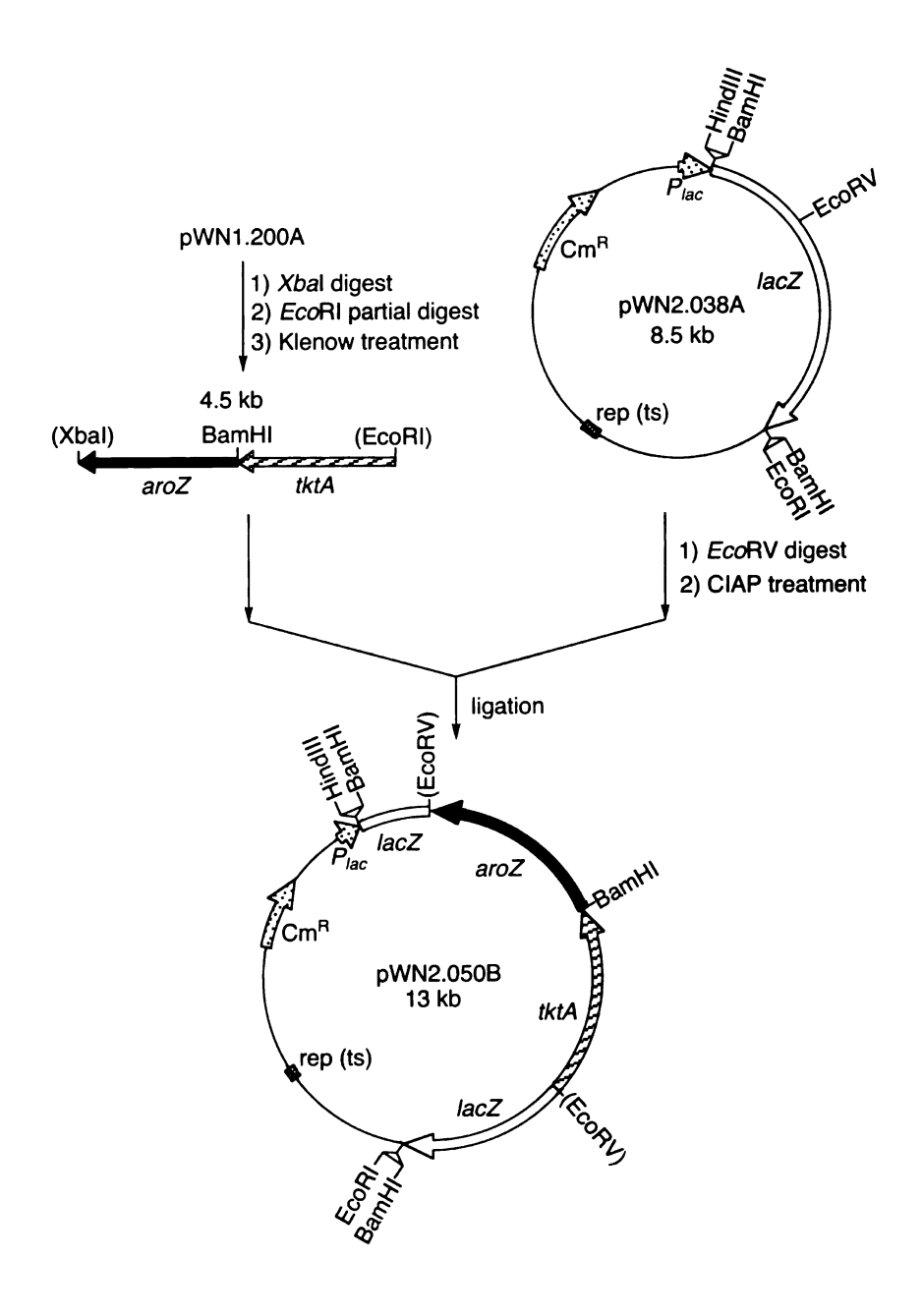


Figure 29. Preparation of plasmid pWN2.050B

Conditions for homologous recombination followed previously published procedures. 115 After transforming E. coli KL7 competent cells with plasmid pWN2.050B, the cells were spread onto LB plates containing Cm. Incubation of the plates at 44 °C, which is a non-permissive temperature for the pSC101 replicon, allows the selection of cells with genomic integration. Subsequent culturing of the resulting cointegrates in LB medium overnight at 30 °C, which is a permissive temperature for the pSC101 replicon, results in the excision of plasmid from genome. Cultures diluted (1:20,000) with LB medium were grown two more cycles at 30 °C for 12 h to enrich rapidly growing cells that had lost the temperature-sensitive replicon. Further release of plasmids was promoted by three cycles of culturing cells in LB medium at 44 °C for 12 h. After serial dilution of each culture, cells were spread onto MacConkey plates containing lactose and incubated at 30 °C for 12 h. White colonies that grew on the plates were further screened on multiple plates to select for the desired E. coli strain. E. coli WN1 was isolated based on the following growth characteristics: growth as a white colony on MacConkey agar containing lactose; no growth on M9 containing aromatic amino acids and aromatic vitamins; growth on M9 containing aromatic amino acids, aromatic vitamins, and serine; growth on LB; and no growth on LB containing Cm.

B. Plasmid Construction

Overview

Four plasmids were employed in this study. The common genetic elements shared by the plasmids include $aroF^{FBR}$, aroY, catA, and serA genes and the P_{aroF} DNA sequence. The $aroF^{FBR}$ gene encodes a feedback insensitive isozyme of 3-deoxy-D-

group o the shi inhibit were accum

> effect encod

3C:[V3

conta

and a

thon

||X||

- 12-

of pla

Colv.

inpin)

this fra

ingfills

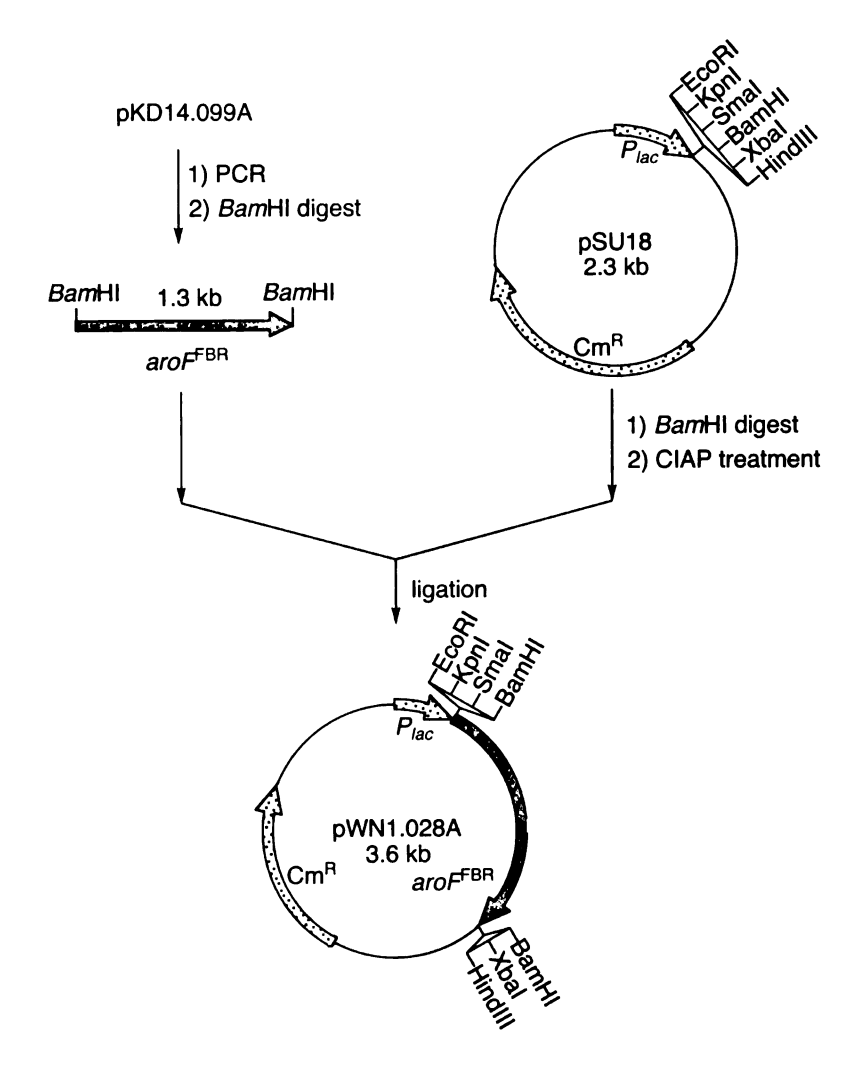
arabino-heptulosonic acid 7-phosphate (DAHP) synthase. Previous research in this group demonstrated that DAHP synthase is the primary gatekeeper of carbon flow into the shikimate pathway. Expression of a DAHP synthase insensitive to the feedback inhibition by the aromatic amino acids resulted in elevated enzyme activity when cells were cultured in medium containing aromatic amino acids and increaseed the accumulation of shikimate pathway metabolites.^{111a} Because the transcription of the aroF^{FBR} gene from its native promoter is regulated by promoter-binding, tyrosineactivated TyrR repressor protein, 116 inclusion of the promoter region (P_{avoF}) , which contains three binding sequences for the TyrR protein, alleviates the down regulation effect caused by TyrR. The Klebsiella pneumoniae protocatechuate decarboxylase encoded by aroY^{109,117} and the Acinetobacter calcoaceticus catechol 1.2-dioxygenase encoded by catA¹¹⁸ are enzymes required for the E. coli synthesis of cis,cis-muconic acid, and are responsible, respectively, for the conversion of protocatechuate into catechol and catechol into cis, cis-muconic aicd. Due to the serA mutation in E. coli KL7 and E. coli WN1 genomes, plasmid-localized serA is necessary for their growth in medium without L-serine supplementation. This provided the nutritional pressure for stable maintenance of plasmids carrying serA by E. coli KL7 and E. coli WN1.

Construction of pWN1.162A and pWN1.184A

A 1.25 kb DNA fragment encoding $aroF^{FBR}$ with its native promoter was amplified from plasmid pKD14.099A and subsequently digested by BamHI. Ligation of this fragment into the BamHI site on pSU18 resulted in pWN1.028A (Figure 30). The $aroF^{FBR}$ gene was transcribed in the same direction as the lac promoter located on pSU18.

Previous experiments verified that the promoter of the *Klebsiella pneumoniae aroY* gene could initiate its own transcription in *E. coli*. ^{106,109} Therefore, a 2.4 kb DNA sequence encoding *aroY* and its promoter was amplified from plasmid pKD9.080A and inserted into the *KpnI* site of pWN1.028A. The *aroY* gene of the resulting plasmid, pWN1.079A (Figure 31), was transcribed in the same direction as *aroF*^{FBR}. Efficient heterologous expression of the *Acinetobacter calcoaceticus catA* gene in *E. coli* was realized by inserting the 1.0 kb PCR product of *catA* with its ribosomal binding site into the *EcoRI* multiple cloning site on pWN1.079A. In the resulting plasmid, pWN1.094A (Figure 32), transcription of *catA* is initiated by the pSU18-encoded *lac* promoter. Insertion of a 1.9 kb *serA* DNA sequence liberated from plasmid pD2625 into the *SmaI* site on pWN1.094A resulted in plasmid pWN1.106A (Figure 33). Subsequent ligation of the *P_{aroF}* DNA fragment ¹¹⁶ into the *XbaI* recognition site on pWN1.106A afforded plasmid pWN1.162A (Figure 34).

Plasmid pWN1.184A (Figure 35) is derived from plasmid pWN1.162A and contains one additional copy of the *aroZ* gene. Digestion of plasmid pSK4.99A with *Bam*HI liberated a 2.3 kb DNA fragment containing the *aroZ* gene and its native promoter. Following treatment with DNA polymerase I Klenow fragment, the DNA product was ligated with linearized pWN1.162A, which had been digested by *HindIII* and treated by Klenow fragment. The *aroZ* gene of pWN1.184A was transcribed in the same orientation as the *lac* promoter of pSU18.



 $\label{eq:figure 30.Preparation of plasmid pWN1.028A. }$

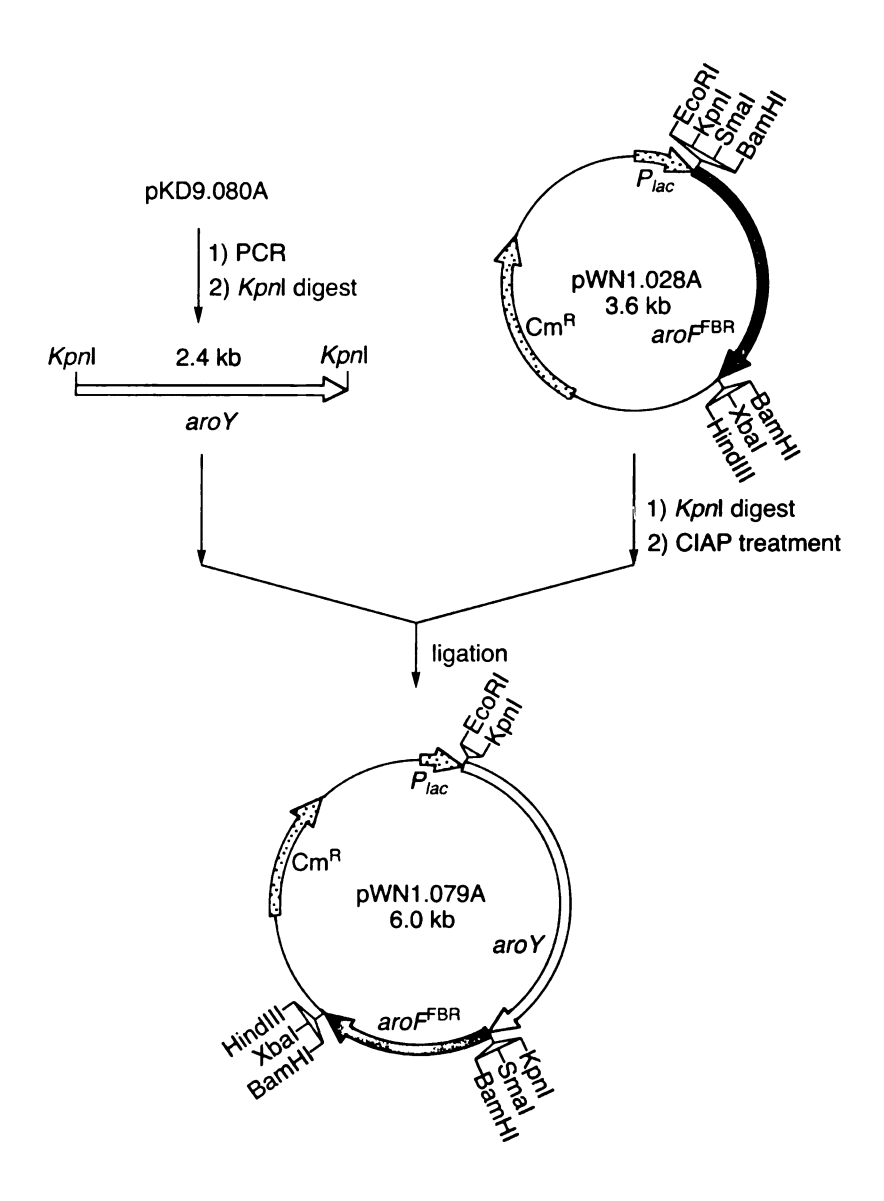


Figure 31. Preparation of plasmid pWN1.079A.

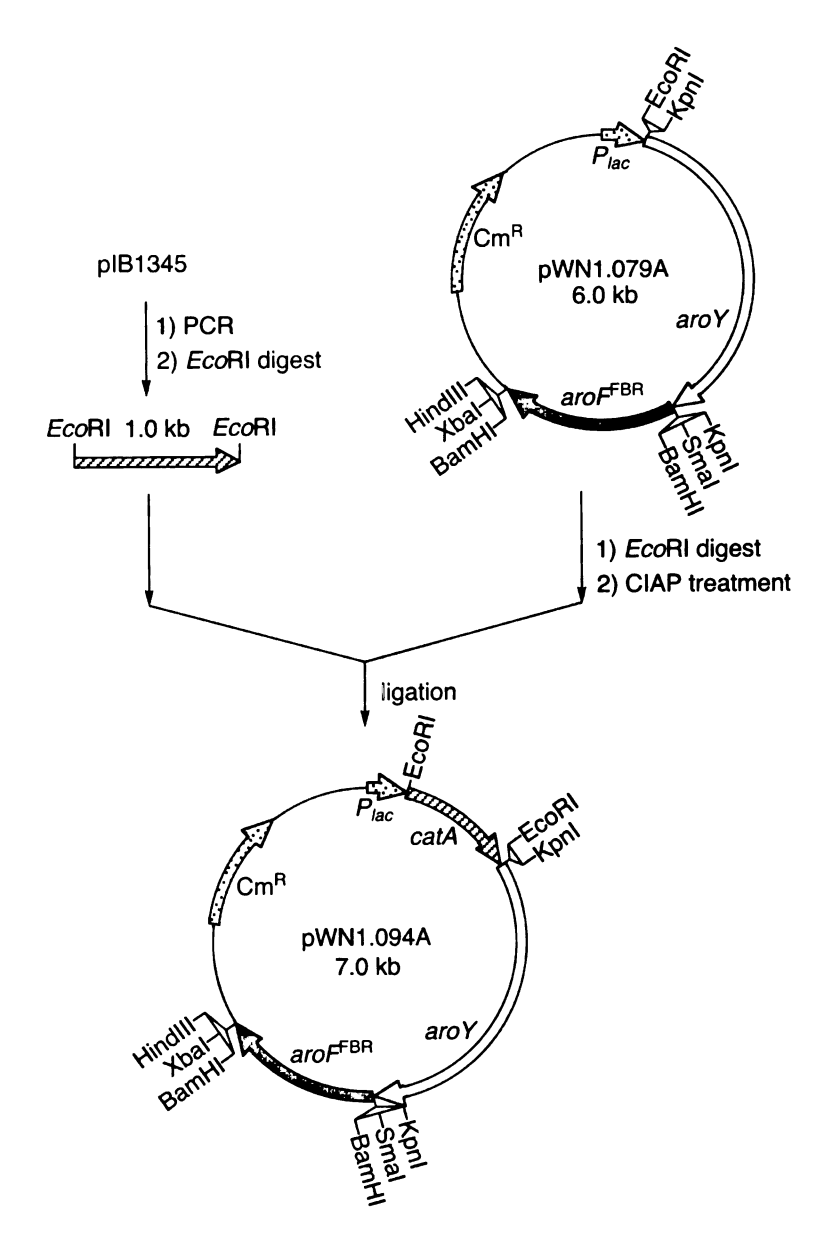
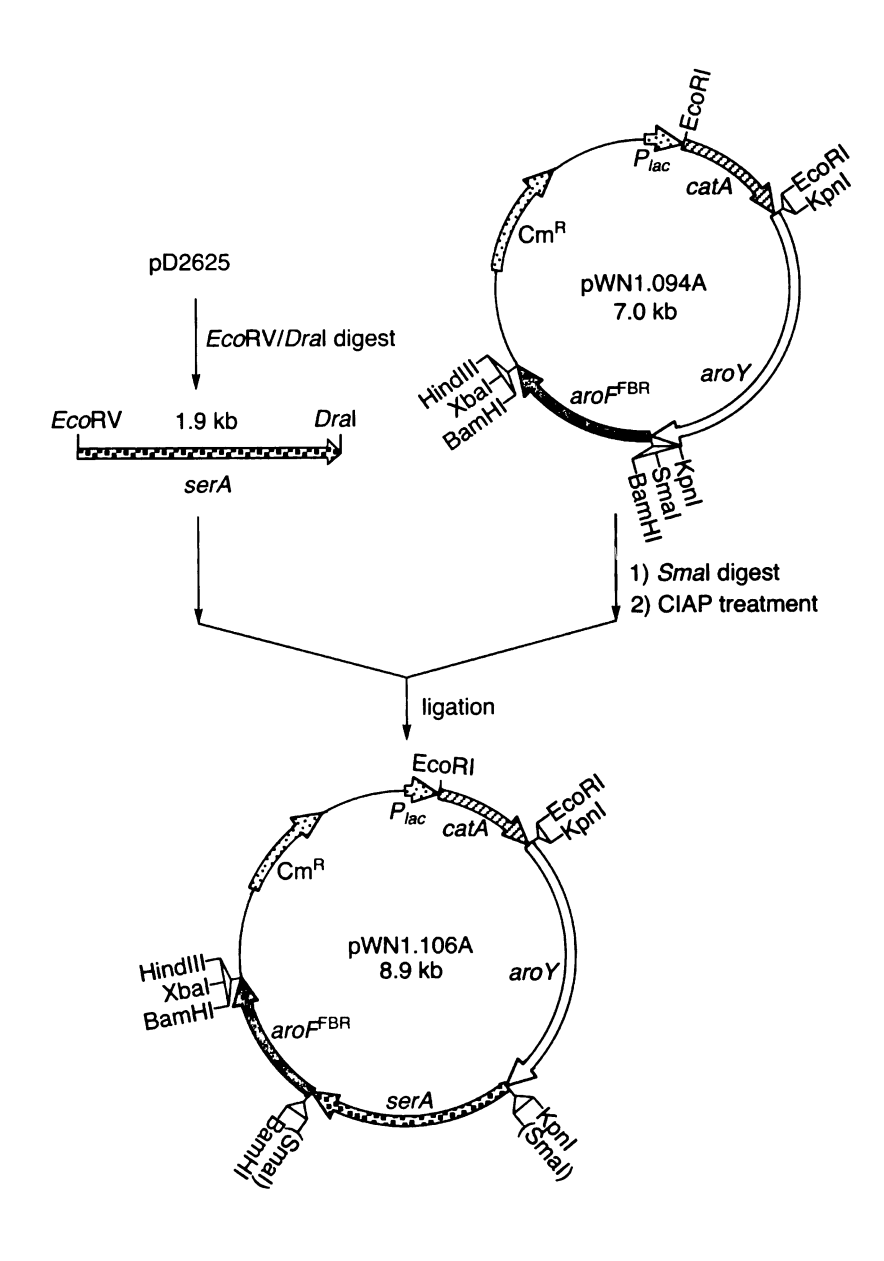


Figure 32. Preparation of plasmid pWN1.094A.



 $\label{eq:Figure 33. Preparation of plasmid pWN1.106A. }$

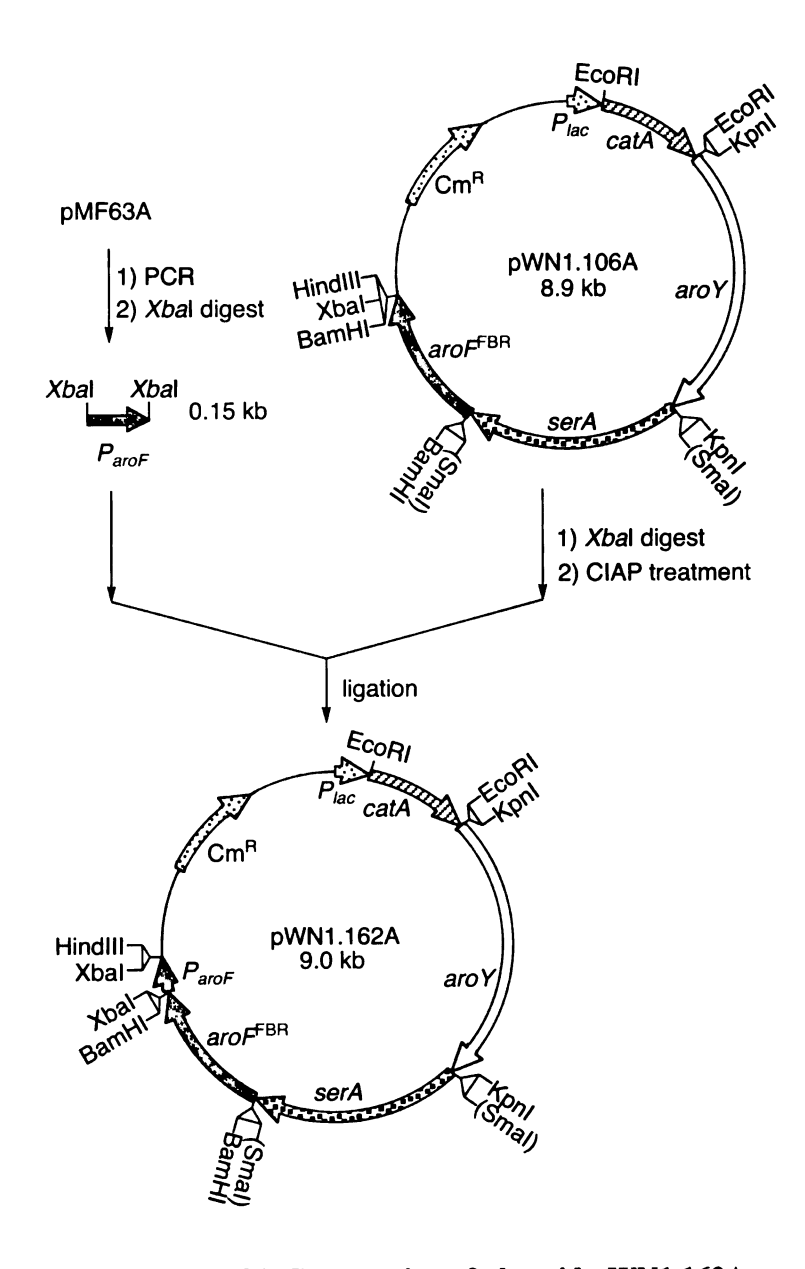


Figure 34. Preparation of plasmid pWN1.162A.

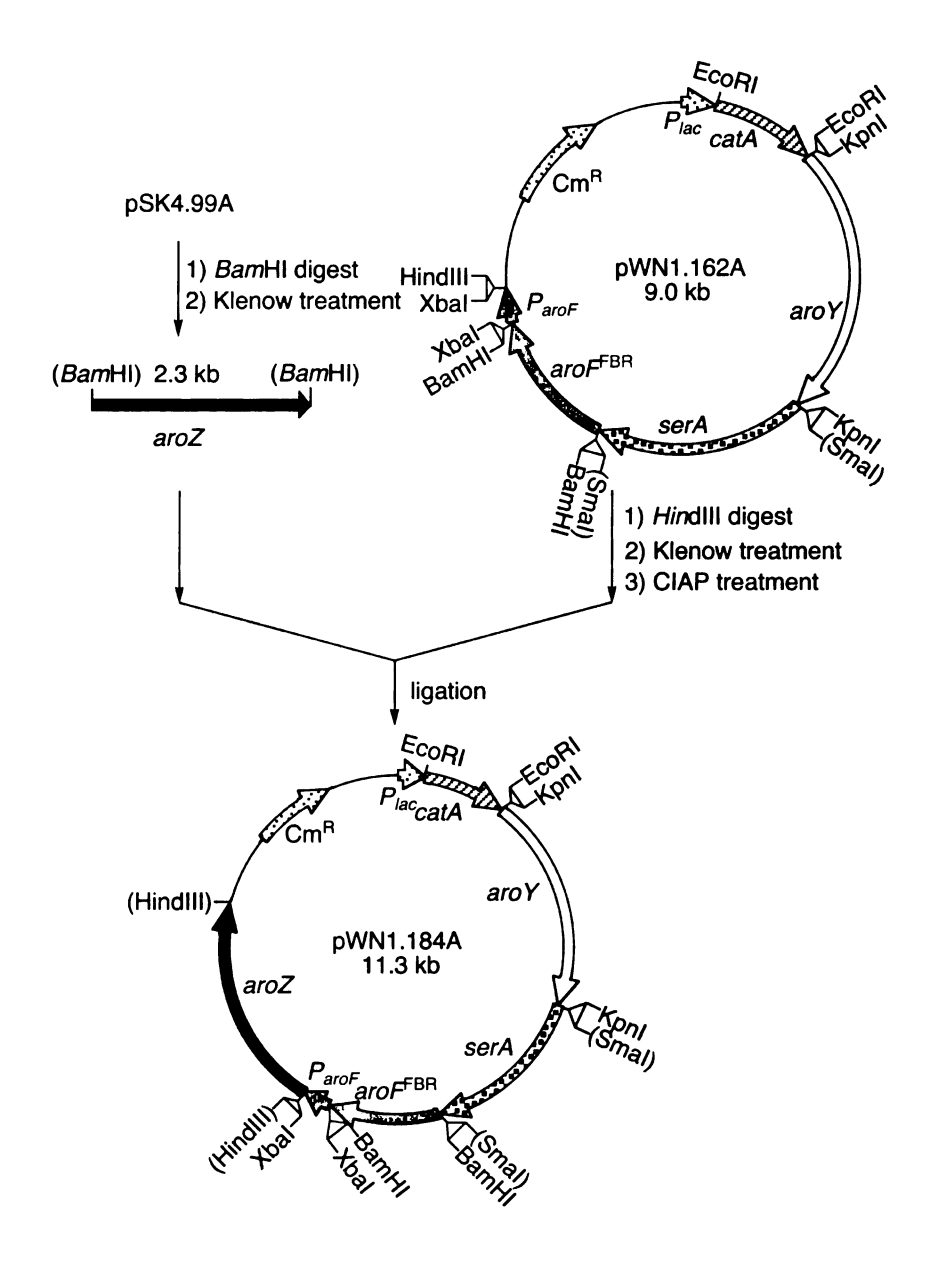


Figure 35. Preparation of plasmid pWN1.184A.

Construction of pWN2.100B

On plasmid pWN2.100B, the transcription of the catA gene was initiated by the tac promoter on pJF118EH.¹¹⁹ Due to the existence of a copy of the plasmid-localized lacl^Q gene, the transcriptional level of catA could be controlled by the IPTG concentration in growth medium. A 1.0 kb DNA fragment containing catA and its native ribosomal binding site was liberated from plasmid pWN1.094A by digestion of *EcoRI*. Insertion of the isolated DNA product into the EcoRI site of pJF118EH resulted in plasmid pWN2.064A (Figure 36). Digestion of plasmid pKD9.046B with HindIII afforded a 2.4 kb DNA fragment containing aroY and its native promoter, which was subsequently treated with Klenow fragment. Plasmid pWN2.064A was digested with BamHI and treated with Klenow fragment. Ligation of the two DNA products resulted in plasmid pWN2.084A (Figure 37). The aroY gene was transcribed in the same orientation as the catA gene. A 3.3 kb DNA fragment containing serA, aro F^{FBR} , and P_{graf} sequences was amplified from the plasmid pWN1.162A. Following digestion with SmaI, the PCR product was ligated with plasmid pWN2.084A, which was linearized by HindIII and treated with Klenow. The transcription of serA and aroY gene on the resulting plasmid, pWN2.100B (Figure 38), was in the opposite direction of tac promoter on pJF118EH.

Construction of pWN2.248

A 2.5 kb DNA fragment containing the *catA* gene with its ribosomal binding site and a downstream gene encoding a protein with unknown function was amplified from plasmid pIB1343.^{118a} The PCR product was ligated into the *Eco*RI site of pJF118EH to afford plasmid pWN2.242A (Figure 39). The transcription of *catA* and the unidentified

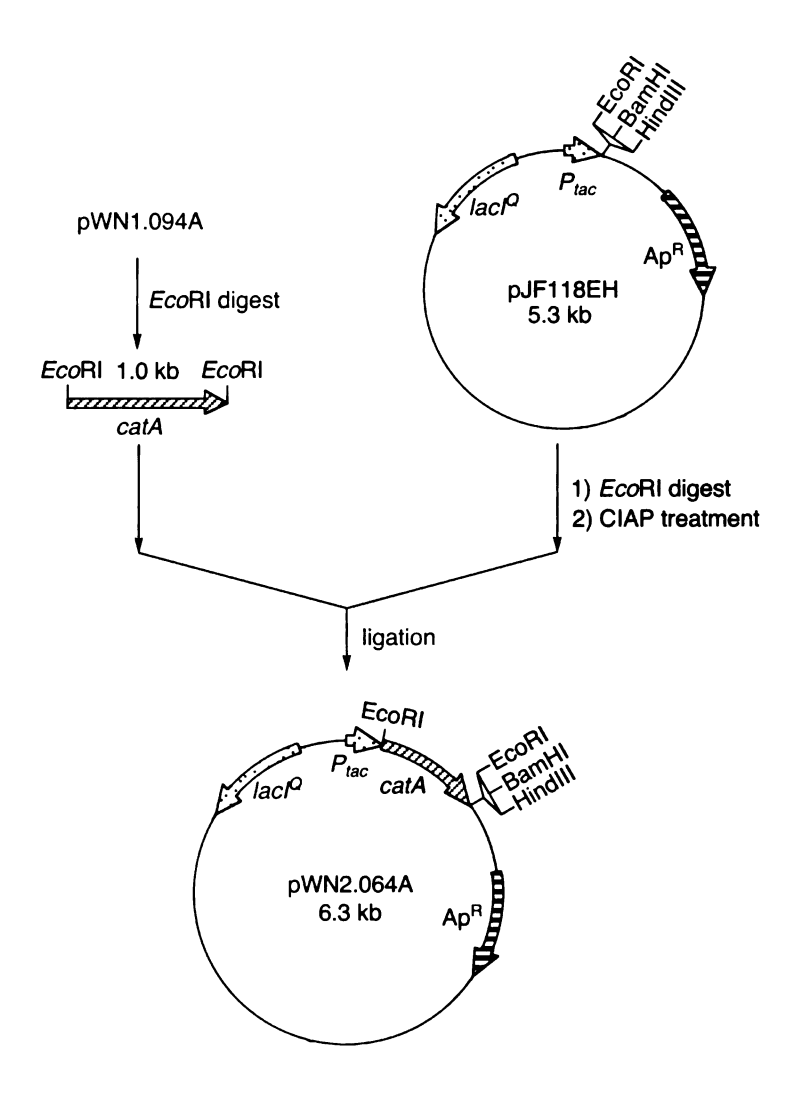


Figure 36. Preparation of plasmid pWN2.064A.

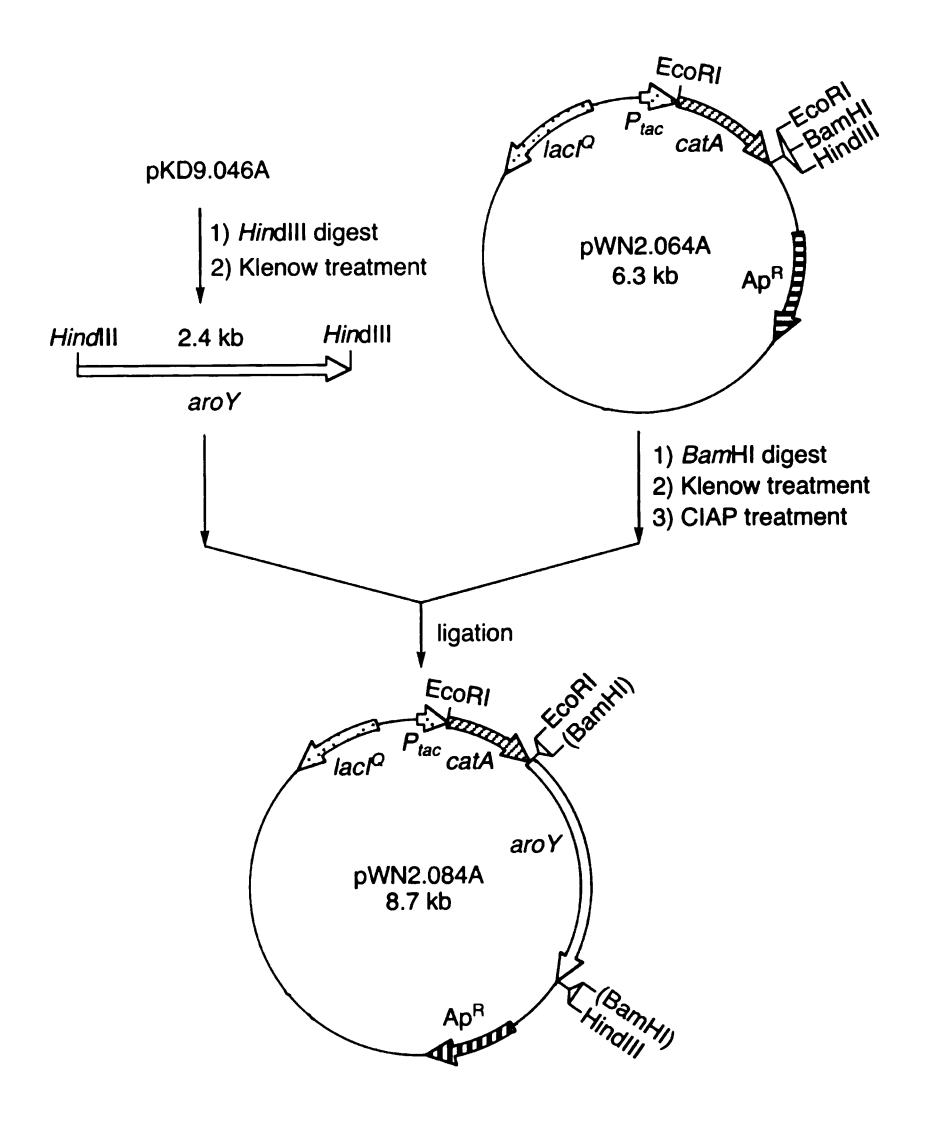


Figure 37. Preparation of plasmid pWN2.084A.

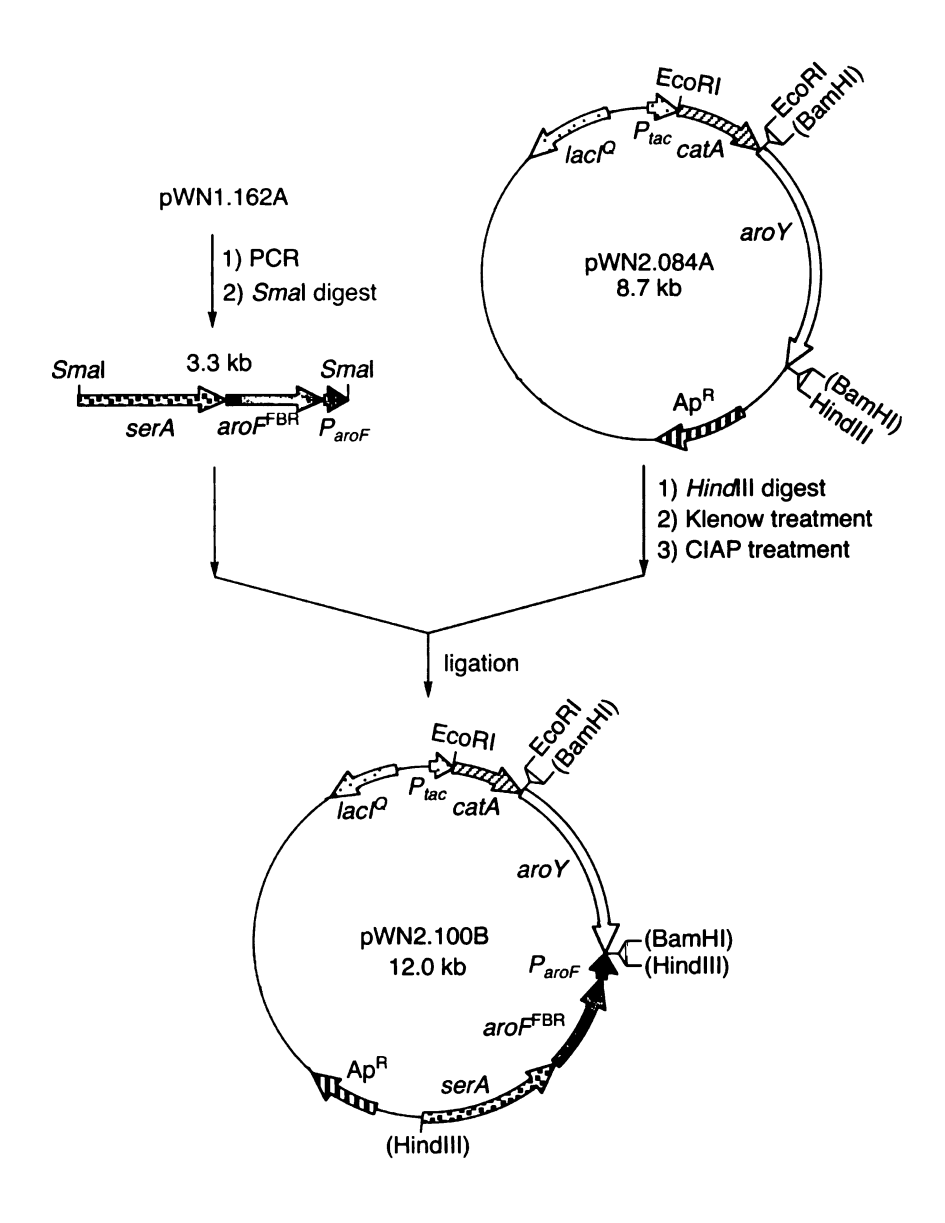


Figure 38. Preparatio of plasmid pWN2.100B.

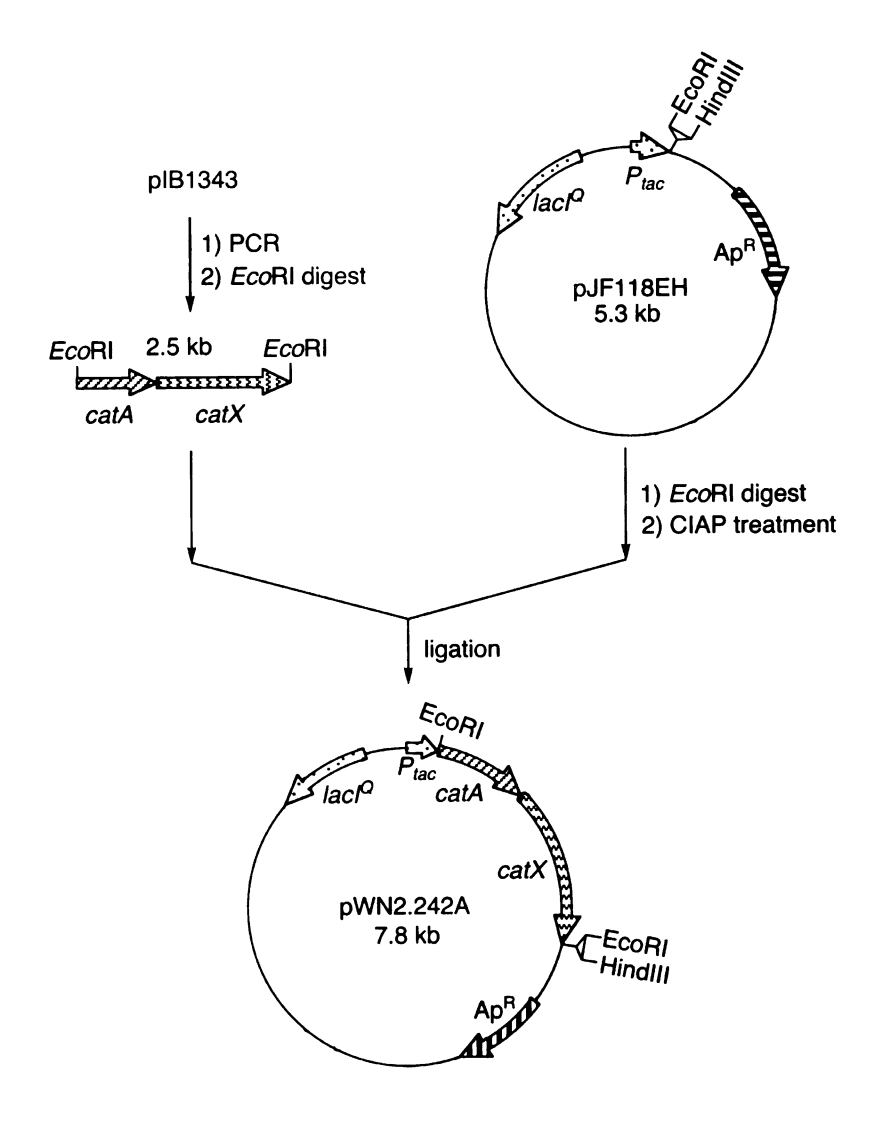


Figure 39. Preparation of plasmid pWN2.242A.

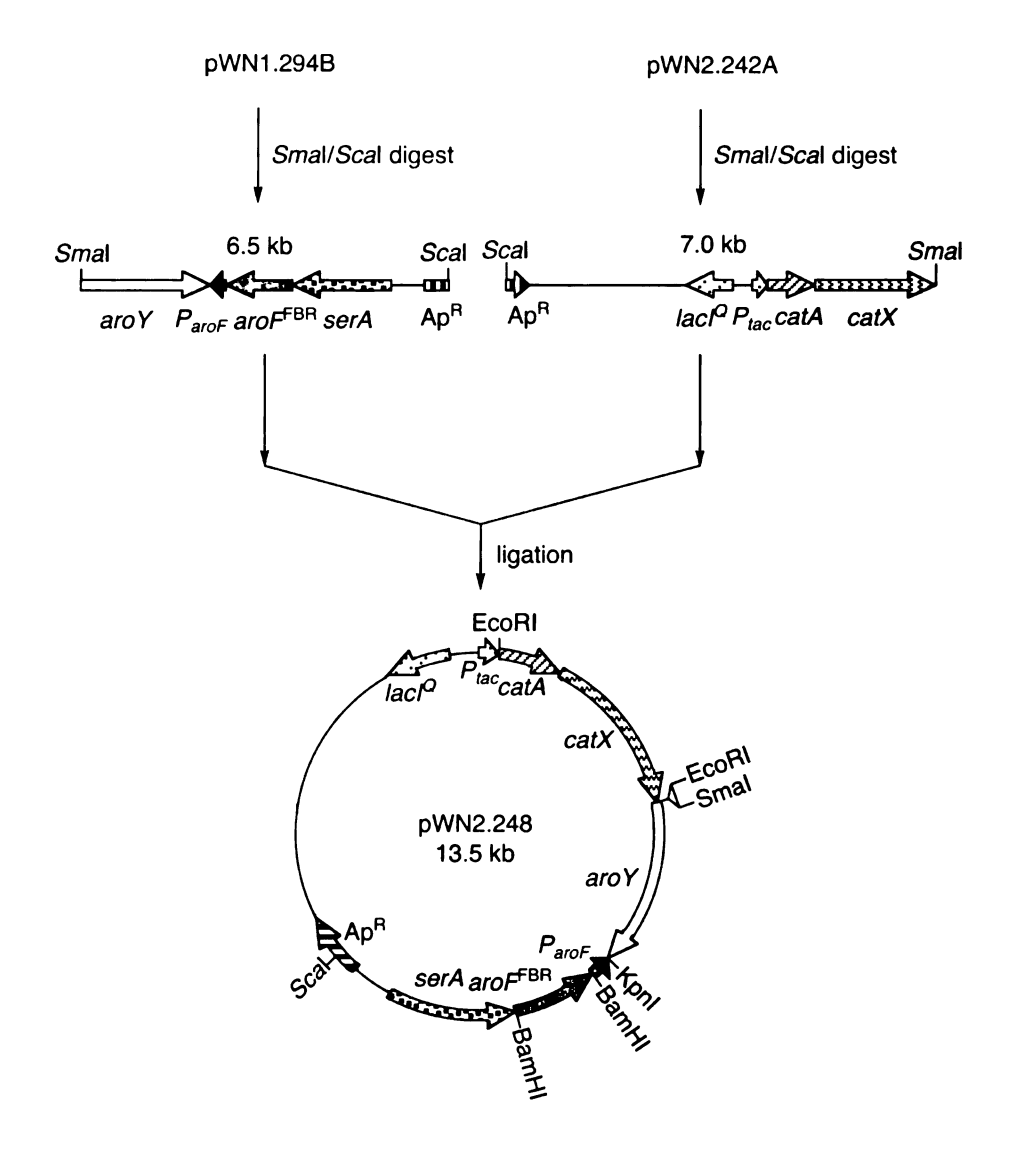


Figure 40. Preparation of plasmid pWN2.248.

šst

wit P₂

pla

Fed

M2

acqi Bra

сеп

jerri

H_:S

Sien

Taji Fed

0, 1

Chia gluci

ĽĽ (

19_{/ 1}

gene was initiated by the tac promoter on pJF118EH. Digestion of plasmid pWN1.294B with SmaI and ScaI liberated a 6.5 kb DNA sequence encoding aroY, serA, $aroF^{FBR}$, and P_{aroF} . Ligation of this fragment with pWN2.242A treated with SmaI and ScaI resulted in plasmid pWN2.248 (Figure 40).

C. Fed-Batch Fermentor Synthesis of cis,cis-Muconic Acid

Fed-Batch Fermentor Conditions

Fermentor-controlled cultivations employed a 2.0 L working capacity B. Braun M2 culture vessel connected to a B. Braun Biostat MD controlled by a DCU-3. Data acquisition utilized a Dell Optiplex Gs⁺ 5166M personal computer (PC) equipped with B. Braun MFCS/Win software (v1.1). Temperature, pH, and glucose feeding were controlled with PID control loops. Temperature was maintained at 36 °C for all fermentations. The pH was maintained at 7.0 by addition of concentrated NH₄OH or 2 N H₂SO₄. Dissolved oxygen (D.O.) was measured using a Mettler-Toledo 12 mm sterilizable O₂ sensor fitted with an Ingold A-type O₂ permeable membrane. D.O. was maintained at 10% air saturation. Antifoam (Sigma 204) was added manually as needed. Fed-batch fermentations were run in duplicate, and reported results represent an average of the two runs.

Fed-batch fermentations were carried out under conditions as described in Chapter 2 with several modifications. The most significant change was the use of glucose as the carbon source in place of glycerol. Inoculants were initially grown in 5 mL of M9 medium for 24 h at 37 °C with agitation. This culture was then transferred to 100 mL of fresh M9 medium, cultured at 37 °C and 250 rpm for an additional 10 h. The

fermentation was initiated (t = 0) when the culture ($OD_{600} = 1.0$ -3.0) was transferred to the fermentor. The initial glucose concentration in the fermentation medium ranged from 20 to 24 g/L according to the growth requirement of different constructs.

The same three-staged method as described in Chapter 2 was employed to maintain D.O. level at 10% through the fermentations. However, the maximum impeller speed was set at 940 rpm, and a glucose solution (65%, w/v) was employed as the carbon source. Under a second set of fermentation conditions, a stainless steel baffle cage consisting of four 1/2" x 5" baffles was placed in the fermentation vessel. Fed-batch cultures with the baffle cage were run using the same conditions employed in the absence of baffles except that the maximum impeller speed was set at a slightly lower value. Appropriate amounts of IPTG stock solution (100 mM) were added to the fermentations of *E. coli* WN1/pWN2.248 at 13 h, 18 h, 24 h, 30 h, 36 h, and 42 h. During a typical 48 h fermentation run, *E. coli* cell growth entered logarithmic phase 6 h after inoculation and reached stationary phase after 24 h. The maximum dry cell weight for each run varied from 20 to 30 g/L.

Synthesis of cis, cis-Muconic Acid Using E. coli KL7/pWN1.162A

The first cis,cis-muconate-synthesizing biocatalyst examined under fed-batch fermentor conditions was $E.\ coli\ KL7/pWN1.162A$. Inclusion of a plasmid-localized $aroF^{FBR}$ gene and plasmid-localized P_{aroF} sequence in KL7/pWN1.162A increased the in vivo activity of DAHP synthase, which is the first and also the rate-determining enzyme in the common pathway.^{111a} Further expression of two genomic copies of the aroB gene eliminated the limitation of 3-dehydroquinate synthase activity. As a result, DAHP

synthesized in the first step could be converted into 3-dehydroquinate efficiently. Therefore, if any other intermediate involved in the biosynthesis of *cis,cis*-muconic acid was detected during the cultivation of *E. coli* KL7/pWN1.162A under fermentor-controlled conditions, it indicated that the enzyme for which the accumulated intermediate was a substrate was a rate-limiting enzyme in *cis,cis*-muconic acid biosynthesis. Future improvement of the biocatalyst would concentrate on increasing the specific activity of the rate-limiting enzyme. On the other hand, if no intermediates were detected in significant concentration when *E. coli* KL7/pWN1.162A was cultured, it would allow us to devote efforts into further increasing the carbon flow directed into *cis,cis*-muconic acid biosynthesis.

Table 7. Product and Byproducts Synthesized by *E. coli* KL7/pWN1.162A after 48 h of Cultivation Under Fermentor-Controlled Conditions.

[ccMA] ^a (g/L)	ccMA yield (%) ^b	[DHS] (g/L)	[Catechol] (g/L)	total yield (%) ^c
20.9	19	6.1	0.1	24

^a Abbreviations: cis,cis-muconic acid (ccMA), 3-dehydroshikimate (DHS); ^b Given as (mol of ccMA)/(mol of glucose); ^c Given as (mol of ccMA + mol of DHS + mol of catechol)/(mol of glucose).

E. coli KL7/pWN1.162A was examined under fed-batch fermentor conditions at pH 7.0, 36 °C, and a D.O. level of 10%. After 48 h of cultivation, 20.9 g/L of cis,cis-muconic acid was synthesized in a 19% (mol/mol) yield from glucose (Figure 41). Intermediates 3-dehydroshikimate and catechol were also produced by the biocatalyst (Table 7). Catechol was only detected at the end of the cultivation in a concentration of 0.1 g/L. However, 3-dehydroshikimate was observed at 12 h and increased throughout the cultivation. 3-Dehydroshikimate formation reached 6.1 g/L and constituted 4.7%

glucose consumed by the microbe. The significant accumulation of 3-dehydroshikimate in the culture medium by *E. coli* KL7/pWN1.162A indicated that the specific activity of 3-dehydroshikimate dehydratase was inadequate.

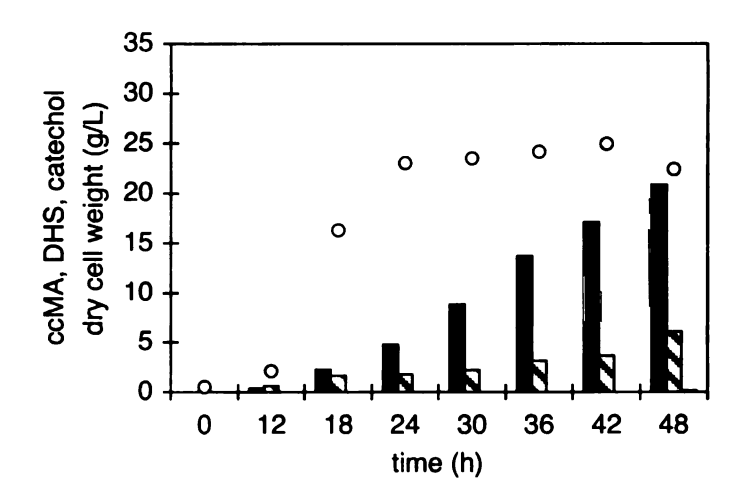


Figure 41. Biosynthesis of *cis,cis*-muconic acid by *E. coli* KL7/pWN1.162A under fed-batch fermentor conditions. • dry cell weight; — *cis,cis*-muconic acid (ccMA); 3-dehydroshikimate (DHS); — catechol.

3-Dehydroshikimate Dehydratase Activity

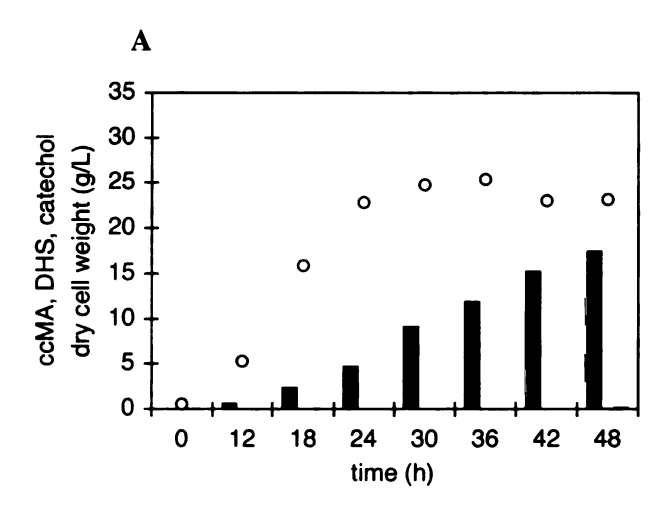
For the purpose of increasing the in vivo activity of 3-dehydroshikimate dehydratase, two approaches were examined. Plasmid pWN1.184A was derived from plasmid pWN1.162A by including one copy of the *aroZ* gene and its native promoter. In a second approach, *E. coli* WN1 was created from *E. coli* KL7, which already carried a *serA::aroBaroZ* insert, by including an extra chromosomal insertion of the *tktAaroZ* cassette into the *lacZ* gene. Therefore, 3-dehydroshikimate dehydratase was expressed from one genome-localized and one plasmid-localized *aroZ* gene in *E. coli* KL7/pWN1.184A, while *E. coli* WN1/pWN1.162A contained two genomic copies of the *aroZ* gene.

Table 8. Product and Byproducts Synthesized by E. coli KL7/pWN1.184A and E. coli WN1/pWN1.162A after 48 h of Cultivation Under Fermentor-Controlled Conditions.

construct	[ccMA] ^a (g/L)	ccMA yield (%) ^b	[DHS] (g/L)	[Catechol] (g/L)	total yield (%) ^c
KL7/pWN1.184A	17.4	21	0.0	0.1	21
WN1/pWN1.162A	31.1	23	2.1	0.3	24

[&]quot;Abbreviations: cis,cis-muconic acid (ccMA), 3-dehydroshikimate (DHS); b Given as (mol of ccMA)/(mol of glucose); c Given as (mol of ccMA + mol of DHS + mol of catechol)/(mol of glucose).

After culturing E. coli KL7/pWN1.184A under fed-batch fermentor conditions for 48 h, no 3-dehydroshikimate was observed in the fermentation broth (Figure 42A). However, this construct only produced 17.4 g/L of cis,cis-muconic acid in a yield of 21% (Table 8). Enzyme assays performed every 12 h indicated that the specific activity of 3dehydroshikimate dehydratase ranged from 0.12 to 0.17 U/mg relative to undetectable activity in E.coli KL7/pWN1.162A (Table 9). At the same time, a twofold to sevenfold decrease of DAHP synthase specific activity was also observed relative to E. coli KL7/pWN1.162A (Table 9). As derivatives of cloning vector pSU18, plasmid pWN1.162A and pWN1.184A have a common p15A replicon, which results in 10-15 copies of plasmid in E. coli host strains. 120 As a consequence, significantly higher 3dehydroshikimate dehydratase expression level was detected in E. coli KL7/pWN1.184A. However, overexpression of 3-dehydroshikimate dehydratase may have imposed a significant metabolic burden. This extra metabolic burden might cause the decreased specific activity of DAHP synthase, which further limits the carbon flow directed into the cis, cis-muconic acid biosynthesis pathway. When E. coli WN1/pWN1.162A was examined under fed-batch fermentor conditions (Figure 42B), no significant change of



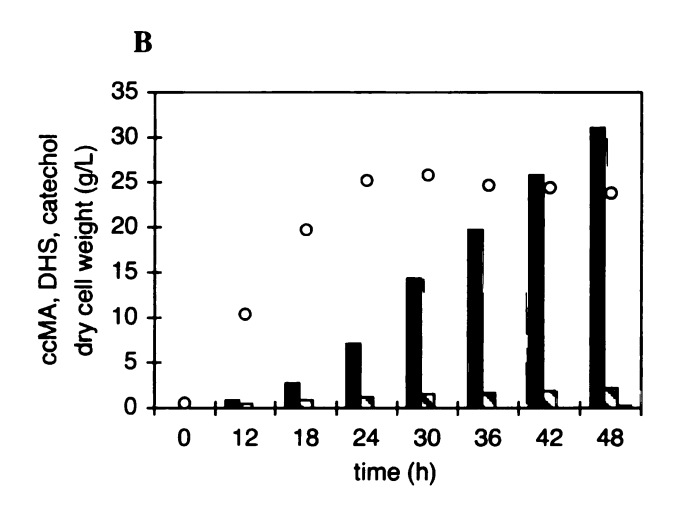


Figure 42. Biosynthesis of cis,cis-muconic acid under fed-batch fermentor conditions. (a) E. coli KL7/pWN1.184A, (b) E. coli WN1/pWN1.162A: • cell dry weight; cis,cis-muconic acid (ccMA); 3-dehydroshikimate (DHS); catechol.

Table 9. DAHP Synthase and 3-Dehydroshikimate Dehydratase Specific Activities.

construct	DAHP synthase activity (U/mg)			DHS dehydratase activity (U/mg)				
	12h	24h	36h	48h	12h	24h	36h	48h
KL7/pWN1.162A	0.32	0.36	0.27	0.15	-	-	-	-
KL7/pWN1.184A	0.11	0.05	0.09	0.09	0.17	0.12	0.15	0.14
WN1/pWN1.162A	0.29	0.35	0.23	0.19	n.d.	n.d.	n.d.	n.d.

^{-:} not measured; n.d.: not detectable.

DAHP synthase activity was observed relative to *E. coli* KL7/pWN1.162A (Table 9). Although the 3-dehydroshikimate dehydratase activity was still undetectable in this construct, it was able to synthesize 31.3 g/L of *cis,cis*-muconic acid in a yield of 23% and accumulated only 2.1 g/L of 3-dehydroshikimate (Table 8). Insertion of the second genomic copy of the *aroZ* gene on *E. coli* WN1 reduced the number of plasmid-localized genes and apparently avoided the detrimental impact associated with expression of plasmid-localized *aroZ* on *cis,cis*-muconic acid biosynthesis.

The Impact of Increased Oxygen Availability on Synthesis of cis,cis-Muconic Acid Using E. coli WN1/pWN1.162A

To further improve the concentration of *cis,cis*-muconic acid synthesized by *E. coli* WN1/pWN1.162A, the impact of increasing the level of oxygen transfer into the fermentation vessel was explored. Inclusion of a stainless steel baffle cage consisting of four 1/2" x 5" baffles in the fermentation vessel accompanied by a slight decrease of the maximum impeller speed from 940 rpm to 900 rpm resulted in an approximately 35% increase in the oxygen transfer rate in the culture medium. Throughout a fed-batch fermentation run, the dissolved oxygen level controls the glucose feeding. Therefore, an

elevated oxygen transfer rate results in an accelerated glucose-feeding rate, which might translate into increased synthesis of *cis*, *cis*-muconic acid.

Table 10. Product and Byproducts Synthesized by *E. coli* WN1/pWN1.162A Under Modified Fed-Batch Fermentor Conditions after 48 h of Cultivation.

[ccMA] ^a (g/L)	ccMA yield	[DHS] (g/L)	[Catechol] (g/L)	total yield (%)°		DAHP synthase activity (U/mg)			
	$(\%)^{b}$	(8,2)	(8,2)		12h	24h	36h	48h	
19.8	15	3.7	3.8	22	0.27	0.28	0.20	0.1	

^a Abbreviations: cis,cis-muconic acid (ccMA), 3-dehydroshikimate (DHS); ^b Given as (mol of ccMA)/(mol of glucose); ^c Given as (mol of ccMA + mol of DHS + mol of catechol)/(mol of glucose).

E. coli WN1/pWN1.162A was examined under the modified fed-batch fermentor conditions. Cell dry weight reached the highest value 30 h after the fermentor's culture medium was inoculated (Figure 43). At the same time point, approximately 0.4 g/L of catechol accumulated in the culture medium. During the rest of the cultivation, a continued accumulation of catechol was accompanied by a decline in dry cell weight and difficulty in controlling the dissolved oxygen level. At 48 h, 3.8 g/L of catechol had been generated, while only 19.8 g/L of cis,cis-muconic acid was synthesized (Table 10). An elevated amount of 3-dehydroshikimate (3.7 g/L) was also observed relative to fermentation runs lacking an installed baffle cage. The accumulation of catechol suggested that insufficient catechol 1,2-dioxygenase activity was expressed when oxygen availability was increased. Earlier research in this group has revealed that catechol could interfere with E. coli metabolism particularly during microbial growth. ¹⁰⁹ Increased formation of catechol might therefore impair cis,cis-muconic acid biosynthesis.

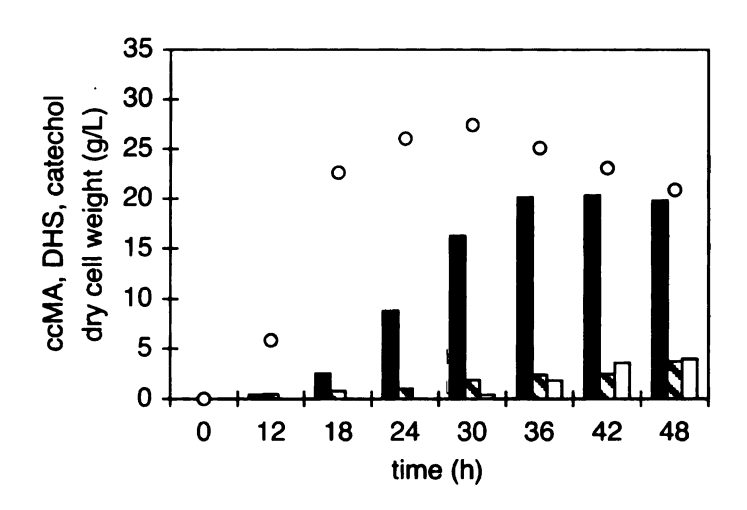


Figure 43. Biosynthesis of cis, cis-muconic acid by E. coli WN1/pWN1.162A when oxygen availability was increased. • cell dry weight; — cis, cis-muconic acid (ccMA); — 3-dehydroshikimate (DHS); — catechol.

Catechol 1,2-Dioxygenase Activity

One approach taken to increase the level of catechol 1,2-dioxygense expression entailed replacement of the *lac* promoter in plasmid pWN1.162A with a strong *tac* promoter. Use of a stronger promoter led to a tighter RNA polymerase binding event, which resulted in a higher transcription level. In order to prevent the possible detrimental effect caused by high-level expression of *catA* gene, cloning vector pJF118EH was chosen to construct the new plasmids. The *lacI*^Q gene located on pJF118EH encodes a *lac* repressor protein, which could repress the transcription initiated by the plasmid-localized *tac* promoter via binding on its *lac* operator region. Lactose and isopropyl β-D-thiogalactopyranoside (IPTG) can alleviate this transcriptional repression by binding with the repressor protein. Therefore, the catechol 1,2-dioxygenase specific activity could be modulated by the amount of IPTG added in the culture medium. As derivatives of pJF118EH, plasmid pWN2.100B and pWN2.248 contained all the genes localized in

plasmid pWN1.162A, while the transcription of the *catA* gene was under the control of a *tac* promoter. As another approach to improve the catechol 1,2-dioxygense activity, plasmid pWN2.248 also carried a 1.5 kb DNA sequence downstream from the *catA* gene. For unknown reasons, inclusion of this downstream DNA sequence has been shown to result in significantly higher catechol 1,2-dioxygenase specific activity.¹²²

In order to evaluate the expression level of catechol 1,2-dioxygenase from each plasmid, pWN1.162A, pWN2.100B, and pWN2.248 were transformed into *E. coli* DH5α, respectively. Single colonies were inoculated into LB medium containing the appropriate antibiotic. The specific activity of catechol 1,2-dioxygenase was assayed in crude cell-free lysate (Table 11). The approximately twofold increase in enzyme activity of *E. coli* DH5α/pWN2.100B relative to *E. coli* DH5α/pWN1.162A indicated the effect of switching gene transcription control from a *lac* promoter to a *tac* promoter. The impact of the expression of the unidentified protein on the expression of the *catA* gene in *E. coli* host was demonstrated by a further sevenfold improvement of catechol 1,2-dioxygenase specific activity in *E. coli* DH5α/pWN2.248.

Table 11. Catechol 1,2-Dioxygenase Specific Activities.

construct	catA gene	catechol 1,2-dioxygenase activity (U/mg)
DH5α/pWN1.162A	P _{lac} -RBS-catA (1.0 kb)	0.13
DH5α/pWN2.100B	P_{tac} -RBS- $catA$ (1.0 kb)	0.30
DH5α/pWN2.248	P_{uac} -RBS- $catA$ (2.5 kb)	2.12

To further examine the effect of elevated catechol 1,2-dioxygenase activity on microbial biosynthesis of *cis,cis*-muconic acid, *E. coli* WN1/pWN2.248 was cultured under modified fed-batch fermentor conditions. The IPTG addition was optimized by

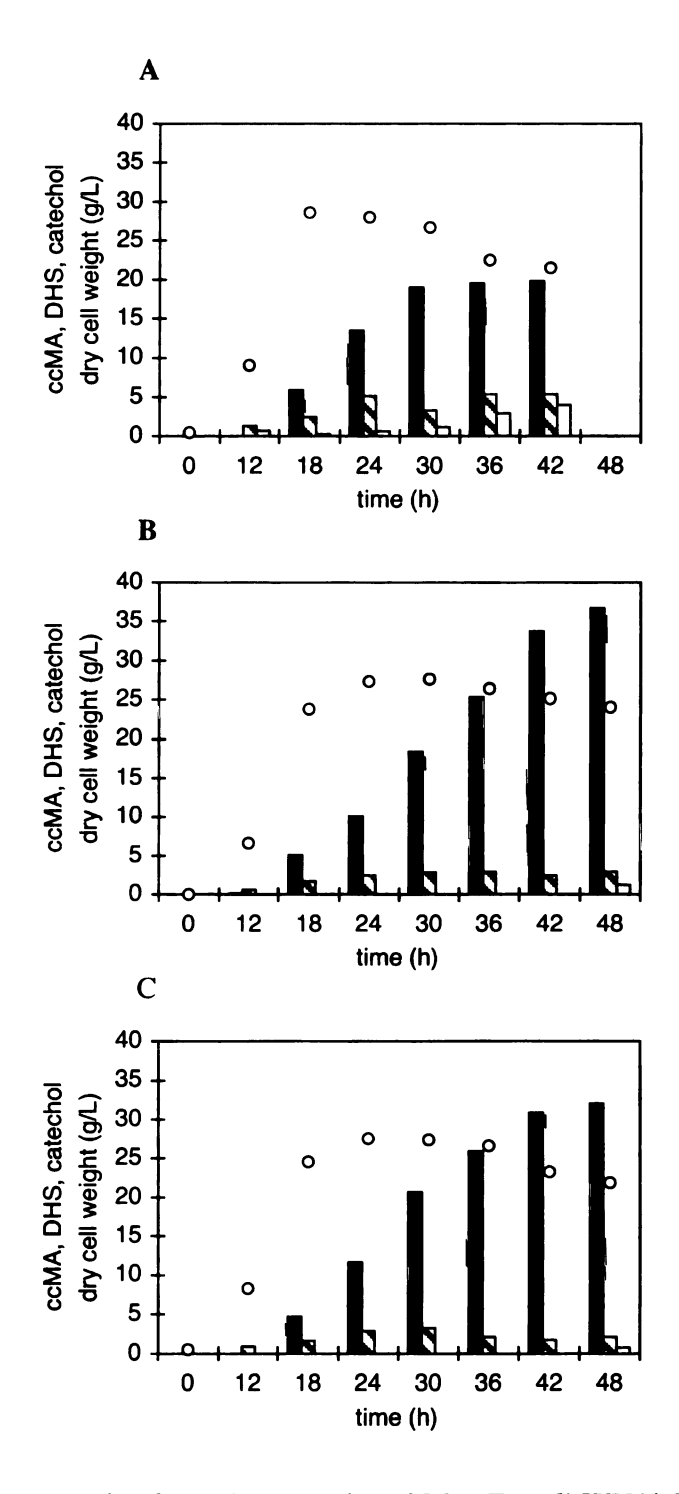


Figure 44. Biosynthesis of cis,cis-muconic acid by E. coli WN1/pWN2.248. IPTG addition at 18, 24, 30, 36, 42 h (a) 6 mg, (b) 12 mg, (c) 24 mg. o cell dry weight; cis,cis-muconic acid (ccMA); 3-dehydroshikimate (DHS); catechol.

Table 12. Product and Byproducts Synthesized by E. coli WN1/pWN2.248 after 48 h of Cultivation Under Fermentor-Controlled Conditions.

IPTG (mg)	[ccMA]" (g/L)	ccMA yield (%) ^b	[DHS] (g/L)	[Catechol]	total yield	DAHP synthase activity (U/mg)			
	(%)			(%)°	12 h	24 h	36 h	48 h	
6 ^d	19.8	15	5.3	3.9	21	0.23	0.29	0.20	-
12	36.8	22	3.0	1.6	24	0.21	0.29	0.17	0.17
24	32.3	19	2.2	0.4	20	0.17	0.20	0.13	0.12

^a Abbreviations: *cis,cis*-muconic acid (ccMA), 3-dehydroshikimate (DHS); ^b Given as (mol of ccMA)/(mol of glucose); ^c Given as (mol of ccMA + mol of DHS + mol of catechol)/(mol of glucose); ^d this fermentation was terminated 42 h after initiation.

observing cell growth characteristics and the concentration of synthesized cis, cismuconic acid. An aliquot of 12 mg of IPTG was added in the fermentation medium approximately 13 h after the fermentation was started to initiate the catechol 1,2dioxygenase expression and the conversion of catechol to cis, cis-muconic acid. The indicated quantities of IPTG were subsequently added at 18, 24, 30, 36, and 42 h to further induce the expression of catechol 1,2-dioxygenase (Table 12, Figure 44). The highest concentration of cis, cis-muconic acid of 36.8 g/L synthesized in 48 h was achieved when 12 mg of IPTG was repeatedly added (Table 12, Figure 44B). Catechol was not detected in the fermentation broth after IPTG addition until 48 h after the run was initiated (Figure 44B), when the concentration was 1.6 g/L. At the same time point, a 3.0 g/L of 3-dehydroshikimate was also observed. When the addition of IPTG was lowered to 6 mg/L at each selected time point, the rate of catechol formation increased (Figure 44A). This increase in catechol formation correlated with a decrease in both cell mass and cis, cis-muconic acid biosynthesis. Due to the difficulty in controlling the D.O. level, the fermentation had to be terminated 42 h after initiation. Along with 19.8 g/L of

cis,cis-muconic acid, the biocatalyst also produced 5.3 g/L of 3-dehydroshikimate and 3.9 g/L of catechol, which counts for approximately 30% of the carbon flow directed into the shikimate pathway (Table 12). Increasing the amount of IPTG repeatedly added from 12 mg to 24 mg reduced the catechol concentration to 0.4 g/L after 48 h of fermentation (Figure 44C). However, increased IPTG concentration in culture medium also resulted in decreased DAHP synthase specific activity, and a reduction in the concentration and yield of synthesized cis,cis-muconic acid (Table 12).

Hydrogenation of cis, cis-Muconic Acid to Adipic Acid

Catalytic hydrogenation was employed for the conversion of *cis,cis*-muconic acid to adipic acid. Following removal of cells by centrifugation, the fermentation broth was treated with activated charcoal to absorb soluble proteins and decolrize the broth. After removal of charcoal by filtration, the resulting filtrate was passed through a 10 kDa molecular weight cut off membrane under 40 psi of nitrogen pressure, followed by a second round of charcoal treatment. The final colorless solution was subjected to hydrogenation employing 5 mol percent of 10% Pt on activated carbon at 500 psi of H₂ pressure at room temperature. After 2.5 h, a 97% conversion of *cis,cis*-muconic acid to adipic acid was achieved.

Discussion and Future Work

A previous report ¹⁰⁶ demonstrated microbial synthesis of *cis,cis*-muconic acid via the designed biosynthetic pathway (Figure 26) under shake flask fermentation conditions employing *E. coli* AB2834/pKD136/pKD8.243A/pKD8.292, a three plasmid biocatalyst

for which the plasmid maintenance was realized by inclusion of antibiotics in the culture medium. In the present study, the biocatalysts were simplified to a single plasmid system by localization of certain cis, cis-muconic acid biosynthetic genes in the genome of host strains through site-specific chromosomal modification. Disruption of the L-serine biosynthetic gene during this modification also allowed plasmid maintenance to be based on nutritional pressure. In the previous study, E. coli AB2834/pKD136/pKD8.243A/ pKD8.292 was initially cultured in rich medium to the early stationary phase of growth followed by resuspension in minimal salts medium containing glucose. 106 The initial growth in rich medium caused an analysis complication since the glucose in the minimal salts medium was not the only carbon source used during the cell growth and synthesis of cis, cis-muconic acid. As a result, the reported 30% (mol/mol) yield likely overestimated the actual yield of cis, cis-muconic acid. During the cultivation of E. coli biocatalysts under fed-batch fermentor conditions employed in this study, the microbial growth and biosynthesis of cis, cis-muconic acid occurred in a single culture medium, which allowed for an accurate estimation of the yield of biosynthesized cis, cis-muconic acid. Additionally, culturing cells under fermentor-controlled conditions provided a culture environment where temperature, pH, dissolved oxygen levels, and glucose addition rates can be controlled. Combined improvements in biocatalyst design and control of culturing conditions resulted in the synthesis of 37 g/L cis,cis-muconic acid by recombinant E. coli strain relative to 2.4 g/L of production in the previous study. 106 Successful conversion of partially purified cis, cis-muconic acid into adipic acid under catalytic hydrogenation conditions using a commonly employed catalyst established a possible route (Figure 26) for the industrial synthesis of adipic acid from glucose.

To estimate the cost of manufacturing adipic acid from glucose, microbial synthesis of L-lysine from D-glucose can be used as a model. Based on a price of \$0.13/kg of D-glucose, the 24% (mol/mol) yield of *cis,cis*-muconic acid synthesized from D-glucose by *E. coli* WN1/pWN2.248, and the 97% (mol/mol) yield for hydrogenation, the estimated cost for manufacturing adipic acid from glucose is \$2.46/kg. This is significantly higher than the current \$1.53/kg price for resin-grade adipic acid. Therefore, further improvements in the concentration and yield of *cis,cis*-muconic acid synthesized from D-glucose are needed.

In wild-type E. coli cells, glucose is transported into the cytoplasm by the phosphoenolpyruvate:carbohydrate phosphotransferase system (PTS). 65 One molecule of phosphoenolpyruvate is converted into pyruvate for each molecule of glucose transported and phosphorylated to form glucose 6-phosphate. Research shows that the generated pyruvate is not apparently recycled back to phosphoenolpyruvate. 125c Therefore, the maximum theoretical yield for converting glucose into cis, cis-muconic acid is 43% (mol/mol). Alternatively, utilization of non-PTS carbon sources such as pentoses and glycerol in cis,cis-muconic acid biosynthesis can circumvent the consumption of phosphoenolpyruvate during glucose transport. As a consequence, the efficiency of carbon utilization by E. coli biocatalysts is improved. Unfortunately, pure, abundant, and inexpensive commercial source of D-xylose, L-arabinose, and glycerol are currently not available. Given that adipic acid is a commodity chemical, the cost of the starting material is one key factor that will determine the market viability of a manufacturing process. Therefore, glucose remains the primary choice for the synthesis of adipic acid using designed route (Figure 26). In Chapter 1 and Chapter 2, strategies developed for

improving the biosynthetic efficiency of shikimate pathway products by *E. coli* biocatalysts from glucose have been discussed, including overexpression of *pps*-encoded phosphoenolpyruvate synthase to recycle pyruvate back to phosphoenolpyruvate¹²⁵ and using alternate glucose transport systems to avoid phosphoenolpyruvate expenditure.¹²⁶ The maximum theoretical yield of shikimate pathway products could thus increase to 86% (mol/mol). A recombinant *E. coli* biocatalyst has been constructed that synthesized 3-dehydroshikimate and associated shikimate pathway byproducts in a total yield of 51% (mol/mol).^{125c}

Although methods to increase the carbon utilization efficiency of E. coli biocatalysts have been established, conversion of this increased carbon flow into cis, cismuconic acid may be problematic. Substantial amounts of 3-deoxy-D-arabinoheptulosonic acid (DAH), 3-dehydroquinate, and gallic acid were synthesized from glucose by E. coli biocatalysts when phosphoenolpyruvate availability was increased during synthesis of 3-dehydroshikimate. The existence of these byproducts in a cis, cismuconic acid fermentation would not only reduce the yield of the desired product, it would also complicate the purification of cis,cis-muconic acid. 3-Dehydroquinate is a biosynthetic intermediate of the shikimate pathway. DAH is exported from the cell's cytoplasm after the dephosphorylation of DAHP, which is the first committed intermediate of the shikimate pathway. To avoid the accumulation of DAH and 3dehydroquinate, 3-dehydroquinate synthase and 3-dehydroquinate dehydratase in vivo specific activity will need to be increased. As an oxidation product of 3dehydroshikimate, the accumulation of gallic acid could be eliminated through an efficient conversion of 3-dehydroshikimate into cis, cis-muconic acid. This will require

increasing the in vivo specific activity of both 3-dehydroshikimate dehydratase and catechol 1,2-dioxygenase. Catechol 1,2-dioxygenase catalyzes the oxidation of catechol to *cis,cis*-muconic acid. Inadequate catechol 1,2-dioxygenase activity results in the accumulation of catechol, which is toxic to *E. coli* biocatalysts. ¹⁰⁹ Therefore, the negative impact of catechol accumulation on the biosynthesis of *cis,cis*-muconic acid is particularly problematic. In addition to increasing the catalytic activity of catechol 1,2-dioxygenase, catechol might also be removed from fermentation broth using resins that specifically bind to catechol.

In comparison with the currently employed industrial synthesis, synthesis of adipic acid from glucose (Figure 26) uses a nontoxic starting material (glucose) derived from a renewable feedstock, and also avoids the generation of N₂O as a byproduct. Therefore, the environmental and health cost associated with synthesis of adipic acid from glucose is significantly lower relative to the current industrial synthesis. Additionally, as petroleum becomes increasingly scarce, 127 utilization of a starting material derived from renewable feedstock instead of petroleum in adipic acid synthesis addresses sustainability issues. These environmental and health-related factors are not currently reflected in the price of adipic acid.

CHAPTER FOUR

MICROBIAL SYNTHESIS OF 1,2,4-BUTANETRIOL FROM D-XYLOSE AND L-ARABINOSE

Background

1,2,4-Butanetriol is mainly used as the synthetic precursor of 1,2,4-butanetriol trinitrate, which is used as an energetic plasticizer for missile propellants and explosives (Figure 45).¹²⁸ In comparison to nitroglycerin, 1,2,4-butanetriol trinitrate possesses superior physical properties including enhanced thermal stability, reduced shock sensitivity, lower volatility, and a sub-zero melting point.¹²⁹ Therefore, substitution of nitroglycerin with 1,2,4-butanetriol trinitrate as an energetic material would not only reduce hazards associated with manufacturing and operating processes, but also improve the operating range of the final product. Nevertheless, the current large-scale production of 1,2,4-butanetriol trinitrate is limited by the availability of its polyol precursor, 1,2,4-butanetriol. In addition to the manufacturing of 1,2,4-butanetriol trinitrate, the two stereoisomers of 1,2,4-butanetriol are also attractive chiral synthons for use in synthetic chemistry.

Figure 45. Structures of 1,2,4-butanetriol and 1,2,4-butanetriol trinitrate.

The current commercial production of 1,2,4-butanetriol relies on NaBH₄ reduction of dimethyl malate in a mixture of C_{2-6} alcohols and tetrahydrofuran (Figure 46). As

might be expected from a stoichiometric reduction, a byproduct salt stream is generated. Each kg of methyl malate reduced by NaBH₄ results in 2-5 kg of borate salts.¹³⁰ The cost of proper disposal of the byproduct salt stream combined with the expense of employing stoichiometric amounts of a reductant limit the use of this reaction to production of relatively small volumes of 1,2,4-butanetriol.

Figure 46. Current commercial synthesis of 1,2,4-butanetriol. (a) NaBH₄, tetrahydrofuran, C₂₋₆ alcohols.

Alternatively, the possibility of synthesizing 1,2,4-butanetriol under catalytic hydrogenation conditions was also explored. Employing a copper-chromium catalyst, dimethyl malate was converted to 1,2,4-butanetriol in a yield of 67% under a H₂ pressure of 5,000 psi.¹³¹ However, the toxicity of the Cr⁶⁺ in the hydrogenation catalyst prohibits the large-scale application of this synthesis. More recently, hydrogenation of aqueous solutions of malic acid using 5% Ru on C was examined in the Frost group. Carboxylates with electron withdrawing groups attached to the adjacent carbon atom are known to be activated towards metal-mediated reduction.¹³² However, the presence of the second unactivated carboxylate group in malic acid requires that the catalyzed reduction be run at higher H₂ pressures. Under a H₂ pressure of 1,000 psi, 25 % (mol/mol) of malic acid was converted into 1,2,4-butanetriol at 135 °C, with 1.3 mol% of 5% Ru on C. Exclusive reduction of the activated carboxylate on malic acid led to the formation of 3,4-dihydroxybutyric acid and 3-hydroxybutyrolactone in a combined yield

Figure 47. Catalytic hydrogenation of malic acid towards 1,2,4-butanetriol. (a) 5,000 psi, $135 \,^{\circ}\text{C}$, $1.3 \, \text{mol}\%$ of Ru ($5\% \, \text{wt.}$) on C, H_2O .

of 60% (mol/mol).¹³³ Further optimization of the hydrogenation condition resulted in complete reduction of malic acid but also formation of a mixture of byproducts. Under a H₂ pressure of 5,000 psi, at 135 °C with 1.3 mol% of 5% Ru on C, 1,2,4-butanetriol was synthesized in a maximum yield of 74% (mol/mol) (Figure 47). The high H₂ pressures and elevated temperature led to C-C and C-O bond cleavage reactions resulting in formation of polyol byproducts (Figure 47) that are difficult to separate from 1,2,4-butanetriol by distillation.¹³³ In addition to the reduced reaction yield and challenging product purification, the quantity and expense of Ru metal required for large-scale hydrogenation of malic acid would constitute a significant cost factor. Although malic acid can be obtained using microbial synthesis and renewable feedstocks,¹³⁴ the problematic catalytic hydrogenation of malic acid limits the utility of this synthetic route.

An alternate synthetic precursor to 1,2,4-butanetriol has been identified by the Frost group (Figure 48). When aqueous solutions of 2-hydroxy-2-buten-4-olide, the lactone form of 4-hydroxy-2-ketobutyric acid, were subjected to catalytic hydrogenation at 125 °C using 1.0 mol% of Ru catalyst (5% Ru on C) under a H₂ pressure of 2,500 psi, 1,2,4-butanetriol was synthesized in a yield of 96% (mol/mol) with no formation of

Figure 48. Chemoenzymatic synthesis of 1,2,4-butanetriol from L-ascorbic acid. (a) Na_2CO_3 , H_2O_2 , 74%; (b) *E. coli* dihydroxy acid dehydratase, 80%; (c) H^+ , EtOAc extraction, 93%; (d) 2,500 psi, 125 °C, 1.0 mol% of Ru on C (5% wt.), H_2O , 96%.

polyol byproducts. 4-Hydroxy-2-ketobutyric acid was synthesized from L-ascorbic acid via the intermediacy of L-threonic acid by a chemoenzymatic route.¹³⁵ In comparison with the hydrogenation of malic acid, the hydrogenation of 2-hydroxy-2-buten-4-olide afforded a significant improvement in reaction yield and product purity. However, the overall yield of 1,2,4-butanetriol synthesized from L-ascorbic acid was only 53% (mol/mol). From an economic standpoint, application of this four-step process at large scale would not be an improvement over the currently employed NaBH₄ reduction of esterified malic acid.

In this chapter, biosynthesis of D- and L-1,2,4-butanetriol has been accomplished by creating biosynthetic pathways not found in nature (Figure 49). The designed biosynthetic pathways (Figure 49) began with the oxidation of D-xylose to D-xylonic acid and L-arabinose to L-arabinonic acid catalyzed by D-xylose dehydrogenase and L-arabinose dehydrogenase, respectively. Conversions of D-xylonic acid to 3-deoxy-D-glycero-pentulosonic acid and L-arabinonic acid to 3-deoxy-L-glycero-pentulosonic acid were catalyzed by D-xylonate dehydratase and L-arabinonate dehydratase, respectively. Further decarboxylation of D- and L-3-deoxy-glycero-pentulosonic acid led to D- and L-3,4-dihydroxybutanal, respectively. Reduction of these aldehydes to D- and L-1,2,4

Figure 49. Biosynthetic pathway of D- and L-1,2,4-butanetriol. Enzymes (a) D-xylose dehydrogenase; (aa) L-arabinose dehydrogenase; (b) D-xylonate dehydratase; (b) L-arabinonate dehydratase; (c) 2-keto acid decarboxylase; (d) alcohol dehydrogenase.

butanetriol was anticipated to employ different alcohol dehydrogenases. Due to the design of the two parallel biosynthetic pathways, D- and L- stereoisomers of 1,2,4-butanetriol could be separately synthesized from D-xylose and L-arabinose. D-Xylonic acid, L-arabinonic acid, 3-deoxy-D-glycero-pentulosonic acid, and 3-deoxy-L-glycero-pentulosonic acid have been identified as metabolic intermediates of certain *Pseudomonas* species. However, D,L-3,4-dihydroxybutanal and D,L-1,2,4-butanetriol has never been isolated from natural resource. The successful biosynthesis of 1,2,4-butanetriol relied on the identification of microbes and enzymes that could catalyze individual synthetic reactions and the construction of biocatalysts that could accomplish the overall conversions of D-xylose into D-1,2,4-butanetriol and L-arabinose into L-1,2,4 butanetriol. In the last part of this chapter, directed evolution methods were applied to improve enzyme-catalyzed decarboxylation of 3-deoxy-D,L-glycero-pentulosonic acid to form D,L-3,4-dihydroxybutanal.

Microbial Synthesis of D- and L-1,2,4-Butanetriol

Microbial synthesis of D- and L-1,2,4-butanetriol proceeded in two steps, with each step being carried out by a different microbe. The first step involved the oxidation of D-xylose or L-arabinose into the corresponding sugar carboxylate. In the second step, D-xylonic acid or L-arabinonic acid purified from the first step was converted into D- or L-1,2,4-butanetriol, respectively.

A. Biosynthesis of D-Xylonic Acid and L-Arabinonic Acid

Overview

D-Xylose is the major component of xylan, which is the most abundant hemicellulose existing in hardwoods. Over millions of years of evolution, microorganisms have developed various pathways to metabolize D-xylose and form a variety of metabolites. Value-added chemicals synthesized from D-xylose include ethanol, was a xylitol, which are and acetone. Over the acetobacter, and Pseudomonas strains also can oxidize D-xylose via a D-xylose dehydrogenase-catalyzed reaction (Figure 50). However, DNA sequence information about genes that encodes D-xylose dehydrogenase is scarce. Hydrolase-catalyzed hydrolysis of the oxidation product, D-xylono-1,5-lactone, yields D-xylonic acid which can be further metabolized by certain Pseudomonas species. L-Arabinose is less abundant in nature relative to D-xylose. L-Arabinose mainly exists as a substituent of side chains in heteroxylans. Microbial oxidation of L-arabinose has been studied in Pseudomonas saccharophila, Microbial oxidation of L-arabinose has been studied in Pseudomonas sp. MSU-1 (Figure 50). L-Arabinose dehydrogenase catalyzes the conversion of L-

arabinose into L-*arabino*-1,4-lactone, which is subsequently hydrolyzed into L-arabinonic acid and utilized as a carbon source. 136,140,141

Figure 50. Microbial oxidation of D-xylose and L-arabinose. (a) D-xylose dehydrogenase; (b) hydrolase; (c) L-arabinose dehydrogenase; (d) hydrolase.

Microbial oxidations of D-xylose to D-xylonic acid have utilized *Pseudomonas* fragi (ATCC 4973) and Gluconobacter oxydans (ATCC 621) under fermentor-controlled conditions. Both strains were able to oxidize pure D-xylose efficiently, while Gluconobacter oxydans (ATCC 621) is less sensitive to inhibitors such as acetic acid and furfural when hemicellulose hydrolyzate was used as the source of D-xylose. However, microbial synthesis of L-arabinonic acid from L-arabinose has not been demonstrated. Furthermore, because the location of L-arabino-1,4-lactone hydrolase is not clear, whether the lactone or the carboxylate form of L-arabinonic acid would accumulate in the culture medium was unknown. In this study, commercially purchased pure D-xylose and L-arabinose were used as the starting material. *Pseudomonas fragi* (ATCC 4973) was used to carry out the oxidation of both D-xylose and L-arabinose.

Pseudomonas fragi (ATCC 4973) is a gram-negative, non-sporeforming eubacteria. ^{142a} Taxonomically, P. fragi is closely related to Pseudomonas putida and

Pseudomonas fluorescens. However, P. fragi is unable to synthesize fluorescent pigments that are commonly produced by P. putida and P. fluorescens. The optimal growth temperature of P. fragi is 30 °C. It can also grow at 4 °C, but not at 37 °C. Head Because this psychrophilic microbe can cause the spoilage of meats, fish, and milk products, research has been focused on its ability to produce exogeneous proteases.

Microbial Synthesis of D-Xylonic Acid

Batch fermentations employed a 2.0 L working capacity B. Braun M2 culture vessel. Utilities were supplied by a B. Braun Biostat MD controlled by a DCU-3. Data acquisition utilized a Dell Optiplex GX200 personal computer (PC) equipped with B. Braun MFCS/Win software (v2.0). Temperature and pH were controlled with PID control loops. Temperature was maintained at 30 °C. The pH was maintained at 6.4 by the addition of 2 N H₂SO₄ and 30% CaCO₃ aqueous slurry. Dissolved oxygen (D.O.) was monitored using a Mettler-Toledo 12 mm sterilizable O2 sensor fitted with an Ingold Atype O₂ permeable membrane. Inoculants were started by introduction of a single colony of P. fragi (ATCC 4973) into 5 mL of D-xylose culture medium. Cultures were grown at 30 °C with agitation at 250 rpm until they were turbid. The cultures were then transferred into 100 mL of fresh D-xylose culture medium and incubated at 30 °C for 12 h with agitation. The inoculants were subsequently transferred into fermentor culture medium to initiate the batch fermentation (t = 0 h). The concentration of D-xylose in the fermentation medium was 100 g/L at 0 h. During the first 24 h of fermentation, cells were growing rapidly (Figure 51). Then the cell growth reached a stationary period for

approximately 12 h. After this phase, the cell growth started again. Although *P. fragi* showed a sigmoid growth character during the fermentation, it was able to produce D-xylonate at a constant rate. After 48 h of culturing, 77 g of D-xylonic acid was synthesized from 100 g of D-xylose in a yield of 70% (mol/mol). D-Xylonic acid was purified as calcium xylonate salt from fermentation medium by ethanol precipitation. Exchange of the calcium salt into a potassium salt was accomplished by passing the calcium xylonate solution through a Dowex 50 (K⁺) column.

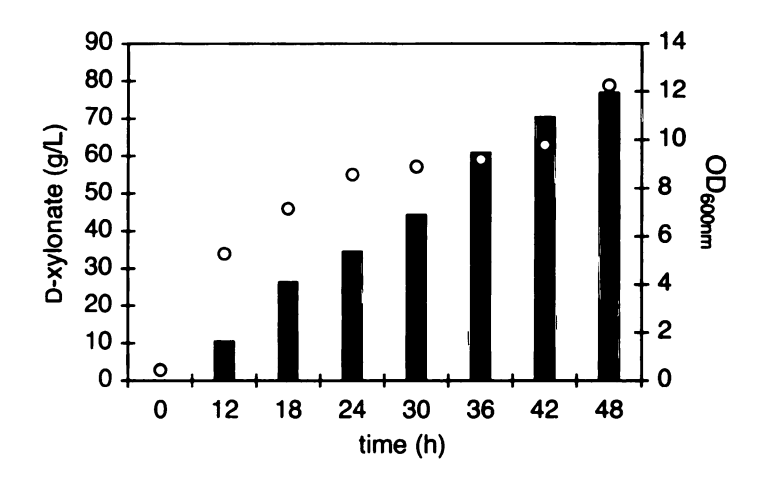


Figure 51. Synthesis of D-xylonic acid by P. fragi (ATCC 4973). \circ OD_{600nm} of P. fragi; \longrightarrow D-xylonate.

Microbial Synthesis of L-Arabinonic Acid

To test the ability of *P. fragi* to oxidize L-arabinose, and further identify whether L-arabinonic acid or its lactone form accumulated in the culture medium, *P. fragi* was examined under shake flask conditions. A single colony of *P. fragi* was introduced into 5 mL of L-arabinose fermentation medium and cultured at 30 °C with shaking for 24 h. This inoculant was subsequently transferred into 100 mL of L-arabinose fermentation medium containing 1 g of L-arabinose. After 24 h of incubation at 30 °C with shaking,

all the L-arabinose was oxidized by the cells, and L-arabino-1,4-lactone was the only metabolite being identified in the culture medium.

P. fragi was further examined under fermentor-controlled conditions. Fermentations were carried out under conditions as described for microbial synthesis of D-xylonic acid with some modifications. The most significant change was the use of L-arabinose as the substrate in place of D-xylose. Additionally, concentrated NH₄OH was used as the base solution together with 2 N H₂SO₄ for pH adjustment. P. fragi cell growth reached stationary phase after 36 h of fermentation (Figure 52). During the first 24 h of cultivation, only L-arabino-1,4-lactone was detected in the culture medium (Figure 52). The hydrolysis of lactone started at 36 h. After 48 h of fermentation, 100 g of L-arabinose was oxidized into 40 g of L-arabino-1,4-lactone and 15 g of L-arabinonic acid in a total yield of 54% (mol/mol). After hydrolysis of L-arabino-1,4-lactone under basic conditions, potassium L-arabinonate was precipitated upon addition of methanol.

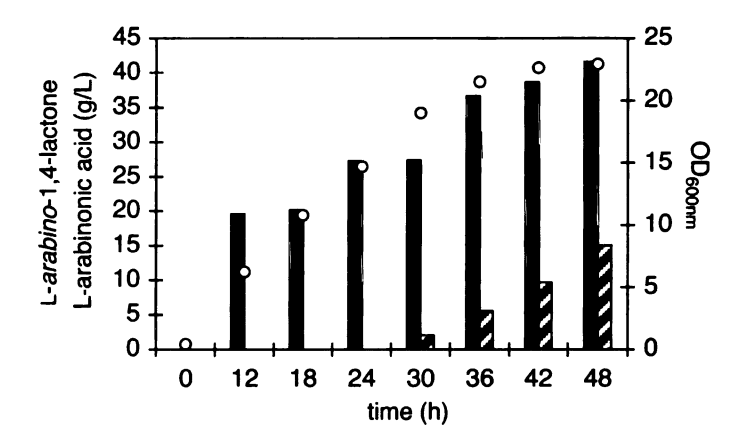


Figure 52. Synthesis of L-arabino-1,4-lactone and L-arabinonic acid by P. fragi.
OD 600nm of P. fragi; L-arabino-1,4-lactone; L-arabinonic acid.

B. D-Xylonate Dehydratase and L-Arabinonate Dehydratase

Overview

Dehydration of D-xylonic acid catalyzed by D-xylonate dehydratase and dehydration of L-arabinonic acid catalyzed by L-arabinonate dehydratase constitute the second reactions in the respective pathways designed for the biosynthesis of D-1,2,4-butanetriol and L-1,2,4-butanetriol (Figure 49). Both enzymes have been proposed to function in the metabolism of pentoses in certain *Pseudomonas* strains, ^{136,140141} and both enzyme activities have been detected in the cell lysates. However, neither the gene nor the protein sequence for either enzyme has been reported. Although *Pseudomonas* strains, which expressed D-xylonate dehydratase and L-arabinonate dehydratase activity as native enzyme activities could potentially be used as the host strain for biosynthesis of 1,2,4-butanetriol, gene sequences for both enzymes are essential for efforts directed at improving the in vivo specific activities of these enzymes and their possible heterologous expression in other microbial hosts.

Two unique catabolic pathways that are similar to the Entner-Doudoroff pathway for glucose-6-phosphate catabolism enable *P. fragi* (ATCC 4973) to use D-xylose or L-arabinose as sole carbon sources for growth. As previously discussed, the first steps of these pathways entail oxidations of the respective carbohydrates into sugar acids (Figure 50). D-Xylonate and L-arabinonate are then dehydrated to form D- and L-3-deoxy-glycero-pentulosonic acid, respectively, by a reaction catalyzed by D-xylonate dehydratase or L-arabinonate dehydratase (Figure 53). A second dehydration leads to 2-ketoglutarate semialdehyde, which is further oxidized to the TCA cycle intermediate 2-ketoglutarate. The routes in *P. fragi* for D-xylose and L-arabinose catabolism therefore

Figure 53. Catabolism of D-xylonic acid and L-arabinonic acid in *P. fragi* (ATCC 4973). (a) D-xylonate dehydratase; (b) 3-deoxy-D-glycero-pentulosonate dehydratase; (c) 2-ketoglutarate dehydrogenase; (d) L-arabinonate dehydratase; (e) 3-deoxy-L-glycero-pentulosonate dehydratase.

converge at 2-ketoglutarate semialdehyde. Intermediates in both pathways including D-xylonate, L-arabinonate, D- and L-3-deoxy-glycero-pentulosonic acid could also be used as sole carbon sources by *P. fragi* for growth. The existence of both D-xylonate dehydratase and L-arabinonate dehydratase in *P. fragi* (ATCC 4973) makes this microbe the focus of efforts for deriving sequence information for both D-xylonate dehydratase and L-arabinonate dehydratase.

Purification of D-Xylonate Dehydratase from P. fragi

Due to the absence of DNA or protein sequence data for D-xylonate dehydratase from any living organisms, classical enzyme purification was used as the first step towards obtaining the genetic information of D-xylonate dehydratase from *P. fragi* (ATCC 4973). The purification was performed using a DE-52 anion exchange column, a hydroxyapatite column, a phenylsepharose column, and an HPLC Resource Q anion exchange column (Table 13). During the purification, D-xylonate dehydratase activity

Table 13. Purification of *P. fragi* D-Xylonate Dehydratase.

	total protein (mg)	total activity (units)	specific activity (unit/mg)	yield (%)	purification fold
cell lysate	7274	215	0.03	100	1.0
DE-52	527	76	0.14	35	4.8
hydroxyapatite	219	66	0.30	31	10
phenylsepharose	24	50	2.10	23	70
Resource Q ^a	11	30	2.91	14	97

^a Approximately 10% of the protein purified from phenylsepharose column was purified using the Resource Q column. Results for total protein and total enzyme activity were then adjusted accordingly.

was monitored by assaying the formation of a 2-keto acid semicarbazone derivative.¹⁴³ After a 97-fold purification, *P. fragi* D-xylonate dehydratase was purified to near homogeneity. Purified protein migrated as a major band on SDS gels with a molecular weight of approximate 60 kDa. The sequence of the NH₂-terminal 12 amino acids was determined for the purified D-xylonate dehydratase (Figure 54) as a prelude for PCR amplification of the encoding gene.

1 6 11 TDSTP KRGRA QL

Figure 54. NH₂-terminal sequence of D-xylonate dehydratase from *P. fragi* (ATCC 4973).

D-Xylonate Dehydratase Activity in E. coli

Using E. coli as the host strain in the biosynthesis of 1,2,4-butanetriol can benefit from the metabolic and regulatory databases along with the genetic engineering

techniques available for this microbe. To determine whether *E. coli* could catabolize D-xylonic acid and L-arabinonic acid, wild-type *E. coli* W3110 was separately cultivated in medium where D-xylonate or L-arabinonate were the sole carbon sources. The observed ability of *E. coli* to utilize D-xylonic acid as a sole source of carbon has not previously been reported. However, L-arabinonic acid was not able to function as the sole source of carbon for *E. coli*. Growth of *E. coli* W3110 on D-xylonic acid raised the question of how this sugar acid was catabolized in *E. coli*.

One possible catabolic pathway of D-xylonic acid in *E. coli* is through the reduction of the sugar acid to D-xylose, which can be catabolized in *E. coli* cells (Figure 55). D-Xylose is isomerized by *E. coli* to D-xylulose and phosphorylated by a kinase. D-Xylulose 5-phosphate is then converted to D-glyceraldehyde 3-phosphate upon transketolase-catalyzed ketol transfer. To examine the role of D-xylose in *E. coli* catabolism of D-xylonic acid, single colonies of *E. coli xylA* strain W945 were inoculated into liquid minimal salts medium containing D-xylose or D-xylonic acid as the sole carbon source. Due to a mutation on the *xylA* gene, *E. coli* W945 can't produce

Figure 55. Catabolism of D-xylose and L-arabinose in E. coli. Enzymes (encoding genes) (a) D-xylose isomerase (xylA); (b) D-xylulose kinase (xylB); (c) transketolase (tktA) or tktB); (d) L-arabinose isomerase (araA); (e) L-ribulose kinase (araB); (f) L-ribulose 5-phosphate 4-epimerase (araD).

functional D-xylose isomerase and thus can't grow on D-xylose. However, *E. coli* W945 was able to grow on D-xylonic acid. This observation excluded D-xylose as an intermediate in *E. coli* catabolism of D-xylonic acid.

Figure 56. E. coli catabolism of D-gluconate and D-galactonate. Enzymes (encoding genes) (a) D-gluconate kinase (gntK); (b) D-gluconate 6-phosphate dehydratase (edd); (c) 3-deoxy-2-keto-D-gluconate 6-phosphate aldolase (eda); (d) D-galactonate dehydratase (dgoD); (e) 3-deoxy-2-keto-D-galactonate kinase (dgoK); (f) 3-deoxy-2-keto-D-galactonate 6-phosphate aldolase (dgoA).

E. coli cells can grow on certain C₆ sugar acids as sole sources of carbon. Catabolism of C₆ sugar acids is exemplified by the catabolism of D-gluconate and D-galactonate (Figure 56).⁶⁶ Both pathways consist of dehydration, phosphorylation, and aldolase-catalyzed cleavage reactions, although these reactions occur in different sequences. The structural similarity between C₅ and C₆ sugar acids indicates that a related catabolic pathway may be responsible for the catabolism of D-xylonate in E. coli. Based on enzyme activity in crude cell lysates, E. coli W3110 cultured on D-xylonic acid expressed a D-xylonate dehydratase activity of 0.012 U/mg, which was fivefold higher relative to the specific activity observed for E. coli W3110 grown on glucose (0.0025 U/mg). This induced enzyme activity suggested that D-xylonate dehydratase may be

responsible for the catabolism of D-xylonate in E. coli and that 3-deoxy-2-keto-Dglycero-pentulosonic acid could be an intermediate in the catabolic pathway. Further analysis of E. coli W3110 culture supernatant by ¹H and ¹³C NMR showed that ethylene glycol and glycolate accumulated during microbial growth on D-xylonic acid. A hypothetical D-xylonate catabolic pathway in E. coli was proposed based on these experimental results (Figure 57). E. coli catabolism of D-xylonate begins with a dehydratase-catalyzed reaction to form 3-deoxy-D-glycero-pentulosonic acid, which is subsequently cleaved by an aldolase to form pyruvate and glycolaldehyde. Pyruvate can be catabolized via the TCA cycle while glycolaldehyde can be catabolized via the glycolate pathway.⁶⁶ As an intermediate in glycolaldehyde catabolism, glycolate could be exported out of the cells. Ethylene glycol could be the reduction product of glycolaldehyde due to intervention of a non-specific alcohol dehydrogenase. The proposed D-xylonate catabolism pathway in E. coli has been identified as part of the Dxylose catabolism pathway in Pseudomonas sp. MSU-1.144 D-Xylonate dehydratase activity and 3-deoxy-D-glycero-pentulosonic acid aldolase activity have been detected in the cell lysate of MSU-1 grown on D-xylose. The 3-deoxy-D-glycero-pentulosonic acid aldolase activity was determined by coupling the cleavage reaction with pyruvate-

Figure 57. Proposed pathway for *E. coli* catabolism of D-xylonic acid. Enzymes (a) D-xylonate dehydratase; (b) 3-deoxy-D-glycero-pentulosonic acid aldolase; (c) alcohol dehydrogenase; (d) glycolaldehyde dehydrogenase.

dependent oxidation of NADH catalyzed by lactate dehydrogenase. However, attempts to detect the 3-deoxy-D-glycero-pentulosonic acid aldolase activity in the cell lysate of *E. coli* W3110 grown on D-xylonic acid were not successful. This result might be explained if 3-deoxy-D-glycero-pentulosonic acid is phosphorylaed prior to its aldolase-mediated cleavage. Irrespective of the steps occurring subsequent to D-xylonate dehydratase, the expression of this enzyme makes *E. coli* W3110 a possible host strain for the biosynthesis of D-1,2,4-butanetriol.

<u>Isolation of Gene Encoding P. fragi (ATCC 4973) L-Arabinonate Dehydratase</u>

Genes encoding enzymes in a given catabolic or biosynthetic pathway are often located closely on the microbial chromosome to form a gene cluster. Thus clustered genes can be isolated by constructing and screening a genomic DNA library of the microorganism. Screening methods can be designed based on the biological function of the pathway encoded by the gene cluster of interest. Obtaining the DNA sequence information for a targeted enzyme through its amino acid sequence requires purification of the targeted enzyme to homogeneity, sequencing the NH₂-terminus or/and COOH-terminus, and obtaining the DNA sequence using PCR with degenerated primers. By contrast, screening a genomic DNA library is a more rapid and less labor-intensive approach. Because of the inability of *E. coli* to use L-arabinonate as a sole source of carbon for growth, isolation of a potential L-arabinonate catabolism gene cluster from *P. fragi* (ATCC 4973) was accomplished by constructing a *P. fragi* genomic DNA library in *E. coli* and screening the *E. coli* strains for an aquired ability to grow on L-arabinonate. Growth on L-arabinonate, in theory, would indicate heterologous expression of the *P*.

fragi chromosomal fragment that contains the L-arabinonate catabolism gene cluster. Since L-arabinonate dehydratase catalyzes the first reaction in the *P. fragi* L-arabinonate catabolic pathway, the gene encoding L-arabinonate dehydratase shall be part of the L-arabinonate catabolism gene cluster.

Genomic DNA was purified from P. fragi (ATCC 4973) and partially digested with Sau3AI. The resulting genomic DNA fragments were ligated into BamHI digested cosmid vector SuperCos 1 to yield concatemers which were then packaged in λ phage. Infection of E. coli BL21(DE3) was followed by plating infected cells on M9 plates containing L-arabinonate as the sole source of carbon to select for growth. Because vector SuperCos 1 carried a DNA fragment encoding resistance to ampicillin, estimation of the transfection efficiency was carried out by plating phage-infected BL21(DE3) cells on LB plates containing ampicillin (Ap). A solution of λ phage and a separate solution of BL21(DE3) cells was also plated on M9 L-arabinonate plates as two negative controls to detect possible contamination. After 66 h of incubation at 37 °C, three colonies formed on phage infected BL21(DE3) plates, which was approximately 0.1% of the number of colonies formed on LB/Ap plates. No colonies formed on the two negative control plates. Purification of the cosmids from the three L-arabinonate-growing colonies followed by analysis of the fragments generated by restriction enzyme digestion indicated that P. fragi genomic DNA with a size of 40-50 kb had been localized in SuperCos 1. These results indicated that a small fragment of P. fragi genomic DNA shared by all three cosmids enabled BL21(DE3) to grow on L-arabinonate.

Restriction enzyme mapping of the three isolated cosmids showed a common 5.0 kb DNA fragment, which was sub-cloned into vector pT7-7. According to the orientation

of the insert relative to a pT7-7-encoded T7 promoter, plasmid pT7-7A and pT7-7B were obtained. To examine whether the 5.0 kb DNA fragment contains the P. fragi Larabinonate catabolism gene cluster, E. coli BL21(DE3) competent cells were transformed with plasmid pT7-7A and pT7-7B respectively. Ten of the single colonies of each transformants were replicated on M9 L-arabinonate plates. After 48 h of incubation at 37 °C, all transformants were able to grow. Therefore, the 5.0 kb DNA fragment encodes enzymes that are sufficient to support E. coli BL21(DE3) to grow on Larabinonate as the sole source of carbon. To further establish that the 5.0 kb DNA fragment also contained the gene encoding L-arabinonate dehydratase, enzyme assays were performed using the cell lysate of BL21(DE3)/pT7-7A and BL21(DE3)/pT7-7B. L-Arabinonate dehydratase activity was monitored by assaying the formation of the semicarbazone derivative of the 2-keto acid. 145 The specific activity was 0.07 U/mg for BL21(DE3)/pT7-7A and 0.11 U/mg for BL21(DE3)/pT7-7B (Table 14). observation showed that the expression of L-arabinonate dehydratase was not affected by the orientation of the 5.0 kb insert. It is very likely that instead of being initiated by the pT7-7-encoded T7 promoter, the transcription of the gene encoding L-arabinonate dehydratase was initiated by a native P. fragi promoter located on the 5.0 kb insert.

Although the 5.0 kb insert could be used to overexpress L-arabinonate dehydratase in an L-1,2,4-butanetriol-synthesizing construct, the DNA sequence of the open reading frame would better serve future metabolic engineering needs such as PCR amplification of the gene. The first step towards identifying the L-arabinonate dehydratase open reading frame entailed a detailed restriction enzyme mapping of the 5.0 kb insert (Figure 58). Small fragments of the 5.0 kb insert were then subcloned into a

Table 14. Sub-Cloning of 5.0 kb P. fragi (ATCC 4973) Genomic DNA Fragments.

constrcut	DNA insert	L-arabinonate dehydratase specific activity (U/mg)	growth on L-arabinonate ^c
BL21(DE3)/pT7-7A"	5.0 kb, BamHI-BamHI	0.07	+
BL21(DE3)/pT7-7B ^b	5.0 kb, BamHI-BamHI	0.11	+
BL21(DE3)/pT7-7C ^a	3.9 kb, PstI-BamHI	0.08	+
BL21(DE3)/pT7-7D ^b	3.9 kb, PstI-BamHI	0.10	+
BL21(DE3)/pT7-7E ^a	2.6 kb, <i>Eco</i> RI- <i>Eco</i> RI	< 0.001	-
BL21(DE3)/pT7-7F ^b	2.6 kb, <i>Eco</i> RI- <i>Eco</i> RI	< 0.001	-
BL21(DE3)/pT7-7G ^a	3.0 kb, SmaI-BamHI	<0.001	-
BL21(DE3)/pT7-7H ^b	3.0 kb, SmaI-BamHI	<0.001	-
BL21(DE3)/pT7-7I ^a	2.6 kb, BamHI-EcoRI	<0.001	-
BL21(DE3)/pT7-7J ^b	2.6 kb, BamHI-EcoRI	<0.001	-

[&]quot; insert in the same orientation relative to pT7-7-encoded T7 promoter, b insert in the opposite orientation relative to plasmid-encoded T7 promoter, +, growth; -, no growth.

pT7-7 vector to generate plasmids that were subsequently transformed into *E. coli* BL21(DE3) to analyze for L-arabinonate dehydratase specific activity (Table 14). Four pairs of such plasmids were constructed, with each pair of plasmids having the fragment localized in two different orientations relative to the pT7-7-encoded T7 promoter. The ability of the DNA fragments to enable growth of *E. coli* BL21(DE3) on L-arabinonate was also examined by replicate plating of BL21(DE3) transformants on M9 L-arabinonate medium (Table 14). Plasmid pT7-7C and pT7-7D contained a 3.9 kb *PstI-BamHI* fragment (Figure 58). BL21(DE3) cells transformed with either plasmids were able to use L-arabinonate as a sole carbon source for growth. The L-arabinonate dehydratase specific activity was 0.08 U/mg in BL21(DE3)/pT7-7C and 0.10 U/mg in BL21(DE3)/pT7-7D (Table 14). However, the rest of the plasmids including pT7-7E and

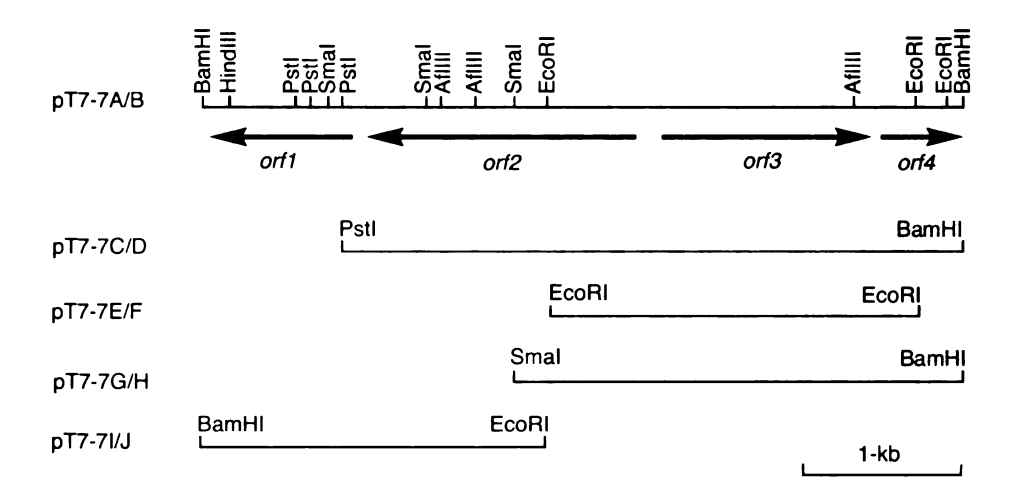


Figure 58. Restriction map of the 5.0 kb *P. fragi* (ATCC 4973) genomic DNA fragment encoding the L-arabinonate catabolic gene cluster. Lightface horizontal lines represent DNA fragments carried by named plasmids. Boldface lines represent open reading frames (*orf*s). Arrows indicate the direction of transcription of each open reading frame.

pT7-7F, which contained a 2.6 kb *Eco*RI-*Eco*RI fragment (Figure 58), pT7-7G and pT7-7H, which contained a 3.0 kb *Sma*I-*Bam*HI fragment (Figure 58), and pT7-7I and pT7-7J, which contained a 2.6 kb *Bam*HI-*Eco*RI fragment (Figure 58), were unable to support the growth of BL21(DE3) on L-arabinonate (Table 14). No L-arabinonate dehydratase activity was detected in the cell lysate of BL21(DE3) transformed with pT7-7E, pT7-7F, pT7-7G, pT7-7H, pT7-7I, and pT7-7J (Table 14). Apparently, the gene encoding L-arabinonate dehydratase was located close to the third *Pst*I site from the 5'-end of the 5.0 kb DNA fragment. Identification of the gene encoding L-arabinonate dehydratase was further facilitated by DNA sequencing. Analysis of the DNA sequence of the 5.0 kb DNA fragment revealed the existence of four open reading frames (*orf*s) (Figure 58). Based on the position of each *orf* on the 5.0 kb DNA fragment, *orf*2 potentially encoded the L-arabinonate dehydratase.

Table 15. L-Arabinonate Dehydratase Specific Activity.

auhatrata	L-arabinonate dehydratase specific activity (U/mg)		
substrate -	BL21(DE3)/pWN5.150A	BL21(DE3)/pWN5.150B	
L-arabinonate	0.21	<0.001	
D-xylonate	<0.001	<0.001	

To further establish that orf2 encoded P. fragi (ATCC 4973) L-arabinonate dehydratase, primers were designed to amplify orf2 together with 18 bp of upstream DNA, which contained a potential ribosomal binding site. The 1.7 kb PCR product was localized into the BamHI site of pT7-7 to yield plasmid pWN5.150A and pWN5.150B. In pWN5.150A, transcription of orf2 is initiated by the pT7-7-encoded T7 promoter (Figure 59). However, no promoter sequence is localized upstream to orf2 in pWN5.150B. As expected, assaying for L-arabinonate dehydratase using the cell lysate of BL21(DE3)/pWN5.150B showed no activity, while BL21(DE3)/pWN5.150A had a specific activity of 0.21 U/mg (Table 15). When D-xylonate was used as the substrate, no detectable dehydratase activity was observed from either strain (Table 15), which indicates orf2-encoded enzyme can't use D-xylonate as its substrate. Incubation of Larabinonate, and the cell lysate of BL21(DE3)/pWN5.150A led to a complete conversion of substrate to 3-deoxy-L-glycero-pentulosonic acid identified by ¹H NMR. Results from both enzyme assay and product analysis for the enzyme-catalyzed reaction confirmed that orf2 encoded a P. fragi L-arabinonate dehydratase, which can be expressed in E. coli as a catalytically active enzyme. Therefore, orf2 was named as aadh (L-arabinonic acid dehydratase) (Figure 60). Amino acid sequence analysis of L-arabinonic acid dehydratase showed this enzyme has high homology to dihydroxy acid dehydratase and

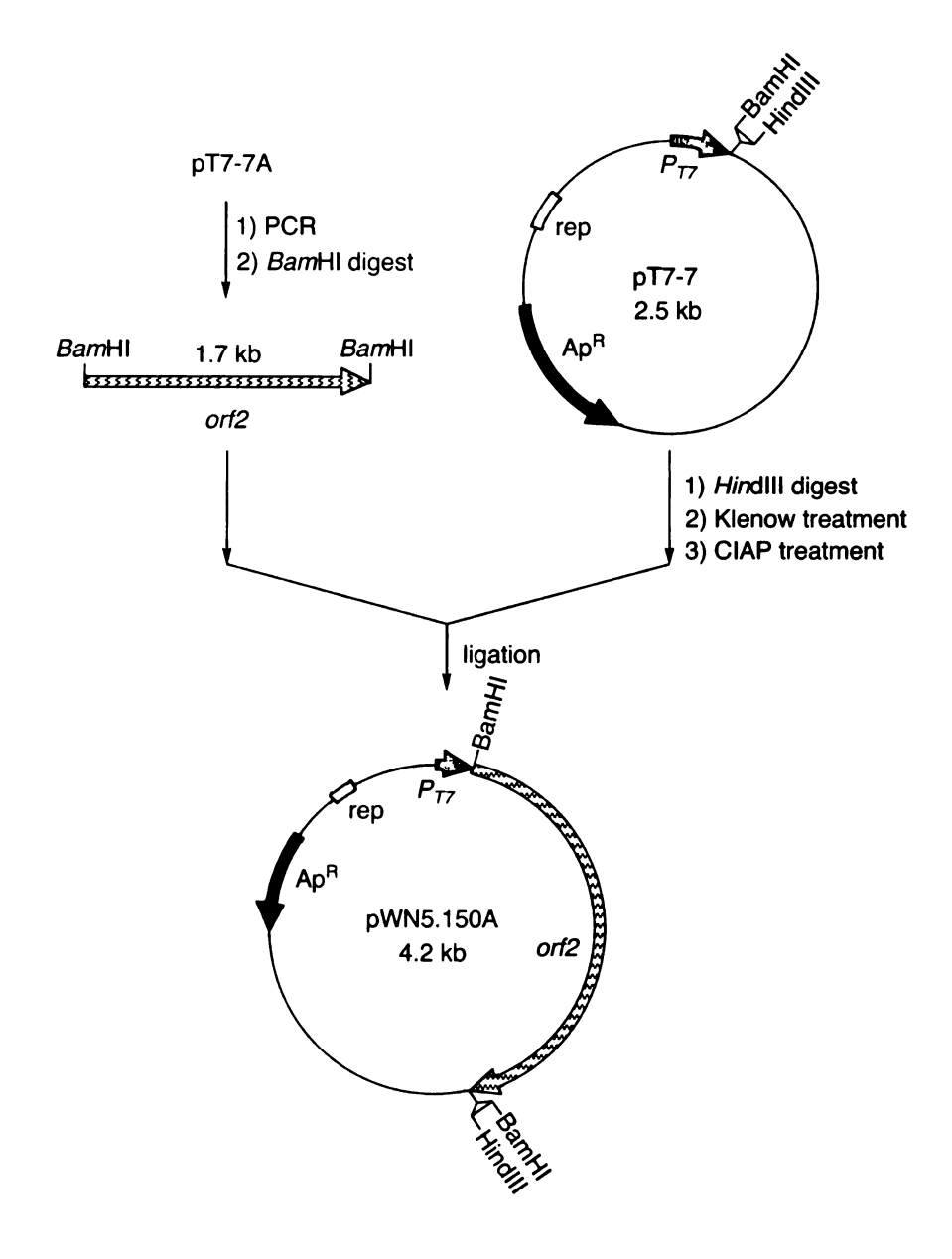


Figure 59. Preparation of plasmid pWN5.150A.

1 ATG TCA GAC AAA TTT CCT CCC CTG CGT TCT GCC CAA TGG TTC GGC AGC GCT GAT AAA AAC GGT TTC ATG S D K F P P L R S A O W F G S A D K N G F M 70 TAC CGC AGC TGG ATG AAG AAC CAG GGC ATT GCC GAT CAT CAG TTC CAG GGC AAA CCC ATC ATC GGT ATC W M N 0 GΙ A D H QF Q G K 139 TGC AAC ACC TGG TCG GAA CTG ACG CCT TGC AAT GCG CAC TTT CGG ACC ATC GCC GAG CAC GTC AAA CGC w s ELTP CNAHFRTI AEHVKR 208 GGT GTG ATC GAG GCC GGT GGT TTC CCG GTC GAG TTC CCG GTG TTT TCC AAC GGC GAA TCC AAT CTG CGA 70 PG V I E A G G F P V E F P V F S N G E S N L R 277 CCT ACC GCC ATG CTG ACG CGC AAT CTG GCG AGC ATG GAT GTG GAA GAA GCC ATT CGC GGT AAC CCG ATC Т A M L T R N L A S M D V E E A I R 346 GAT GGC GTG GTG CTG TTG ACC GGT TGC GAC AAA ACC ACC CCG GCG CTG TTG ATG GGC GCG GCC AGC TGC V V L L T G C D K T T P A L L M GAASC 415 GAT GTC CCG GCC ATT GTG GTC ACC GGT GGG CCG ATG CTG AAC GGC AAG CAC AAA GGC AAG GAC ATC GGC GPMLN 484 GCC GGG ACC ATC GTC TGG CAG ATG CAC GAG TCC TAC AAA GCC GGC ACC ATC AGC CTC GAC GAA TTC CTC 162 ► A G T I V W Q M H E S Y K A G T I S 553 TCG GCC GAG GCC GGC ATG TCG CGC TCG GCG GGC ACC TGC AAC ACC ATG GGT ACG GCC TCG ACC ATG GCC A E A G M S R AGTCNTMGT S 622 TGC ATG GCT GAA GCC CTG GGC ACC TCG CTG CCC CAT AAC GCG GCC ATC CCG GCG GTG GAT TCG CGC CGC 208 C M A E A L G T S L P H N A A I P A V D 691 TAT GTG CTG GCC CAT ATG TCG GGC ATG CGC GCC GTC GAG ATG GTC CGC GAA GAT TTG CGC CTG TCC AAA LAHMS G M R A V EMVRED 760 GTG TTG ACC CGG GAA GCC TTT GAA AAT GCG ATC AGG GTC AAT GCC GCC ATT GGC GGT TCG ACC AAC GCC 254 V L T R E A F E N A I R V N A A I G G S T N A 829 GTG ATT CAC CTC AAG GCC ATC GCC GGG CGG ATC GGC GTG GAC CTG GAG CTG GAT GAT TGG ACC CGC ATA 277 VIHLKAIAGRIG V D L E L D D W T R I 898 GGG CAG GGC ACA CCG ACC CTG GTG GAC TTG CAG CCG TCG GGT CGT TTC CTG ATG GAA GAG TTC TAC TAT 300 PG QG TPTL V D L QP S G R F L M E E F Y Y 967 GCC GGA GGC CTG CCG GCC GTG TTG CGG CGC TTG GGT GAG AAC GGC CTG ATA CCC AAT CCA CAC GCG TTG 323▶ A G G L P AVLRR LGEN GLIPNP 1036 ACC GTC AAC GGC CAG AGT TTG TGG GAG AAC GTT AAA AAC TCA CCG ATC TAT GGT GAC GAC GAA GTT ATC LWENVKN S P 1105 CGC GCA ATC GAT AAC CCG CTG GTG GCC GAC GGC GGT ATC TGT GTA TTG CGC GGC AAC CTG GCG CCT CTG 369▶ R A I D N P LVADGGI CVLRGNLAP 1174 GGC GCG GTA CTC AAG CCA TCC GCT GCG ACC CCG GCC CTG ATG AAG CAT CGC GGA CAG CCC GTG GTA TTC SAATPALMKHRGQP 1243 GAG AAC TTC GAC ATG TAC AAG GCC CGC ATC AAT GAC CCT GAG CTG GCG GTC ACT GCC GAC TCG ATT CTG D M ARINDP Y K ELAV Т ADSIL 1312 GTG ATG AAG AAC TGT GGA CCA AAG GGT TAC CCG GGC ATG GCC GAA GTG GGC AAC ATG GGC CTG CCC GCC N G P K G Υ Р G M A Ε G N M С 1381 AAG CTG CTG GCT CAG GGC GTG ACC GAT ATG GTG CGC ATT TCC GAT GCC CGC ATG AGC GGC ACG GCG TAC 461 K L L A Q G V T D M V R I S D A R M S G T A Y 1450 GGC ACA GTG GTG CTG CAC GTA GCA CCG GAA GCC GCG GCC GGC GGG CCA CTG GCG GCT GTG CAG GAA GGT 484▶ G T V V L H V A P E A A A G G P L A A V 1519 GAC TGG ATT GAA CTG GAC TGC GCC ACT GGA CGC CTG CAC CTG GAT ATC AGC GAG GCC GAA CTG ACC GCT 507 D W I E L D C A T GRLHLDISEAELTA 1588 CGC CTG GCC GAT ATC GAG CCG CCA AAA AAC CTG TTG ATT GGC GGC TAT CGC CAG CTC TAC ATC GAC CAT ADI EPPKNLLI G G Y R Q L 1657 GTC ATG CAG GCT GAC CAA GGC TGC GAC TTC GAT TTC CTG GTG GGC TGC CGA GGA TCG CAA GTA CCC CGT 553 V M Q A D Q G C D F D F L V G C R G S Q V P R 1726 CAT TCC CAC TGA 576 H S H

Figure 60. The DNA sequence of P. fragi (ATCC 4973) L-arabinonate dehydratase.

Table 16. Annotation of Loci in the L-Arabinonate Catabolic Gene Cluster.

gene	proposed function
orfl	transcription regulator
orf3	carbohydrate transport protein
orf4	unknown

phosphogluconate dehydratase. The possible functions of other ORFs on the 5.0 kb DNA fragment were assigned based on sequence homology (Table 16).

C. 2-Keto Acid Decarboxylase and Alcohol Dehydrogenase

Overview

Decarboxylation of 3-deoxy-D,L-glycero-pentulosonic acid to form D,L-3,4-dihydroxybutanal followed by reduction of D,L-3,4-dihydroxybutanal to form D,L-1,2,4-butanetriol constitutes two enzyme-catalyzed steps required for 1,2,4-butanetriol biosynthesis (Figure 49). Because there is no precedent in nature of enzymes that can catalyze either conversion, various 2-keto acid decarboxylases and alcohol dehydrogenases were screened for activities towards nonnative substrates 3-deoxy-D,L-glycero-pentulosonic acid and D,L-3,4-dihydroxybutanal.

In pursuing 2-keto acid decarboxylase and alcohol dehydrogenase activities, racemic 3-deoxy-D,L-glycero-pentulosonic acid and racemic D,L-3,4-dihydroxybutanal were chemically synthesized (Figure 61). 3-Deoxy-D,L-glycero-pentulosonic acid was prepared by the condensation between oxaloacetate and glycolaldehyde (Figure 61A). The reaction was carried out in a phosphate buffer (50 mM, pH 7.0) at room temperature overnight followed by lowering the pH to 3.0 with Dowex 50 (H⁺) and degassing for 30

Figure 61. Chemical synthesis of 3-deoxy-D,L-glycero-pentulosonic acid and D,L-3,4-dihydroxybutanal. (a) 50 mM phosphate buffer, pH 7.0; (b) Dowex 50 (H⁺), pH 3.0, 75%; (c) acetone, p-toluenesulfonic acid, 85%; (d) PCC, CH_2Cl_2 , 45%; (e) Dowex 50 (H⁺), 100%.

min. The product was purified by anion exchange columns (Dowex 1X8) and characterized by ¹H NMR, ¹³C NMR, and high-resolution mass spectrometry. Synthesis of D,L-3,4-dihydroxybutanal started from protecting D,L-1,2,4-butanetriol with acetone in the presence of *p*-toluenesulphonic acid (Figure 61B). A 9:1 (mol:mol) mixture of D,L-butane-1,2,4-triol 1,2-acetonide and D,L-butane-1,2,4-triol 2,4-acetonide was obtained and isolated in 85% yield. ¹⁴⁷ After PCC catalyzed oxidation, ¹⁴⁸ D,L-3,4-dihydroxybutanal acetonide was separated from D,L-2,4-dihydroxybutanal acetonide using flash chromatography in 45% yield. Deprotection of D,L-3,4-dihydroxybutanal acetonide was carried out quantitatively in the presence of cation exchange resin (Dowex 50 (H⁺)). ¹⁴⁹ The deprotected product was characterized by ¹H and ¹³C NMR spectroscopy ¹⁵⁰ and high-resolution mass spectrometry.

Screening for Alcohol Dehydrogenase Activity

Based on the cofactor requirement, alcohol dehydrogenase can be divided into

three major categories, NAD(P)-dependent dehydrogenases, NAD(P)-independent enzymes that use pyrroloquinoline quinone, heme or cofactor F420 as cofactor, and FAD-dependent oxidases. To screen for catalytic activity suitable for the conversion of D,L-3,4-dihydroxybutanal to D,L-1,2,4-butanetriol, four NAD-dependent alcohol dehydrogenases were tested. *Zymomonas mobilis* alcohol dehydrogenase I (encoded by *adhA*) and alcohol dehydrogenase II (encoded by *adhB*) catalyze the conversion from acetaldehyde into ethanol during ethanol fermentation. AdhA is a long-chain (337 amino acids) zinc-dependent enzyme, while AdhB is an iron-activated enzyme. Research showed that AdhA could also catalyze the reduction of butanal. The *dhaT*-encoded 1,3-propanediol dehydrogenase catalyzes the conversion of 3-hydroxypropanal into 1,3-propanediol in the anaerobic glycerol catabolic pathway in *Klebsiella pneumoniae*. DhaT is also an iron-activated enzyme. Additionally, commercially available horse liver alcohol dehydrogenase (HLADH) was also tested. HLADH is a zinc-dependent enzyme with broad substrate specificity.

NAD-dependent alcohol dehydrogenases catalyze reversible conversions between alcohols and aldehydes. AdhA, AdhB, DhaT, and HLADH were first examined by assaying their activity in the oxidative reaction using D,L-1,2,4-butanetriol as substrate. The possible oxidation reaction was followed spectrophotometrically by monitoring the formation of NADH at 340 nm. Enzyme assays of AdhA, AdhB, or DhaT were carried out in the cell lysate of *E. coli* strains that expressed the corresponding enzymes, while commercially purchased HLADH was directly used. The catalytic activity of each enzyme towards its native substrate was also determined. Catalytic activity towards 1,2,4-butanetriol was detected for AdhA, DhaT, and HLADH, but not AdhB. A

Table 17. Alcohol Dehydrogenase Activities.

anguma	construct	alcohol dehydrogenase specific activity (U/mg)		
enzyme		native substrate	D,L-1,2,4-butanetriol	
AdhA	DH5α/pLOI135	73 (ethanol) ^a	0.06	
AdhB	DH5α/pLOI295	50 (ethanol)	<0.001	
HLADH	purchased	2.6 (ethanol)	0.1	
DhaT	DH5α/pWN5.022A	0.66 (1,3-propanediol)	0.003	

^a name of the native substrate in parenthesis.

comparison between the specific ativities for native substrate and nonnative substrate showed that HLADH was the most active dehydrogenase towards 1,2,4-butanetriol (Table 17). Because 1,2,4-butanetriol has two primary alcohols and one secondary alcohol, the question arose as to which alcohol was being oxidized. Therefore, the reduction reaction was monitored by incubation of each enzyme with D,L-3,4-dihydroxybutanal and NADH. The in vitro reaction also included glucose 6-phosphate and glucose 6-phosphate dehydrogenase to regenerate NADH (Figure 62). GC analysis of the reaction mixtures showed 1,2,4-butanetriol was formed in reactions catalyzed by

Figure 62. In vitro reaction of alcohol dehydrogenase.

AdhA, DhaT, and HLADH, but not in reaction catalyzed by AdhB. Enzyme-catalyzed reactions in both oxidative and reductive directions confirmed that AdhA, DhaT, and HLADH were able to catalyze the conversion of D,L-3,4-dihydroxybutanal into D,L-1,2,4-butanetriol. The successful identification of alcohol dehydrogenase activity suitable for reduction of D,L-3,4-dihydroxybutanal provided a means for appraising 2-keto acid decarboxylases for the coversion of 3-deoxy-D,L-glycero-pentulosonic acid into D,L-3,4-dihydroxybutanal, which was the last enzyme activity required for biosynthesis of D,L-1,2,4-butanetriol from pentoses.

Screening for 2-Keto Acid Decarboxylase Activity

Six thiamine diphosphate-dependent enzymes that catalyze nonoxidative decarboxylation of 2-keto acids were examined for their catalytic activities towards 3-deoxy-D,L-glycero-pentulosonic acid. Pyruvate decarboxylase functions in ethanol-producing microbes and catalyzes the conversion of pyruvate to acetaldehyde. The pdc-encoded pyruvate decarboxylase from Acetobacter pasteurianus, 154a Zymobacter palmae, 154b and Zymomonas mobilis 154c together with commercially available pyruvate decarboxylase from Saccharomyces cerevisae were tested. Other 2-keto acid decarboxylases examined included mdlC-encoded benzoylformate decarboxylase from Pseudomonas putida 155 and ipdC-encoded indole 3-pyruvate decarboxylase from Erwinia herbicola. 156 Benzoylformate decarboxylase functions in the mandelate pathway and catalyzes the conversion of benzoylformate to benzaldehyde. Indole 3-pyruvate decarboxylase is involved in the biosynthesis of indole 3-acetic acid and catalyzes the conversion of indole 3-pyruvate to indole acetaldehyde.

Table 18. 2-Keto Acid Decarboxylase Activities.

anzyma		2-keto acid decarboxylase specific activity (U/mg)		
enzyme	construct	native substrate	3-deoxy-D,L-glycero- pentulosonic acid	- BT°
PDC	purchased	6.1 (pyruvate) ^d	<0.001	-
Pdc^a	ER1648/pJAM304	47 (pyruvate)	< 0.001	-
Pdc ^b	DH5α/pJAM3440	31 (pyruvate)	<0.001	_
Pdc^{c}	TC4/pLOI276	20 (pyruvate)	< 0.001	-
MdlC	DH5α/pWN5.238A	11 (benzoylformate)	0.001	+
IpdC	DH5α/pWN5.284A	10 (indole 3-pyruvate)	<0.001	-

^a from Acetobacter pasteurianus, ^b from Zymobacter palmae, ^c from Zymomonas mobilis, ^d name of the native substrate in parenthesis, ^c BT, 1,2,4-butanetriol.

The catalytic activity of the candidate 2-keto acid decarboxylases towards 3-deoxy-D,L-glycero-pentulosonic acid was first examined by coupling the potential decarboxylation reaction with HLADH-catalyzed reduction of D,L-3,4-dihydroxybutanal. The reaction was followed by monitoring the consumption of NADH. Enzyme assays were carried out in the cell lysate of *E. coli* strains that expressed the candidate enzyme, except for *S. cerevisiea* pyruvate decarboxylase, which was used as purchased. Based on the coupling enzyme assay, only benzoylformate decarboxylase showed detectable activity towards the nonnative substrate (Table 18). All candidate enzymes were active towards their native substrates. To further confirm this observation, in vitro enzymatic reactions were also set up by incubation of each 2-keto acid decarboxylase with the mixture of 3-deoxy-D,L-glycero-pentulosonic acid, thiamine diphosphate, NADH, and HLADH for 24 h. After removal of proteins and unreacted substrate, the reaction mixture was analyzed by ¹H NMR. 1,2,4-Butanetriol was only unambiguously detected

in the reaction catalyzed by benzoylformate decarboxylase. Therefore, the results of both enzyme assay and product analysis showed that benzoylformate decarboxylase could catalyze the decarboxylation of the racemic 3-deoxy-D,L-glycero-pentulosonic acid to form D,L-3,4-dihydroxybutanal.

Because the C-3 stereogenic carbon atom in 3-deoxy-D,L-glycero-pentulosonic acid might affect substrate binding, the catalytic activity of benzoylformate decarboxylase towards each stereoisomer of 3-deoxy-glycero-pentulosonic acid was examined. Syntheses of D- and L-3-deoxy-glycero-pentulosonic acid were accomplished via enzymatic reactions. Incubation of D-xylonic acid with purified P. fragi D-xylonate dehydratase afforded 3-deoxy-D-glycero-pentulosonic acid. Similarly, incubation of L-arabinonic acid with the cell lysate of BL21(DE3)/pWN5.150A, which expressed P. fragi L-arabinonate dehydratase, afforded 3-deoxy-L-glycero-pentulosonic acid. After removal of protein, the product of each enzymatic reaction was incubated with benzoylformate decarboxylase, thiamine diphosphate, NADH, and HLADH for 24 h. ¹H NMR analysis showed that 1,2,4-butanetriol was formed in both reactions. The total yield of 1,2,4-butanetriol from D-xylonic acid was 9%, while the total yield from L-arabinonic acid was 10%. This observation established that benzoylformate decarboxylase catalyzed decarboxylation of D and L isomer of 3-deoxy-glycero-pentulosonic acid at a similar rate.

With *mdlC*-encoded benzoylformate decarboxylase-catalyzed decarboxylation of both stereoisomers of 3-deoxy-*glycero*-pentulosonic acid, and *adhA*-encoded along with *dhaT*-encoded alcohol dehydrogenases catalyzing the reduction of 3,4-dihydroxybutanal, all of the enzyme activities required for the conversion of D-xylonate into D-1,2,4-butanetriol and the conversion of L-arabinonate into L-1,2,4-butanetriol have been

identified. Research efforts therefore were focused on the design and construction of 1,2,4-butanetriol-synthesizing microbes.

D. Microbial Synthesis of D- and L-1,2,4-Butanetriol

Construction of a D-1,2,4-Butanetriol-Synthesizing Microbe

Biosynthesis of D-1,2,4-butanetriol from D-xylonic acid requires a D-xylonic acid transport system and the activities of three enzymes including D-xylonate dehydratase, 2keto acid decarboxylase, and alcohol dehydrogenase. The observation that E. coli could use D-xylonic acid as the sole source of carbon for growth indicated that a native E. coli transport system could transport D-xylonic acid from the culture medium into the cytoplasm. Discovery of the D-xylonate dehydratase activity in E. coli W3110 simplified the biocatalyst design by reducing the number of enzymes requiring heterologous expression in E. coli. However, the ability of E. coli to catabolize D-xylonic acid raised the question as to whether the low decarboxylase activity of mdlC-encoded benzoylformate decarboxylase towards 3-deoxy-D-glycero-pentulosonic acid could compete with the catabolic pathway to divert carbon flow into the biosynthesis of D-1,2,4-butanetriol. To address this question, E. coli W3110/pWN5.238A was cultured in 5 mL of M9 medium containing D-xylonic acid as the sole source of carbon. The pJF118EH-derived plasmid pWN5.238A carried mdlC, lacl^Q, and an ampicillin resistance gene (Figure 63). Therefore, plasmid maintenance was achieved by addition of ampicillin to the culture medium. Transcription of benzoylformate decarboxylaseencoding mdlC was initiated by the pJF118EH-localized tac promoter, which was under the control of Lac repressor protein encoded by lacI^Q. Expression of MdlC was induced

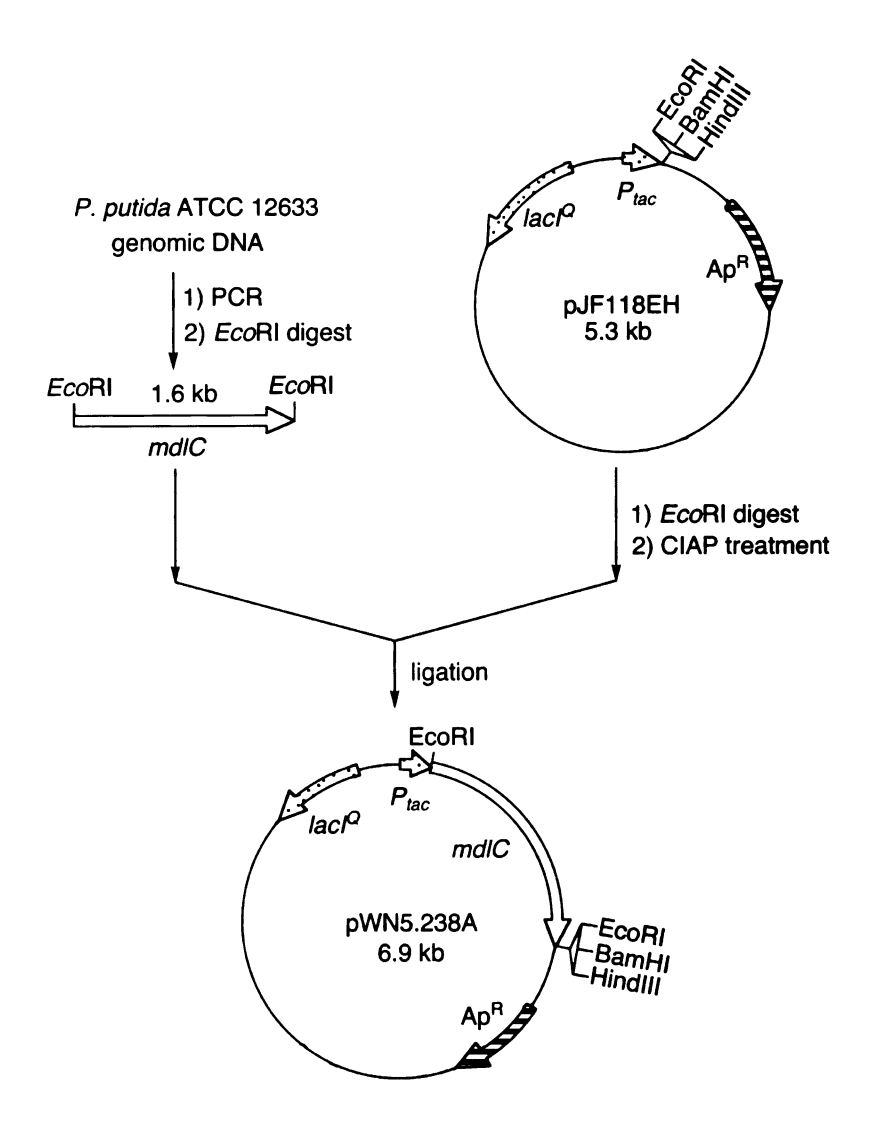


Figure 63. Preparation of plasmid pWN5.238A.

by addition of IPTG to the culture medium to a final concentration of 0.5 mM when the OD₆₀₀ of the cell culture reached 0.4. Cultivation for 36 h after IPTG addition was followed by ¹H NMR analysis of the solutes in the culture supernatant. Ethylene glycol and glycolate were the only metabolites that could be unambiguously identified. The decarboxylation product, D-3,4-dihydroxybutanal was not observed. Therefore, the catalytic activity of benzoylformate decarboxylase was not enough to compete for 3-deoxy-D-glycero-pentulosonic acid when *E. coli* W3110 was grown on D-xylonic acid.

To relieve the competition for 3-deoxy-D-glycero-pentulosonic acid, E. coli strains were cultured in a rich medium containing D-xylonic acid. The presence of alternate carbon source was intended to slow the rate of D-xylonic acid catabolism. As a consequence, 3-deoxy-D-glycero-pentulosonic acid derived from D-xylonic acid might be diverted into the biosynthesis of D-1,2,4-butanetriol. E. coli W3110/pWN5.238A, E. coli JWF1/pWN5.238A, E. coli KL3/pWN5.238A, and E. coli DH5 α /pWN5.238A were cultured in 5 mL of LB medium containing Ap (Table 19). When the OD₆₀₀ of cell culture reached 0.4, D-xylonic acid was added into culture medium to a final concentration of 0.1 M. At the same time, mdlC-encoded benzoylformate decarboxylase expression was induced with the addition of IPTG to a final concentration of 0.5 mM. 'H NMR analysis of the culture supernatant revealed that E. colil W3110/pWN5.238A, E. coli JWF1/pWN5.238A, and E. coli KL7/pWN5.238A completely consumed D-xylonic acid 36 h after the IPTG induction. Ethylene glycol and glycolate were still the only Dxylonic acid-derived metabolites that accumulated. However, approximately 50% of the initial D-xylonic acid remained in the culture medium of E. coli DH5α/pWN5.238A. Additionally, an unexpected 15 mM of 1,2,4-butantriol was produced by this strain

Table 19. E. coli Growth Characteristic in D-Xylonic Acid and Synthesis of 1,2,4-Butanetriol.

strain	relevant characteristics	growth on D-xylonic acid	BT ^b production ^c
W3110	wild type	+	_
JWF1	lacI ^Q serA::aroB	+	-
KL3	aroE353 serA::aroB	+	_
DH5α	lacZ∆M15 hadR recA	+/-	+

^a cells started to grow seven days after the inoculation, ^b BT, 1,2,4-butanetriol, ^c the indicated host strain was transformed with pWN5.238A and cultured in LB medium containing D-xylonic acid.

(Table 19). This observation indicated that benzoylformate decarboxylase catalyzed the decarboxylation of part of the 3-deoxy-D-glycero-pentulosonic acid derived from the catabolism of D-xylonic acid by *E. coli* DH5α. The accumulation of 1,2,4-butanetriol instead of D-3,4-dihydroxybutanal indicated that an unidentified *E. coli* alcohol dehydrogenase was able to catalyze the reduction of the aldehyde. As a consequence, a D-1,2,4-butanetriol-synthesizing *E. coli* construct only requires the heterologous expression of *mdlC*-encoded benzoylformate decarboxylase to catalyze the synthesis of D-1,2,4-butanetriol from D-xylonic acid. Native D-xylonate dehydratase and alcohol dehydrogenase activities in *E. coli* catalyze the remaining two reactions required for the overall conversion.

A second conclusion from this experiment is that $E.\ coli\ DH5\alpha$ is a better host strain for biosynthesis of D-1,2,4-butanetriol relative to $E.\ coli\ W3110$, JWF1, and KL3. Production of 1,2,4-butanetriol by $E.\ coli\ DH5\alpha$ seemingly is due to a slower rate of D-xylonic acid catabolism. When single colonies of $E.\ coli\ W3110$, JWF1, KL3, and DH5 α were respectively inoculated into M9 D-xylonic acid medium, $E.\ coli\ DH5\alpha$ cells started

growing seven days after the inoculation, while other strains started growing 12 h after the inoculation. The genetic basis for the slower rate of D-xylonic acid catabolism in E. $coli\ DH5\alpha$ remains to be identified.

With the identification of host strain $E.\ coli$ DH5 α and the determination that mdlC-encoded benzoylformate decarboxylase is the only enzyme requiring heterologous expression, D-1,2,4-butanetriol-synthesizing $E.\ coli$ DH5 α /pWN6.186A was constructed. Plasmid pWN6.186A was derived from pWN5.238A by insertion of a kanamycin resistance gene (Figure 64). As a consequence, plasmid maintenance in $E.\ coli$ DH5 α /pWN6.186A was achieved by inclusion of kanamycin in the culture medium. This approach avoids possible plasmid loss caused by decreasing concentrations of ampicillin in the culture medium due to β -lactamase-catalyzed hydrolysis.

Construction of an L-1,2,4-Butanetriol-Synthesizing Microbe

Biosynthesis of L-1,2,4-butanetriol from L-arabinonic acid required the activities of three enzymes including *aadh*-encoded L-arabinonate dehydratase, *mdlC*-encoded benzoylformate decarboxylase, and an alcohol dehydrogenase, while a transport system was required for bringing the starting material from the culture medium into the *E. coli* cytoplasm. However, the observation that *E. coli* can't use L-arabinonate as the sole source of carbon for growth raised a question about whether such a transport system was native to *E. coli*. Additionally, the observation that *E. coli* alcohol dehydrogenase was capable of catalyzing the reduction of D-3,4-dihydroxybutanal raised a second question with respect to whether this enzyme was capable of reducing L-3,4-dihydroxybutanal to L-1,2,4 butanetriol.

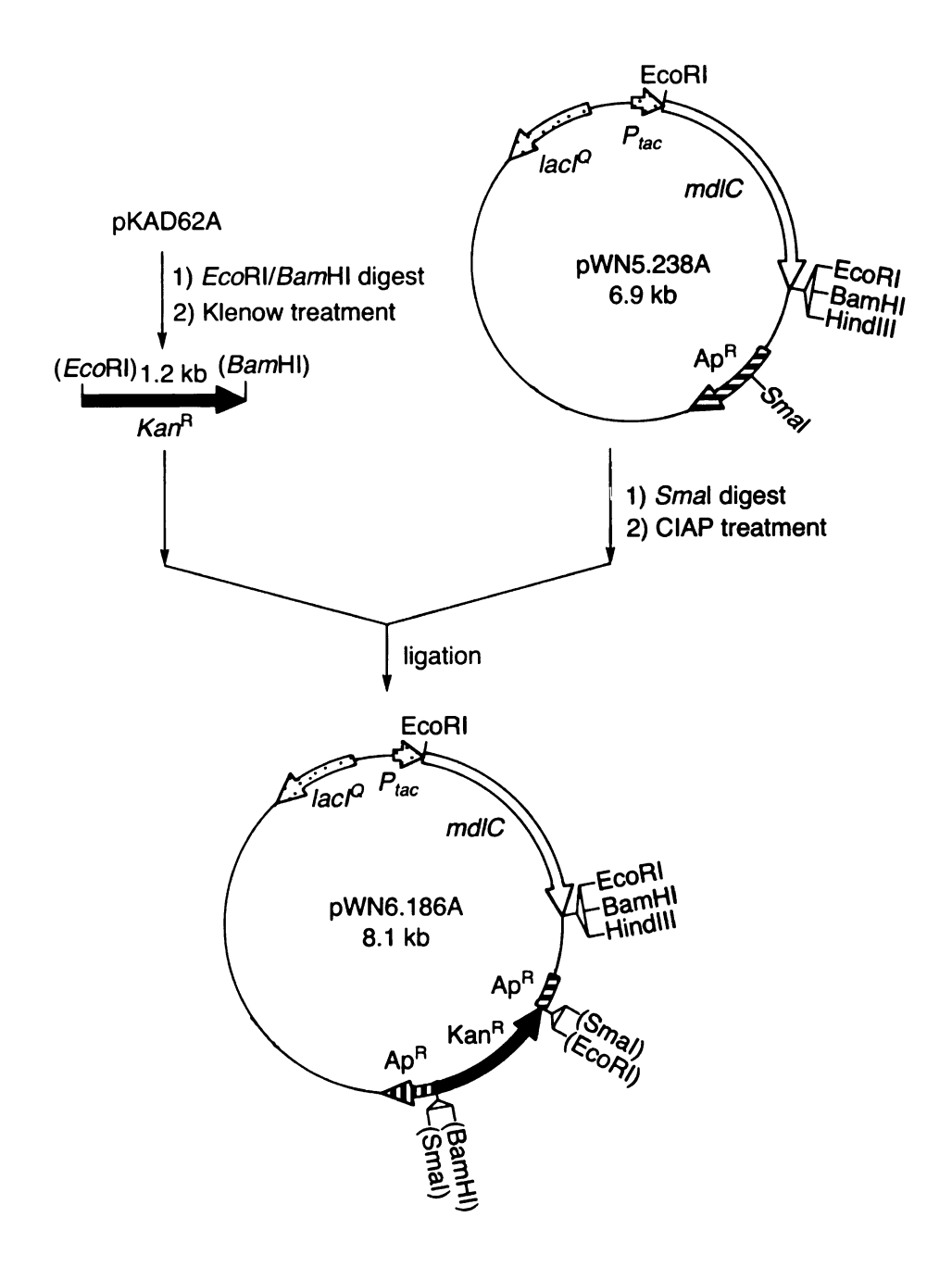


Figure 64. Preparation of plasmid pWN6.186A.

To answer the above two questions, E. coli BL21(DE3)/pWN6.086A was constructed. As a derivative of plasmid pWN5.150A (Figure 59), plasmid pWN6.086A carried aadh, mdlC, $lacI^Q$, and an ampicillin resistance gene (Figure 65). As a consequence, when E. coli BL21(DE3)/pWN6.086A was cultured in medium containing L-arabinonic acid, an E. coli L-arabinonic acid transport system would be implicated by a decrease in the conentration of L-arabinonic acid in the culture supernatant. Furthermore, if E. coli alcohol dehydrogenase was catalytically active towards L-3,4-dihydroxybutanal, the reduction product, L-1,2,4-butanetriol would accumulate in the culture supernatant. LB medium containing ampicillin was inoculated with E. coli BL21(DE3)/pWN6.086A. When the OD_{600} of the culture reached 0.4, L-arabinonic acid was added to the culture medium to a final concentration of 0.1 M. At the same time, aadh-encoded L-arabinonate dehydratase and *mdlC*-encoded benzoylformate decarboxylase expression was induced with the addition of IPTG to a final concentration of 0.5 mM. ¹H NMR analysis of the culture supernatant of E. coli BL21(DE3)/pWN6.086A after the IPTG induction revealed a constant L-arabinonic acid concentration in the initial 24 h and a slight drop at 36 h (Table 20). No L-3,4-dihydroxybutanal or L-1,2,4-butanetriol was detected. This indicated that it was unlikely that E. coli BL21(DE3) transported L-arabinonic acid into its cytoplasm in significant amounts.

Isolation of the *P. fragi* (ATCC 4973) aadh gene led to the identification of gene orf3, which encoded a protein with high homology to sugar transport proteins (Table 16). The expression of Orf3 together with L-arabinonate dehydratase and an orf4-encoded protein with unknown function allows *E. coli* to grow on L-arabinonic acid (Table 15). To examine whether the orf3-encoded protein functions as an L-arabinonic acid transport

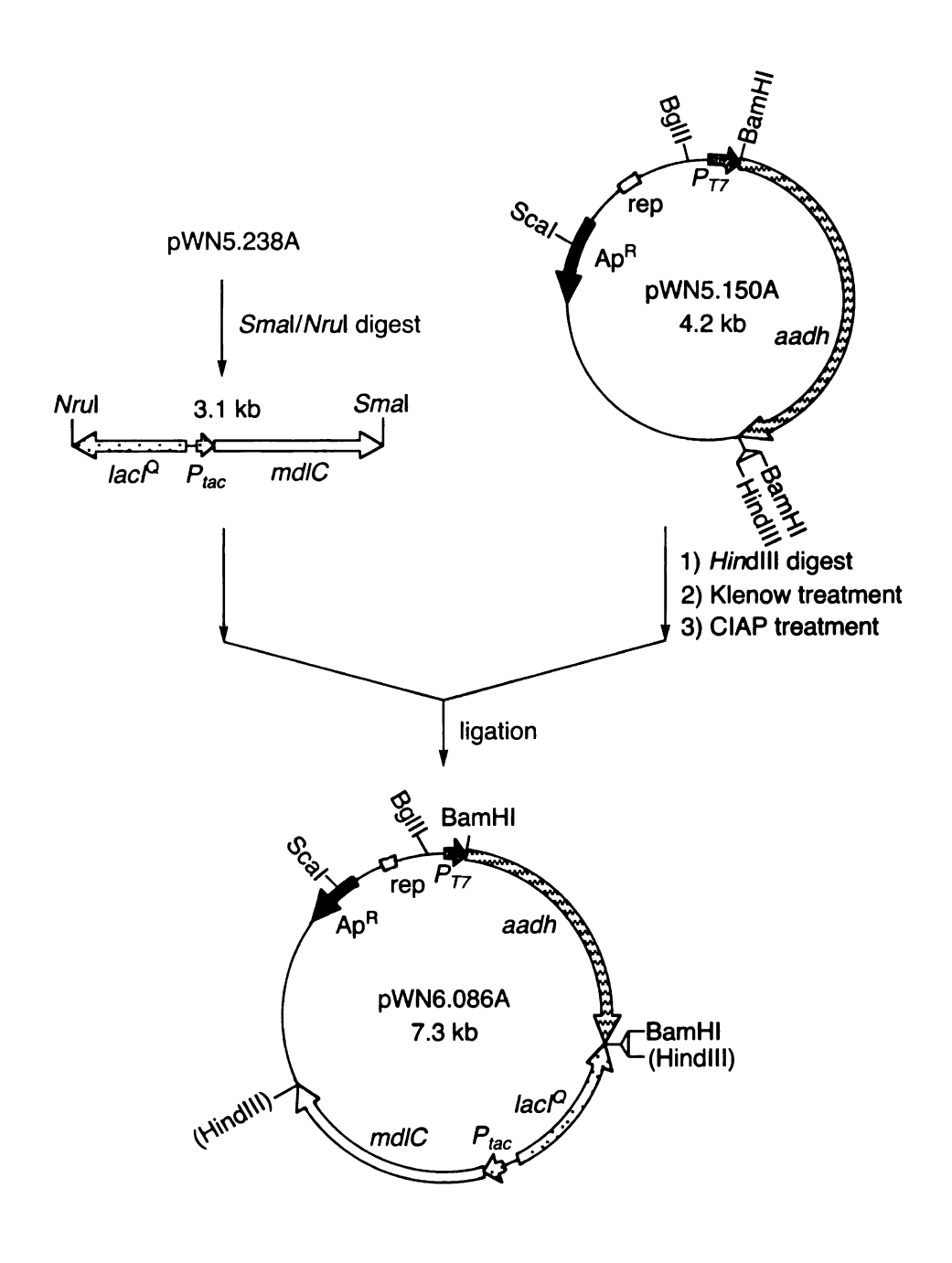


Figure 65. Preparation of plasmid pWN6.086A.

protein, orf3 was amplified using PCR and subsequently inserted into vector pKK223-3 to afford plasmid pWN6.120A (Figure 66). Digestion of pWN6.120A with BamHI liberated a 1.7 kb DNA fragment containing P_{tac} -orf3, which was cloned into pWN6.086A to afford pWN6.126A (Figure 67). The ability of E. coli BL21(DE3)/pWN6.126A to transport L-arabinonic acid was examined using the same method as for E. coli BL21(DE3)/pWN6.086A. Within 36 h after IPTG induction, the concentration of L-arabinonic acid in the culture medium has steadily decreased (Table 20). At the same time, the concentration of 1,2,4-butanetriol steadily increased. Formation of 3,4-dihydroxybutanal was not detected. Therefore, orf3 likely encoded a P. fragi L-arabinonic acid transport protein (Figure 69). Gene orf3 was renamed as aatp (Larabinonic acid transport protein). The formation of 1,2,4-butanetriol also showed that an unidentified E. coli alcohol dehydrogenase could catalyze the reduction of L-3,4dihydroxybutanal. Insertion of a kanamycin resistance gene into plasmid pWN6.126A resulted in pWN6.222A (Figure 68). E. coli BL21(DE3)/pWN6.222A was examined under fed-batch fermentor conditions.

Table 20. Cultivation of *E. coli* in Medium Containing L-Arabinonate.

time ^a (h)	BL21(DE3)/pWN6.086A		BL21(DE3)/pWN6.126A	
	L-arabinonic acid (mM)	BT ^b (mM)	L-arabinonic acid (mM)	BT (mM)
0	120	0	117	0
12	121	0	91	4.5
24	118	0	81	7.5
36	110	0	76	8.0

^a When IPTG and L-arabinonic acid were added to the culture medium, time = 0 h; ^b BT, 1,2,4-butanetriol.

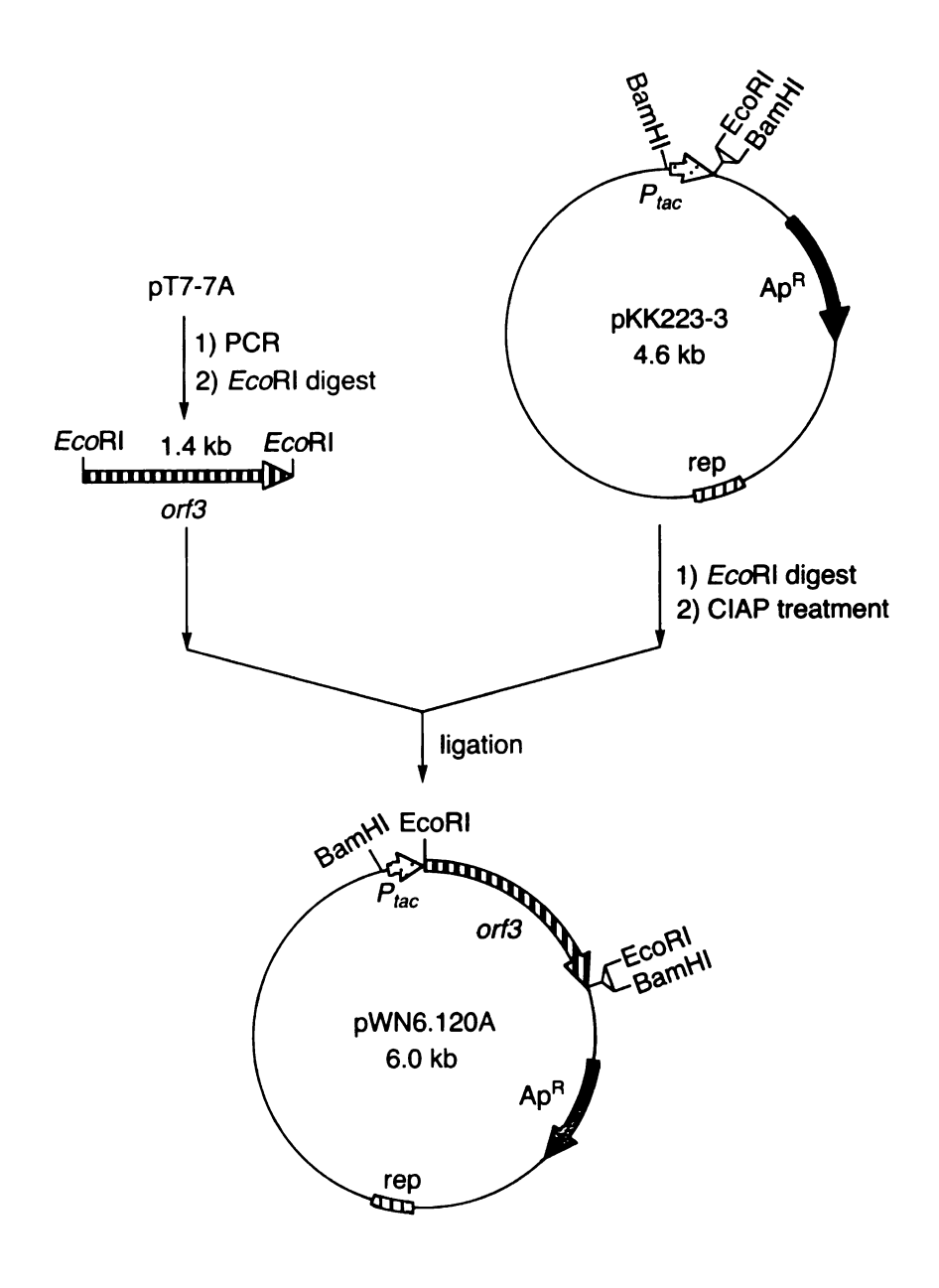


Figure 66. Preparation of plasmid pWN6.120A.

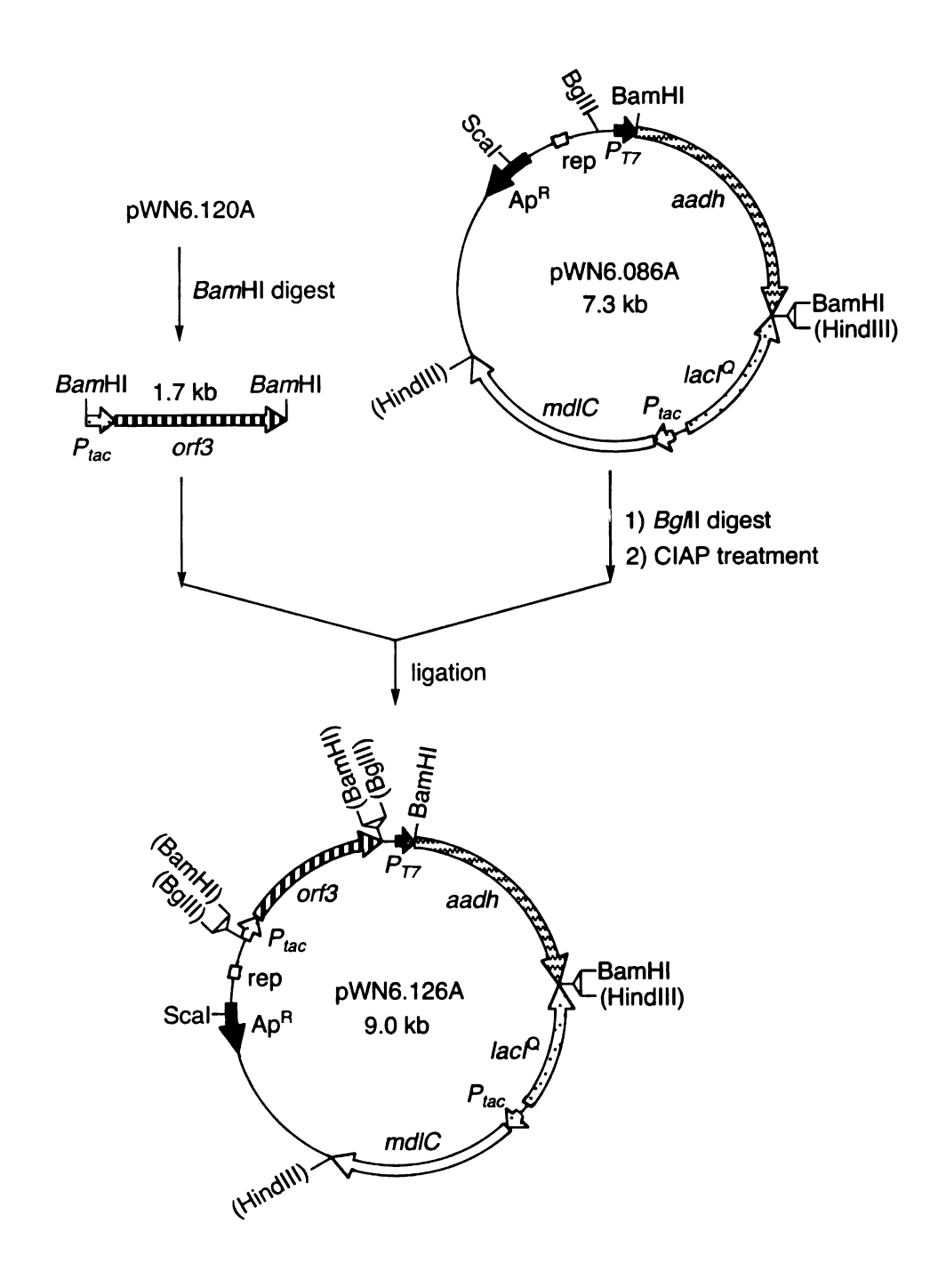


Figure 67. Preparation of plasmid pWN6.126A.

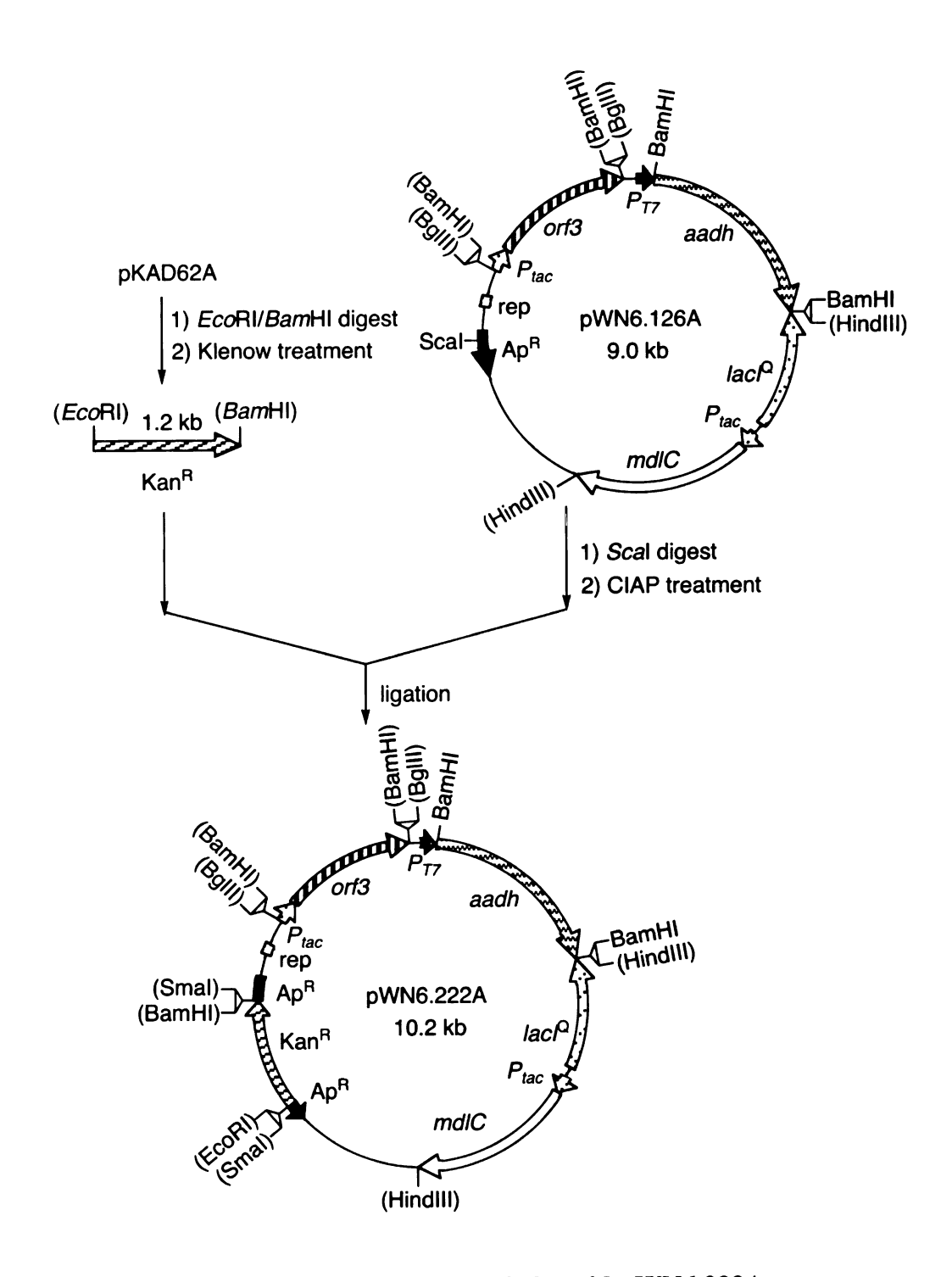


Figure 68. Preparation of plasmid pWN6.222A.

1 ATG GGA GAC CGT CTC ATG AGC CAG GAA CTC CGG CTT ATT CGT CGC ATT ACG CTT AAA CTC ATT CCC TTC 1 M G D R L M S Q E L R L I R R I T L K L I P F 70 CTG ATC CTG CTG TAC CTG ATT GCT TAT GTA GAT CGT TCC GCG GTG GGC TTT GCA AAG CTG CAC ATG GGC 24 L I L L Y L I A Y V D R S A V G F AKLHM 139 GCG GAT ATC GGC ATT GGC GAT GCC GCC TAT GGC CTG GGC GCC GGG CTG TTT TTC ATT GGC TAT TTC CTG 208 ATG GAA ATC CCC AGC AAC CTG ATG CTC GAG CGT TTC GGC GCC CGG CGC TGG TTT GCC CGG ATC ATG GTC I P S N L M L E R F GARRWF A R 277 ACC TGG GGC GCC ATC ACC ATT GGC ATG GCC TTT GTG CAG GGG CCG CAC AGC TTC TAT GTC ATG CGT TTC GMAF 0 G P н 346 CTG CTG GGG GTC GCC GAA GCG GGG TTC TTT CCT GGC GTG CTG TAC TAC ATC ACC CAA TGG TTT CCG GTC LGVAEAGFFP G V L 415 CGC CAT CGC GGC AAG ATC CTG GGC CTG TTT ATC CTC TCG CAA CCA ATC GCC ATG ATG ATC ACC GGG CCC 139▶ R H R G K I L G L F I L S Q P I A M M I Т 484 GTG TCT GGC GGC TTG CTT GGC ATG GAT GGC ATC CTT GGC CTG CAT GGC TGG CAA TGG CTG TTT ATT GTG 162 \blacktriangleright V S G G L L G M D G I L G L H G W Q W L F I 553 ATC GGC ACG CCC GCC ATT CTG TTG ACC TGG CCC GTA CTG CGT TAC TTG CCG GAC GGC CCG CAA CAG GTC V L R GPOOV622 AAG TGG ATG GAT CAG GGT GAA AAG GAC TGG CTG CAA GGC GAG CTG GAA AAG GAC TTG CAA GCC TAC GGC QGELEKD 208▶ K W M D QGEKDWL LQAY 691 CAG ACC CGT CAT GGC AAC CCG TTG CAT GCT CTG AAA GAC AAG CGC GTA TTG CTG CTT GCG CTG TTC TAC 231 PQTRHGNPLHALKDKRVLL 760 CTG CCC GTC ACC CTG AGT ATT TAC GGG CTG GGG CTG TGG CTG CCA ACG TTG ATC AAA CAG TTT GGC GGC 254 L P V T L S I Y G L G L W L P T L I K Q F G G 829 AGT GAT TTG AGC ACC GGG TTC GTG TCT TCG GTG CCC TAT GTC TTC GGC ATT ATC GGC TTG CTC ATC ATC 277▶ S D L S T G F V S S V P YVFGII GLL 898 CCT CGC AGT TCC GAC CGC CTC AAT GAT CGC TAT GGC CAC CTG GCA GTG CTC TAT GTG CTG GGC GCC ATC SSDRLNDR G H L V L Υ Α 967 GGG CTG TTC TTC AGC GCC TGG CTG ACG GTG CCG ATG CTG CAA CTG GCG GCC TTG AGC CTG GTG GCA TTC FSAWLT V P M L QLAA 1036 TCG TTG TTT TCC TGT ACC GCC ATC TTC TGG ACA TTA CCG GGA CGC TTC TTC GCC GGT GCC AGC GCC GCC W Т ΑI G R 1105 GCC GGC ATT GCC CTG ATC AAC TCG GTG GGC AAC CTG GGT GGC TAC ATC GGA CCG TTT GTG ATC GGT GCG S Α N V G N L G G G P 1174 CTC AAG GAA TAC ACC GGC AAC CTC GCC TCG GGC TTG TAC TTC CTG AGC GGG GTG ATG CTG TTC GGG CTC 392 L K E Y T G N L A S G L Y F L S G V M L 1243 TTC CTG ACG TTC GTG GTG TAT CGC ACC CTC GAG CGT AAA CAC GTG CTC CAG TCG AGC GAA TTT GCC GCC Т LERKHVLQSSEFAA 415 F L T F V V Υ R 1312 AGC GCC CGC GCG GCG ACC CAT CTT TAA 438 S A R A A T H L

Figure 69. The DNA sequence of an L-arabinonic acid transport protein from P. fragi (ATCC 4973).

Biosynthesis of D- and L-1,2,4-Butanetriol

Biosynthesis of D- and L-1,2,4-butanetriol were carried out under fed-batch fermentor conditions. The same fed-batch fermentor equipment as described in Chapter 2 and Chapter 3 was employed. Fermentations were run at 33 °C, pH 7.0, and the dissolved oxygen (D.O.) level was maintained at 20%. The initial glucose concentration in the fermentation medium was 22 g/L for the synthesis of D-1,2,4-butanetriol and 12 g/L for the synthesis of L-1,2,4-butanetriol.

The same three-staged method as described in Chapter 2 was employed to maintain D.O. level at 20%. However, glucose (650 g/L) was used as the feedstock. At the beginning of the third controlling stage, D-xylonic acid or L-arabinonic acid was added to the culture medium. At the same time, protein expression was induced by the addition of IPTG to the culture medium to a final concentration of 0.5 mM. After culturing *E. coli* DH5α/pWN6.186A under fed-batch fermentor conditions for approximately 10 h, IPTG and D-xylonic acid (10 g) were added to the fermentor. An additional 6 h of cultivation resulted in the accumulation of 1.6 g/L of 1,2,4-butanetriol in

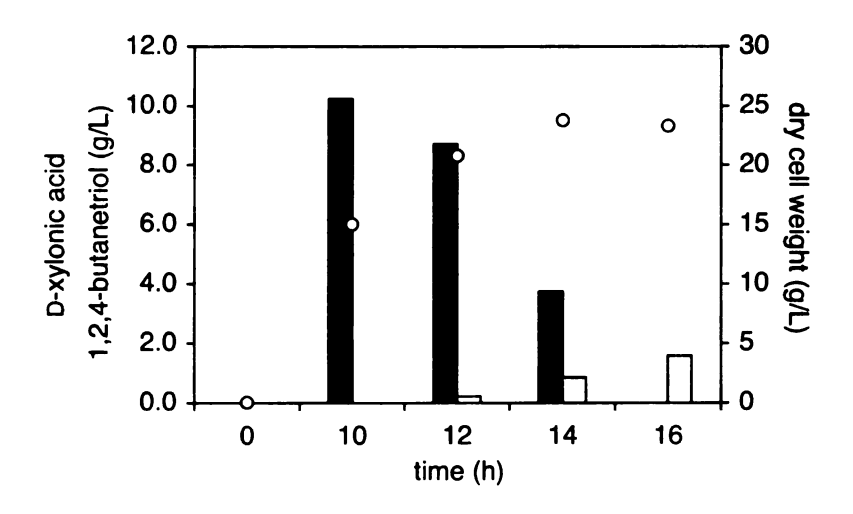


Figure 70. Biosynthesis of D-1,2,4-butanetriol by E. coli DH5\(\alpha\)/pWN6.186A. \(\circ\) cell dry weight; \(\begin{array}{c} D-xylonic acid; \(\begin{array}{c} \begin{array}{c} 1,2,4-butanetriol. \end{array}

25% (mol/mol) yield (Figure 70). E. coli DH5α/pWN6.186A also synthesized ethylene glycol (0.1 g/L) in a 3% (mol/mol) yield. Ethylene glycol has been identified as a product of E. coli D-xylonic acid catabolism. Its accumulation shows that E. coli can catabolize D-xylonic acid under fed-batch fermentor conditions. However, because E. coli can also use ethylene glycol as a carbon source, 66 the amount of ethylene glycol detected in the culture medium can not be used to estimate the amount of D-xylonic acid being used for producing cell mass. Relative to E. coli DH5α/pWN6.186A, fermentorcontrolled cultivation of E. coli BL21(DE3)/pWN6.222A reached the third D.O. controlling stage earlier. Approximately 4.5 h after the initiation of the fermentation, IPTG and L-arabinonic acid (10 g) were added to the culture medium. A significant decrease in cell dry weight was observed over the next 4 h. After an additional 6 h of cultivation, E. coli BL21(DE3)/ pWN6.222A synthesized 2.4 g/L of 1,2,4-butanetriol in 35% (mol/mol) yield (Figure 71) and 0.09 g/L of ethylene glycol in 2 % (mol/mol) yield. The accumulation of ethylene glycol during synthesis of L-1,2,4-butanetriol indicated that 3-deoxy-D-glycero-pentulosonic acid was catabolized by E. coli via a similar pathway

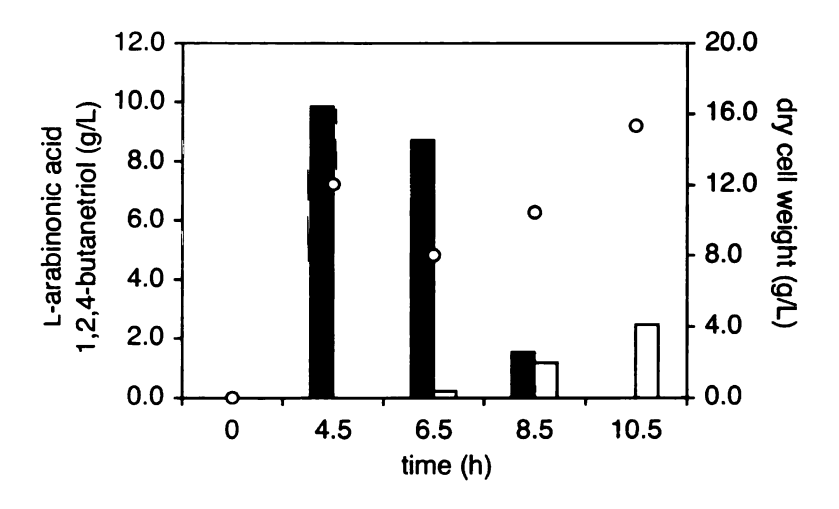


Figure 71. Biosynthesis of L-1,2,4-butanetriol by E. coli BL21(DE3)/pWN6.222A. o cell dry weight; L-arabinonic acid; 1,2,4-butanetriol.

used for catabolism of the corresponding D- stereoisomer. During synthesis of L-1,2,4-butanetriol from L-arabinonic acid, 3-deoxy-glycero-pentulosonic acid was also observed in culture supernatant at 6.5 h and 8.5 h. This observation suggested that mdlC-encoded benzoylformate decarboxylase activity was a limiting factor in the biosynthesis of L-1,2,4-butanetriol.

To determine the enantiomeric purity of microbial synthesized 1,2,4-butanetriol, fermentation broth of $E.\ coli\ DH5\alpha/pWN6.186A$ and $E.\ coli\ BL21(DE3)/pWN6.222A$ were partially purified and derivatized using Mosher reagent, (S)-(+)- α -methoxy- α -(trifluoromethyl) phenylacetyl chloride. Analysis of 1,2,4-butanetriol Mosher ester using an HPLC Chiralpak column revealed that the ee% of microbial synthesized D- and L-1,2,4-butanetriol were 99% and >99%, respectively.

<u>Directed Evolution of Benzoylformate Decarboxylase to Improve</u> <u>Microbial Synthesis of 1,2,4-Butanetriol</u>

A. Background

Biosynthesis of 1,2,4-butanetriol (Figure 49) was designed around *P. fragi* D-xylose and L-arabinose catabolism and *E. coli* D-xylonic acid catabolism. As the point at which 1,2,4-butanetriol biosynthesis diverges from D-xylose and L-arabinose catabolism, the decarboxylation of 3-deoxy-glycero-pentulosonate stereoisomers catalyzed by benzoylformate decarboxylase occupies a critical position in the overall biosynthesis. As observed from both in vitro enzyme assay and in vivo synthesis of 1,2,4-butanetriol, benzoylformate decarboxylase showed low catalytic activity towards 3-deoxy-glycero-pentulosonate stereoisomers. Therefore, improving the activity of this decarboxylase is essential for improving the yields and concentrations of biosynthesized 1,2,4-butanetriol.

Since its first application about one decade ago¹⁵⁷, directed evolution has rapidly become a powerful tool used in protein engineering research.¹⁵⁸ Directed evolution allows significant improvement of enzyme performance without the input of any structural or mechanistic information. Alternatively, studies of the mutants obtained from directed evolution experiments can help to understand basic questions related to protein folding, ligand-receptor binding, and enzyme evolution.¹⁵⁹ Various PCR-based techniques such as error-prone PCR,¹⁶⁰ DNA shuffling,¹⁶¹ and stagger-extended PCR¹⁶² have been employed in directed evolution efforts. Such evolved enzymes have demonstrated altered substrate specificity or improved stability and catalytic activity under a variety of conditions.

The *mdlC*-encoded benzoylformate decarboxylase from *Pseudomonas putida* (ATCC 12633) functions in the mandelate metabolic pathway, which enables several closely related microorganisms to utilize both *R* and *S*-mandelate as a sole source of carbon for growth. Two crystal structures are available for benzoylformate decarboxylase. In this section, directed evolution methods were applied to improve the catalytic activity of benzoylformate decarboxylase towards 3-deoxy-D,L-*glycero*-pentulosonic acid. The *mdlC* gene was first subjected to error-prone PCR to generate the mutant enzyme library designated as E1. Genes encoding mutant enzymes with elevated activity towards 3-deoxy-D,L-*glycero*-pentulosonic acid were subsequently recombined through DNA shuffling to generate the mutant library designated as S2. The ability of mutant benzoylformate decarboxylase to support microbial synthesis of D-1,2,4-butanetriol was further evaluated by a small-scale shake flask experiment. Additionally, DNA sequencing results of benzoylformate decarboxylase variants obtained from the

directed evolution efforts revealed the possible structural bases for improved catalytic activity with respect to decarboxylation of 3-deoxy-D,L-glycero-pentulosonic acid.

B. Directed Evolution of Benzoylformate Decarboxylase

Construction of Benzoylformate Decarboxylase Mutant Libraries

Two PCR-based DNA sequence randomization methods including error-prone PCR and DNA shuffling were used in the directed evolution of benzoylformate decarboxylase. PCR products were inserted into protein expression vector pJF118EH and subsequently transformed into *E. coli* DH5α to generate mutant library E1 and S2. Inclusion of an *Eco*RI restriction enzyme site on the sense primer and a *Bam*HI restriction enzyme site on the anti-sense primer allowed digestion of the PCR product with both restriction enzymes and ligation of the digestion product into vector pJF118EH digested by the same restriction enzymes. As a consequence, the insert DNA can only be located into the vector in a defined orientation. This directional cloning strategy ensured that the inserted gene would be expressed off a *tac* promoter located upstream from the *Eco*RI recognition site on pJF118EH. Due to the expression of a plasmid-encoded Lac repressor protein, *tac* promoter initiated transcription of mutant genes in different clones could be regulated by the addition of IPTG. Analysis of the mutant library showed an insertion frequency of approximately 90% during the cloning step.

The wild type *mdlC* gene (1587 bp), which encodes *Pseudomonas putida* (ATCC 12633) benzoylformate decarboxylase, was first subjected to random mutagenesis using error-prone PCR. To determine a PCR amplification condition that introduced a limited number of mutations over the entire gene, ¹⁶⁴ three mutant libraries were generated using

PCR in three different concentrations of MnCl₂ (0.1 mM, 0.2 mM, and 0.5 mM). DNA sequencing of these three mutant libraries revealed an average mutation frequency of 0.12, 0.25 and 0.90%, which corresponded to 1.9 bp, 3.9 bp, and 14 bp changes on a gene of 1587 bp. Since the desired mutation frequency in directed evolution experiments ranges from 2-5 bp per gene, 164 error-prone PCR used for generating the E1 library was run at 0.2 mM MnCl₂. Based on in vitro enzymatic reactions, approximately 50% of the mutants of E1 library could catalyze the decarboxylation of 3-deoxy-D,L-glyceropentulosonic acid. As the second stage of directed evolution, DNA shuffling was employed to recombine genes of benzoylformate decarboxylase mutants in route to identification of improved decarboxylase activity relative to 3-deoxy-D,L-glyceropentulosonic acid. To facilitate the formation of blunt-ended digestion products and further improve the efficiency of the primerless PCR reaction, 165 random fragmentation using DNaseI was carried out in the presence of MnCl₂. Digestion time was controlled to afford DNA fragments of 50-100 bp lengths as the major products. Approximately 42% of the mutants generated in this fasion catalyzed the decarboxylation of 3-deoxy-D,Lglycero-pentulosonic acid.

Development of a Screening Method

Designing reliable and efficient methodology for the identification of mutant isozymes possessing the desired improved catalytic properties is the most challenging and rate-limiting step in directed evolution. Decarboxylase activities of benzoylformate decarboxylase mutants towards 3-deoxy-D,L-glycero-pentulosonic acid

were screened using a direct assay to detect the formation of the decarboxylation product of the in vitro enzymatic reactions.

Figure 72. Reaction of Purpald with D,L-3,4-dihydroxybutanal and 3-deoxy-D,L-glycero-pentulosonic acid.

Purpald (4-amino-3-hydrazino-5-mercapto-1,2,4-triazole) (Figure 72) and Schiff's reagent (Figure 73) were examined for use as a chromogenic indicator in the screening assay. To test the selectivity of Purpald and Schiff's reagent for the decarboxylation product, D,L-3,4-dihydroxybutanal, over the substrate, 3-deoxy-D,L-glycero-pentulosonic acid, each dye molecule was incubated, respectively, with chemically synthesized aldehyde and 2-keto acid. The absorbance spectrum (from 190 nm to 900 nm) of each reaction was then analyzed. The reaction product of Purpald and D,L-3,4-dihydroxybutanal had a λ_{max} (wavelength of maximum absorbance) at 542 nm. Incubation of Purpald with 3-deoxy-D,L-glycero-pentulosonic acid first resulted in a λ_{max} at 344 nm. However, intensity of this signal steadily decreased and the intensity of a new signal at 544 nm steadily increased. This observation indicated that the 2-keto acid derivative of Purpald is unstable, which may be converted to the aldehyde derivative

Figure 73. Reaction of Schiff's reagent with D,L-3,4-dihydroxybutanal.

through a decarboxylation reaction (Figure 72). Schiff's reagent is also referred to as leucofuchsin, which is derived from the reaction of pararosaniline with sulfuric acid¹⁶⁷ (Figure 73). Incubation of Schiff's reagent with D,L-3,4-dihydroxybutanal restored the pararosanilline chromophore and afforded a product with λ_{max} at 548 nm, while the reaction of Schiff's reagent and 3-deoxy-D,L-glycero-pentulosonic acid resulted in no signal in the visible light range from 380 nm to 750 nm. Therefore, Schiff's reagent was used in the screening assay.

Screening of benzoylformate decarboxylase mutant libraries was carried out in a 96 well format. Single colonies from mutant libraries were inoculated and cultured in 96 well growth blocks. Protein expression was induced with IPTG. Following harvesting of cells by centrifugation, cell pellets were incubated with BugBuster protein extraction reagent. Protein concentrations determined by Bradford assay revealed a relatively uniform cell lysing process among different clones with a variation < 10% of soluable protein. The crude cell lysates were then incubated with 3-deoxy-D,L-glyceropentulosonic acid. After quenching the reaction with trichloroacetic acid, the

decarboxylation product D,L-3,4-dihydroxybutanal was derivatized by addition of Schiff's reagent to the reaction mixture. Formation of the chromophore was monitored using a microplate reader. A calibration curve of the absorbance of the derivatization product at 550 nm relative to the concentration of authentic D,L-3,4-dihydroxybutanal showed a nonlinear relationship, with the sensitivity of the assay increase as the concentration of D,L-3,4-dihydroxybutanal increased from 1 mM to 10 mM. Under the employed reaction conditions, neither 3-deoxy-D,L-glycero-pentulosonic acid nor the Bugbuster reagent reacted with Schiff's reagent to cause background absorbances.

Isolation of Benzoylformate Decarboxylase Mutants

A total number of 6.3×10^3 independent clones from the E1 library were subjected to the screening procedure. Forty mutants with improved catalytic activity towards 3-deoxy-D,L-glycero-pentulosonic acid were subjected to a second round of screening using the same assay with duplicated samples. Plasmids encoding mutant benzoylformate decarboxylases were isolated from four mutants that showed the highest activity in the re-screening. Mutant genes amplified from these four plasmids were named E1-1, E1-2, E1-3, and E1-4. Randomization of the four mutant genes using DNA shuffling resulted in library S2. The first round of screening of 3.9×10^3 independent clones from the S2 library afforded eighty mutants with further improved catalytic activity, which were subjected to a second round of screening. Thirty-six mutants with higher activities for the decarboxylation of 3-deoxy-D,L-glycero-pentulosonic acid were identified.

Differences between the in vitro reaction environment used in the screening and the in vivo reaction environment of the intact cells include substrate availability, competing reactions, and enzyme stability. Since the ultimate purpose of this directed evolution effort was to increase the in vivo activity of benzoylformate decarboxylase towards 3-deoxy-D,L-glycero-pentulosonic acid, it was necessary to test the performance of benzoylformate decarboxylase mutants in intact *E. coli* cells. Plasmids were isolated from the thirty-six clones isolated from the S2 library and transformed into *E. coli* W3110. Single colonies of *E. coli* W3110 expressing wild-type and mutant benzoylformate decarboxylase were inoculated into M9 medium containing D-xylonic acid as the sole source of carbon. After inducing the protein expression with IPTG, cells were cultured for an additional 36 h. The culture supernatants were derivatized using bis(trimethylsilyl)trifluoro-acetamide and injected on an HP-5 capillary gas chromatography column. The concentration of 1,2,4-butanetriol was quantified relative to an internal standard of dodecane based on a calibtration curve. Expression of eighteen

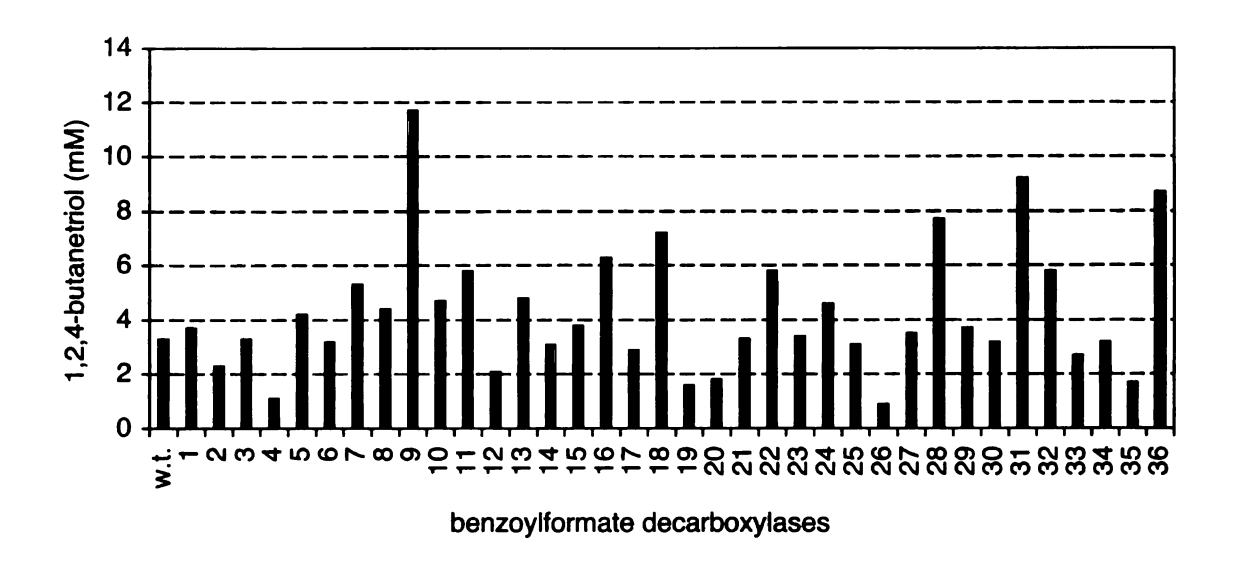


Figure 74. 1,2,4-Butanetriol production by *E. coli* W3110 expressing wild-type and mutant benzoylformate decarboxylases.

benzoylformate decarboxylase mutants in E. coli W3110 afforded increased biosynthesis of 1,2,4-butanetriol relative to the wild-type enzyme. Twofold to threefold increase in biosynthesis of 1,2,4-butanetriol was observed for E. coli W3110 containing mutant 9, 28, 31, or 36. These four best mutants were named S2-9, S2-28, S2-31, and S2-36, respectively. Expression of the rest of the eighteen mutants in E. coli W3110 resulted in approximately the same or lower concentrations of 1,2,4-butanetriol in the culture medium. Although this observation can be explained by different enzyme activities under in vivo and in vitro environment, one additional possibility existed. When benzoylformate decarboxylase mutants were screened for improved activity towards the nonnative substrate, the racemic mixture of 3-deoxy-glycero-pentulosonic acid was used Therefore, selected mutants could have had improved in the in vitro screens. performance towards both enantiomers or alternatively, towards one single enantiomer. However, the in vivo experiment was conducted in medium containing only D-xylonic acid. As a consequence, only 3-deoxy-D-glycero-pentulosonic acid is available inside the cells. Therefore, mutants with improved activity towards either both enantiomers or the D- isomer could lead to the observed increased 1,2,4-butanetriol biosynthesis. To examine whether the benzoylformate decarboxylase mutant isozymes obtained via directed evolution have altered stereoselectivity relative to 3-deoxy-D,L-glyceropentulosonic acid, the enantiomeric purity of 3,4-dihydroxybutanal synthesized in vitro by wild-type benzoylformate decarboxylase and four mutant isozymes was analyzed. The four benzoylformate decarboxylase mutants were chosen so that mutants that synthesized the highest concentration of 1,2,4-butanetriol (S2-9 and S2-36) and mutants that synthesized the lowest concentration of 1,2,4-butanetriol (S2-4 and S2-26) were

Table 21. Enantiomeric Purity Analysis of 1,2,4-Butanetriol Synthesized in the in vitro Enzymatic Reactions.

benzoylformate decarboxylase	wild-type	S2-9	S2-36	S2-4	S2-26
ee% of L-1,2,4 butanetriol	5.5	5.5	4.3	14.1	15.6

included. After removal of protein and unreacted substrate from the in vitro enzymatic reaction mixture, the aldehyde was reduced to 1,2,4-butanetriol using NaBH₄. Mosher ester of thus formed 1,2,4-butanetriol was injected on an HPLC Chiralpak AD column to determine the enantiomeric excess (*ee%*, Table 21). The results showed that wild-type benzoylformate decarboxylase, mutant S2-9, and S2-36 slightly prefer the L- isomer of 3-deoxy-*glycero*-pentulosonic acid as substrate (Table 21). This stereoselectivity favoring the L-stereoisomer was increased for mutant S2-4 and S2-26 (Table 21). Therefore, altered stereoselectivity is one possible reason for the low 1,2,4-butanetriol synthesis observed in intact cells for mutants selected for improved catalytic activity in the in vitro enzyme screens.

Characterization of Selected Mutants

To determine the nucleotide and amino acid substitutions in benzoylformate decarboxylase mutants with improved activity towards 3-deoxy-D,L-glycero-pentulosonic acid, mutants from the E1 library, E1-1, E1-2, E1-3, and E1-4, together with mutants S2-9, S2-28, S2-31, and S2-36 were subjected to DNA sequencing (Table 22). Mutants of the E1 library contained 2-3 nucleotide exchanges, which corresponded to 1-3 amino acid changes. All four mutants displayed an approximately 1.5-fold increase in decarboxylase activity towards 3-deoxy-D,L-glycero-pentulosonic acid in the in vitro enzyme assays.

Table 22. Characterization of Benzoylformate Decarboxylase Mutants.

generation	name	base substitutions	amino acid substitutions	
E1	E1-1	G248T/T810A/A1342G	S83I/F175L/T448A	
E1	E1-2	A164C/G248C	D55A/S83T	
E1	E1-3	A1328G/C1389T/A1414G	Q443R/A460V/N472D	
E1	E1-4	T42C/A1025T	silent/E342V	
S 2	S2-9	A164C/C1389T	D55A/A460V	
S2	S2-28	T42C/A164C/G1141A/A1328G/ C1389T	silent/D55A/A381T/Q443R/ A460V	
S2	S2-31	T42C/A164C/G248C/A1025T	silent/D55A/S83T/E342V	
S2	S2-36	T42C/A164C/A1025T/A1342G	silent/D55A/E342V/T448A	

Recombination of the four mutants resulted in 2-5 nucleotide changes and 2-4 amino acid changes in the four selected mutants from the S2 library. They showed a twofold to threefold increase in specific activity towards 3-deoxy-D,L-glycero-pentulosonic acid in the in vitro enzyme assays. The four mutants from the S2 library share one common D55A mutation. Mutant S2-9 and S2-28 share an A460V mutation, while mutant S2-31 and S2-36 share an E342V mutation. To obtain more insight into the altered specific activity of mutants S2-9, S2-28, S2-31, and S2-36, wild-type benzoylformate decarboxylase and the four mutants were expressed as recombinant 6-His tagged protein and purified to near homogeneity using Ni-NTA agrose resin. The kinetic parameters of the purified proteins were determined using the racemic 3-deoxy-D,L-glycero-pentulosonic acid as substrate (Table 23). All the mutant enzymes have lower affinity and are less active towards benzoylformate relative to the wild-type enzyme (Table 23). The significantly decreased catalytic activity (k_{cu}/K_m) of mutant S2-9 and S2-28

Table 23. Kinetic Data of Wild-Type and Mutant Benzoylformate Decarboxylases.

	benzoylformate			3-deoxy-D,L-glycero-pentulosonate		
	K_m (μM)	k_{cat} (s ⁻¹)	$\frac{k_{cal}/K_m}{(M^{-1} s^{-1})}$	K_m (mM)	k_{cat} (min ⁻¹)	$\frac{k_{cal}/K_m}{(\mathrm{M}^{-1}\mathrm{min}^{-1})}$
wild type	74	124	1.7×10^6	4.3	4.3	1×10^3
S2-9	93	2.4	2.6×10^4	3.7	6.8	1.8×10^3
S2-28	175	2.6	1.5×10^4	3.9	6.8	1.7×10^3
S2-31	90	36	4×10^5	4.0	5.6	1.4×10^3
S2-36	79	25	3.1×10^{5}	3.7	5.6	1.5×10^3

(Table 23) towards benzoylformate was accompanied by improved k_{ca}/K_m towards 3deoxy-D,L-glycero-pentulosonic acid. Mutant S2-31 and S2-36 also showed increased catalytic efficiency (Table 23) towards 3-deoxy-D,L-glycero-pentulosonic acid. The kinetic data indicated that the impact on the decarboxylation of 3-deoxy-D,L-glyceropentulosonic acid attendant with the mutations shared by S2-9 and S2-28, and by the mutations shared by S2-31 and S2-36. According to the benzoylformate decarboxylase crystal structure, amino acid residue A460 is situated in the enzyme active site. The amide hydrogen of A460 forms a hydrogen bond with the oxygen of the β phosphate group of the thiamine diphosphate cofactor. Substitution of alanine with a branched amino acid valine may altered the positioning of the cofactor and amino acid residues in the active site. Substitution of alanine with leucine at this same position has resulted in a benzoylformate decarboxylase mutant with improved catalytic activity towards long aliphatic chain 2-keto acids including 2-ketobutyrate, 2-ketopentanoat, and 2ketohexanoate.¹⁶⁸ Residues E342 and D55 are not located in the active site. Their contributions to the improved catalytic activity towards 3-deoxy-D,L-glyceropentulosonic acid can not be readily interpreted. The E342V and D55A mutations may serve as additional examples of enzyme activity altered by amino acid changes that are distant from the active site. 169a

Discussion and Future Work

As an energetic plasticizer, 1,2,4-butanetriol trinitrate has superior physical properties relative to widely used nitroglycerin. However, the expense of its precursor, racemic 1,2,4-butanetriol (\$70-\$90/kg), limits the application of 1,2,4-butanetriol trinitrate for military and civilian purposes. Substantial reductions in the cost of 1,2,4butanetriol could lead to expanded and, ultimately, complete substitution of 1,2,4butanetriol trinitrate for nitroglycerin. Given the prominent role of nitroglycerin has played in high energy material chemistry dating back to its incorporation into the first dynamite formulation developed by Alfred Nobel, this would also be a significant achievement from a historical perspective. The major costs associated with current 1,2,4butanetriol synthesis include the disposal of byproduct borate salts and stoichiometric use of NaBH₄. Therefore, attempts to improve 1,2,4-butantriol synthesis have focused on exploring approaches to catalytically reduce malic acid. Although catalytic hydrogenation of malic acid doesn't produce a salt stream as a reaction byproduct, the cost of the metal catalyst (Ru) required for large-scale production is a significant consideration. Additionally, due to the formation of a number of polyol byproducts, purification of 1,2,4-butanetriol from this reaction is difficult. In the designed microbial synthesis of 1,2,4-butanetriol (Figure 49), the problematic reduction of a carboxylate is replaced with the straightforward reduction of an aldehyde. In comparison with the metal

catalyst required for hydrogenation and the NaBH₄ required for stoichiometric reduction, cost of growing the microbial catalyst is negligible. A salt stream is, however, generated when growing microbial catalysts.

Microbial synthesis of 1,2,4-butanetriol presents several interesting features that haven't been explored by other approaches. First of all, experimental results show that Dand L-1,2,4-butanetriol can be separately synthesized in high optical purity by providing microbial biocatalysts with D-xylose or L-arabinose as the starting material. The physical properties of racemic mixtures are typically different from those of the pure enantiomers. However, due to the limited availability of optically pure D- and L-1,2,4-butanetriol, the energetic material properties of a single enantiomer of 1,2,4-butanetriol trinitrate haven't been characterized. Microbial synthesis of 1,2,4-butanetriol therefore offers the possibility to mix D- and L-1,2,4-butanetriol in different ratios and test the physical properties of nitration product of these mixtures, which may lead to the discovery of a better energetic plasticizer. Since racemic 1,2,4-butanetriol can be easily obtained by mixing D- and L- isomers in a 1:1 ratio, satisfying the requirement of current racemic 1,2,4-butanetriol trinitrate manufacturing is not difficult using the microbial synthesis. Secondly, biosynthesis of the enantiomers of 1,2,4-butanetriol allows access to a variety of chiral synthons. Finally, renewable feedstocks are used as the source of the D-xylose and L-arabinose used as starting materials in the microbial synthesis of 1,2,4-butanetriol. In comparison with glucose, fewer products have been manufactured using pentoses as starting materials. As major components of hemicellulose, D-xylose and L-arabinose streams that are pure and inexpensive may become available in the future. Exploiting routes to convert these carbohydrates into value-added chemicals is thus highly desirable.

In this research, enzyme activities necessary for the biosynthesis of 1,2,4-butanetriol were identified. D-Xylose and L-arabinose were then respectively converted into D- and L-1,2,4-butanetriol in a combined yield of 18% (mol/mol) and 19% (mol/mol) by using two microbial biocatalysts for each conversions. As proof-of-concept experiments, these results established the viability of microbial synthesis of 1,2,4-butanetriol and also set the foundation for future improvements. For the present, the concentration and yield of 1,2,4-butanetriol microbially synthesized from pentoses can not yet justify commercialization of this route.

Further optimization of the current 1,2,4-butantriol biosynthesis could start with the identification of every biosynthetic intermediate and byproduct that accumulate in the culture medium. Metabolites that have been so far identified include ethylene glycol and 3-deoxy-L-glycero-pentulosonic acid. The accumulation of these molecules indicated insufficient 2-keto acid decarboxylase activity. Formation of 3,4-dihydroxybutyric acid has also been detected.

One alternative to the two-microbe biosynthesis of 1,2,4-butanetriol is to construct a single microbe that can directly convert pentose into 1,2,4-butanetriol enantiomer. Due to its unique catabolism of pentoses (Figure 53), *P. fragi* is the ideal host strain. Cultivation of recombinant *P. fragi* expressing 2-keto acid decarboxylase and alcohol dehydrogenase in D-xylose could directly afford 3-deoxy-D-glycero-pentulosonic acid. Carbon flow diverted by the 2-keto acid decarboxylase would dictate the concentration and yield of D-1,2,4-butanetriol. Similarly, cultivation of the same recombinant *P. fragi* strain in L-arabinose in theory could afford L-1,2,4-butanetriol. Therefore, biosynthesis of D- or L-1,2,4-butanetriol can be accomplished using the same

microbe by switching between D-xylose and L-arabinose as the starting material. In comparison with the two-microbe synthesis, the single microbe synthesis would avoid intermediate purification steps. However, realization of this simplified biosynthesis may also require a significant amount of metabolic engineering. Expression of wild-type and mutant benzoylformate decarboxylase in *P. fragi* cultured on D-xylose or L-arabinose didn't lead to the accumulation of 3,4-dihydroxybutanal or 1,2,4-butanetriol (data not included). This result indicated that the catalytic activity of benzoylformate decarboxylase may be insufficient to siphon carbon flow into biosynthesis of 1,2,4-butanetriol. To increase the in vivo availability of 3-deoxy-glycero-pentulosonic acid, the catalytic activities of enzymes catalyzing its catabolism may need to be reduced.

Central to biosynthesis of 1,2,4-butanetriol using either two-microbe or single-microbe synthesis is how to improve the in vivo catalytic activity of the 2-keto acid decarboxylase. The catalytic efficiency (k_{ca}/K_m) of benzoylformate decarboxylase has been improved 40%-80% using directed evolution. However, directed evolution of a single enzyme often suffers from the limited sequence diversity. Currently, DNA family shuffling appears to be the best option for generating a highly diversified gene library. Application of this method to more efficiently evolve 2-keto acid decarboxylase activity towards 3-deoxy-glycero-pentulosonic acid will require future identification of a group of genes with a substantial level of DNA sequence identity and encode enzymes that can catalyze the decarboxylation of 3-deoxy-glycero-pentulosonic acid.

CHAPTER FIVE

EXPERIMENTAL

General Methods

A. Chromatography

Gas chromatography was performed on an Agilent 6890N equipped with an HP-5 capillary column (30 m x 0.25 mm x 0.25 micron). Temperature programming began with an initial temperature of 120 °C for 3 min. The temperature was increased to 210 °C at a rate of 15 °C/min, and held at the final temperature for 1 min. The split injector was maintained at a temperature of 300 °C and the FID detector was kept at 350 °C. Samples analyzed by gas chromatography were derivatized using bis(trimethylsilyl)trifluoro-acetamide and quantified relative to an internal standard of dodecane.

HPLC analysis was performed on an Agilent 1100 HPLC installed with ChemStation acquisition software (Rev. A.08.03). Columns used in the enantiomeric purity analysis of 1,2,4-butanetriol include Chiralpak AD column (Daicel Chemical, 4.6 mm x 250 mm) and Chirapak ADH column (Daicel Chemical, 4.6 mm x 250 mm). Protein purification utilized the same HPLC system equipped with a Pharmacia Resource Q column (6.4 mm x 30 mm, 1 mL). Solvents were routinely filtered through 0.45-μm membranes (Gelman Science) prior to use.

Dowex 50 (H⁺) and Dowex 1 1X8-400 (Cl⁻) were purchased from Aldrich-Sigma. Previously used Dowex 50 (H⁺) was cleaned by treatment with bromine. An aqueous suspension of resin was adjusted to pH 14 by addition of solid KOH. Bromine was added to the solution until the suspension turned a golden yellow color. Additional bromine

was added (1-2 mL) to obtain a saturated solution. The mixture was left to stand at room temperature overnight, and the Dowex 50 resin was collected by filtration and washed exhaustively with water followed by 6 N HCl. Dowex 50 (H⁺) was stored at 4 °C. AG-1X8 (acetate form and chloride form) and hydroxyapatite Bio-Gel HTP gel were purchased from Bio-Rad. Phenylsepharose was purchased from Pharmacia. Diethylaminoethyl cellulose (DEAE) was purchased from Whatman. Ni-NTA resin was purchased from Qiagen.

B. Spectroscopic Measurements

 1 H NMR and 13 C NMR spectra were recorded on either a Varian VX-300 or a Varian VXR-500 FT-NMR spectrometer. Chemical shifts for 1 H NMR and 13 C NMR spectra were reported in parts per million (ppm) relative to sodium 3-(trimethylsilyl)propionate-2,2,3,3-d₄ (TSP, $\delta = 0.0$ ppm) with D₂O as the solvent. UV and visible measurements were recorded on a Perkin-Elmer Lambda 3b UV-vis spectrophotometer or on a Hewlett Packard 8452A Diode Array Spectrophotometer equipped with HP 89532A UV-Visible Operating Software. Measurements of multiple samples in microplates were carried out using a Benchmark microplate reader (Bio-Rad Laboratories) equipped with Microplate Manager III Macintosh Data Analysis and Kinetics Software.

C. Bacterial Strains and Plasmids

E. coli DH5 α [F' endA1 hsdR17($r_K m_K^{\dagger}$) supE44 thi-1 recA1 gyrA relA1 $\phi 80lacZDM15$ $\Delta(lacZYA-argF)_{UI69}$] and E. coli RB791 (W3110 lacL81 Q) were obtained

previously in this laboratory. E. coli W3110, E. coli AB2834 [tsx-352 supE42 λ aroE353 malA352 (λ -)], E. coli Lin 4393 [fhuA22 phoA8 fadL701 relA1 glpR2 pit-10 spoT1 glpK22(fbR) rrnB-2 mcrB1 creC510] and E. coli W945 [thr-1 araC14 leuB6 lacY1 glnV44 galK2 rfbD1 mgl-51 malT1 (LamR) xylA5 mtl-1 thi-1] were obtained from the E. coli Genetic Stock Center at Yale University. E. coli KL364c (AB2834 serA::aroB) and E. coli KL7¹⁰⁷ (AB2834 serA::aroBaroZ) were previously constructed in this laboratory. E. coli BL21 (DE3) [E. coli B F^- dcm ompT hsdS(r_{B^-} m_{B^-}) gal λ (DE3)] was purchased from Novagen. Pseudomonas fragi (ATCC 4973), Pseudomonas putida (ATCC 12633) and Klebsiella pneumoniae (ATCC 25955) were purchased from American Type Culture Collection. E. coli ER1648/pJAM304^{154a} and E. coli DH5α/pJAM3440^{154b} were obtained from Professor J. Maupin-Furlow (University of Florida). E. coli TC4/pLOI276^{154c} and plasmids pLOI135^{152b} and pLOI295^{152a} were obtained from Professor L. O. Ingram (University of Florida). Plasmid pJF118EH was Plasmid obtained from Professor M. Bagdasarian (Michigan State University). pMAK705¹⁷⁰ was obtained from Professor S. R. Kushner (University of Georgia). Plasmids pIB1343^{118a} and pIB1345^{118a} were obtained from Professor L. Nicolas Ornston (Yale University). Cosmid pMB2¹⁵⁶ was obtained from Professor S. E. Lindow (University of California at Berkeley). Plasmid pD2625 was obtained from Genencor Inc. Plasmid pKK223-3¹⁷¹ and pT7-7¹⁷² were obtained previously by this laboratory. Plasmid pKD14.099A, pKD9.080A, pKD9.046B, pKD11.291A, pMF63A, pKL5.17A, pSK4.023A, pSK4.99A, pKAD62A, and pJG7.246 were previously constructed in this laboratory. Plasmid pQE30 was purchased from Qiagen. Cosmid vector SuperCos 1 was purchased from Stratagene.

D. Storage of Bacterial Strains and Plasmids

All bacterial strains including Escherichia coli, Pseudomonas fragi, Pseudomonas putida, and Klebsiella pneumoniae were stored at -78 °C in glycerol. Plasmids were transformed into E. coli DH5α or E. coli JM109 for long-term storage. Preparation of bacteria glycerol freeze samples started from introduction of a single colony of the desired strain picked from an agar plate into 5 mL medium. E. coli strains were cultured in LB medium containing appropriate amount of antibiotics at 37 °C with agitation for 12 h. Pseudomonas fragi (ATCC 4973) and Pseudomonas putida (ATCC 12633) were cultured in nutrient broth at 30 °C with agitation for 24 h. Klebsiella pneumoniae (ATCC 25955) was cultured in ATCC medium 561 at 30 °C with agitation for 24 h. Glycerol freeze samples were prepared by addition 0.75 mL of bacteria culture to 0.25 mL of sterile 80% (v/v) aqueous glycerol solution. The solutions were mixed, allowed to stand at room temperature for 2 h, and then stored at -78 °C.

E. Culture Medium

Bacto tryptone, Bacto yeast extract, nutrient broth, casamino acids, agar, and MacConkey agar base were purchased from Difco. Casein hydrolysate was obtained from Sigma. Nutrient agar was purchased from Oxoid.

All solutions were prepared in distilled, deionized water. LB medium¹⁷³ (1 L) contained Bacto tryptone (10 g), Bacto yeast extract (5 g), and NaCl (10 g). LB-glucose medium contained glucose (10 g), MgSO₄ (0.12 g), and thiamine hydrochloride (0.001 g) in 1 L of LB medium. LB-freeze buffer contained K₂HPO₄ (6.3 g), KH₂PO₄ (1.8 g), MgSO₄ (1.0 g), (NH₄)₂SO₄ (0.9 g), sodium citrate dihydrate (0.5 g) and glycerol (44 mL)

in 1 L of LB medium. M9 salts 173 (1 L) contained Na₂HPO₄ (6 g), KH₂PO₄ (3 g), NH₄Cl (1 g), and NaCl (0.5 g). M9 minimal medium¹⁷³ contained D-glucose (10 g), MgSO₄ (0.12 g), and thiamine hydrochloride (0.001 g) in 1 L of M9 salts. Other M9 media contained carbon sources (10 g) including D-lactose, L-arabinose, glycerol, D-xylonate, or L-arbinonate in place of D-glucose in M9 minimal medium. For example, M9 glycerol medium contained glycerol (10 g), MgSO₄ (0.12 g), and thiamine hydrochloride (0.001 g) in 1 L of M9 salts. M9 L-arabinose medium also contained 0.4% (w/v) casamino acids, which was added into the M9 salts solution before autoclave. M9 medium (1 L) was supplemented where appropriate with L-phenylalanine (0.040 g), L-tyrosine (0.040 g), Ltryptophan (0.040 g), p-hydroxybenzoic acid (0.010 g), potassium p-aminobenzoate (0.010 g), and 2,3-dihydroxybenzoic acid (0.010 g). L-Serine was added to a final concentration of 40 mg/L where indicated. Antibiotics were added where appropriate to the following final concentrations: ampicillin (Ap), 50 µg/mL; chloramphenicol (Cm), 20 μg/mL; kanamycin (Kan), 50 μg/mL; tetracycline (Tc), 12.5μg/mL. Stock solutions of antibiotics were prepared in water with the exceptions of chloramphenicol which was prepared in 95% ethanol and tetracycline which was prepared in 50% aqueous ethanol. Aqueous stock solutions of isopropyl-β-D-thiogalactopyranoside (IPTG) were prepared at various concentrations. Solutions of LB medium, M9 inorganic salts, MgSO₄, D-glucose, D-lactose, glycerol and L-arabinose were autoclaved individually and then mixed. Solutions of potassium D-xylonate, potassium L-arabinonate, aromatic amino acids, aromatic vitamins, L-serine, thiamine hydrochloride, antibiotics, and IPTG were sterilized through 0.22-um membranes. MacConkey plates (1 L) contained MacConkey agar base (40 g) and D-lactose (10 g). Other solid media were prepared by addition of Difco agar to a final concentration of 1.5% (w/v) to the liquid medium.

Pseudomonas fragi and Pseudomonas putida were grown either in nutrient broth or on solid nutient agar plates. Nutrient broth and nutrient agar were prepared according to procedures recommended by the manufactures. Klebsiella pneumoniae was cultured in liquid or on solid ATCC medium 561. ATCC medium 561 (800 mL) contained yeast extract (1 g), casein hydrolysate (1.4 g), K₂HPO₄ (0.6 g), MgSO₄ (0.5 g), K₂SO₄ (1 g), and glycerol (20 mL). Solid ATCC medium 561 was prepared by addition of Difco agar to a final concentration of 1.5% (w/v) to the liquid medium.

The standard fermentation medium (1 L) utilized in Chapter 2 and Chapter 3 contained K₂HPO₄ (7.5 g), ammonium iron (III) citrate (0.3 g), citric acid monohydrate (2.1 g), L-phenylalanine (0.7 g), L-tyrosine (0.7 g), L-tryptophan (0.35 g), and concentrated H₂SO₄ (1.2 mL). Fermentation medium was adjusted to pH 7.0 by addition of concentrated NH₄OH before autoclaving. The following supplements were added immediately prior to initiation of the fermentation: D-glucose or glycerol (as specified), MgSO₄ (0.24 g), *p*-hydroxybenzoic acid (0.010 g), potassium *p*-aminobenzoate (0.010 g), 2,3-dihydroxybenzoic acid (0.010 g), and trace minerals including (NH₄)₆(Mo₇O₂₄)·4H₂O (0.0037 g), ZnSO₄·7H₂O (0.0029 g), H₃BO₃ (0.0247 g), CuSO₄·5H₂O (0.0025 g), and MnCl₂·4H₂O (0.0158 g). IPTG stock solution was added as necessary to the indicated final concentration. Carbon sources including glucose feed solution and glycerol feed solution, and MgSO₄ (1 M) solution were autoclaved separately. Glucose feed solution (650 g/L) was prepared by combining 300 g of glucose and 280 mL of H₂O. Glycerol feed solution (600 g/L) was prepared by combining 300 g of glycerol with 270 mL of

 H_2O . Solutions of aromatic vitamins, trace minerals, and IPTG were sterilized through 0.22- μ m membranes. Antifoam (Sigma 204) was added to the fermentation broth as needed.

F. General Fed-Batch Fermentor Conditions

Fermentations employed a 2.0 L working capacity B. Braun M2 culture vessel. Utilities were supplied by a B. Braun Biostat MD controlled by a DCU-3. Data acquisition utilized a Dell Optiplex Gs⁺ 5166M personal computer (PC) equipped with B. Braun MFCS/Win software (v1.1) or a Dell Optiplex GX200 personal computer (PC) equipped with B. Braun MFCS/Win software (v2.0). Temperature, pH, and carbon source feeding were controlled with PID control loops. pH was maintained at 7.0 by addition of concentrated NH₄OH or 2 N H₂SO₄. Dissolved oxygen (D.O.) was measured using a Mettler-Toledo 12 mm sterilizable O₂ sensor fitted with an Ingold A-type O₂ permeable membrane. Inoculants were started by introduction of a single colony picked from an agar plate into 5 mL of M9 medium. Cultures were grown at 37 °C with agitation at 250 rpm until they were turbid and subsequently transferred to 100 mL of M9 medium. Cultures were grown at 37 °C and 250 rpm for an additional 10 h. The inoculant ($OD_{600} = 1.0-3.0$) was then transferred into the fermentation vessel and the batch fermentation was initiated (t = 0 h).

Three staged methods were used to maintain D.O. concentrations at desired air saturation during the fermentations. With the airflow at an initial setting of 0.06 L/L/min, the D.O. concentration was maintained by increasing the impeller speed from its initial set point of 50 rpm to its preset maximum rate. With the impeller speed constant, the

mass flow controller then maintained the D.O. concentration by increasing the airflow rate from 0.06 L/L/min to a preset maximum of 1.0 L/L/min. At constant impeller speed and constant airflow rate, the D.O. concentration was finally maintained at the desired air saturation for the remainder of the fermentation by oxygen sensor-controlled carbon source feeding. At the beginning of this stage, the D.O. concentration fell below the desired air saturation due to residual initial carbon source in the medium. This lasted for approximately 10 min to 30 min before carbon source feeding commenced. The carbon source feed PID control parameters were set to 0.0 s (off) for the derivative control (τ_D) and 999.9 s (minimum control action) for the integral control (τ_1). X_P was set to 950% to achieve a K_P of 0.1.

G. Analysis of Fermentation Broth

Samples (5-10 mL) of fermentation broth were removed at the indicated timed intervals. Cell densities were determined by dilution of fermentation broth with water (1:100) followed by measurement of absorption at 600 nm (OD_{600}). Dry cell weight of *E. coli* cells (g/L) was calculated using a conversion coefficient of 0.43 g/L/ OD_{600} . The remaining fermentation broth was centrifuged to obtain cell-free broth.

For the biosythhesis of 3-dehydroshikimate, cis,cis-muconic acid, D-xylonate, and L-arabinonate, solute concentrations in the cell-free broth were quantified by ¹H NMR. A portion (0.5-2.0 mL) of the cell-free broth was concentrated to dryness under reduced pressure, concentrated to dryness one additional time from D_2O , and then redissolved in D_2O containing a known concentration of the sodium salt of 3-(trimethylsilyl)propionic-2,2,3,3-d₄ acid (TSP, Lancaster Synthesis Inc.). Concentrations were determined by

comparison of integrals corresponding to each compound with the integral corresponding to TSP ($\delta = 0.00$ ppm) and were converted by response factors determined using authentic materials. Compounds were quantified using the following resonances: 3deoxy-D-arabino-heptulosonic acid (DAH, δ 1.81, t, 1 H); 3-dehydroquinate (DHQ, δ 4.38, d, 1 H); 3-dehydroshikimate (DHS, δ 4.28, d, 1 H); cis,cis-muconic acid (δ 6.02, d, 2 H); catechol (δ 6.90, m, 4 H); gallic acid (GA, δ 7.02, s, 2 H); D-xylonic acid (δ 4.08, d, 1 H); L-arabinonic acid (δ 4.24, dd, 1 H); and L-arabino-1,4-lactone (δ 4.64, d, 1 H). A standard concentration curve was determined for metabolites using solutions of authentic samples. Concentrations were calculated by application of the following response factor: 3-dehydroshikimate, 0.95; 3-dehydroquinate, 0.89; 3-deoxy-D-arabino-heptulosonic acid, 1.22; gallic acid, 1.36; cis, cis-muconic acid, 0.96; D-xylonic acid, 0.85; L-arabinonic acid, 0.88. For the biosynthesis of 1,2,4-butanetriol, the concentration 1,2,4-butanetriol in cell-free broth was quantified by GC analysis. A portion of the fermentation broth (0.5-1.0 mL) was concentrated to dryness under reduced pressure, and the residue was redissolved in pyridine (0.9 mL). To this pyridine solution, dodecane (0.1 mL) and bis(trimethylsilyl)trifluoroacetamide (BSTFA, 2 mL, 7.53 mmol) were sequentially added. Silvation of 1,2,4-butanetriol was carried out at room temperature with stirring for 10 h. Samples were then analyzed using gas chromatography.

H. Genetic Manipulations

General

Recombinant DNA manipulations generally followed procedures described by Sambrook.¹⁷⁴ Restriction enzymes were purchased from Gibco BRL or New England

Biolabs. T4 DNA ligase, large fragment of DNA polymerase I (Klenow fragment) and dNTP's were purchased from Invitrogen. Calf intestinal alkaline phosphatase was purchased from New England Biolabs. Fast-Link DNA ligase was purchased from Epicentre Technologies. Agrose (electrophoresis grade) was purchased from Invitrogen.

Phenol was prepared by addition of 0.1% (w/v) 8-hydroxyquinoline into distilled phenol. Two extractions of phenol with an equal volume of 1 M Tris-HCl (pH 8.0) were followed by extraction with 0.1 M Tris-HCl (pH 8.0) until the pH of the aqueous layer was greater than 7.6. Phenol was stored under an equal volume of 0.1 M Tris-HCl (pH 8.0) at 4 °C. SEVAG was a mixture of chloroform and isoamyl alcohol (24:1, v/v). TE buffer contained 10 mM Tris-HCl (pH 8.0) and 1 mM Na₂EDTA (pH 8.0). Endostop solution (10X concentrated) contained 50% glycerol (v/v), 0.1 M Na₂EDTA (pH 7.5), 1% sodium dodecyl sulfate (SDS) (w/v), 0.1% bromophenol blue (w/v), and 0.1% xylene cyanole FF (w/v) and was stored at 4 °C. Prior to use, 1 mL of 10X Endostop was mixed with 0.12 mL of DNase-free RNase. DNase-free RNase was prepared by dissolving 10 mg RNase in 1 mL of 10 mM Tris-HCl (pH 7.5) and 15 mM NaCl. Following inactivation of the DNase activity by heating at 100 °C for 15 min, the solution was stored at -20 °C.

PCR (Polymerase Chain Reaction)

Regular PCR amplifications were carried out as described by Sambrook.¹⁷⁴ Each reaction (0.1 mL) contained 10 mM KCl, 20 mM Tris-HCl (pH 8.8), 10 mM (NH₄)₂SO₄, 2 mM MgSO₄, 0.1% Triton X-100, dATP (0.2 mM), dCTP (0.2 mM), dGTP (0.2 mM), dTTP (0.2 mM), template DNA (0.02 μg-1 μg), 0.5 μM of each primer, and 2 units of

Vent polymerase. Primers were synthesized by the Macromolecular Structure Facility at Michigan State University.

Determination of DNA Concentration

In order to determine the concentration of DNA, an aliquot (10 μ L) of sample was diluted to 1 mL in TE and the absorbance at 260 nm was measured relative to TE. The DNA concentration was calculated based on the fact that the absorbance at 260 nm of a 50 μ g mL⁻¹ of plasmid DNA is 1.0.

Large Scale Purification of Plasmid DNA

Routine purification of plasmid DNA on a large scale followed a modified alkaline lysis procedure described by Sambrook.¹⁷⁴ A single colony of a strain containing the desired plasmid was inoculated into a 2 L Erlenmeyer flask containing LB (500 mL) and the appropriate antibiotics. Following incubation in a gyratory shaker (250 rpm) at 37 °C for 12-14 h, cells were harvested by centrifugation (4 000g, 5 min, 4 °C) and then resuspended in 10 mL of cold GETL solution [50 mM glucose, 20 mM Tris-HCl (pH 8.0), 10 mM Na₂EDTA (pH 8.0)] into which lysozyme (5 mg mL⁻¹) had been added immediately prior to use. The suspension was kept at room temperature for 5 min. Addition of 20 mL of 1% sodium dodecyl sulfate (w/v) in 0.2 N NaOH was followed by gentle mixing and storage on ice for 15 min. A 15 mL aliquot of ice-cold solution containing 3 M KOAc (prepared by mixing 60 mL of 5 M KOAc, 11.5 mL of glacial acetic acid and 28.5 mL of water) was added. Vigorous shaking of the mixture resulted in formation of a white precipitate. Following storage on ice for 10 min, the sample was

centrifuged (48 000g, 20 min, 4 °C) to remove cellular debris. The resulting supernatant was transferred equally to two centrifuge tubes, then mixed with isopropanol (0.6 volume) to precipitate DNA. After the samples were stored at room temperature for 15 min, the DNA was recovered by centrifugation (20 000g, 20 min, 4 °C). The DNA pellet was then rinsed with 70% ethanol and dried.

The isolated DNA was dissolved in 3 mL TE and transferred to a 15 mL Corex tube. The solution was thoroughly mixed with 3 mL of cold 5 M LiCl, then centrifuged (12 000g, 10 min, 4 °C) to remove high molecular weight RNA. The clear supernatant was transferred to a Corex tube, treated with an equal volume of isopropanol (6 mL) and was gently mixed. The precipitated DNA was collected by centrifugation (12 000g, 10 min, 4 °C), rinsed with 70% ethanol and dried. After redissolving the DNA pellet in 0.5 mL of TE containing DNase-free RNase (20 μg/mL), the solution was transferred to a 1.5 mL microcentrifuge tube and stored at room temperature for 30 min. Following addition of 0.5 mL of 1.6 M NaCl containing 13% PEG-8000 (w/v), the solution was mixed and centrifuged (microcentrifuge, 5 min, 4 °C) to recover the precipitated DNA. The supernatant was discarded and the pellet was dissolved in 0.4 mL of TE. The sample was sequentially extracted with phenol (0.4 mL), phenol and SEVAG (0.4 mL each) and finally SEVAG (0.4 mL). 10 M NH₄OAc (10 mL) was added to the aqueous DNA solution. After thorough mixing, 95% ethanol (1 mL) was added to precipitate the DNA. The sample was left at room temperature for 5 min and then centrifuged (microcentrifuge, 5 min, 4 °C). The resulting DNA pellet was rinsed with 70% ethanol, dried, and dissolved in 0.2-0.5 mL of TE.

For the purpose of DNA sequencing, purification of plasmid DNA employed a Qiagen Plasmid Maxi Kit purchased from Qiagen. The manufacture's procedure was followed during the experiment, and the resulting DNA was dissolved in sterile water to facilitate DNA sequencing.

Small Scale Purification of Plasmid DNA

A single colony of a strain containing the desired plasmid was inoculated into LB (5 mL) containing the appropriate antibiotics. Following incubation at 37 °C with agitation (250 rpm) overnight, cells were harvested from 3 mL of culture in a 1.5 mL microcentrifuge tube by centrifugation. The cell pellet was resuspended in 0.1 mL of cold GETL solution into which lysozyme (5 mg mL⁻¹) was added immediately before use. The sample was kept on ice for 10 min. Addition of 0.2 mL of 1% sodium dodecyl sulfate (w/v) in 0.2 N NaOH was followed by gentle mixing and storage on ice for 5-10 min. To the resulting sample was added 0.15 mL of cold 3 M KOAc solution. The mixture was shaken vigorously and then stored on ice for 5 min. Following removal of precipitated cellular debris by centrifugation (microcentrifuge, 20 min, 4 °C), the supernatant was transferred to a fresh microcentrifuge tube and extracted with phenol and SEVAG (0.2 mL each). The aqueous DNA solution was transferred to a fresh microfuge tube and mixed well with 1 mL of 95% ethanol. After storage at room temperature for 5 min, DNA was precipitated by centrifugation (15 min, room temperature). The DNA pellet was rinsed with 70% ethanol, dried, and redissolved in 50-100 µL of TE. DNA isolated using this method was used for restriction enzyme analysis.

Purification of Genomic DNA

Genomic DNA purification from all bacterial strains including E. coli, Pseudomonas fragi, Pseudomonas putida, and Klebsiella, pneumoniae followed a modified procedure described by Wilson.¹⁷⁵ A single colony of the bacteria was inoculated into a 500 mL Erlenmeyer flask containing 100 mL culture medium. Cultures of E. coli strains were incubated in a gyratory shaker (250 rpm) at 37 °C for 12 h. Cultures of Pseudomonas fragi, Pseudomonas putida, and Klebsiellas pneumoniae were incubated in a gyratory shaker (250 rpm) at 30 °C for 24 h. Cells were harvested by centrifugation (4 000g, 5 min, 4 °C), and were resuspended in 9.5 mL of TE and transferred to a small (45 mL) centrifuge bottle. Following mixing with SDS (0.5 mL, 10 % w/v) and freshly prepared proteinase K (0.05 mL, 20 mg mL⁻¹), the sample was incubated at 37 °C for 1 h with gentle, periodic mixing. Aqueous NaCl (5 M, 1.8 mL) was added to the cell suspension, which was mixed thoroughly, and 1.5 mL of CTAB/NaCl solution (aqueous solution containing 0.041 g mL⁻¹ of NaCl and 0.1 g mL⁻¹ of hexadecyltrimethylammonium bromide) was added. After mixing, the sample was incubated at 65 °C for 20 min. The solution was divided into two Corex tubes, and the contents of each tube were extracted with an equal volume of SEVAG. The organic and aqueous layers were separated by centrifugation (6 000g, 10 min, 4 °C), and the clear, aqueous layer was transferred to two fresh Corex tubes. All transfers of DNA-containing solutions were carried out using large-bore pipette tips to minimize shearing of the genomic DNA. Genomic DNA was precipitated by addition of 0.6 volumes of isopropanol. After storage at room temperature for 2 h, threads of DNA were spooled onto a flame-sealed Pasteur pipette and transferred to a single Corex tube containing 70%

ethanol. Following a brief rinse with ethanol, the DNA was dried and resuspended in 1 mL of TE containing RNase (0.1 mg mL⁻¹). The resulting mixture was stored at 4 °C overnight to allow the DNA to dissolve completely. After sequential extractions with phenol (1 mL) and SEVAG (1 mL), the aqueous layer was transferred to a Corex tube and thoroughly mixed with 0.1 mL of 3 M NaOAc (pH 5.2). DNA was precipitated by addition of 95% ethanol (3 mL) and stored at room temperature for 1.5 h. The DNA threads were spooled onto a flame-sealed Pasteur pipette and briefly rinsed in 1 mL of 70% ethanol. The spooled DNA was transferred to a 1.5 mL microfuge tube, dried, and redissolved in 0.5 mL of TE. Genomic DNA was stored at 4 °C.

Restriction Enzyme Digestion of DNA

Restriction enzyme digests were performed in buffers provided by the enzyme suppliers. A typical restriction enzyme digest contained approximately 1 μg of DNA (in 10 μL of TE), 2 μL of restriction enzyme buffer (10X concentration), 1 μL of bovine serum albumin (BSA) (2 mg mL⁻¹), 1 μL of restriction enzyme and 6 μL TE. After incubation at 37 °C for 1-2 h, the sample was mixed with 2 μL of Endostop (10X concentrated) and analyzed by agarose gel electrophoresis. When DNA was required for cloning experiments, restriction digestion was terminated by addition of 1 μL of 0.5 M Na₂EDTA (pH 8.0). Following extraction with phenol and SEVAG (0.1 mL each), DNA was thoroughly mixed with 0.1 volume of 3 M NaOAc (pH 5.2) and precipitated by addition of 3 volumes of 95% ethanol. After storage at -78 °C for 3 h, precipitated DNA was recovered by centrifugation (15 min, 4 °C), rinsed with 0.1 mL of 70% ethanol and centrifuged (15 min, 4 °C). DNA was dried and redissolved in TE. Alternatively DNA

was isolated from the restriction digestion mixture utilizing Zymoclean DNA Clean and Concentrate Kit (Zymo Research) following the protocol recommended by the manufacturer.

Agarose Gel Electrophoresis

Agarose gels were run in TAE buffer containing 40 mM Tris-acetate and 2 mM EDTA (pH 8.0). Gels typically contained 0.7% agarose (w/v) in TAE buffer. DNA fragments smaller than 1 kb were resolved in 2% agarose. Addition of ethidium bromide (0.5 μg mL⁻¹) to the agarose allowed for visualization of DNA fragments under ultraviolet exposure. Two sets of DNA size markers were employed to estimate the size of DNA fragments between 0.5 kb and 23 kb: λ DNA digested with *Hin*dIII resulted in bands of 23.1 kb, 9.4 kb, 6.6 kb, 4.4 kb, 2.3 kb, 2.0 kb, and 0.6 kb, and λ DNA digested with *Eco*RI and *Hin*dIII resulted in bands of 21.2 kb, 5.1 kb, 5.0 kb, 4.3 kb, 3.5 kb, 2.0 kb, 1.9 kb, 1.6 kb, 1.4 kb, 0.9 kb, 0.8 kb, and 0.6 kb. For DNA fragments smaller than 1 kb, a 100 bp DNA ladder purchased from Invitrogen was utilized as a DNA size marker.

<u>Isolation of DNA from Agarose</u>

The band of agarose containing the DNA of interest was excised from argrose gel using a razor blade under long wavelength UV light (365 nm) to avoid damages to DNA. The excised agarose was transferred into a 1.5 mL microfuge tube. Two methods were used to isolate the DNA from the agarose. The first method involved chopping the agarose plug thoroughly with a razor blade and transfering it to a 0.5 mL microfuge tube, which was packed tightly with glass wool and had an 18 gauge hole at the bottom. While

centrifuging for 5 min using a Beckman microfuge, the aqueous solution was collected in a 1.5 mL microfuge tube. The DNA was precipitated from the aqueous soltion by addition of 3 M NaOAc (pH 5.2, 0.1 vol) and 95% ethanol (2-3 vol) as previously described. DNA was subsequently redissolved in TE. In a second method, the DNA was isolated from the agarose plug using Zymoclean Gel DNA Recovery Kit (Zymo Research) by following manufacturer recommended procedure.

Treatment of Vector DNA with Calf Intestinal Alkaline Phosphatase

Plasmids digested with a single restriction enzyme were dephosphorylated to prevent self-ligation. Digested vector DNA was dissolved in TE or sterile H_2O (88 μ L). To this sample was added 10 μ L of dephosphorylation buffer (10X concentration) and 2 μ L of calf intestinal alkaline phosphatase (2 units). The reaction was incubated at 37 °C for 1 h. The phosphatase was inactivated by addition of 1 μ L of 0.5 M EDTA (pH 8.0) followed by heat treatment (65 °C, 20 min). After sequential extraction with phenol and SEVAG (100 μ L each) to remove protein, the DNA was precipitated as previously described and redissolved in TE.

Treatment of DNA with Klenow Fragment

DNA fragments with recessed 3' termini were modified to blunt-ended fragments by treatment with the Klenow fragment of *E. coli* DNA polymerase I. Since the Klenow fragment works well in common restriction enzyme buffers, there was no need to purify the DNA after restriction digestion and prior to filling recessed 3' termini. To a 20 μ L of digested DNA sample (0.8-2 μ g) was added 2 μ L of a solution containing 25 mM of each

of the four dNTP's and 2.5 units of Klenow fragment. After thorough mixing, the reaction was allowed to stand at room temperature for 20 min. The Klenow reaction was quenched either by sequential extraction with equal volume of phenol and SEVAG or by addition of Endostop (10X concentrated, 2 µL). DNA isolation from the resulting aqueous solution employed either DNA precipitation or agarose gel electrophoresis as previously described.

Ligation of DNA

DNA ligations using T4 DNA ligase were designed to result in a molar ratio of 1:3 between vector and insert DNA. A typical ligation reaction contained 0.1 μg vector DNA, 0.05 to 0.2 μg insert DNA, 2 μL of T4 ligation buffer (5X concentration), 1 μL of T4 DNA ligase (2 units), and TE to a final volume of 10 μL. The reaction was carried out at 16 °C for at least 4 h. In an alternative method, the Fast-link DNA Ligation Kit (Epicentre Technologies) was employed according to the procedures recommended by the manufacturer. Ligation mixture was used to transform chemically competent cells without purification. Inorganic salts and protein was removed from the ligation reactions using Zymoclean DNA Clean and Concentrate Kit prior to transforming electrocompetent cells.

Preparation and Transformation of Competent Cells

Chemically competent and electrocompetent cells were prepared using procedures modified from Sambrook.¹⁷⁴ Preparation of chemically competent cells started with introduction of a single colony into 5 mL LB containing appropriate antibiotics.

Following incubation at 37 °C with agitation overnight, 1 mL of the culture was transferred to a 500 mL Erlenmeyer flask containing 100 mL LB and appropriate antibiotics. The cells were cultured in a gyratory shaker (250 rpm, 37 °C) until they reached the mid-log phase of growth (OD₆₀₀ = 0.4-0.6). The culture was transferred to a centrifuge bottle that was previously sterilized with bleach and rinsed with sterile water. The cells were harvested by centrifugation (4 000g, 5 min, 4 °C) and the supernatant was discarded. All manipulations were carried out on ice during the remaining part of the procedure. Cells were resuspended in 100 mL of ice-cold 0.9% NaCl (w/v), harvested by centrifugation, and resuspended in 50 mL of ice-cold 100 mM CaCl₂. The suspension was stored on ice for a minimum of 30 min and centrifuged (4 000g, 5 min, 4 °C). The resulting cell pellet was resuspended in 4 mL of ice-cold 100 mM CaCl₂ (v/v) containing 15% glycerol (v/v). Aliquots (0.25 mL) were dispensed into ice-cold 1.5 mL sterile microfuge tubes and immediately frozen in liquid nitrogen. Competent cells were stored at -78 °C without significant loss of transformation efficiency over a period of six months.

Prior to transformation, frozen chemically competent cells were thawed on ice for about 5 min. An aliquot of plasmid (1 to 10 µL) or DNA ligation mixture was added to thawed competent cells (0.1 mL). After gentle mixing, the solution was kept on ice for 30 min. The cells were then heat shocked at 42 °C for 2 min and subsequently stored on ice for 1 min. LB (0.5 mL) was added to the cells, and the sample was incubated at 37 °C for 1 h without agitation. Cells were harvested using microcentrifugation (30 s), resuspended in 0.1 mL of LB and plated onto an LB plate containing the appropriate antibiotics. If the transformation was to be plated onto minimal medium plates, the cells

were washed once with an aliquot of M9 salts (0.5 mL). After resuspension in fresh M9 salts (0.1 mL), the cells were spread onto the plates. Competent cells that were not transformed with any DNA, were subjected to the same transformation procedure. Such treated cells were plated onto LB plates to check the viability of the competent cells, and were also plated onto selection medium to verify the absence of contaminations.

Preparation of electrocompetent cells followed the same procedure as described above for cell growth and harvest. Harvested cells were then washed with two portions (250 mL each) of ice-cold sterile double distilled water. After the second treatment with water, cells were collected by centrifugation (4 000g, 5 min, 4 °C) and resuspended in 50 mL of aqueous 10% glycerol (v/v) solution. The cell suspension was centrifuged (4 000g, 5 min, 4 °C). The resulting cell pellet was gently resuspended in 5 mL of ice-cold aqueous 10% glycerol. Aliquots (0.25 mL) of cells were dispensed into ice-cold sterile microfuge tubes, frozen in liquid nitrogen, and stored at -78 °C.

Electroporation was performed in Bio-Rad Gene Pulser cuvettes with an electrode gap of 0.2 cm. The cuvettes were chilled on ice for 5 min prior to use. Plasmid DNA (dissolved in sterile water, 1-5 μ L) or purified DNA ligation reaction was mixed with 0.1 mL of electrocompetent cells. After storage on ice for 5 min, the solution was transferred to a chilled cuvette. Moisture on the outer surface of the cuvette was removed before it was placed in the sample chamber of Bio-Rad Gene Pulser. The instrument was set at 2.5 kvolts, 25 μ F, and 200 Ohms. A single pulse was applied to the sample which typically resulted in a time constant of 4-5 ms. The cuvette was removed, and 0.5 mL of LB was added into it. Contents of the cuvette were transferred to a 1.5 mL microfuge tube, incubated at 37 °C for 1 h, and plated on the appropriate selective medium.

I. Enzyme Assays

General

Cells were collected by centrifugation at 4 000g and 4 °C for 5 min. Harvested cells were resuspended in the appropriate buffer and subsequently disrupted by two passages through a French press (16,000 psi, SLM Aminco). Cellular debris was removed by centrifugation (48 000g, 20 min, 4 °C). Protein concentrations were determined using the Bradford dye-binding method. A standard curve was prepared using bovine serum albumin. Protein assay solution was purchased from Bio-Rad.

DAHP Synthase

DAHP synthase was assayed according to the procedure described previously.¹⁷⁷ D-Erythrose 4-phosphate¹⁷⁸ (E4P) and phosphoenolpyruvate¹⁷⁹ used in the assay were synthesized by this group following literature procedures. Resuspension buffer contains potassium phosphate buffer (50 mM, pH 6.5), phosphoenolpyruvate (10 mM) and CoCl₂ (0.05 mM). Cellular lysate was diluted in potassium phosphate (50 mM), phosphoenolpyruvate (0.5 mM), and 1,3-propanediol (250 mM), pH 7.0. A diluted solution of D-erythrose 4-phosphate (E4P) was first concentrated to 12 mM by rotary evaporation and neutralized with 5 N KOH. Two solutions were prepared and incubated separately at 37 °C for 5 min. The first solution (1 mL) contained E4P (6 mM), phosphoenolpyruvate (12 mM), ovalbumin (1 mg mL⁻¹), and potassium phosphate (25 mM), pH 7.0. The second solution (0.5 mL) consisted of the diluted lysate. After the two solutions were mixed (time = 0), aliquots (0.15 mL) were removed at timed intervals and quenched with 10% (w/v) trichloroacetic acid (0.1 mL). Precipitated protein was

removed by centrifugation, and the product DAHP in each sample was quantified using a thiobarbituric acid assay¹⁸⁰ as described below.

An aliquot (0.1 mL) of DAHP containing sample was reacted with 0.1 mL of H_3PO_4 (8.2 M) containing $NaIO_4$ (0.2 M) at 37 °C for 5 min. The reaction was quenched by addition of 0.5 mL of H_2SO_4 (0.1 M) containing $NaAsO_2$ (0.8 M) and Na_2SO_4 (0.5 M). The mixture was vortexed until a dark brown color disappeared. Upon addition of a 3 mL of 0.04 M thiobarbituric acid in 0.5 M Na_2SO_4 (pH 7), the sample was heated at 100 °C for 15 min. The sample was cooled, and the pink chromophore was extracted into distill cyclohexanone (4 mL). The aqueous and the organic layers were separated by centrifugation (2 000g, 15 min). The absorbance of the organic layer was measured at 549 nm (ε = 68,000 L mol⁻¹ cm⁻¹). One unit of DAHP synthase activity was defined as the formation of 1 µmol of DAHP per min at 37 °C.

Glycerol Kinase

Glycerol kinase was assayed according to the procedure described by Lin.⁷⁵ Resuspension buffer contained Tris-HCl (60 mM, pH 7.5) and MgCl₂ (10 mM). The assay was based on measuring the formation of ¹⁴C-sn-glycerol 3-phosphate from ¹⁴C-glycerol at 37 °C. The reaction mixture (300 μL) contained the following: 60 mM Tris-HCl, 0.1mM ¹⁴C-glycerol (uniformly labeled, 0.5 μCi/μmole, Sigma), 10 mM ATP, 10 mM MgCl₂, and appropriately diluted cell crude lysate. Aliquots (30 μL) were removed from the reaction at timed intervals, applied to a disc of DEAE filter paper, and immediately dropped into 80% aqueous ethanol. Each disc was then washed with water to remove unreacted glycerol. After drying, each filter was subjected to scintillation

counting. The amount of sn-glycerol 3-phosphate (μ mol) bound to the DEAE filter paper was calculated by multiplying the reading from the scintillation counter (μ Ci) by two. One unit of glycerol kinase activity was defined as the formation of 1 μ mol of sn-glycerol 3-phosphate per min at 37 °C.

Catechol 1,2-Dioxygenase

Catechol 1,2-dioxygenase was assayed according to the procedure described by Hayaishi. Resuspension buffer contained Tris-HCl (50 mM, pH 7.5), MgCl₂ (5 mM), (NH₄)₂SO₄ (5 mM), EDTA (1 mM), DTT (1 mM) and 10% glycerol (v/v). The enzymatic reaction (1 mL) contained potassium phosphate (100 mM, pH 7.5), catechol (250 μM) and an appropriate amount of crude cellular lysate. Catechol 1,2-dioxygenase activity was measured spectrophotometrically by monitoring the formation of *cis*, *cis*-muconic acid at 260 nm. One unit of catechol 1,2-dioxygenase activity was defined as the formation of 1 μmol of *cis*, *cis*-muconic acid per min at 24 °C. A molar extinction coefficient of 16,000 M⁻¹cm⁻¹ (260 nm) was used for *cis*, *cis*-muconic acid. ¹⁸¹

3-Dehydroshikimate Dehydratase

3-Dehydroshikimate dehydratase activity was assayed by measuring the formation of protocatechuic acid at 290 nm. Cells resuspension buffer contained Tris-HCl (100 mM, pH 7.5) and MgCl₂ (2.5 mM). The assay solution contained Tris-HCl (100 mM, pH 7.5), MgCl₂ (2.5 mM), 3-dehydroshikimic acid (1 mM), and an appropriate amount of cell lysate in a total volume of 1 mL. The reaction was initialized upon the addition of the enzyme. Enzyme activity was measured spectrophotometrically by monitoring the

formation of protocatechuic acid at 290 nm. One unit of 3-dehydroshikimate dehydratase activity was defined as the formation of 1 µmol of protocatechuic acid per min at room temperature. A molar extinction coefficient of 3,890 M⁻¹cm⁻¹ (290 nm) was used for protocatechuic acid.¹⁸²

Transketolase

Transketolase was measured using a coupled enzyme assay described by Paoletti. The assay solution (1 mL) contained triethanolamine buffer (150 mM, pH 7.6), MgCl₂ (5 mM), thiamine pyrophosphate (0.1 mM), NADP (0.4 mM), β -hydroxypyruvate (0.4 mM), D-erythrose 4-phosphate (0.1 mM), glucose 6-phosphate dehydrogenase (3 units), and phosphoglucose isomerase (10 units). To avoid the background absorbance caused by the residual amount of D-glucose-6-phosphate existing in the solution of D-erythrose 4-phsphate, the assay solution was incubated at room temperature, and the absorbance at 340 nm was monitored for several minutes. After all the D-glucose-6-phosphate in the solution of D-erythrose 4-phosphate reacted, an aliquot of transketolase-containing solution was added to the reaction mixture. The reaction was monitored at 340 nm for 10 min. One unit of transketolase activity was defined as the formation of 1 µmol of NADPH (ϵ = 6220 M⁻¹ cm⁻¹) per min.

D-Xylonate Dehydratase and L-Arabinonate Dehydratase

D-Xylonate dehydratase and L-arabinonate dehydratase activity were assayed according to procedures described by Dahms. The 2-keto acid formed during the reaction was quantified as its semicarbazone derivative. Resuspension buffer contained

Tris-HCl (50 mM, pH 8.0) and MgCl₂ (10 mM). Two solutions were prepared and incubated separately at 30 °C for 3 min. The first solution (150 μL) contained Tris-HCl (50 mM, pH 8.0), MgCl₂ (10 mM) and an appropriate amount of cell lysate. The second solution (25 μL) contained potassium D-xylonate or potassium L-arabinonate (0.1 M). After the two solutions were mixed (time = 0), aliquots (30 μL) were removed at timed intervals and mixed with semicarbazide reagent (200 μL), which contained 1% (w/v) of semicarbazide hydrochloride and 0.9% (w/v) of sodium acetate in water. Following incubation at 30 °C for 15 min, each sample was diluted to 1 mL with H₂O. Precipitated protein was removed by centrifugation. The absorbance of semicarbazone was measured at 250 nm. One unit of D-xylonate dehydratase or L-arabinonate dehydratase activity was defined as the formation of 1 μmol of 2-keto acid per min at 30 °C. A molar extinction coefficient of 10,200 M⁻¹cm⁻¹ (250 nm) was used for 2-keto acid semicarbazone derivatives.

2-Keto Acid Decarboxylase

The specific activities of 2-keto acid decarboxylases including pyruvate decarboxylase, indole 3-pyruvate decarboxylase, and benzoylformate decarboxylase were determined by coupling the decarboxylation reaction with aldehyde-dependent oxidation of NADH by equine liver alcohol dehydrogenase. Resuspension buffer contained sodium phosphate (50 mM, pH 6.5) and MgCl₂ (10 mM). The enzyme assay solution (1 mL) contained sodium phosphate (50 mM, pH 6.5), MgCl₂ (10 mM), thiamine pyrophosphate (0.15 mM), NADH (0.2 mM), and an appropriate amount of cell lysate. When pyruvate decarboxylase was assayed for specific activity on pyruvate, equine liver

alcohol dehydrogenase (0.05 U) and pyruvate (5 mM) were also included in the assay.¹⁵⁴ When indole 3-pyruvate decarboxylase was assayed for specific activity on indole 3-pyruvate, equine liver alcohol dehydrogenase (0.05 U) and indole 3-pyruvate (1 mM) were also included in the assay. When benzoylformate decarboxylase was assayed for specific activity on benzoylformate, equine liver alcohol dehydrogenase (0.05 U) and benzoylformate (2 mM) were also included in the assay.¹⁵⁵ When 2-keto decarboxylases were assayed for specific activity on 3-deoxy-D,L-*glycero*-pentulosonic acid, equine liver alcohol dehydrogenase (1 U) and 3-deoxy-D,L-*glycero*-pentulosonate (50 mM) were also included in the assays. Enzyme activity was measured spectrophotometrically by monitoring the oxidation of NADH at 340 nm. One unit of 2-keto acid decarboxylase was defined as the conversion of 1 μmol of NADH (ε = 6,220 M⁻¹cm⁻¹) per min at room temperature.

Alcohol Dehydrogenase

The enzyme activities of alcohol dehydrogenases including *adhA*-encoded alcohol dehydrogenase II^{152a} and *adhB*-encoded alcohol dehydrogenase II^{152b} of *Zymomonas mobilis*, horse liver alcohol dehydrogenase, and 1,3-propanediol oxidoreductase¹⁵³ were measured in the oxidative direction by monitoring the formation of NADH. Resuspension buffer for *adhA*-encoded alcohol dehydrogenase I and *adhB*-encoded alcohol dehydrogenase II contained potassium phosphate (30 mM, pH 6.5), sodium ascorbate (10 mM), and Fe(NH₄)₂(SO₄)₂ (0.5 mM).¹⁵² Enzyme assays (1 mL) of AdhA, AdhB, and horse liver alcohol dehydrogenase on the native substrate contained Tris-HCl (30 mM, pH 8.5), NAD (1 mM), appropriate amount of cell lysate, and ethanol (1

mM). ¹⁵² Cell resuspension buffer for 1,3-propanediol oxidoreductase contained potassium carbonate (100 mM, pH 9.0) and ammonium sulfate (35 mM). ¹⁵³ When the specific activity of 1,3-propanediol oxidoreductase on native substrate was measured, the enzyme assay solution (1 mL) contained potassium carbonate (100 mM, pH 9.0), NAD (1 mM), appropriate amount of cell lysate, and 1,3-propanediol (0.1 mM). ¹⁵³ When the above four alcohol dehydrogenases were assayed for specific activity on nonnative substrate, 1,2,4-butanetriol (50 mM) was included in the assay in place of the native substrate. Enzyme activity was measured spectrophotometrically by monitoring the formation of NADH at 340 nm. One unit of alcohol dehydrogenase was defined as the formation of 1 µmol of NADH ($\varepsilon = 6,220 \text{ M}^{-1}\text{cm}^{-1}$) per min at room temperature.

Protein SDS-PAGE Analysis

Protein SDS-PAGE analysis followed the procedure described by Harris. Preparation of a 10% separating gel started from mixing 3.33 mL of 30% (w/v) aqueous acrylamide stock solution containing N,N'-methylene-bisacrylamide (0.8% (w/v)), 2.5 mL of 1.5 M Tris-HCl (pH 8.8), and 4 mL of distilled deionized water. After degassing the solution using a water aspirator for 30 min, 0.1 mL of 10% (w/v) aqueous ammonium persulfate solution, 0.1 mL 10% (w/v) aqueous SDS solution, and 0.005 mL of N, N, N', N'-tetramethylethylenediamine (TEMED) were added. The mixture was mixed thoroughly and poured into a 0.1 cm-width gel cassette to about 1.5 cm below the top of the gel cassette. *t*-Amyl alcohol was overlaid on top of the solution and the gel was allowed to polymerize for 1 h at rt. The stacking gel was prepared by mixing 1.7 mL 30% acrylamide stock solution containing N,N'-methylene-bisacrylamide (0.8% (w/v)),

2.5 mL Tris-HCl solution (0.5 M, pH 6.8), and 5.55 mL of distilled deionized water. After degassing for 30 min, 0.1 mL of 10% ammonium persulfate, 0.1 mL 10% SDS, and 0.01 mL of TEMED was added, and the solution was mixed thoroughly. t-Amyl alcohol was removed from the top of the gel cassette, which was subsequently rinsed with water and wiped dry. After insertion of the comb, the gel cassette was filled with stacking gel solution, and the stacking gel was allowed to polymerize for 1 h at rt. After removal of the comb, the gel cassette was installed into the electrophoresis apparatus. The electrode chamber was then filled with electrophoresis buffer containing glycine (192 mM), Tris base (25 mM), and 0.1% SDS (w/v). Following dilution with Laemmli sample buffer (10 μL, Sigma S-3401) consisting of 4% SDS, 20% glycerol, 10% 2-mercaptoethanol, 0.004% bromophenol blue, and Tris-HCl (125 mM, pH 6.8), each protein sample (10 μL) was heated at 100 °C for 10 min. Samples and markers (MW-SDS-200, Sigma) were then loaded into the sample wells and the gel was run under constant current at 30 mA until the blue tracking dye (bromophenol blue) reached the interface of stacking gel and separating gel. The protein gel was then run at a higher current (50 mA). When the blue tracking dye reaches the bottom of the gel, electrophoresis was terminated. The protein gel was subsequently removed from the cassette and submerged in 10% (w/v) aqueous trichloroacetic acid solution with constant shaking for 30 min. The protein gel was then transferred into a solution containing 0.1% (w/v) Comassie Brilliant Blue R, 45% (v/v) MeOH, 10% (v/v) HOAc in H₂O and stained with constant shaking for 4 h. Destaining of the protein gel was carried out in a solution containing 45% (v/v) MeOH, 10% (v/v) HOAc in H₂O for 2-3 h. For long-term storage, SDS-PAGE gels were sealed in plastic bags containing 10% glycerol.

CHAPTER TWO

A. Strain Constructions

E. coli KL3.21

E. coli KL3^{64c} competent cells were transformed with plasmid pKL5.17A^{64c} then spread onto M9 glycerol plates supplemented with aromatic amino acids and vitamins. Following incubation at 37 °C, single colonies of transformants were streaked out on fresh M9 glycerol plates supplemented with aromatic amino acids and vitamins. Single colonies with an enhanced growth rate were further streaked out on M9 glycerol plates supplemented with aromatic amino acids and vitamins for additional three rounds. One randomly chosen colony was cultured under fermentor-controlled conditions using glycerol as the sole carbon source. Fermentor-controlled cultivation followed the same procedure for microbial synthesis of 3-dehydroshikimate. An aliquot of cells were taken from the fermentor at 24 h time point. Cells were diluted with M9 salts, and spread onto M9 glycerol plates supplemented with aromatic amino acids and aromatic vitamins. Incubation of the plates at 37 °C resulted in the formation of single colonies with different sizes. A randomly chosen single colony with an enhanced growth rate was inoculated into 5 mL LB medium and grown at 37 °C for 12 h. Culture was then diluted in LB (1:20,000), and three more cycles of growth at 37 °C for 12 h were carried out to promote plasmid loss. Serial dilutions of cell culture from the last growth cycle were spread onto LB plate. Single colonies formed on this plate were screened on multiple plates for loss of plasmid and maintenance of E. coli KL3 phenotype: growth on M9 glycerol containing serine, aromatic amino acids and aromatic vitamins; no growth on M9 glycerol supplemented with aromatic amino acids and aromatic vitamins; no growth

on M9 glycerol containing serine and shikimic acid; no growth on LB containing Cm. The resulting strain was named KL3.21.

Plasmid pWN3.062A

This 12.3 kb pJF118EH-based plasmid encoded aroF^{FBR}, P_{aroF}, glpK^{FBR}, serA, and tktA. Ligation of a 1.25 kb aro F^{FBR} DNA fragment into pJF118EH afforded pJY1.131. PCR amplification of the promoter region of the aroF gene from pMF63A¹⁸⁵ utilized the following primers containing BamHI restriction sequences: 5'-GCGGATCC AAAGGGAGTGTAAATTTAT and 5'-GCGGATCCCCTCAGCGAGGATGACGT. Insertion of the resulting 0.15 kb DNA fragment into the BamHI site of pJY1.131 resulted in pSK1.171A. Using genomic DNA isolated from E. coli Lin4393 as template, a 1.5 kb glpK^{FBR} DNA fragment was amplified using PCR employing the following primers containing *EcoRI* restriction sequences: 5'-CGGAATTCGCCATGACTGAAAAAAAAT and 5'-CGGAATTCGCTTATTCGTCGTGTTCTT. Digestion of the PCR product with EcoRI followed by ligation into the EcoRI site of pSK1.171A afforded pWN3.042A. A 1.9 kb serA-encoding fragment was liberated from pD2625 by digestion with EcoRV and DraI. Ligation of the serA fragment into the SmaI site of pWN3.042A yielded pWN3.052A. Digestion of pSK4.203 with BamHI released a 2.2 kb fragment encoding the tktA gene, which was subsequently treated with Klenow fragment. Plasmid pWN3.052A was digested with HindIII and treated with Klenow fragment. Ligation of the two DNA fragments with blunt ends afforded pWN3.062A.

Plasmid pWN3.120A

This 12.3 kb plasmid was constructed employing the same cloning strategy for pWN3.062A. Using genomic DNA of *E. coli* RB791 as template, a 1.5 kb *glpK* DNA fragment was amplified using the same primers as those used for *glpK*^{FBR} amplification from Lin43. Localization of the PCR product into pSK1.171A resulted in pWN3.118A. Insertion of the 1.9 kb *serA* fragment into pWN3.118A yielded pWN3.119A. Ligation of the 2.2 kb *tktA* fragment into pWN3.119A resulted in pWN3.120A.

B. Microbial Synthesis of 3-Dehydroshikimate

Fed-batch fermentations were performed as described in the General Methods section. The carbon source was glycerol. The initial glycerol concentration in the fermentation medium ranged from 17 to 22 g/L. Three staged methods were used to maintain D.O. at 10% throughout the fermentations. Fermentations were run at a maximum impeller speed of 1100 rpm. IPTG stock solution (50 mM, 0.08 mL) was added to fermentations of *E. coli* KL3.21/pWN3.120A at 16 h, 24 h, 30 h, 36 h, and 42 h, while the same amount of IPTG was added into fermentations of *E. coli* KL3.21/pWN3.062A at 17 h, 24 h, 30 h, 36 h, and 42 h.

CHAPTER THREE

A. Strain Constructions

E. coli WN1

E. coli WN1 was prepared by homologous recombination of a tktAaroZ gene cassette into the lacZ locus of E. coli KL7. Construction of tktAaroZ cassette began

with digestion of pSK4.023A¹⁸⁶ with *Bam*HI to yield a 2.2 kb fragment encoding *tktA*. Following treatment of the *tktA* fragment with Klenow fragment, the DNA was ligated into the *Sma*I site of pSK4.99A¹⁸⁶ to afford pWN1.200A.

To direct recombination of the *tktAaroZ* cassette into the *lacZ* gene of *E. coli* KL7,¹⁰⁷ the *tktAaroZ* cassette was flanked by the *lacZ* gene sequence using the following procedure. The 1.9 kb open reading frame of *lacZ* was amplified from *E. coli* RB791 genomic DNA using the following primers containing *BamHI* restriction sequences: 5'-CGGGATCCATGACCATGATTACGG and 5'-CGGGATCCTTATTTTTGACACCA CAC. The amplified PCR product was digested with *BamHI* and subsequently inserted into the *BamHI* site of pMAK705 to afford pWN2.038A. Digestion of pWN1.200A with *XbaI* followed by partial digestion with *EcoRI* liberated a 4.5 kb *tktAaroZ* gene cassette, which was treated by Klenow fragment. The 4.5 kb DNA fragment was resolved from other DNA pieces on an agarose gel and was subsequently ligated into pWN2.038A linearized with *EcoRV* to afford pWN2.050B.

Homologous recombination was carried out using the same procedure as previously described. Competent E. coli KL7 cells were transformed with pWN2.050B and spread onto LB plates containing Cm. After passaging the cointegrates through multiple growth cycles as previously described, serial dilutions of each culture were spread onto MacConkey plates containing lactose and incubated at 30 °C for 12 h. White colonies that grew on the plates were further screened on multiple plates to select for the desired recombination product. E. coli KL7 lacZ::tktAaroZ was isolated based on the following growth characteristics: growth as a white colony on MacConkey agar containing lactose; no growth on M9 containing aromatic amino acids and aromatic

vitamins; growth on M9 containing aromatic amino acids, aromatic vitamins, and serine; growth on LB; and no growth on LB containing Cm. E. coli KL7 lacZ::tktAaroZ was renamed WN1.

Further confirmation that *E. coli* WN1 possessed the *tktAaroZ* insert relied on amplification of a 2.0 kb DNA fragment located in the middle of *tktAaroZ* gene cassette. PCR reactions utilized the following primers: 5'-CGGAATTCGTCTCAGAATGCTAT CGAAG and 5'-CGGAATTCTTGAAGATCTCCAGCGACCA. When using *E. coli* WN1 genomic DNA as template, a 2.0 kb amplification product was obtained. When using *E. coli* KL7 genomic DNA as template, no 2.0 kb fragment was produced. Digestion of the 2.0 kb PCR product with *AflIII*, *AvaI*, *BamHI*, and *NruI* afforded DNA fragments of the expected sizes based on the sequence of the *tktAaroZ* cassette.

Plasmid pWN1.162A

Plasmid pWN1.162A is a pSU18⁸⁶ derivative. It encoded *aroF*^{FBR}, *aroY*, *catA*, *serA*, and *P*_{aroF}. PCR amplification of a 1.25 kb *aroF*^{FBR} DNA fragment from pKD14.099A¹⁰⁶ utilized primers containing *Bam*HI restriction sequences: 5'-GCGGATCCAAAGGGAGTGTAAATTTAT and 5'-GCGGATCCTCTTAAGCCACG CGAGCCGT. Digestion of the resulting DNA with *Bam*HI followed by ligation into the *Bam*HI site of pSU18 afforded pWN1.028A. The *Klebsiella pneumoniae aroY* gene was amplified from pKD9.080A¹⁰⁶ using following primers containing *Kpn*I restriction sequences: 5'-GGGGTACCGCTTATCAATAAAGCATA and 5'-GGGGTACCCTTGC ACTATTTACCC GA. Localization of the resulting 2.4 kb *aroY* locus into the *Kpn*I site of pWN1.028A resulted in pWN1.079A. The open reading frame of the *Acinetobacter*

calcoaceticus catA locus was amplified with its native ribosomal binding site from pIB1345^{118a} employing the following primers containing *Eco*RI restriction sequences: 5'-CGGAATTCGTCGACAGATAAGTT and 5'-CGGAATTCGAACCATTTTGGTGT.

The 1.0 kb catA DNA fragment was cloned behind the *P*_{lac} promoter on pWN1.079A by insertion into its *Eco*RI site to afford pWN1.094A. A 1.9 kb serA-encoding fragment was liberated from pD2625 by digestion with *Eco*RV and *DraI*. Ligation of the serA fragment into the *SmaI* site on pWN1.094A yielded pWN1.106A. PCR amplification of the promoter region of aroF gene from pMF63A¹⁸⁵ utilized the following primers containing *XbaI* restriction sequences: 5'-GCTCTAGAGAATTCAAAGGGAGTGTA and 5'-GCTCTAGACCTCAGCGAGGATGACGT. Insertion of the resulting 0.15 kb DNA fragment into the *XbaI* site of pWN1.106A afforded pWN1.162A.

Plasmid pWN1.184A

Digestion of pSK4.99A¹⁸⁶ with *Bam*HI released a 2.3 kb fragment encoding the *aroZ* gene, which was subsequently treated with Klenow fragment. Plasmid pWN1.162A was digested with *Hin*dIII and treated with Klenow fragment. Ligation of the two DNA fragments with blunt ends afforded pWN1.184A.

Plasmid pWN2.100B

This 11.9 kb plasmid is a pJF118EH-derived plasmid that encoded catA, aroY, serA, $aroF^{FBR}$, and P_{aroF} . Digestion of pWN1.094A with EcoRI released a 1.0 kb catA gene that included its native ribosomal binding site along with the open reading frame. Localization of the resulting DNA fragment into the EcoRI site of pJF118EH yielded

pWN2.064A. Digestion of pKD9.046B¹⁰⁶ with *Hin*dIII liberated a 2.4 kb *aroY* fragment, which was subsequently treated with Klenow fragment. Plasmid pWN2.064A was digested with *Bam*HI and treated with Klenow fragment. Ligation of the two blunt end fragments of DNA afforded pWN2.084. PCR amplification of the *serAaroF*^{FBR}P_{aroF} gene cassette from pWN1.162A utilized the following primers containing *Sma*I restriction sequences: 5'-TCCCCCGGGTAAATAGTGCAAGG and 5'-TCCCCCGGGATGACGT AACGATAA. Digestion of the resulting 3.3 kb DNA with *Sma*I followed by ligation into the Klenow fragment-treated *Hin*dIII site of pWN2.084 afforded pWN2.100B.

Plasmid pWN2.248

This 13.5 kb plasmid is a pJF118EH-derived plasmid that encoded *catA*, *aroY*, *serA*, *aroF*^{FBR}, and *P*_{aroF}. A 2.5 kb *catA* DNA fragment containing an additional 1.5 kb of downstream DNA sequence was amplified from pIB1343^{118a} employing the following primers containing *EcoRI* restriction sequences: 5'-CGGAATTCGGTCGACAGA TAAGTTT and 5'-CGGAATTCTGCTTGAG TTGATTGGC. Digestion of the resulting 2.5 kb DNA fragment with *EcoRI* followed by insertion into the *EcoRI* site of pJF118EH resulted in pWN2.242A. Double digestion of pWN1.294B with *SmaI* and *ScaI* liberated a 6.5 kb *aroYserAaroF*^{FBR}*P*_{aroF} fragment. Ligation of the resulting DNA fragment into pWN2.242A linearized with *SmaI* and *ScaI* afforded pWN2.248.

B. Microbial Synthesis of cis, cis-Muconic Acid

Fed-batch fermentations were performed as described in the General Methods section. D-Glucose was used as the carbon source. The initial glucose concentration in

the fermentation medium ranged from 20 to 24 g/L. Fermentations that did not require baffles were run with a maximum impeller speed of 940 rpm. Fed-batch cultures employed a stainless steel baffle cage (four 1/2" x 5" baffles) were run with a maximum impeller speed of 900 rpm. IPTG stock solution (100 mM, 0.5 mL) was added to fermentations of *E. coli* WN1/pWN2.248 at 13 h, 18 h, 24 h, 30 h, 36 h, and 42 h.

C. Hydrogenation of cis, cis-Muconic Acid to Adipic Acid

Fermentation broth was centrifuged at 14 000g for 20 min, and the broth was decaned from the pelleted cells. The resulting broth was combined with Darco KB-B activated carbon (Aldrich, 20 g/L of broth) and swirled at 250 rpm for 2 h. After filtration through Whatman 5 filter paper, the filtrate was passed via pressurized filtration through a membrane possessing a molecular weight cut off of 10 kDa. The resulting filtrate was then treated a second time with activated carbon as described above.

Hydrogenation reactions were performed using a Parr HTHP 4575 that was equipped with mechanic stirring, a pressure indicator, and temperature control. The pretreated fermentation broth (250 mL) containing 150 mM *cis,cis*-muconate was mixed with 10% platinum on activated carbon (3.614 g, 5 mol percent) in a glass liner, which was fitted into the metal container of Parr hydrogenation apparatus. H₂ was flushed through the system three times. The hydrogenation reaction was carried out at 500 psi of H₂ pressure at 25 °C, with stirring for 2.5 h. The reaction was then filtered through Celite to remove catalysts. The concentration of *cis,cis*-muconic acid and adipic acid in the resulting filtrate were determined by gas chromatography. A portion of the filtrate (0.5-1.0 mL) was concentrated to dryness under reduced pressure, and the residue was

redissolved in pyridine (0.9 mL). To this pyridine solution, dodecane (0.1 mL) and bis(trimethylsilyl)trifluoroacetamide (BSTFA, 2 mL, 7.53 mmol) were sequentially added. Silyation was carried out at room temperature with stirring for 10 h. Samples were then analyzed using GC and quantified relative to an internal standard of dodecane.

CHAPTER FOUR

A. Purification of D-Xylonate Dehydratase from *Pseudomonas fragi* (ATCC 4973) Buffers

Buffers used for purification of D-xylonate dehydratase from *P. fragi* included buffer A: Tris-HCl (50 mM, pH 8.0), MgCl₂ (2.5 mM), DTT (1.0 mM), PMSF (0.25 mM); buffer B: Tris-HCl (50 mM, pH 8.0), MgCl₂ (2.5 mM), DTT (1.0 mM), PMSF (0.25 mM), NaCl (500 mM); buffer C: potassium phosphate (2.5 mM, pH 8.0), MgCl₂ (2.5 mM), DTT (1.0 mM), PMSF (0.25 mM); buffer D: potassium phosphate (250 mM, pH 8.0), MgCl₂ (2.5 mM), DTT (1.0 mM), PMSF (0.25 mM); buffer E: Tris-HCl (50 mM, pH 8.0), MgCl₂ (2.5 mM), DTT (1.0 mM), PMSF (0.25 mM), (NH₄)₂SO₄ (1 M).

Purification of D-Xylonate Dehydratase

Cultivation of *P. fragi* for protein purification used a liquid medium described by Weimberg. ^{136a} This liquid medium (1 L) contained KH₂PO₄ (4.5 g), Na₂HPO₄ (4.7 g), NH₄Cl (1 g), CaCl₂ (0.01 g), ferric ammonium citrate (0.1 g), MgSO₄ (0.25 g), corn steep liquor (0.1 g). Growth of an inoculant was initiated by introduction of a single colony of *P. fragi* from a nutrient agar plate into 100 mL of the liquid medium containing D-xylose (0.25 g). The cells were cultured at 30 °C with agitation for 24 h. The resulting cell

culture was transferred into a 2 L fermentor vessel that contained 1 L of the liquid medium with 10 g of D-xylose. Fermentor-controlled cultivation was carried out at 30 °C, pH 6.5 with an impeller speed of 650 rpm for 48 h. Cells were harvested by centrifugation at 8 000g and 4 °C for 10 min.

All protein purification manipulations were carried out at 4 °C. D-Xylonate dehydratase specific activity was assayed as described in the General Methods section. P. fragi cells (150 g, wet weight) were resuspended in 250 mL of buffer A and disrupted by two passages through a French press cell at 16,000 psi. Cellular debris was removed by centrifugation (48 000g, 20 min, 4 °C). The cell lysate was applied to a DEAE column (5 x 18 cm) equilibrated with buffer A. The column was washed with 1 L of buffer A followed by elution with a linear gradient (1.75 L + 1.75 L, buffer A/buffer B). Fractions containing D-xylonate dehydratase were combined and concentrated to 100 mL. After dialysis against buffer C (3 x 1 L), the protein was loaded onto a hydroxyapatite column (2.5 x 35 cm) equilibrated with buffer C. The column was washed with 350 mL of buffer C and eluted with a linear gradient (850 mL + 850 mL, buffer C/buffer D). Fractions containing D-xylonate dehydratase were combined and concentrated to 30 mL. After dialysis against buffer E (3 x 300 mL), the protein solution was applied to a phenylsepharose column (2.5 x 15 cm) equilibrated with buffer E. The column was washed with 200 mL of buffer E followed by elution with a linear gradient (400 mL + 400 mL, buffer E/buffer A). Fractions containing D-xylonate dehydratase were combined and concentrated to 15 mL. After dialysis against buffer A (3 x 150 mL), protein samples (15 x 0.1 mL) were loaded on a Resource Q (6.4 mm x 30 mm, 1 mL) column equilibrated with buffer A. The column was washed with 25 mL of a 90:10 (v/v) mixture

of buffer A and buffer B, and eluted with a linear gradient of NaCl (50 mM to 200 mM) in buffer A over 20 min. Fractions containing D-xylonate dehydratase were combined and concentrated to 0.5 mL. After dialysis against buffer A (3 x 10 mL), the enzyme was quick frozen in liquid nitrogen and stored at -80 °C. The NH₂-terminal of purified D-xylonate dehydratase was sequenced by the Genomic Technology Support Facility at Michigan State University.

B. Pseudomonas fragi Genomic DNA Library Construction

Pseudomonas fragi (ATCC 4973) genomic DNA was isolated according to the procedure described by Wilson.¹⁷⁵ The DNA was partially digested with Sau3AI under controlled conditions to afford fragments in the range of 30 kb to 42 kb. The resulting DNA fragments were ligated into cosmid vector SuperCos 1, which had been digested with BamHI. The ligated DNA was packaged using the Gigapack* III XL packaging extract (Stratagene) using the procedure supplied by the manufacturer. After addition of the ligated DNA into Gigapack* III XL packaging extract, the solution was thoroughly mixed and incubated at room temperature for 2 h. The mixture was then diluted with 500 μL of SM buffer containing Tris-HCl (50 mM, pH 7.5), NaCl (100 mM), MgSO₄ (8 mM), and gelatin (0.01%, w/v). To remove proteins, 20 μL of chloroform was added to the sample and subsequently separated from the aqueous layer by microfugation. The supernatant containing the phage was used to transfected E. coli BL21(DE3) cells.

Preparation of E. coli BL21(DE3) cells used for phage transfection started by introduction of a single colony into 5 mL LB medium containing $MgSO_4$ (10 mM) and maltose (0.2 %, w/v). Following incubation at 37 °C for 4 h with agitation, the cells were

harvested by microfugation at 500g for 10 min. The cells were resuspended in appropriate volume of MgSO₄ (10 mM) to reach an OD₆₀₀ of 0.5. An aliquot (25 μL) of BL21(DE3) cells was added to a sterile test tube containing appropriate amount of phage solution. After incubation at room temperature for 30 min, LB medium (0.2 mL) was added and cells were cultured at 37 °C for one hour with occasional agitation. Cells were harvested by microcentrifugation (30 s) and washed one time with an aliquot of M9 salts (0.5 mL). Cells were resuspended in fresh M9 salts (0.1 mL) and spread onto solid M9 medium containing L-arabinonate as the single carbon source. The plates were incubated at 37 °C. Three colonies formed after 66 h of incubation. Cosmids purified from the three colonies were subjected to restriction enzyme digestion.

C. Plasmids

Plasmid pWN5.150A

This 4.2 kb plasmid is a pT7-7-derived plasmid that encoded the *Pseudomonas* fragi aadh gene. PCR amplification of a 1.7 kb aadh DNA fragment from pT7-7A (Chapter Four) utilizes primers containing BamHI restriction sequences: 5'-GAGGATCCCAATAAGAGCCCGCCATAA and 5'-ACGGATCCTACTCAGTGGGA ATGACGG. Digestion of the resulting DNA with BamHI followed by insertion into the BamHI site of pT7-7 resulted in pWN5.150A.

Plasmid pWN5.022A

This 6.5 kb plasmid is a pJF118EH-derived plasmid that encoded the *Klebsiella* pneumoniae dhaT gene. PCR amplification of a 1.2 kb dhaT DNA fragment from

Klebsiella pneumoniae (ATCC 25955) genomic DNA utilized the following primers containing BamHI restriction sequences: 5'-ACGGATCCGCGAGAAGGTATATTA TGAGC and 5'-TCGGATCCCCTCGTTAACACTCAGAATGC. Digestion of the resulting DNA fragment with BamHI followed by insertion into the BamHI site of pJF118EH resulted in pWN5.022A.

Plasmid pWN5.284A

This 7.0 kb plasmid derived from pJF118EH. It encoded the *Erwinia herbicola ipdC* gene. PCR amplification of a 1.7 kb DNA fragment from pMB2¹⁵⁶ utilized the following primers containing *Eco*RI restriction sequences: 5'-CGGAATTCTGAAAGG AACGCGCAATGTC and 5'-GTGAATTCTGAATCTTAGCCGCCGTTGC. Digestion of the resulting DNA with *Eco*RI followed by insertion into the *Eco*RI site of pJF118EH resulted in pWN5.284A.

Plasmid pWN5.238A

This 6.9 kb plasmid derived from pJF118EH and encoded the *Pseudomonas* putida mdlC gene. PCR amplification of a 1.6 kb DNA fragment from the genomic DNA of *Pseudomonas* putida (ATCC 12633) used the following primers containing *Eco*RI restriction sequences: 5'-CGGAATTCGATTCACCATTTGGTAAGAGA and 5'-CGGAATTCTCTGGCTCATGGCTTACCTCA. Digestion of the resulting reaction product with *Eco*RI followed by insertion into the *Eco*RI site of pJF118EH afforded pWN5.238A.

Plasmid pWN6.186A

This 8.1 kb plasmid is derived from plamid pWN5.238A. Digestion of pKAD62A¹⁸⁸ with *Eco*RI and *Bam*HI liberated a 1.2 kb DNA fragment encoding a kanamycin resistance gene, which was subsequently treated with Klenow fragment. Ligation of the resulting DNA with pWN5.238A previously digested with *Sca*I afforded pWN6.186A.

Plasmid pWN6.120A

This 6.0 kb plasmid is a pKK223-3-derived plasmid that encoded the *Pseudomonas fragi aatp* gene. PCR amplification of the *aatp* gene from pT7-7A (Chapter Four) utilized the following primers containing *Eco*RI restriction sequences: 5'-CGGAATTCACTGAGAGCTGATCCTGG and 5'-CGGAATTCTAAACGCATAACG GTGTC. Digestion of the PCR product with *Eco*RI followed by insertion into the *Eco*RI site of pKK223-3 resulted in pWN6.120A.

Plasmid pWN6.222A

This 10.1 kb plasmid is a pT7-7-derived plasmid that encoded aadh, aatp, mdlC, $lacI^Q$, and the kanamycin resistance gene. Digestion of pWN5.238A with NruI and SmaI liberated a 3.0 kb DNA fragment containing $lacI^QP_{lac}mdlC$ cassette. Insertion of the resulting DNA into pWN5.150A which was previously digested with HindIII and incubated with Klenow fragment afforded pWN6.086A. Digestion of pWN6.120A with BamHI liberated a 1.7 kb DNA fragment encoding $P_{tac}aatp$ cassette, which was subsequently inserted into the BgIII site of pWN6.086A to yield pWN6.126A. Digestion

of pKAD62A with *Eco*RI and *Bam*HI liberated a 1.2 kb DNA fragment encoding the kanamycin resistance gene, which was treated with Klenow fragment. Ligation of the resulting DNA with pWN6.126A that was previously digested with *Sca*I afforded pWN6.222A.

D. Microbial Oxidation of Pentoses

Fermentor-Controlled Cultivation Conditions

Fermentations employed a 2.0 L working capacity B. Braun M2 culture vessel. Utilities were supplied by a B. Braun Biostat MD controlled by a DCU-3. The fermentor-controlled cultivations were carried out at 30 °C, with an impeller speed of 650 rpm and an airflow at 0.5 L/L/min. The culture medium was maintained at pH 6.4 by addition of 2 N H₂SO₄ and 30% CaCO₃ for oxidation of D-xylose or concentrated NH₄OH for oxidation of L-arabinose.

Fermentation medium^{139a} (1 L) for microbial oxidation of D-xylose or L-arabinose contained K₂HPO₄ (2 g), KH₂PO₄ (1 g), (NH₄)₂SO₄ (5 g) and yeast extract (6 g). The following supplements were added immediately prior to initiation of the fermentation: D-xylose or L-arabinose (as specified), MgSO₄ (0.24 g). Solutions of D-xylose and L-arabinose were prepared by combining 100 g of D-xylose or L-arabinose with 90 mL of H₂O. Solutions D-xylose, L-arabinose, and MgSO₄ (1 M) were autoclaved separately. Inoculants were started by introduction of a single colony of *Pseudomonas fragi* picked from a nutrient agar plate into 5 mL of fermentation medium. Cultures were grown at 30 °C with agitation at 250 rpm until they were turbid (~24 h) and subsequently transferred to 100 mL of fermentation medium. Cultures were grown at 30 °C and 250 rpm for an

additional 12 h. The inoculant ($OD_{600} = 1.0\text{-}3.0$) was then transferred into the fermentation vessel and the batch fermentation was initiated (t = 0 h). Samples (5-10 mL) of fermentation broth were removed at 6 h intervals. Cell densities were determined by dilution of fermentation broth with water (1:100) followed by measurement of absorption at 600 nm (OD_{600}).

Purification of Fermentation Products

Fermentation broth was centrifuged at 14 000g for 20 min and the cells were discarded. The resulting supernatant was combined with Darco KB-B activated carbon (20 g/L of broth), and swirled at 250 rpm for 2 h. After filtration through Whatman 5 filter paper, the filtrate was treated a second time with activated carbon as described above. Purification of D-xylonate followed a procedure modified from Buchert. Activated charcoal-treated fermentation broth (1-1.1 L) was concentrated to 250 mL, and ethanol (3 ethanol:1 broth, v/v) was added to the solution. The solution was chilled at -20 °C for approximately 12 h to precipitate calcium D-xylonate. The ethanol was then decanted, and precipitated calcium xylonate was dried under vacuum (95% recovery based on D-xylonate quantified in crude fermentation broth). Calcium xylonate (50 g) was dissolved in warm H₂O (100 mL). The solution was passed through a Dowex-50 (K⁺ form, 300 mL) column to obtain potassium xylonate.

Activated charchoal-treated fermentation broth (1-1.1 L) resulting from microbial oxidation of L-arabinose was concentrated to 100 mL by rotary evaporation. The pH of the solution was adjusted to 12.0 by addition of solid KOH. Hydrolysis of L-arabino-1,4-lactone to L-arabinonate was carried out at room temperature with stirring for overnight.

The solution was then neutralized by addition of concentrated HCl, and methanol (5 methanol:1 broth, v/v) was added. The resulting solution was chilled at 4 °C for 12 h. Precipitated potassium arabinonate was filtered and dried under vacuum (92% recovery based on L-arabinonate and L-arabino-1,4-lactone quantified in the fermentation broth).

E. Microbial Synthesis of 1,2,4-Butanetriol

Fermentor-Controlled Cultivation Conditions

Fed-batch fermentations were performed as described in the General Methods section. Fermentor-controlled cultivations were carried out at 33 °C. Addition of concentrated NH₄OH or 2 N H₂SO₄ was employed to maintain pH at 7.0. For microbial synthesis of D- or L-1,2,4-butanetriol, fermentation medium (1 L) contained Bacto tryptone (20 g), Bacto yeast extract (10 g) and NaCl (5 g). The following supplements were added immediately prior to initiation of the fermentation: K₂HPO₄ (3.75 g), glucose, MgSO₄ (0.24 g), and thiamine hydrochloride (0.34 g). Kanamycin (0.1 g) was added into the culture medium at the same time. Solutions of K₂HPO₄ (50 mM, pH 7.0), glucose, and MgSO₄ (1 M) were autoclaved separately. Solutions of thiamine hydrochloride (0.1 g/mL), kanamycin (50 mg/mL), IPTG (0.5 M), potassium D-xylonate (1 M), and potassium L-arabinonate (1 M) were sterilized through 0.22 μm membrane.

Inoculants were started by introduction of a single colony picked from an agar plate into 5 mL of LB-glucose medium containing kanamycin. Cultures were grown at 37 °C with agitation at 250 rpm until they were turbid. An aliquot (0.5 mL) of this culture was subsequently transferred to 100 mL of LB-glucose medium containing kanamycin, which was grown at 37 °C and 250 rpm for an additional 10 h. The inoculant

 $(OD_{600} = 1.0-3.0)$ was then transferred into the fermentation vessel and the batch fermentation was initiated (t = 0 h). The initial glucose concentration in the fermentation medium was 22 g/L for microbial synthesis of D-1,2,4-butanetriol and 12 g/L for microbial synthesis of L-1,2,4-butanetriol.

The same three staged methods described in General Methods section were used to maintain D.O. concentrations to 20% throughout the fermentor-controlled cultivations. At the initiation of the final D.O. controlling stage, solution of potassium D-xylonate (12 g) or potassium L-arabinonate (12 g) was added to the culture medium together with IPTG solution (1 mL, 0.5 M). The concentration of 1,2,4-butanetriol in the culture medium was quantified by GC analysis.

Analysis of 1,2,4-Butanetriol for Enantiomeric Purity

Fermentation broth was centrifuged at 14 000g for 20 min, and the cells were discarded. The resulting supernatant was combined with Darco KB-B activated carbon (20 g/L of broth), and swirled at 250 rpm for 2 h. The activated carbon was removed by filtration through Whatman 5 filter paper. Resulting filtrate was treated a second time with activated carbon as described above. An aliquot (200 mL) of activated carbon-treated fermentation broth was concentrated to 20 mL using rotary evaporation. The resulting solution was eluted through a Dowex 1 (1X8-400, hydroxide form) column with water. The eluant was neutralized by addition of Dowex 50 (H⁺ form) resin, and the resin was removed by filtration. The filtrate was concentrated under vacuum to give an approximately 85% recovery of 1,2,4-butanetriol.

To a 1,2,4-butanetriol (0.0027 g, 0.025 mmol) in pyridine (0.2 mL), CH₂Cl₂ (0.3 mL), p-dimethylaminopyridine (0.005 g), and (S)-(+)- α -methoxy- α -(trifluoromethyl) phenylacetyl chloride (0.026 g, 0.1 mmol) were sequentially added. The mixture was stirred at room temperature overnight and passed through a disposable pipette containing silica gel, which was eluted with 3 mL of CH₂Cl₂. The eluant was dried under vacuum, and the residue was redissolved in CH₂Cl₂ (3 mL) and washed with 1% NaHCO₃ (5 mL) and H₂O (2 x 5 mL). The CH₂Cl₂ layer was concentrated under vacuum to give the 1,2,4butanetriol Mosher ester. Mosher esters of D- and L-1,2,4-butanetriol were analyzed on an Agilent 1100 HPLC equipped with a Chiralpak AD column (Daicel Chemical, 4.6 mm x 250 mm), which had been equilibrated with hexane/2-propanol (98:2, v/v). The column was eluted with the same solvent mixture at a rate of 1.25 mL/min, while the eluant was monitored at 260 nm. The retention time of D- and L-1,2,4-butanetriol Mosher ester were 14.4 min and 8.1 min, respectively. Mixtures of authentic D- and L-1,2,4-butanetriol in varied weight ratio were derivatized using Mosher's reagent and further analyzed by HPLC. A calibration curve was generated by plotting the peak area ratio of D- and L-1,2,4-butanetriol Mosher esters against the weight ratio of D- and L-1,2,4-butanetriol in above mixed authentic samples.

F. Directed Evolution of Benzoylformate Decarboxylase

Construction of Benzoylformate Decarboxylase Mutant Libraries

DNA sequence randomization was carried out in two steps: random mutagenesis of the complete *mdlC* gene (1587 bp) by error-prone PCR to generate library E1 and recombination of improved benzoylformate decarboxylase mutants from library E1 by

DNA shuffling to generate library S2. Randomized *mdlC* DNA sequences from either library were digested with *Eco*RI and *Bam*HI followed by agarose gel isolation and extraction. The resulting 1.6 kb DNA fragment was ligated into *Eco*RI and *Bam*HI digested pJF118EH. *E. coli* DH5α competent cells were transformed with the ligation mixture using electroporation and spread onto LB plates containing ampicillin.

Error-Prone PCR

Error-prone PCR was carried out using sense primer containing *Eco*RI restriction sequence 5'-CGGAATTCGATTCACCATTTGGTAAGAGA and anti-sense primer containing *Bam*HI restriction sequence 5'-TGGGATCCTCATGGCTTACCTCACTT. The mutagenic PCR reaction (0.1 mL) contained Tris-HCl (20 mM, pH 8.4), KCl (50 mM), template DNA (pWN5.238A, 0.025 μg), dATP (0.2 mM), dGTP (0.2 mM), dCTP (1.0 mM), dTTP (1.0 mM), MgCl₂ (7 mM), primers (0.5 μM each), *Taq* polymerase (1.5 units, Invitrogen) and MnCl₂ (0.2 mM). PCR reactions were carried out for 35 cycles using the following cycle conditions: 94 °C for 30 s, 55 °C for 60 s and 72 °C for 100 s.

DNA Shuffling

Genes encoding benzoylformate decarboxylase mutants with improved 3-deoxy-D,L-glycero-pentulosonic acid decarboxylase activity obtained from the E1 library were amplified by standard PCR employing *Pfu* turbo polymerase using the two primers listed above. DNA shuffling of these mutants followed a modified procedure described by Stemmer.¹⁶¹ A random fragmentation of mutant DNA with DNase I was carried out in the presence of Tris-HCl (20 mM, pH 7.5), MnCl₂ (10 mM), DNase I (0.03 units), and 1

μg of the PCR product of each mutant DNA in a total volume of 50 μL at room temperature for 11 min. The digestion reaction was terminated by addition of endostop solution. DNA fragments of 50-100 bp were purified from 2.5% low melting point agarose gel by electrophoresis onto DE81 ion-exchange paper (Whatman), elution with 1 M NaCl, and ethanol precipitation. The resulting DNA precipitate was redissolved in sterile H₂O (10 μL). Reassembly of the purified DNA fragments was realized by a primerless PCR reaction (50 μL) that contained Tris-HCl (20 mM, pH 8.4), KCl (50 mM), dNTP (0.2 mM), *Taq* polymerase (2.5 units), and the purified DNA fragments (5 μL). The PCR program was: one cycle of denaturation at 94 °C for 3 min followed by 60 cycles of 1 min denaturation at 94 °C, 1 min hybridization at 55 °C and 1 min plus 5 s per cycle elongation at 72 °C and finally a 10 min step at 72 °C. The PCR products were purified using Zymoclean DNA Clean and Concentrate Kit. An aliquot (5 μL) of the reassembled DNA was amplified by a standard PCR reaction employing *Pfu* turbo polymerase using the two primers listed above.

Screening of Benzoylformate Decarboxylase Mutant Libraries

Screening of benzoylformate decarboxylase mutant libraries was carried out in 96-well format. A typical round of screening started with inoculation of 93 single colonies from the mutant library together with two colonies of *E. coli* DH5α/pWN5.238A into individual wells on a 96-well flat-bottom block (Qiagen, 2 mL per well), which was loaded with LB-freeze buffer containing Ap (1.0 mL/well). As a control, well H-12 contained only growth medium. Cells were cultured at 37 °C with agitation at 300 rpm for 12 h. An aliquot (50 μL) of each culture was transferred to a

sterilized 96-well microplate, which was stored at -80 °C as a masterplate. A second 50 μL aliquot of each culture was inoculated into a second 96-well flat-bottom block, which was loaded with LB medium containing Ap (1.0 mL/well). Inoculants were incubated at 37 °C and 300 rpm for 100 min, and protein expression was induced by the addition of IPTG to a final concentration of 0.5 mM. Cells were incubated at 37 °C and 300 rpm for an additional 6 h and harvested by centrifugation at 3000 rpm for 10 min. The pelleted cells were resuspended in 150 µL of lysis buffer, which contained potassium phosphate (50 mM, pH 6.5), MgCl₂ (5 mM), benzonase nuclease (25 units/mL) and 10 x BugBuster protein extraction reagent (Novagen, 15 µL). Cells were lysed at 30 °C for 30 min with shaking. An aliquot (50 µL) of each cell lysate was then transferred to corresponding wells in a fresh 96 well microplate containing MgCl₂ (5 mM), thiamine diphosphate (0.5 mM), and D,L-3-deoxy-glycero-pentulosonic acid (10 mM) in 50 µL of potassium phosphate buffer (50 mM, pH 6.5). The decarboxylation reaction mixtures were incubated at 30 °C with shaking for 4 h, quenched by addition of 30 µL of 10% trichloroacetic acid solution. Protein precipitates were removed by centrifugation at 4000 rpm for 10 min. An aliquot (50 µL) of each supernatant was mixed with 50 µL of Schiff's reagent in a 96-well microplate and incubated at room temperature for 30 min. The formation of red dye was monitored by measuring the absorbance at 550 nm relative to well H12 using a Benchmark microplate reader (Bio-Rad Laboratories).

Schiff's reagent was prepared by dissolving pararosaniline (1 g) and sodium metabisulphite (1.9 g) in HCl (100 mL, 0.15 M). The solution was incubated at room temperature with agitation for 2 h. Activated charcoal (0.5 g) was then added to the solution, and the mixture was shaken for 2 min at room temperature. Removal of the

activated charcoal by filtration resulted in light yellow-colored Schiff's reagent, which was stored in a brown bottle at 4 °C.

Biosynthesis of 1,2,4-Butanetriol by E. coli W3110 Expressing Wild-Type and Mutant Benzoylformate Decarboxylase

Single colony of *E. coli* W3110 transformants was inoculated into 5 mL of M9 D-xylonate medium containing Ap and incubated at 37 °C with agitation for 36 h. An aliquot (100 μL) of culture was transferred into 5 mL M9 D-xylonate medium containing Ap, and the inoculant was incubated at 37 °C with agitation. When cell growth reached exponential rate, protein expression was induced by addition of IPTG to culture medium to a final concentration of 0.5 mM. Cells were cultured at 37 °C with agitation for an additional 48 h. An aliquot (2 mL) of cell culture was withdrawn, and the cells were removed with centrifugation. The resulting supernatant was dried under vacuum, derivatized with bis(trimethylsilyl)trifluoroacetamide, and analyzed by GC.

<u>Purification of Recombinant 6-His Tagged Benzoylformate Decarboxylase</u>

Purification of benzoylformate decarboxylase was facilitated by cloning *mdlC* gene into plasmid pJG7.246.¹⁸⁹ Derived from protein expression vector pQE30, plasmid pJG7.246 contained an extra 1.3 kb DNA fragment encoding the *lacl^Q* gene inserted into the *PstI* site of pQE-30. PCR amplification of wild-type or mutant *mdlC* gene utilized following primers containing *BamHI* restriction sequences: 5'-AGGGATCCATGGCTTC GGTACACGGCA and 5'-TGGGATCCTCATGGCTTACCTCACTT. Digestion of the 1.6 kb DNA fragment with *BamHI* followed by insertion into the *BamHI* site of pJG7.246 resulted in pWN7.088A-X (X is the name of the insert).

Single colony of E. coli DH5α/pWN7.088A-X was inoculated into 5 mL LB medium containing Ap. Inoculants were cultured at 37 °C with agitation for overnight. Cells were subsequently transferred into 500 mL of LB containing Ap and grown at 37 °C with agitation. When the OD_{600nm} of the inoculants reached 0.4-0.6, IPTG was added to the culture medium to a final concentration of 0.5 mM. Cells were grown for an additional 4 h, then harvested by centrifugation at 4 000g and 4 °C for 5 min. Harvested cells were resuspended in 16 mL of resuspension buffer, which contains potassium phosphate (50 mM, pH 6.5) and MgCl₂ (5 mM). Cell resuspension was subsequently disrupted by two passages through a French press (16,000 psi). Cell debris were removed by centrifugation at 48 000g for 20 min at 4 °C. Resulting cell-free lysate was mixed with 4 mL of Ni-NTA agarose resin (50% slurry (w/v)), and the mixture was stirred at 4 °C for one hour. The lysate resin slurry was then transferred to a polypropylene column (Qiagen), and the column was washed with wash buffer (2 x 16 mL), which contains K₂HPO₄ (50 mM, pH 8.0), imidazole (20 mM), and NaCl (300 mM). The 6-His tagged protein was eluted from the column by washing with elution buffer (2 x 4 mL), which contains K₂HPO₄ (50 mM, pH 8.0), imidazole (250 mM), and NaCl (300 mM). The eluted protein was dialyzed against cell resuspension buffer. Protein samples were analyzed using SDS-PAGE.

Analysis of Decarboxylation Product of 3-Deoxy-D,L-glycero-pentulosonic Acid for Enantiomeric Purity

Cultures were initiated by introduction of a single colony of desired *E. coli* strain into 5 mL LB medium containing Ap. Inoculants were grown at 37 °C with agitation for 12 h, and an aliquot (1 mL) of culture was subsequently transferred to 100 mL LB

medium containing Ap. Cultures were grown at 37 °C with agitation. When the OD_{600nm} of the inoculants reached 0.4-0.6, IPTG was added to the culture medium to a final concentration of 0.5 mM. Cells were cultured at 37 °C with agitation for an additional 6 h and harvested by centrifugation at 4 000g and 4 °C for 5 min.

Harvested cells were resuspended in 5 mL of resuspension buffer, which contained potassium phosphate (50 mM, pH 6.5) and MgCl₂ (5 mM). Cell resuspension was subsequently disrupted by two passages through a French press (16,000 psi). Cell debris were removed by centrifugation at 48 000g and 4 °C for 20 min. An aliquot (4 mL) of the resulting cell-free lysate was incubated with a mixture of 3-deoxy-D,Lglycero-pentulosonic acid (10 mM), MgCl₂ (5 mM), and thiamine diphosphate (0.5 mM) in 26 mL of potassium phosphate buffer (50 mM, pH 6.5). The enzymatic reaction was incubated at 30 °C for 4 h with stirring, then was quenched by addition of concentrated hydrochloric acid to reach pH 2.0. Precipitated protein was removed by centrifugation at 48 000 g for 20 min at 4 °C. The solution was neutralized, concentrated to approximately 3 mL, and loaded on a Dowex 1X8 column (20 mL), which was subsequently washed with water (60 mL). The flow-through and wash fraction were combined and concentrated to approximately 10 mL. To this solution, NaBH₄ (20 mg) was added. Reduction reaction was carried out at room temperature with stirring overnight and quenched by addition of Dowex 50 (H⁺) resin. The resulting mixture was passed through a short Dowex 50 (H⁺) column and concentrated to dryness. Boric acid was removed as an azeotrope with methanol (6x). The resulting residue was redissolved in water. The concentration of 1,2,4-butanetriol was quantified by ¹H NMR.

Derivatization of 1,2,4-butanetriol using (S)-(+)-α-methoxy-α-(trifluoromethyl) phenylacetyl chloride followed the same procedure described in previous section. The Mosher esters of 1,2,4-butanetriol were analyzed using an Agilent 1100 HPLC equipped with a Chiralpak AD-H column (Daicel Chemical, 4.6 mm x 250 mm), which had been equilibrated with hexane/2-propanol (90:10, v/v). The column was eluted with a linear gradient of 2-propanol (10%-2% in hexane) over 15 min at a rate of 1.25 mL/min, while the eluant was monitored at 260 nm. The retention time of D- and L-1,2,4-butanetriol Mosher ester was, respectively, 6.3 min and 4.7 min. Mixtures of authentic D- and L-1,2,4-butanetriol in varied weight ratio were derivatized using Mosher's reagent and further analyzed by HPLC. A calibration curve was generated by plotting the peak area ratio of D- and L-1,2,4-butanetriol Mosher esters against the weight ratio of D- and L-1,2,4-butanetriol in above mixed authentic samples.

REFERENCES

- ¹ Pannuri, S.; DiSanto, R.; Kamat, S. In Kirk-Othmer Encyclopedia of Chemical Technology Online; Biocatalysis, 2003, Wiley.
- ² Ball, P.; Ziemelis, K.; Allen, L. *Nature*, **2001**, 409, 225.
- ³ Nielsen, P. H.; Malmos, H.; Damhus, T.; Diderichsen, B.; Nielsen. H. K.; Simonsen, M.; Schiff, H. E.; Oestergaard, A.; Olsen, H. S.; Eigtved, P.; Nielsen, T. K. In *Kirk-Othmer Encyclopedia of Chemical Technology Online*; Enzyme Application, Industrial, 1994, Wiley.
- ⁴ Strohl, W. R. In *Biotechnology of Antibiotics*, 2nd ed.; Strohl W. R., Ed; Marcel Dekker, Inc.: NY, 1997.
- ⁵ (a) Asano, Y.; Tani, Y.; Yamada, H. Agricultural Biol. Chem. 1980, 44, 2251. (b) Yamada, H. In New Frontiers in Screening for Microbial Biocatalysts; Kieslich, K., van de Beek, C. P., de Bont, J. A. M., van den Tweel, W. J. J., Eds.; Elsevier: Amsterdam, 1998. (c) Kobayashi, M.; Shimizu, S. Curr. Opin. Chem. Biol. 2000, 4, 95.
- ⁶ (a) Draths, K. M.; Knop, D. R.; Frost, J. W. J. Am. Chem. Soc. 1999, 121, 1603. (b) Frost, J. W.; Frost, K. M.; Knop, D. R. WO 2000044923 A1 20000803. (c) Knop, D. R.; Draths, K. M.; Chandran, S. S.; Barker, J. L.; von Daeniken, R.; Weber, W.; Frost, J. W. J. Am. Chem. Soc. 2001, 123, 10173. (d) Chandran, S. S.; Yi, J.; Draths, K. M.; von Daeniken, R.; Weber, W.; Frost J. W. Biotech. Prog. 2003, 19, 808.
- ⁷ Bar, A. In *Alternative Sweeteners*, 2nd ed.; Nabors, L. O., Gelardi, R. C. Ed.; Marcel Dekker, Inc.: NY, 1991; p358.
- ⁸ Thomas, S. M.; DiCosimo, R.; Nagarajan, V. Trends Biotechnol. 2002, 20, 238.
- ⁹ (a) Louwrier, A. Biotechnol. Appl. Biochem. 1998, 27, 1. (b) Aristidou, A.; Penttila, M. Curr. Opin. Biotechnol. 2000, 11, 187.
- ¹⁰ Niu, W.; Draths, K. M.; Frost, J. W. Biotechnol. Prog. **2002**, 18, 201.
- ¹¹ Niu, W.; Molefe, M. N.; Frost, J. W. J. Am. Chem. Soc. 2003, 125, 12998.
- ¹² (a) Haslam, E. *The Shikimate Pathway*; Wiley: New York, 1974. (b) Pittard, A. J. In *Escherichia coli and Salmonella: Cellular and Molecular Biology*, 2nd ed.; Neidhardt, F. C., Ed.; ASM Press: Washington, DC, 1996; p458. (c) Herrmann, K. M. *Plant Cell* **1995**, 7, 907. (d) Herrmann, K. M.; Weaver, L. M. *Annu. Rev. Plant Physiol. Plant Mol. Biol.* **1999**, 50, 473.

- ¹⁴ (a) Dewick, P. M. Nat. Prod. Rep. 1998, 15, 17. (b) Knaggs, A. R. Nat. Prod. Rep. 2003, 20, 119.
- ¹⁵ Herrmann, K. M. In *Amino Acids: Biosynthesis and Genetic Regulation*; Herrmann, K. M., Somerville, R. L., Eds.; Addison-Wesley: Reading, 1983: p301.
- ¹⁶ Blattner, F. R.; Plunkett, G. III; Bloch, C. A.; Perna, N. T.; Burland, V.; Riley, M.; Collado-Vides, J.; Glasner, J. D.; Rode, C. K.; Mayhew, G. F.; Gregor, J.; Davis, N. W.; Kirkpatrick, H. A.; Goeden, M. A.; Rose, D. J.; Mau, B.; Shao, Y. *Science* **1997**, 277, 1453.
- ¹⁷ (a) McCandliss, R. J.; Herrmann, K. M. *Proc. Natl. Acad. Sci. USA* **1978**, 75, 4810. (b) Stephens, C. M.; Bauerle, R. *J. Biol. Chem.* **1991**, 266, 20810.
- ¹⁸ Carpenter, E. P.; Hawkins, A. R.; Frost, J. W.; Brown, K. A. *Nature* **1998**, *394*, 299.
- ¹⁹ (a) Turner, M. J.; Smith, B. W.; Haslam, E. J. Chem. Soc., Perkin Trans. 1 1975, 1, 52. (b) Gourley, D. G.; Shrive, A. K.; Polikarpov, I.; Krell, T.; Coggins, J. R.; Hawkins, A. R.; Isaacs, N. W.; Sawyer, L. Nat. Struct. Biol. 1999, 6, 521.
- ²⁰ (a) Anton, I. A.; Coggins, J. R. *Biochem. J.* **1988**, 249, 319. (b) Michel, G.; Roszak, A. W.; Sauve, V.; Maclean, J.; Matte A.; Coggins, J. R.; Cygler, M.; Lapthorn, A. J. J. *Biol. Chem.* **2003**, 278, 19463. (c) Vogan, E. *Structure* **2003**, 11, 902.
- ²¹ (a) DeFeyter, R. C.; Pittard, J. J. Bacteriol. **1986**, 165, 226. (b) DeFeyter, R. C.; Pittard, J. J. Bacteriol. **1986**, 165, 331. (c) DeFeyter, R. C.; Pittard, J. J. Bacteriol. **1986**, 165, 233. (d) Løbner-Olesen, A.; Marinus, M. G. J. Bacteriol. **1992**, 174, 525.

- ²³ Duncan, K.; Coggins, J. R. *Biochem. J.* **1986**, 234, 49. (b) Duncan, K.; Lewendon, A.; Coggins. J. R. *FEBS Lett.* **1984**, 165, 121. (c) Schonbrunn, E.; Eschenburg, S.; Shuttleworth, W. A.; Schloss, J. V.; Amrhein, N.; Evans, J. N. S.; Kabsch, W. *Proc. Natl. Acad. Sci. USA* **2001**, 98, 1376.
- ²⁴ White, P. J.; Millar, G.; Coggins, J. R. Biochem. J. 1988, 251, 313.
- ²⁵ (a) Macheroux, P.; Schmid, J.; Amrhein, N.; Schaller, A. *Planta* **1999**, 207, 325. (b) Maclean, J.; Ali, S. *Structure* **2003**, *11*, 1499. (c) Quevillin-Cheruel, S.; Leulliot, N.; Meyer, P.; Graille, M.; Bremang, M.; Blondeau, K.; Sorel, I.; Poupon, A.; Janin, J.; van Tilbeurgh, H. *J. Biol. Chem.* **2004**, 279, 619.

²² Heatwole, V. M.; Somerville, R. L. J. Bacteriol. **1992**, 174, 331.

- ²⁶ Coggins, J. R.; Abell, C.; Evans, L. B.; Frederickson, M.; Robinson, D. A.; Roszak, A. W.; Lapthorn, A. P. *Biochem. Soc. Trans.* **2003**, *31*, 548.
- ²⁷ (a) Franz, J. E.; Mao, M. K.; Sikorski, J. A. In *Glyphosate: A Unique*, *Global Herbicide*; American Chemical Society Monograph, Washington, DC, 1996. (b) Sikorski, J. A.; Gruys, K. J. Acc. Chem. Res. 1997, 30, 2.
- ²⁸ Sweeney, W. A.; Bryan, P. F. In Kirk-Othmer Encyclopedia of Chemical Technology Online; BTX Processing, 1992, Wiley.
- ²⁹ Eggeling, L.; Sahm, H. In *Metabolic Engineering*; Lee, Y. S., Papoutsakis, E. T., Eds.; Marcel Dekker, Inc.:N.Y., 1999; p155.
- ³⁰ Araki, K.; Ozeki, T. In Kirk-Othmer Encyclopedia of Chemical Technology Online; Amino Acids, 2003, Wiley.
- ³¹ Oyama, K. In *Chirality in Industry*; Collins, A. N., Sheldrake, G. N., Crosby, J., Eds.; Wiley: UK, 1992: p237.
- ³² Murdock, D.; Ensley, B. D.; Serdar, C.; Thalen, M. Biotechnology 1993, 11, 381.
- ³³ (a) Hanessian, S.; Beaulieu, P.; Dube, D. *Tetrahedron Lett.* **1986**, 27, 2332. (b) Flack, J. R.; Yadagiri, P. J. Org. Chem. **1989**, 54, 5851. (c) Molin, H.; Pring, B. G. *Tetrahedron Lett.* **1985**, 26, 677. (d) Montchamp, J.-L.; Piehler, L. T.; Frost, J. W. J. Am. Chem. Soc. **1992**, 114, 4453. (e) Widlanski, T.; Bender, S. L.; Knowles, J. R. J. Am. Chem. Soc. **1989**, 111, 2299.
- ³⁴ Ran, N.; Knop, D. R.; Draths, K. M.; Frost, J. W. J. Am. Chem. Soc. 2001, 123, 10927.
- ³⁵ Krumenacker, L.; Costantini, M.; Potal, P.; Sentenac, J. In *Kirk-Othmer Encyclopedia of Chemical Technology Online*; Hydroquinone, Resorcinol, and Catechol, 1995, Wiley.
- ³⁶ Richman, J. E.; Chang. Y.-C.; Kambourakis, S.; Draths, K. M.; Almy, E.; Snell, K. D.; Strasburg, G. M.; Frost, J. W. J. Am. Chem. Soc. **1996**, 118, 11587.
- ³⁷ (a) Kambourakis, S.; Draths, K. M.; Frost, J. W. J. Am. Chem. Soc. **2000**, 122, 9042. (b) Kambourakis, S.; Frost, J. W. J. Org. Chem. **2000**, 65, 6904.
- ³⁸ (a) Barker J. L.; Frost, J. W. *Biotechnol. Bioeng.* **2001**, *76*, 376. (b) Amaratunga, M.; Lobos, J. H.; Johnson, B. F.; Williams, D. U.S. Patent 6,030,819, 2000.
- ³⁹ Draths, K. M.; Frost, J. W. J. Am. Chem. Soc. 1995, 117, 2395.
- ⁴⁰ Li, K.; Frost, J. W. J. Am. Chem. Soc. 1998, 120, 10545.

- ⁴¹ (a) Rao, S. R.; Ravishankar, G. A. J. Sci. Food Agric. **2000**, 80, 289. (b) Priefert, H.; Rabenhorst, J.; Steinbuchel, A. Appl. Microbiol. Biotechnol. **2001**, 56, 296.
- ⁴² (a) Aiba, S.; Tsunekawa, H.; Imanaka, T. *Appl. Environ. Microbiol.* **1982**, *43*, 289. (b) Tsunekawa, H.; Imanaka, T.; Aiba, S. *J. Gen. Microbiol.* **1980**, *118*, 253.
- ⁴³ (a) Weaver, L. M.; Herrmann, K. M. J. Bacteriol. **1990**, 172, 6581. (b) Draths, K. M.; Pompliano, D. L.; Conley, D. L.; Frost, J. W.; Berry, A.; Disbrow, G. L.; Staversky, R. J.; Lievense, J. C. J. Am. Chem. Soc. **1992**, 114, 3956. (c) Ray, J. M.; Yanofsky, C.; Bauerle, R. J. Bacteriol. **1988**, 170, 5500.
- ⁴⁴ Venkat, K.; Backman, K.; Hatch, R. T. Food Biotechnol. 1990, 4, 547.
- ⁴⁵ Li, K.; Mikola, M. R.; Draths, K. M.; Worden, R. M.; Frost, J. W. *Biotechnol. Bioeng.* **1999**, *64*, 61.
- ⁴⁶ (a) Draths, K. M.; Frost, J. W. J. Am. Chem. Soc. **1990**, 112, 1657. (b) Frost, J. W. U.S. Patent 5,168,056, 1992.
- ⁴⁷ Lu, J.; Liao, J. C. Biotechnol Bioeng. 1997, 53, 132.
- ⁴⁸ (a) Miller, J. E.; Backman, K. C.; O'Connor, M. J.; Hatch, R. T. J. Ind. Microbiol. **1987**, 2, 143. (b) Gosset, G.; Yong-Xiao, J.; Berry, A. J. Ind. Microbiol. **1996**, 17, 47.
- ⁴⁹ (a) Patnaik, R.; Liao, J. C. Appl. Environ. Microbiol. **1994**, 60, 3903. (b) Patnaik, R.; Spitzer, R. G.; Liao, J. C. Biotechnol. Bioeng. **1995**, 46, 361.
- ⁵⁰ Yi, J.; Li, K.; Draths, K. M.; Frost, J. W. Biotechnol. Prog. **2002**, 18, 1141.
- ⁵¹ Snoep, J. L.; Arfman, N.; Yomano, L. P.; Fliege, R. K.; Conway, T.; Ingram, L. O. J. Bacteriol. **1994**, 176, 2133.
- ⁵² Flores, N.; Xiao, J.; Berry, A.; Bolivar, F.; Valle, F. Nature Biotechnol. 1996, 14, 620.
- ⁵³ Yi, J.; Draths, K. M.; Li, K.; Frost, J. W. Biotechnol. Prog. 2003, 19, 1450.
- ⁵⁴ (a) Patnaik, R.; Spitzer, R. G.; Liao, J. C. *Biotechnol. Bioeng.* **1995**, 46, 361. (b) Li, K.; Frost, J. W. *Biotechnol. Prog.* **1999**, 15, 876.
- 55 (a) Madison, L. L.; Huisman, G. W. Microbiol. Mol. Biol. Rev. 1999, 63, 21. (b) Tan, I. K. P. In Kirk-Othmer Encyclopedia of Chemical Technology Online; Polyhydroxyalkanoates, 2003, Wiley.

- ⁵⁶ (a) Schmid, A.; Dordick, J. S.; Hauer, B.; Kiener, A.; Wubbolts, M.; Witholt, B. *Nature* **2001**, 409, 258. (b) Schoemaker, H. E.; Mink, D.; Wubbolts, M. G. *Science* **2003**, 299, 1694.
- ⁵⁷ (a) Schmidt-Dannert, C. *Biochemistry* **2001**, 40, 13126. (b) Arnold, F. H. *Nature* **2001**, 409, 253.
- ⁵⁸ Bolon, D. N.; Voigt, C. A.; Mayo, S. L. Curr. Opin. Chem. Biol. 2002, 6, 125.
- ⁵⁹ Johnson, E. A.; Schroeder, W. Adv. Biochem. Eng. 1995, 53, 119.
- ⁶⁰ (a) Edge, R.; McGarvey, D. J.; Truscott, T. G. J. Photochem. Photobiol. **1997**, 41, 189. (b) Singh, D. K.; Lippman, S. M. Oncology NY **1998**, 12, 1643.
- ⁶¹ (a) Wang, C. W.; Liao, J. C. *Biotechnol. Bioeng.* **1999**, 62, 235. (b) Albrecht, M.; Takaichi, S.; Steiger, S.; Wang, Z. Y.; Sandmann, G. *Nat. Biotechnol.* **2000**, 18, 843. (c) Sandmann, G. *ChemBioChem* **2002**, 3, 629. (d) Lee, P. C.; Schmidt-Dannert, C. *Appl. Microbiol. Biotechnol.* **2002**, 60, 1.
- ⁶² Schmidt, C.; Umeno, D.; Arnold, F. H. Nature Biotechnol. 2000, 18, 750.
- ⁶³ Whistler, R. L.; Daniel, J. R. In Kirk-Othmer Encyclopedia of Chemical Technology Online; Starch, 1997, Wiley.
- ⁶⁴ (a) Patnaik, R.; Liao, J. C. Appl. Environ. Microbiol. **1994**, 60, 3903. (b) Patnaik, R.; Spitzer, R. G.; Liao, J. C. Biotechnol. Bioeng. **1995**, 46, 361. (c) Li, K.; Mikola, M.; Draths, K. M.; Worden, R. M.; Frost, J. W. Biotechnol. Bioeng. **1999**, 64, 61.
- ⁶⁵ Postma, P. W.; Lengeler, J. W.; Jacobson, G. R. In *Escherichia coli and Salmonella: Cellular and Molecular Biology*, 2nd ed.; Neidhardt, F. C., Ed.; ASM Press: Washington, DC, 1996; p1149-1174.
- ⁶⁶ Lin E. C. C. In *Escherichia coli and Salmonella: Cellular and Molecular Biology*, 2nd ed.; Neidhardt, F. C., Ed.; ASM Press: Washington, DC, 1996; p307-342.
- ⁶⁷ Thompson, N. S. In Kirk-Othmer Encyclopedia of Chemical Technology Online; Hemicellulose, 1995, Wiley.
- 68 Li, K.; Frost, J. W. Biotechnol. Prog. 1999, 15, 876.
- ⁶⁹ Moniruzzaman, M.; Dien, B. S.; Ferrer, B.; Hespell, R. B.; Dale, B. E.; Ingram, L. O.; Bothast, R. J. *Biotechnol. Lett.* **1996**, *18*, 985.
- ⁷⁰ Havashi, S.-I.: Lin, E. C. C. J. Biol. Chem. **1967**, 242, 1030.

- ⁷¹ (a) Weiner, J. H.; Heppel, L. A. *Biochem. Biophys. Res. Commun.* **1972**, 47, 136. (b) Schryvers, A.; Lohmeier, E.; Weiner, J. H. *J. Biol. Chem.* **1978**, 253, 783.
- ⁷² (a) Yi, J.; Li, K.; Draths, K. M.; Frost, J. W. *Biotechnol. Prog.* **2002**, *18*, 1141. (b) Yi, J.; Draths, K. M.; Li, K.; Frost, J. W. *Biotechnol. Prog.* **2003**, *19*, 1450.
- ⁷³ (a) Hwang, S. O.; Gil, G. H.; Cho, Y. J.; Kang, K. R.; Lee, J. H.; Bae, J. C. Appl. Microbiol. Biotechnol. 1985, 22, 108. (b) Aiba, S.; Tsunekawa, H.; Imanaka, T. Genet. Ind. Microorg., Proc. Int. Symp., 4th 1983, 183. (c) Gibson, J. M.; Thomas, P. S.; Thomas, J. D.; Barker, J. L.; Chandran, S. S.; Harrup, M. K.; Draths, K. M.; Frost, J. W. Angew. Chem., Int. Ed. 2001, 40, 1945.
- ⁷⁴ (a) Koch, J. P.; Hayashi, S.-I.; Lin, E. C. C. J. Biol. Chem. **1964**, 239, 3106. (b) Schweizer, H.; Boos, W.; Larson, T. J. J. Bacteriol. **1985**, 116, 563.
- ⁷⁵ Zwaig, N; Kistler, W. S.; Lin, E. C. C. J. Bacteriol. **1970**, 102, 753.
- ⁷⁶ (a) Berman, M.; Lin, E. C. C. *J. Bacteriol.* **1971**, *105*, 113. (b) Zwaig, N.; Lin. E. C. C. *Science*, **1966**, *153*, 755. (c) Liu, Z. W.; Faber, R.; Feese, M.; Remington, S. J.; Pettigrew, D. W. *Biochemistry* **1994**, *33*, 10120.
- ⁷⁷ Morrison, L. R. In Kirk-Othmer Encyclopedia of Chemical Technology Online; Glycerol, 1994, Wiley.
- ⁷⁸ Biebl, H.; Zeng, A.-P.; Menzel, K.; Deckwer, W.-D. Appl. Microbiol. Biotechnol. **1998**, 50, 24.
- ⁷⁹ Lee, P. C.; Lee, W. G.; Lee, S. Y.; Chang, H. N. Biotechnol. Bioeng. 2001, 72, 41.
- ⁸⁰ Pittard, J.; Wallace, B. J. J. Bacteriol. 1966, 91, 1494.
- 81 Draths, K. M.; Frost, J. W. J. Am. Chem. Soc. 1990, 112, 9630.
- ⁸² (a) Snell, K. D.; Frost, J. W. J. Am. Chem. Soc. **1993**, 115, 11581. (b) Snell, K. D.; Draths, K. M.; Frost, J. W. J. Am. Chem. Soc. **1996**, 118, 5605.
- 83 Weaver, L. M.; Herrmann, K. M. J. Bacteriol. 1990, 172, 6581.
- ⁸⁴ Mikola, M. R.; Widman, M. T.; Worden, R. M. Appl. Biochem. Biotechnol. 1998, 70, 905.
- 85 Cobbett, C. S.; Delbridge, M. L. J. Bacteriol. 1987, 169, 2500.
- 86 Bartolome, B.; Jubete, Y.; Martinez, E.; de la Cruz, F. Gene 1991, 102, 75.

- ⁸⁷ (a) Lowry, O. H.; Carter, J.; Ward, J. B.; Glaser, L. J. Biol. Chem. **1971**, 246, 6511. (b) Lin, E. C. C. Ann. Rev. Microbiol. **1976**, 30, 535.
- 88 Sprenger, G. A. Biochim. Biophys. Acta 1993, 1216, 307.
- ⁸⁹ Fraenkel, D. G. In *Escherichia coli and Salmonella: Cellular and Molecular Biology*, 2nd ed.; Neidhardt, F. C., Ed.; ASM Press: Washington, DC, 1996; p189-199.
- ⁹⁰ (a) Draths, K. M.; Frost, J. W. J. Am. Chem. Soc. **1990**, 112, 1657. (b) Draths, K. M.; Pompliano, D. L.; Conley, D. L.; Frost, J. W.; Berry, A.; Disbrow, G. L.; Staversky, R. J.; Lievense, J. J. Am. Chem. Soc. **1992**, 114, 3956.
- 91 Thorner, J. W.; Paulus, H. J. Biol. Chem. 1973, 248, 3922.
- ⁹² Pettigrew, S. W.; Liu, W. Z.; Holmes, C.; Meadow, N. D.; Roseman, S. *J. Bacteriol*. **1996**, *178*, 2846.
- 93 Freedberg, W. B.; Kistler, W. S.; Lin, E. C. C. J. Bacteriol. 1971, 108, 137.
- 94 Paisley, M. A. In Kirk-Othmer Encyclopedia of Chemical Technology Online; Biomass Energy, 2003, Wiley.
- 95 (a) Flores, N.; Xiao, J.; Berry, A.; Bolivar, F.; Valle, F. Nat. Biotechnol. 1996, 14, 620.
 (b) Chen, R.; Yap, W. M. G. J.; Postma, P. W.; Bailey, J. E. Biotechno. Bioeng. 1997, 56, 583.
- 96 Holms, H. FEMS Microbiol. Rev. 1996, 19, 85.
- ⁹⁷ Oppenheim, J. P.; Dickerson, G. L. In Kirk-Othmer Encyclopedia of Chemical Technology Online; Adipic Acid, 2003, Wiley.
- 98 Dickinson, R. E.; Cicerone, R. J. Nature 1986, 319, 109.
- 99 Thiemens, M. H.; Trogler, W. C. Science 1991, 251, 932.
- ¹⁰⁰ (a) Uriarte, A. K.; Rodkin, M. A.; Gross, M. J.; Kharitonov, A. S.; Panov, G. I. Studies in Surface Science and Catalysis 1997, 110, 857. (b) Panov, G. I.; Sheveleva, G. A.; Kharitonov, A. S; Romannikov, V. N.; Vostrikova, L. A. Appl. Catal. 1992, 82, 31.
- ¹⁰¹ (a) Sato, K.; Aoki, M.; Noyori, R. *Science* **1998**, 281, 1646. (b) Deng, Y.; Ma, Z.; Wang, K.; Chen, J. *Green Chem.* **1999**, 1, 275. (c) Besson, M.; Blackburn, A.; Gallezot, P.; Kozynchenko, O.; Pigamo, A.; Tennison, S. *Top. Catal.* **2000**, 13, 253. (d) Raja, R.; Sankar, G.; Thomas, J. M. *Angew. Chem. Int. Ed.* **2000**, 39, 2313.

- ¹⁰² Cheng, Q.; Thomas, S. M.; Kostichka, K.; Valentine, J. R.; Nagarajan, V. J. Bacteriol. **2000**, 182, 4744.
- ¹⁰³ Sweeney, W. A.; Bryan, P. F. In Kirk-Othmer Encyclopedia of Chemical Technology Online; BTX Processing, 1992, Wiley.
- ¹⁰⁴ Lewis, R. J. Carcinogenically Active Chemicals; Van Nostrand Reinhold: New York, 1991; p68.
- ¹⁰⁵ O'Connor, S. R.; Farmer, P. B.; Lauder, I. J. Pathol. 1999, 189, 448.
- ¹⁰⁶ Draths, K. M.; Frost, J. W. J. Am. Chem. Soc. 1994, 116, 399.
- ¹⁰⁷ Li, K.; Frost, J. W. J. Am. Chem. Soc. 1998, 120, 10545.
- ¹⁰⁸ Pittard, J.; Wallace, B. J. J. Bacteriol. **1966**, 91, 1494.
- ¹⁰⁹ Draths, K. M.: Frost, J. W. J. Am. Chem. Soc. **1995**, 117, 2395.
- ¹¹⁰ Snell, K. D.; Draths, K. M.; Frost, J. W. J. Am. Chem. Soc. 1996, 118, 5605.
- ¹¹¹ (a) Li, K.; Mikola, M. R.; Draths, K. M.; Worden, R. M.; Frost, J. W. *Biotechnol. Bioeng.* **1999**, *64*, 61. (b) Draths, K. M.; Knop, D. R.; Frost, J. W. *J. Am. Chem. Soc.* **1999**, *121*, 1603.
- ¹¹² Draths, K. M.; Pompliano, D. L.; Conley, D. L.; Frost, J. W.; Berry, A.; Disbrow, G. L.; Staversky, R. J.; Lievense, J. C. *J. Am. Chem. Soc.* **1992**, *114*, 3956.
- ¹¹³ Li, K. Ph.D. Thesis, Michigan State University, 2000.
- ¹¹⁴ (a) Court, D. L.; Sawitzke, J. A.; Thomason, L. C. Annu. Rev. Genet. **2002**, 36, 361. (b) Hanin, M.; Paszkowaki, J. Curr. Opin. Plant Biol. **2003**, 6, 157.
- ¹¹⁵ (a) Hamilton, C. M.; Akdea, M.; Washburn, B. K.; Babitzke, P.; Kushner, S. R. J. Bacteriol. **1989**, 171, 4617; (b) Ohta, K.; Beall, D. S.; Mejia, J. P.; Shanmugam, K. T.; Ingram, L. O. Appl. Environ. Microbiol. **1991**, 57, 893.
- ¹¹⁶ (a) Garner, C. C.; Herrmann, K. M. *J. Biol. Chem.* **1985**, 260, 3820. (b) Cobbett, C. S.; Delbridge, M. L. *J. Bacteriol.* **1987**, 169, 2500.
- ¹¹⁷ Patel, J. C.; Grant, D. J. W. Antonie van Leeuwenhoek 1969, 35, 53.
- ¹¹⁸ (a) Neidle, E. L.; Ornston, L. N. J. Bacteriol. **1986**, 168, 815. (b) Hayaishi, O.; Katagiri, M.; Rothberg, S. **1957**, 229, 905.

- ¹¹⁹ Furste, J. P.; Pansegrau, W.; Frank, R.; Blocker, H.; Scholz, P.; Bagdasarian, M.; Lanka, E. Gene 1986, 48, 119.
- ¹²⁰ Bartolome, B.; Jubete, Y.; Martinez, E.; de la Cruz, F. Gene 1991, 102, 75.
- ¹²¹ Knop, D. R. Ph.D. Thesis, Michigan State University, 2001.
- ¹²² Neidle, E. L.; Hartnett, C.; Bonitz, S.; Ornston, L. N. J. Bacteriol. 1988, 170, 4874.
- ¹²³ Frost, J. W.; Lievense, J. New J. Chem. **1994**, 18, 341.
- ¹²⁴ Chemical Market Reporter, **2001**, 259 (22).
- ¹²⁵ (a) Patnaik, R.; Liao, J. C. Appl. Environ. Microbiol. **1994**, 60, 3903. (b) Patnaik, R.; Spitzer, R. G.; Liao, J. C. Biotechnol. Bioeng. **1995**, 46, 361. (c) Yi, J.; Li, K.; Draths, K. M.; Frost, J. W. Biotechnol. Prog. **2002**, 18, 1141.
- ¹²⁶ (a) Yi, J.; Draths, K. M.; Li, K.; Frost, J. W. *Biotechnol. Prog.* **2003**, *19*, 1450. (b) Flores, N.; Xiao, J.; Berry, A.; Bolivar, F.; Valle, F. *Nature Biotechnol.* **1996**, *14*, 620.
- ¹²⁷ Campbell, C. J.; Laherrere, J. H. Sci. Am. 1998, 278, 78.
- ¹²⁸ Lindner, V. In Kirk-Othmer Encyclopedia of Chemical Technology Online; Explosives, 1994, Wiley.
- ¹²⁹ CPIA/M3 Solid Propellant Ingredients Manual; The Johns Hopkins University, Chemical Propulsion Information Agency: Whiting School of Engineering, Columbia, MD, 2000.
- (a) Monteith, M. J.; Schofield, D.; Bailey, M. Int. Patent Appl. WO 98/08793, 1998.
 (b) Ikai, K.; Amagasake-shi, H. EU Patent Appl. EP 1,061,060 A1, 1999.
- ¹³¹ Adkins, H.; Billica, H. R. J. Am. Chem. Soc. 1948, 70, 3121.
- ¹³² (a) Folkers, K.; Adkins, H. J. Am. Chem. Soc. **1932**, 54, 1145. (b) Trenner, N. R.; Bacher, F. A. J. Am. Chem. Soc. **1949**, 71, 2352. (c) Zhang, Z.; Jackson, J. E.; Miller, D. J. Appl. Cat. A **2001**, 219, 89.
- ¹³³ Molefe, M. N.; Frost, J. W. Unpublished results.
- ¹³⁴ Blair, G. T.; DeFraties, J. J. In Kirk-Othmer Encyclopedia of Chemical Technology Online; Hydroxy Dicarboxylic Acids, 1995, Wiley.
- ¹³⁵ Molefe, M. N.; Niu, W.; Frost, J. W. Unpublished results.

- ¹³⁶ (a) Weimberg, R. J. Biol. Chem. **1961**, 236, 629. (b) Weimberg, R. J. Biol. Chem. **1959**, 234, 727.
- ¹³⁷ Thompson, N. S. In Kirk-Othmer Encyclopedia of Chemical Technology Online; Hemicellulose, 1995, Wiley.
- ¹³⁸ (a) Ho, N. W.; Chen, Z.; Brainard, A. P. Appl. Environ. Microbiol. **1998**, 64, 1852. (b) Silva, S. S.; Felipe, M. G.; Mancilha, I. M. Appl. Biochem. Biotechnol. **1998**, 72, 331. (c) Fond, O.; Engasser, J. M.; Matta-El-Amouri, G.; Petitdemange, H. Biotechnol. Bioeng. **1986**, 26, 160.
- ¹³⁹ (a) Buchert, J.; Viikari, L.; Linko, M.; Markkanen, P. *Biotechol. Lett.* **1986**, 8, 541. (b) Buchert, J.; Puls, J.; Poutanen, K. *Appl. Microbiol. Biotechnol.* **1988**, 28, 367.
- ¹⁴⁰ (a) Schimz, K. L.; Kurz, G. Hoppe-Seyler's Z. Physiol. Chem. **1973**, 354, 1238. (b) Schimz, K. L.; Kurz, G. Biochem. Soc. Trans. **1975**, 3, 1087.
- ¹⁴¹ Dahms, A. S.; Anderson, R. L. J. Biol. Chem. 1972, 247, 2228.
- 142 (a) Lysenko, O. J. Gen. Microbiol. 1961, 25, 379. (b) De Vos, P.; Van Landschoot, A.; Segers, P.; Tytgat, R.; Gillis, M.; Bauwens, M.; Rossau, R.; Goor, M.; Pot, B.; Kersters, K.; Lizzaraga, P.; De Ley, J. Int. J. Sys. Bacteriol. 1989, 39, 35. (c) Tarrant, P. J. V.; Pearson, A. M.; Price, J. F.; Lechowich, R. V. Appl. Microbiol. 1971, 22, 224. (d) Gillespie, N. C. J. Appl. Bacteriol. 1981, 50, 29. (e) Alanis, E.; Lara, P.; Guerrero I. Food Chem. 1999, 67, 45.
- ¹⁴³ Dahms, S. A.; Donald, A. Methods in Enzymol. 1982, 90, 302.
- ¹⁴⁴ Dahms, S. A. Biochem. Biophys. Res. Commun. 1974, 60, 1433.
- ¹⁴⁵ Anderson, R. L.; Dahms, S. A. Methods in Enzymol. 1975, 42C, 305.
- ¹⁴⁶ Stoolmiller A. C. Methods in Enzymol. 1975, 41, 101.
- ¹⁴⁷ Borjesson, L; Welch, C. J. Tetrahedron 1992, 48, 6325.
- ¹⁴⁸ Mori, K.; Takigawa, T.; Matsuo, T. Tetrahedron 1978, 35, 933.
- ¹⁴⁹ Andre, C.; Bolte, J.; Demuynck, C. Tetrahedron Asymmetry 1998, 9, 1359.
- ¹⁵⁰ Synder, J.; Serianni, A. S. Carbohydr. Res. 1991, 210, 21.
- ¹⁵¹ Reid, M. F.; Fewson, C. A. Crit. Rev. Microbiol. 1994, 20, 13.

- 152 (a) Keshav, K. F.; Yomano, L. P.; An, H. J.; Ingram, L. O. J. Bacteriol. 1990, 172, 2491. (b) Conway, T.; Sewell, G. W.; Osman, Y. A.; Ingram, L. O. J. Bacteriol. 1987, 169, 2591.
- ¹⁵³ (a) Tong, I. T.; Liao, H. H.; Cameron, D. C. Appl. Environ. Microbiol. **1991**, *57*, 3541. (b) Johnson, E. A.; Lin, E. C. C. J. Bacteriol. **1987**, *169*, 2050.
- 154 (a) Raj, K. C.; Ingram, L. O.; Maupin-Furlow, J. A. Arch. Microbiol. 2001, 176, 443.
 (b) Raj, K. C.; Talarico, L. A.; Ingram, L. O.; Maupin-Furlow, J. A. Appl. Environ. Microbiol. 2002, 68, 2869. (c) Conway, T.; Osman, Y. A.; Konnan, J. I.; Hoffmann, E. M.; Ingram, L. O. J. Bacteriol. 1987, 169, 949.
- ¹⁵⁵ Tsou, A. Y.; Ransom, S. C.; Gerlt, J. A.; Buechter, D. D.; Babbitt, P. C.; Kenyon, G. L. *Biochemistry* **1990**, *29*, 9856.
- ¹⁵⁶ Brandl, M. T.; Lindow, S. E. Appl. Environ. Microbiol. 1996, 62, 4121.
- ¹⁵⁷ Chen, K.; Arnold, F. H. Proc. Nat. Acad. Sci. USA 1993, 93, 5618.
- ¹⁵⁸ (a) Powell, K. A.; Ramer, S. W.; Cardayre, S. B.; Stemmer, W. P. C.; Tobin, M. B.; Longchamp, P. F.; Huisman, G. W. *Angew. Chem. Int. Ed.* **2002**, *40*, 3948. (b) Schmidt-Dannert, C. *Biochemistry* **2001**, *40*, 13125. (c) Tao, H.; Cornish, V. W. *Curr. Opin. Chem. Biol.* **2002**, *6*, 858.
- ¹⁵⁹ Arnold, F. H.; Wintrode, P. L.; Miyazaki, K.; Gershenson, A. *Trends Biochem. Sci.* **2001**, 26, 100.
- ¹⁶⁰ (a) Cadwell, R. C.; Joyce, G. F. *PCR Method. Appl.* **1992**, 2, 28. (b) Leung, D. W.; Chen, E.; Goeddel, D. V. *Technique* **1989**, *1*, 11.
- ¹⁶¹ (a) Stemmer, W. P. C. *Nature* **1994**, *370*, 389. (b) Stemmer, W. P. C. *Proc. Natl. Acad. Sci. USA* **1994**, *91*, 10747.
- ¹⁶² Zhao, H.; Giver, L.; Shao, Z.; Affholter, J. A.; Arnold, F. H. Nature Biotechnol. 1998, 16, 258.
- ¹⁶³ (a) Hasson, M. S.; Muscate, A.; McLeish, M. J.; Polovnikova, L. S.; Gerlt, J. A.; Kenyon, G. L.; Petsko, G. A.; Ringe, D. *Biochemistry* **1998**, *37*, 9918. (b) Polovnilova, E. S.; McLeish, M. J.; Sergieko, E. A.; Burgner, J. T.; Anderson, N. L.; Bera, A. K.; Jordan, F.; Kenyon, G. L.; Hasson, M. *Biochemistry* **2003**, *42*, 1820.
- ¹⁶⁴ Zhao, H.; Moore, J. C.; Volkov, A. A.; Arnold, F. H. In *Manual of Industrial Microbiology and Biotechnology*; Demain, A. L., Davis, J. E., Eds; ASM Press: Washington, DC, 1999; p597-604.

- ¹⁶⁵ (a) Lorimer, I. A. J.; Pastan, I. Nucleic Acids Res. 1995, 23, 3067. (b) Zhao, H.; Arnold, F. H. Nucleic Acids Res. 1997, 25, 1307.
- (a) Cohen, N.; Abramov, S.; Dror, Y.; Freeman, A. Trend. Biotechnol. 2001, 19, 507.
 (b) Olsen, M.; Iverson, B.; Georgiou, G. Curr. Opion. Biotechnol. 2000, 11, 331.
- ¹⁶⁷ Kiernan, J. A. *Histological and histochemical methods: Theory and practice* 3rd ed.; Butterworth Heinemann: Oxford, UK, 1999.
- ¹⁶⁸ Siegert, P.; Pohl, M.; Kneen, M. M.; Pogozheva, I. D.; Kenyon, G. L.; McLeish, M. J. Oxidative Stress and Disease 2004, 11, 275.
- 169 (a) Oue, S.; Okamoto, A.; Yano, T.; Kagamiyana, H. J. Biol. Chem. 1999, 274, 2344.
 (b) Stefan, A.; Radeghieri, A.; Rodriguez, A.; Hochkoeppler, A. FEBS Lett. 2001, 493, 139.
- ¹⁷⁰ Hamilton, C. M.; Aldea, M.; Washburn, B. K.; Babitzke, P.; Kushner, S. R. J. Bacteriol. **1989**, 171, 4617.
- ¹⁷¹ Brosius, J.; Holy, A. *Proc. Natl. Acad. Sci. USA*, **1984**, *81*, 6929.
- ¹⁷² Tabor, S.; Richardson, C. C. *Proc. Natl. Acad. Sci. USA*, **1987**, *84*, 4767.
- ¹⁷³ Miller, J. H. Experiments in Molecular Genetics; Cold Spring Harbor Laboratory: Plainview, NY, 1972.
- ¹⁷⁴ Sambrook, J.; Russell, D. W. *Molecular Cloning: A Laboratory Manual*, 3rd ed.; Cold Spring Harbor Laboratory: Cold Spring Harbor, NY, 2001.
- ¹⁷⁵ Wilson K. In Current Protocols in Molecular Biology; Ausubel, F. M.; Brent, R.; Kingston, R. E.; Moore, R. E.; Seidman, J. G.; Smith, J. S.; Struhl, K. Eds.; Wiley: NY, 1987.
- ¹⁷⁶ Bradford, M. M. Anal. Biochem. 1976, 72, 248.
- ¹⁷⁷ Schoner, R.; Herrmann, K. M. J. Biol. Chem. 1976, 251, 5440.
- ¹⁷⁸ Sieben, A. S.; Perlin, A. S.; Simpson, F. J. Can. J. Chem. 1966, 44, 663.
- ¹⁷⁹ (a) Clark, V. M.; Kirby, A. J. *Biochem Prep.* **1966**, *11*, 101. (b) Hirschbein, B. L.; Mazenod, F. P.; Whitesides, G. M. J. Org. Chem. **1982**, 47, 3765.
- ¹⁸⁰ Gollub, E.; Zalkin, H.; Sprinson, D. B. Methods in Enzymol. 1971, 17A, 349.
- ¹⁸¹ Hayaishi, O.; Katagiri, M.; Rothberg, S. J. Biol. Chem. 1957, 229, 905.

¹⁸² Strøman, P.; Reinert, W. R.; Giles, N. H. J. Biol. Chem. 1978, 253, 4593.

¹⁸³ Paoletti, F.; Williams, J. F.; Horecker, B. L. Anal. Biochem. **1979**, 95, 250.

¹⁸⁴ Harris, E. L. V.; Angal, S. In *Protein Purification Methods: A Practical Approach*; Oxford University Express: Oxford, New York, Tokyo, 1989.

¹⁸⁵ Farabaugh, M. A. M.S. Thesis, Michigan State University, 1996.

¹⁸⁶ Kambourakis, S. Ph.D. Thesis, Michigan State University, 2000.

Miller, J. H. A Short Course in Bacterial Genetics: A Laboratory Manual and Handbook for Escherichia coli and Related Bacteria; Cold Spring Harbor Laboratory Press: Plainview, NY, 1992.

¹⁸⁸ Dell, K. A.; Frost, J. W. J. Am. Chem. Soc. 1993, 115, 11581-11589.

¹⁸⁹ Guo, J. Ph.D. Thesis, Michigan State University, 2004.